Volume 2, Number 1 January-February 1994

ISSN: 0869-5938

STRATIGRAPHY AND GEOLOGICAL CORRELATION

Official English Translation of *Stratigrafiya, Geologicheskaya Korrelyatsiya*

Editor-in-Chief
Boris S. Sokolov

Academician, Russian Academy of Sciences
Counsellor of the Presidium of the Russian Academy of Sciences

Journal of the Fundamental and Applied Aspects of Stratigraphy and the Correlation of Geologic Events and Processes in Time and Space

МАИК НАУКА/INTERPERIODICA PUBLISHING

Stratigraphy and Geological Correlation

(*Stratigrafiya. Geologicheskaya Korrelyatsiya*)

Published 6 times a year
by МАИК Наука/Interperiodica Publishing (Russia)
Distributed worldwide by Interperiodica
ISSN: 0869-5938

Editor-in-Chief
Boris S. Sokolov
Academician, Russian Academy of Sciences,
Counsellor of the Presidium of Russian Academy of Sciences

Address for correspondence: Staromonetnyi per. 22, Moscow 109180 Russia
Phones: 7-(095) 231-2164; Fax: 7-(095) 233-5590.

Deputy Editor-in-Chief
Mikhail A. Semikhatov
Corresponding Member of the Russian Academy of Sciences
Head of Laboratory, Geological Institute,
Russian Academy of Sciences

Assistant Editor
Aleksei B. Herman
Senior Scientist,
Geological Institute,
Russian Academy of Sciences

EDITORIAL BOARD

Mikhail A. Akhmet'ev
Dr. Sci. (Geol.-Min.),
Head of Laboratory, Geological Institute,
Russian Academy of Sciences

Aleksandr S. Alekseev
Professor, Department of Paleontology,
Moscow State University

Mikhail N. Alekseev
Dr. Sci. (Geol.-Min.),
Chief Scientist, Geological Institute,
Russian Academy of Sciences

Ivan A. Basov
Dr. Sci. (Geol.-Min.),
Deputy Director, Institute of the Lithosphere,
Russian Academy of Sciences

Michael G. Basset
Professor, National Museum of Wales,
Cardiff, UK

William A. Berggren
Professor, Department of Geology and
Geophysics, Woods Hole Oceanographic
Institute, USA

Elena V. Bibikova
Dr. Sci. (Geol.-Min.), Chief Scientist,
Vernadskii Institute of Geochemistry
and Analytical Chemistry,
Russian Academy of Sciences

Nikita A. Bogdanov
Corresponding Member of the Russian Academy
of Sciences, Director, Institute of the
Lithosphere, Russian Academy of Sciences

Kiyotaka Chinzei
Professor, Institute of Geology,
University of Tokyo, Tokyo, Japan

Nikolai M. Chumakov
Dr. Sci. (Geol.-Min.),
Chief Scientist, Geological Institute,
Russian Academy of Sciences

Yurii B. Gladenkov
Dr. Sci. (Geol.-Min.),
Deputy Director, Geological Institute,
Russian Academy of Sciences

Dmitrii L. Kaljo
Professor, Institute of Geology, Tallinn, Estonia

Victor E. Khain
Member of the Russian Academy of Sciences,
Chief Scientist, Institute of the Lithosphere,
Russian Academy of Sciences

Lidiya A. Nevesskaya
Dr. Sci. (Biol.), Laboratory Chief, Institute of
Paleontology, Russian Academy of Sciences

Aleksandr G. Ponomarenko
Dr. Sci. (Biol.), Chief Scientist, Institute of
Paleontology, Russian Academy of Sciences

Jurgen Remane
Professor, Institute de Géologie,
Université de Neuchâtel, Switzerland

Aleksei Yu. Rozanov
Dr. Sci. (Geol.-Min.),
Director, Institute of Paleontology,
Russian Academy of Sciences

Boris A. Sokolov
Dr. Sci. (Geol.-Min.),
Professor, Dean, Faculty of Geology,
Moscow State University

Otto Walliser
Professor,
Göttingen University, Göttingen, Germany

Sun Weigo
Professor, Nanjing Institute of Geology
and Paleontology, Academia Sinica, China

Victor A. Zakharov
Dr. Sci. (Geol.-Min.),
Head of Laboratory, Institute of Geology,
Geophysics, and Minerology,
Siberian Branch, Russian Academy
of Sciences, Novosibirsk

Aleksandr I. Zhamoida
Corresponding Member of the Russian Academy
of Sciences, Russian Geological Institute,
St. Petersburg

Staff Editor Tamara V. Trishkina

Editor of the English Translation Anatolii Ya. Sharas'kin, Dr. Sci. (Geol.-Min.)

SCOPE

Stratigraphy and Geological Correlation (Stratigrafiya. Geologicheskaya Korrelyatsiya) is the only journal in the world designed to provide comprehensive coverage of the fundamental and applied aspects of stratigraphy and the correlation of geological events and processes in time and space. Articles are based on the results of multidisciplinary research, and are directed toward researchers, university professors, students, and geologists interested in understanding stratigraphy and the chronological features of the world's geological record.

SUBSCRIPTION OFFICE

INTERPERIODICA
P.O. BOX 1831, BIRMINGHAM, AL 35201-1831 USA
PHONE: (800) 633-4931; (205) 995-1567 (outside US and Canada); FAX: (205) 995-1588

PUBLISHER

МАИК НАУКА/INTERPERIODICA PUBLISHING
PROFSOYUZNAYA UL. 90, MOSCOW, 117864 RUSSIA
PHONE: 7-(095) 336-0066; FAX: 7-(095) 336-0666

SUBSCRIPTION PRICE

US $591 (North America), $645(other). A 5% discount is given on 2-year orders. Subscriptions may be entered at any time. Orders may be placed at agencies or directly. 5% discount to all subscription agencies. Cancellations not allowed except for duplicate payment. Prepayment required.
Advance payment required in US$/US bank. MasterCard/Visa accepted. Checks payable to *Stratigraphy and Geological Correlation* or Interperiodica.

Journal founded in 1993.

Original Russian Edition Copyright © 1994 by the Russian Academy of Sciences
and the Division of Geology, Geophysics, Geochemistry, and Mining Sciences.
English Translation Copyright © 1994 by МАИК Наука/Interperiodica Publishing (Russia).

CONTENTS

Volume 2, Number 1, 1994

Simultaneous English language translation of the journal is available from МАИК НАУКА/Interperiodica Publishing (Russia). *Stratigraphy and Geological Correlation* ISSN 0869-5938.

Uranium-Lead Age of the Sumian Acid Magmatic Rocks in Northern Karelia

O. A. Levchenkov, A. A. Nikolaev, E. S. Bogomolov, and S. Z. Yakovleva 1

Rubidium-Strontium Geochronology of Proterozoic Metamorphic Rocks in North Korea

I. M. Gorokhov, Choi Won Cheng, V. A. Glebovitskii, A. V. Baskakov, A. K. Buiko, S. A. Bushmin, Kim Yong Muk, Kim Reh Soo, Kim Choo Ryol, I. N. Krylov, E. P. Kutyavin, N. N. Mel'nikov, N. E. Morozov, and I. S. Sedova 7

Microfossils in Cherts from the Mesoproterozoic (Middle Riphean) Debengda Formation, the Olenek Uplift, Northeastern Siberia

V. N. Sergeev, A. H. Knoll, S. P. Kolosova, and P. N. Kolosov 19

Dynamics of Graptolite Diversity across the Wenlock–Ludlow Boundary

T. N. Koren' 34

Paleozoic Coral Reefs in Russia

L. N. Bol'shakova, M. R. Gekker, R. V. Goryunova, V. N. Dubatolov, A. B. Ivanovskii, V. N. Kosmynin, V. A. Luchinina, B. S. Sokolov, and Yu. I. Tesakov 40

Main Morphological Events in the Evolution of Paleozoic Cephalopods

I. S. Barskov, M. F. Bogoslovskaya, F. A. Zhuravleva, G. N. Kiselev, L. F. Kuzina, T. B. Leonova, V. N. Shimanskii, and S. V. Yatskov 49

Palynology of the Lower Permian Deposits in Northeastern Syria

O. P. Yaroshenko and I. Bach Imam 56

Changes in the Taxonomic and Ecologic Composition of Shelf Benthic Assemblages at the Permian–Triassic Boundary

L. A. Nevesskaya 68

Radiolarians as Indicators of Triassic Climate in Northeast Asia

N. Yu. Bragin 75

Evolution of the Jurassic Tethyan Foraminifera

K. I. Kuznetsova 80

Upper Eocene Olistostromes on the Southern Slope of the Greater Caucasus

F. D. Maisadze 88

Correlation of Development Stages of the Paleogene Diatom Flora from Marine Epicontinental and Oceanic Basins

Z. I. Glezer 95

Climatic Optima during the Cenozoic in West Siberia Deduced from Palynological Data

V. S. Volkova and I. A. Kul'kova 99

Stratigraphy and Geological Correlation, Vol. 2, No. 1, 1994, pp. 1 - 6. Translated from Stratigrafiya. Geologicheskaya Korrelyatsiya, Vol. 2, No. 1, 1994, pp. 3 - 9.
Original Russian Text Copyright © 1994 by Levchenkov, Nikolaev, Bogomolov, Yakovleva.
English Translation Copyright © 1994 by Interperiodica Publishing (Russia).

Uranium-Lead Age of the Sumian Acid Magmatic Rocks in Northern Karelia

O. A. Levchenkov*, A. A. Nikolaev, E. S. Bogomolov*, and S. Z. Yakovleva***

**Institute of Precambrian Geology and Geochronology, Russian Academy of Sciences, nab. Makarova 2, St.Petersburg, 199034 Russia*
***Institute of Geology, Karelian Research Center, Russian Academy of Sciences, Pushkinskaya ul. 11, Petrozavodsk, 185610 Russia*

Recieved March 18, 1993

Abstract – Morphologic features and U-Pb isotope ages of zircons from Sumian metarhyolites of the Lekhta structure as well as from two granite massifs of a single rhyolite–granite volcano-plutonic association were studied. Two zircon generations were distinguished within the granite–granite-porphyry–rhyolite sequence. Zircons of the first generation P–G morphologic type in the most deep-seated magmatites are considered "pervasive" for the above facial types. They crystallized at 2449.3 ± 3.7 Ma. Zircons of the second generation, regarded minerals typical of rocks occurring at shallow depth (especially of volcanic facies), were dated as 2442.8 ± 4.8 Ma. This age reliably estimates the timing of the Sumian acid volcanism within the Lekhta structure.

A complex of acid metavolcanics and associated volcanosedimentary rocks, traditionally considered a typical representative of the Sumian Superhorizon of the lower Proterozoic regional stratigraphic sequence, is a significant constituent of the Karelides in the eastern part of the Baltic shield. The Sumian rocks unconformably overlie the Lopian strata and signal an abrupt change of geotectonic regimes at the Archean–Proterozoic boundary. Their isotopic dating allows us to estimate the upper geochronological parameters of the boundary.

Our investigations, carried out for many years in areas of widespread Sumian metarhyolites (the Lekhta and Panayarvi structures), led us to the justified conclusion that the metarhyolites belong to the lower Proterozoic. The U-Pb dating of zircons from these rocks allowed us to estimate the time-range of the metarhyolites within the 2400 - 2500 Ma interval (Krats *et al.*, 1976; Sakko, 1971; Silvennoinen, 1972). The data agrees with available geological observations, and does not contradict the 2500 ± 50 Ma age of the Archean–Proterozoic boundary adopted in the modern geochronological scale of the Precambrian.

A subsequent study of the U-Pb isotope systems in zircons from quartz porphyries showed a notable dispersion of their data points on the concordia plot, explained by one of two causes: repeated disturbances of zircon isotope systems or mixing of zircon generations of different ages.

A method (Levchenkov *et al.*, 1985), more complex than the Wetherill's model (1956), was proposed for the interpretation of U-Pb errochronous relationships under additional assumptions concerning the evolution of isotopic systems. The calculations resulted in ages exceeding 2700 Ma. This isotope dating was considered as a tentative estimation of the metarhyolite age under proposed constraints concerning the geochemical history of the studied zircons.

The mixing of non-coeval crystals, regarded as a second cause for the appearance of U-Pb errochronous relationships, was not investigated.

The publication of this model's results led to their inadequate interpretations by specialists in general geology. This led to far-reaching but, unfortunately, premature conclusions that the Sumian should be considered as a member of the upper Archean complex (Svetov and Sviridenko, 1989) and that the general trends in the evolution of Lopian magmatism should be reevaluated (Kolychev, 1991). An ambiguity in the understanding of the chronostratigraphic position of the rocks under discussion prompted the present study.

On the other hand, the problem of possibly, comagmatic but heterofacial metarhyolites in the Early Karelids of northern Karelia, which, presumably form the petrologically and geochronologically unified rhyolite-granite volcano-plutonic association (Sudovikov, 1934; Bilibina and Dashkova, 1957; Gilyarova, 1957; Kheiskanen *et al.*, 1977; Hackman and Wilkman, 1929), has been previously discussed in regional geological literature. Geological, petrographic, and petrochemical criteria used do not contradict such an assumption. In this case, the Kormanka and Nuorunen granite massifs and, to a lesser extent, small charnokite bodies in the Vichan area were considered possible plutonic analogs of the metarhyolites.

Thus, the objectives of our work were as follows: (1) to obtain genetic information on the accessory zircons as a basis for subsequent geological and petrologic interpretation of isotope data for both the metarhyolites and their possible plutonic analogs,

(2) U-Pb isotope dating of Sumian volcanism and granite magmatism in order to solve the above problems.

This article presents our results for samples collected from the central and eastern parts of the Lekhta structure (Fig. 1). These are the extrusive proper and volcano-sedimentary (pyroclastic) rocks of rhyolite composition, as well as samples of associated probably subvolcanic bodies. These samples allowed us to obtain representative material for a mineralogical study of zircon.

To estimate the degree of the lateral stability of the zircon population throughout the studied area, we also studied zircons from quartz porphyry of the Tsipringa Lake area, which turned out to be mineralogically similar to the other zircons under study.

Plutonic rocks are represented by granites of the Kormanka massif, whereas hypabyssal (including subvolcanic) rocks are granite porphyries of the Kosozero–Tiroyarvi–Tukhkala area.

It should be stressed that we selected areas for the study regarding above all the present state of the problem as well as the results of previous investigations. Therefore, our task was limited to the mineralogical and geochronological verification of already existing hypotheses.

On the basis of our own experience and available facts, we arrived at the assumption that the zircons from genetically identical but heterofacial magmatic rocks can be characterized by individual features of their population, being analogous to each other in certain qualitative mineralogical features observed amid varieties.

In case of a positive response to these assumptions, a comparative analysis of zircon generations from different facial rock groups is believed to be of interest, and to result in the recognition of zircon generations typomorphic of volcanic and plutonic rocks.

To obtain accessory zircon for mineral analysis, 100 - 300-g samples, crushed to 0.25 mm in size, were cleaned of their magnetic minerals without elutriation and then separated in bromoform. All the obtained concentrates of heavy minerals were subjected to a manual sorting and separation of the available zircons.

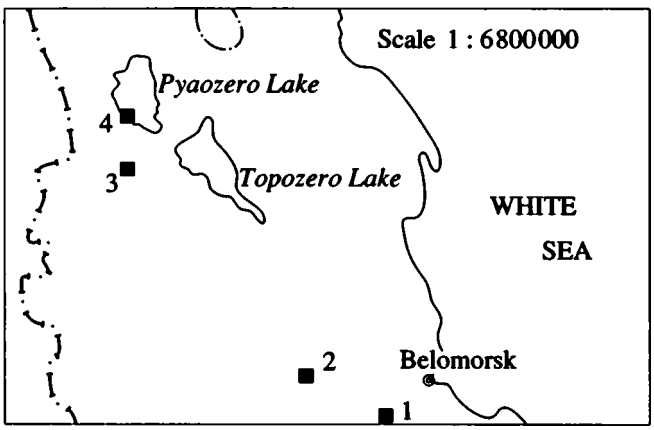

Fig. 1. Scheme of the study areas: 1, 2 – the Lekhta structure, 3 – Tiroyarvi–Tukhkala area, 4 – Kormanka area.

The principal mineralogical characteristics included traditional features of zircons: color, luster, transparency, size, coefficient of elongation and flattening, types of zonation, the degree to which they are idiomorphic and euhedral, specific features of crystal surfaces, etc. Relative ages of separated groups of individuals were determined using directly observed relationships between them. Taking into account the enumerated criteria, we identified genetically similar groups of individuals (generations), and, if it was possible, their morphotypes (Pupin, 1980).

In the samples studied, a quantitative role of certain generations was assessed. For their petrogenetic classification we estimated the presence and relative role of a certain generation within the general zircon population, dependant on the intensity of zircon-forming geological process (Nikolaev, 1980).

The isotope study of zircons was carried out using only carefully selected monogenerations.

According to the above method, we studied 38 zircon samples from matarhyolites, 7 from the hypabyssal granite-porphyries, and 4 from the granites. The study allowed us to make the following conclusions.

Accessory zircon of the rocks studied is represented by a population uniform in its mineralogical features but heterogenous in composition, i.e., containing a number of generations.

Crystals of the first generation comprise a wide spectrum of morphologic types lacking any definite breaks in the mineral-formation and having a gradual transition of one morphotype to an other, reflected in a regular variation in the relative abundance of the simple crystal forms. The morphotypes are the crystal assemblages of a single generation formed under evolving physicochemical conditions of crystallizing magma (Fig. 2a).

Grains of the first generation have smooth, flat, and lustrous surfaces with occasionally noticeable spiral microstructures of the layer growth. Certain crystals show evidence of corrosion (microcavernous surfaces), probably the result of local corrosion. The elongation coefficient is uniform, on average equal to 2.7; flattened forms are unusual. Inclusions of irregularly oriented and corroded tiny grains of yellow zircon and white apatite are extremely rare. Occasionally, the crystals of the described group are overgrown with zircons of the second generation.

The second generation consists of light-rose and yellow crystals and their fragments varying in morphology from elongated-prismatic to needlelike, and having elongation coefficients from 5 to 10. They are easily distinguished by their well expressed, coarse symmetric zoning, whose 3 - 4 zones differ in transparency. Occasionally, zircons of the first generation are overgrown by zircons of the second generation. Small disperse microinclusions of an ore mineral are common

in them; sometimes microinclusions of biotite, feldspar, and white quartz can be observed as well.

Euhedral and subhedral crystals are rare and represented by the J–D-morphotypes (Fig. 2b). Fragments, often devoid of dipiramidal forms, are typical of this generation.

Crystal faces are lustrous. However, rough, usually iron-plated face surfaces, the result of a partial post-crystallization corrosion are often observed.

Based on the above features, we assume that the zircons of the first generation were crystallized under a narrow interval of physicochemical conditions of a magma oversaturated with the zircon-forming components.

The two other subordinate zircon varieties are attributed to a special group represented by less abundant, small, brown or greenish-grey, short-prismatic, and often fractured crystals. Preliminary determinations of their apparent ages using the ion thermoemission method yielded ages exceeding 2500 Ma.

One more variety is represented by rare microinclusions of resorbed zircon grains in the crystals of the first generation. Relations between the individuals of this group and any real geological process were not established, suggesting their xenogenous nature. The subordinate zircons varieties were excluded from samples used for age determinations.

The relative abundance of the first and second zircon generations in the granite–granite-porphyry–rhyolite sequence suggests the following conclusions: (1) Zircons of the first generation are generally pervasive in all types of the rock facies. Undoubtedly, the P–G morphotypes are most abundant in the deep-seated rocks, which are probably related to fractional crystallization of a granite melt. (2) Zircons of the second generation are considered typomorphic minerals of shallow, especially volcanic facies. Its relative abundance in the general population is more prominent in the extrusive rocks than in the granite-porphyry; and increases from 1 - 3% in the latter to 25 - 30% in extrusive rocks. The second zircon generation may have formed under conditions of a shallow subsurface crystallization.

For the isotopic age determinations, zircon samples from the Lekhta metarhyolites and Kormanka granites were separated into fractions corresponding to crystal-morphology, degree of transparency, and size. In order to remove chemically disturbed phases, a part of the zircon sample of the first type separated from the metarhyolites was treated by hydrofluoric acid at $T = 210°C$ for 4 hours (fraction no. 6). Three fractions (nos. 5, 9, and 10) were obtained using an abrasive treatment of crystals of the first and second generations.

The zircons decomposition and the extraction of Pb and U were performed using a modification of Krogh's method (Krogh, 1973). The experimental level of Pb contamination did not exceeded 0.5 ng; for U this value was less than 0.01 ng.

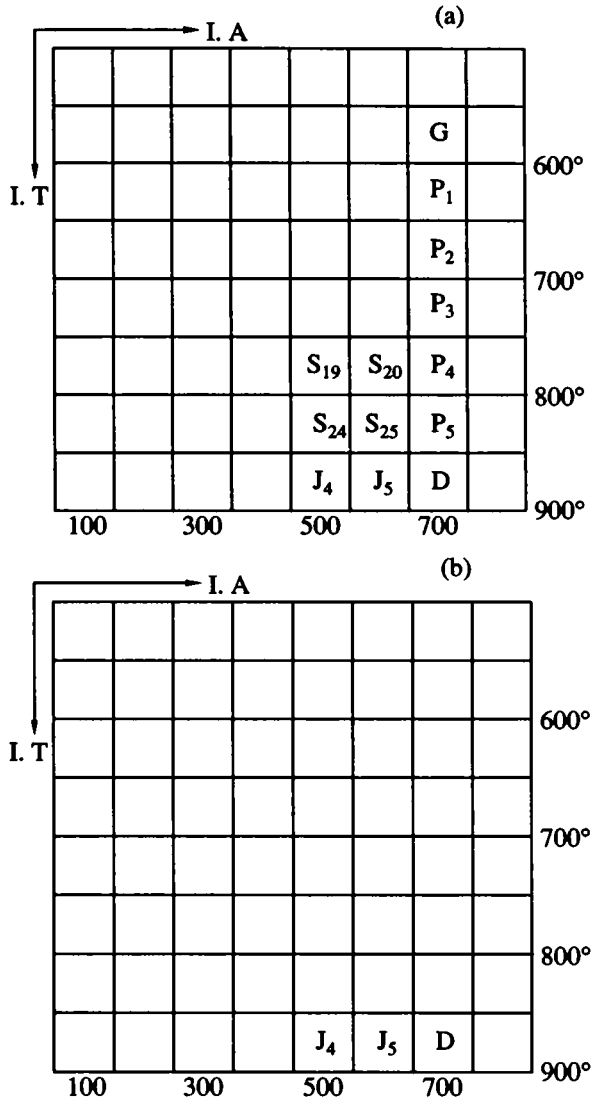

Fig. 2. Schematic typologic diagrams for zircons of the first (a) and second (b) generations.

The isotopic compositions of Pb and U were measured using the multicollector mass-spectrometer MAT-261. Analytical errors in the measurements of U/Pb isotope ratios did not exceed 1.0%. The calculated correlation coefficients of measurement errors for U/Pb isotopic ratios are equal to 0.98.

The Pb and U/Pb isotopic ratios, isochrone parameters, and ages were calculated using Ludwig's programs (Ludwig, 1990). The following constants were used: $\lambda_{238} = 0.155125 \times 10^{-9}$ years, $\lambda_{235} = 0.984850 \times 10^{-9}$ years, and $^{238}U/^{235}U = 137.88$.

All the studied fractions of both zircon types from metarhyolites contain small concentrations of uranium, varying from 46.8 to 78.3 ppm. The table shows Th/U ratios in zircons, which appeared in the course of crystallization. The ratios were calculated for each fraction on the basis of the lead isotope composition and zircon formation time (Levchenkov and Yakovleva, 1985). The Th/U ratios in the fractions are relatively constant

Lead and uranium isotopes in zircons

No.	Fraction, number of the analysis	Fraction weight, mg	Content, ppm		Measured isotopic ratios			Atom ratios		Age, Ma	Th/U
			uranium	lead	$^{206}Pb/^{204}Pb$	$^{206}Pb/^{207}Pb$	$^{206}Pb/^{208}Pb$	$^{206}Pb/^{238}Pb$	$^{207}Pb/^{235}Pb$		
	No. 610 - 101, quartz porphyry, the Lekhta structure										
1	Type-1, gross	1.42	78.3	27.3	575	6.3724	4.5968	0.28824	5.3456	2157.6	0.43
2	Type-1 (P_{1-3}), −150	2.82	46.8	28.0	190	4.5315	2.5009	0.40309	8.5670	2392	0.65
3	Type-1 (D), −200	2.57	60.3	31.4	1080	6.0960	4.1180	0.42796	8.9956	2374	0.56
4	Type-1 (D), +100	1.65	75.9	40.2	1965	6.0914	4.1158	0.43961	9.5733	2433.7	0.61
5	Type-1 (D), +100, at	0.95	61.2	33.5	1150	5.9102	3.8604	0.45111	9.8582	2439.7	0.62
6	Type-1 (D), NDHF	–	8.2 ng	5.0 ng	299.3	4.9806	3.1032	0.46297	10.150	2445.1	0.58
7	Type-2 (J_{4-5} - D), +150	2.28	61.5	33.1	978	5.8802	3.5625	0.43260	9.3861	2427.5	0.67
8	Type-2 (J_{4-5} - D), −150	4.19	66.6	34.1	2320	6.1738	3.6051	0.41299	8.9232	2420.4	0.70
9	Type-2 (J_{4-5} - D), +100	2.28	73.6	39.9	4485	6.2175	3.7244	0.44309	9.6658	2437	0.70
10	Type-2 (J_{4-5} - D), at	1.86	64.7	35.4	2225	6.1120	3.7080	0.44596	9.7235	2435.8	0.69
11	Type-2, gross, at	2.83	58.8	30.2	2520	6.1692	3.9493	0.42287	9.1698	2426.5	0.64
	No. 1, granite-porphyry, the Tiroyarvi Lake area										
12	Type-1 (J_{4-5} - D), gross	2.58	266	109	2855	6.4113	3.5590	0.32894	6.8792	2364.9	0.73
	No. 404 - 1, granite, the Kormanka massif										
13	Type-1 (J_{4-5})	0.70	230	91.9	468.4	5.5998	3.4860	0.31125	6.5065	2364.2	0.59
14	Type-1 (J_{4-5})	0.61	70.5	36.4	626.0	5.6257	4.0132	0.42574	9.2671	2433.0	0.53
15	Type-1 (J_{4-5}) transparent	0.58	83.8	43.6	795.0	5.7448	4.3346	0.43276	9.4544	2439.2	0.51

Note: Size of zircon fractions is indicated in μm; at is the abrasive treatment; NDHF is the zircon fraction unliquidated in HF.

with their values changing from 0.4 to 0.7; their variations in the first generation zircons are higher than in the second generation crystals. The narrow range of Th/U ratios in the zircons of the second generation (Fig. 3) confirms the earlier assumption, based on their morphological features, that this generation crystallized under a limited interval of physicochemical conditions.

The age values calculated by the $^{207}Pb/^{206}Pb$ ratio in zircons of the first generation vary considerably, from 2445.1 (no. 6) to 2157.6 Ma (no. 1), which indicates a disturbance of the isotope systems of the minerals studied. Therefore, in order to determine the time of the zircon formation, an isochrone method was used. Two fractions were excluded from consideration: fraction no. 1, with the most distorted Pb/U ratios, and frac-

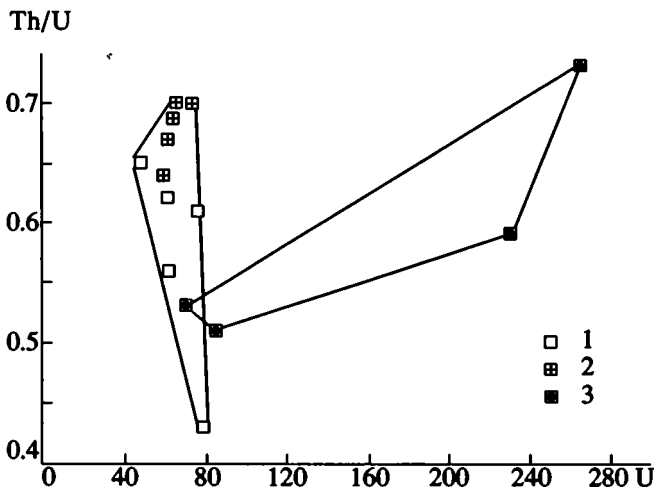

Fig. 3. The Th/U-U plot for zircons from quartz porphyry (1 – first generation, 2 – second generation), granite porphyry, and granite (3 – third generation).

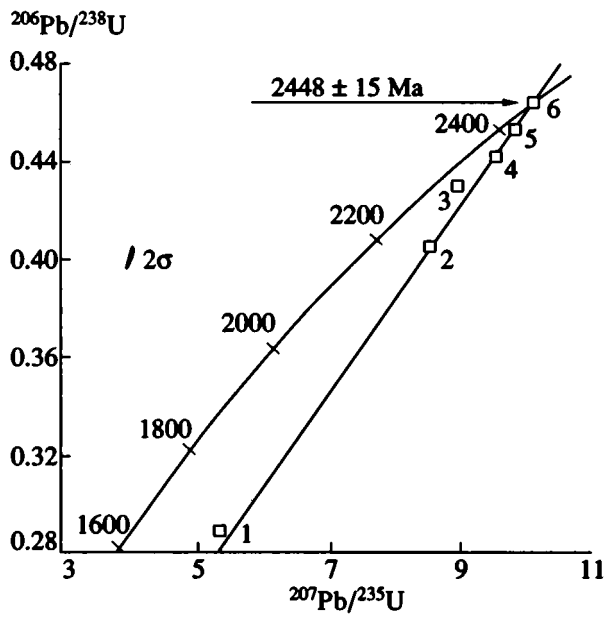

Fig. 4. The concordia plot for zircons of the first generation from quartz porphyry of the Lekhta structure. The point numbers on Figs. 4, 5, and 6 correspond to the sample numbers in Table.

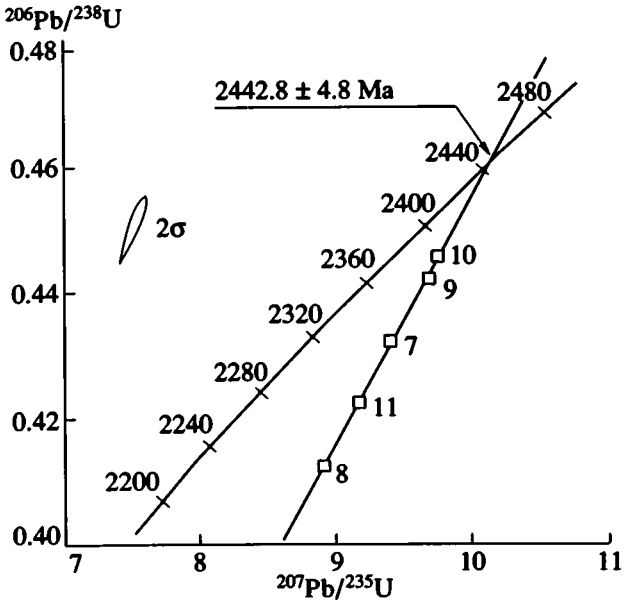

Fig. 5. The concordia plot for zircons of the second generation from quartz porphyry of the Lekhta structure.

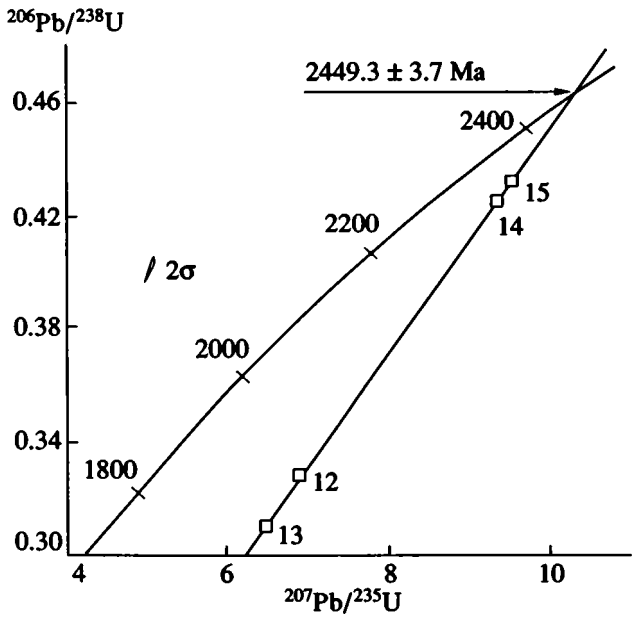

Fig. 6. The concordia plot for zircons of the first generation from granite porphyry of the Tiroyarvi Lake area and granite of the Kormanka massif.

tion no. 3, certain grains of which have rims composed of a later zircon generation.

The isochrone, calculated by the Pb/U ratios in zircon fractions of the first group, yielded 2448 ± 15 Ma age, and MSWD = 2.4 (Fig. 4). The MSWD exceeding unity probably resulted from the thin rims of a late zircon generation around some early grains that are most noticeable in the fraction no. 3.

The U isotopic composition and Th/U ratio in zircons of the second generation ($J_{4.5}$–D) do not differ from the same parameters in zircons of the first generation, though their Th/U ratios vary within a considerably narrower range (Fig. 3, the table). However, according to the measured $^{206}Pb/^{204}Pb$ isotope ratios, these two zircon morphotypes differ somewhat in their common lead content. Such features, along with the zircons crystallization temperatures estimated using Pupin's systematics of zircon morphology (Pupin, 1980), indicate that these minerals were crystallized from an evolving melt.

The $^{207}Pb/^{206}Pb$ ages of zircon fractions of the second group vary from 2420.4 (no. 8) to 2437 Ma (no. 9). Their isochrone age corresponds to 2442.8 ± 4.8 Ma; MSWD = 0.87 (Fig. 5).

The investigation results confirmed previously noted data dispersion points (Levchenkov *et al.*, 1985) on the corcordia diagram for the bulk zircon samples from the quartz porphyry, which prompted a reevaluation of their isotope age based on the U-Pb errochrone interpretation. The following is evidence of the data points dispersion:

(1) The data points of two zircon generations form two different isochrone relationships, whereas the points of the no. 1 and no. 3 fractions plot outside of these isochrones.

(2) As previously noted, the bulk samples contained two subordinate zircon varieties, the ages of which, according to the thermoemission data, exceeded 2500 Ma. Undoubtedly, these zircon varieties contaminating the analyzed bulk samples influence the dispersion of the data points on the Wetherill's plot.

However, the age measurements, performed accounting for the zircon generation types and the level of their crystal perfection, showed the presence of a concordant age phase, which subsequently excludes the possibility of interpreting the isotope data as it was considered by Levchenkov *et al.* (1985).

The same work reports the $^{207}Pb/^{206}Pb$ isotopic age of apatite, estimated using the common lead correction made in accordance with the Stacey and Kramers' model (Stacey and Kramers, 1975). This apatite age also appears to be exagerated. According to the studies by Ovchinnikova and her colleagues (personal communications), when the measured $^{206}Pb/^{204}Pb$ ratio does not exceed 30 such a correction for the apatite age calculation results in considerably older isotopic ages.

First generation zircons from granites of the Kormanka massif and the Tiroyarvi Lake area belong to the $J_{4.5}$–D morphologic type. According to a number of geochemical features, such as the content of uranium, of common lead, and Th/U ratio, these zircons do not differ considerably from zircons of the quartz porphyry. The exception, zircon fractions from two granite samples containing 230 and 266 ppm of U (the table, no. 12 and no. 13).

The isochrone age of zircon crystallization in the Kormanka massif (the table, nos. 13, 14, and 15) is 2449.3 ± 3.7 Ma, (MSWD =1.2). The data point of the zircon bulk sample from the graniteporphyry of the Tiroyarvi Lake area (the table, no. 12; Fig. 6) plots on the same isochrone.

The ages obtained for zircons from granites do not differ (within the limits of analytical errors) from the ages of the first zircon generation in the quartz porphyry (Fig. 6). Therefore, the formation of the first generation zircon, which is considered "pervasive" for all the studied rock facies, took place simultaneously 2449.3 ± 3.7 Ma ago. This value, as it was measured more accurately, is accepted as the age of the zircon crystallization.

The isotopic age (2442.8 ± 4.8 Ma) of the second zircon generation, formed during the subsurface crystallization, seems the most reliable estimate of the acid volcanism age of the Lekhta structure.

REFERENCES

Bilibina, T.V. and Dashkova, A.D., Characteristics of Some Precambrian Granites of Northern Karelia (the Nuorunen Intrusive Complex), *Petrogr. Sb. `VSEGEI*, 1957, vol. 21, no. 2, pp. 39 - 47.

Gilyarova, M.A., Quartz Porphyries and Keratophyres of Central Karelia, *Uchen. Zap. LGU, Ser. Geol. Nauk*, 1957, issue 8, no. 215, pp. 58 - 83.

Hackman, V. and Wilkman, P., *Suomen Geologinen Yleis Kartta*, Lehti D6, Kuolajarvi, Helsinki, 1929.

Kheiskanen, K.I., Golubev, A.I., and Bondar', L.F., *Orogennyi Vulkanizm* (Orogenic Volcanism), Leningrad: Nauka, 1977.

Kolychev, E.A., The Sumian Volcanic Rocks of the Baltic Shield and Tectonic Environment of Their Formation, *Izv. Akad. Nauk SSSR, Ser. Geol.*, 1991, no. 2, pp. 3 - 13.

Kratz, K.O., Levchenkov, O.A., Shuleiko, I.K., *et al.*, Age Boundaries of the Yatulian Complex of Karelia, *Dokl. Akad. Nauk SSSR*, 1976, vol. 231, pp. 1191 - 1194.

Krogh, T.E., A Low-Contamination Method for Hydrothermal Decomposition of Zircon and Extraction of U and Pb for Isotopic Age Determinations, *Geochim. Cosmochim. Acta*, 1973, vol. 37, no. 3, pp. 485 - 494.

Levchenkov, O.A., Yakovleva, S.Z., Krylov, I.N., *et al.*, On Isotopic Age of the Sumian Quartz Porphyries of the Lekhta Structure in Karelia, *Izotopnoe Datirovanie Protsessov Vulkanizma i Osadkoobrazovaniya* (Isotopic Dating of Processes of Volcanism and Sedimentation), Moscow: Nauka, 1985, pp. 154 - 161.

Levchenkov, O.A. and Yakovleva, S.Z., A Possibility to Calculate Th/U Ratio Using Isotope Composition of Lead in Zircons, *Sovremennye Dannye Izotopnoi Geokhimii i Kosmokhimii* (Modern Data on Isotope Geochemistry and Cosmochemistry), Leningrad: Nauka, 1985, pp. 136 - 142.

Ludwig, K.R., *Isoplot for MS-DOS Version 2.00*, Open-File Report 88 - 557, 1990.

Nikolaev, A.A., On the Formation of Zircon Generations Related to Granite-Forming Processes, *Zapiski Vsesoyuzn. Mineral. Obshch.*, 1980, vol. 6, pp. 681 - 686.

Pupin, J.P., Zircon and Granite Petrology, *Contrib. Mineral., and Petrol.*, 1980, vol. 73, no. 3, pp. 207 - 220.

Sakko, M., Varhais-Karijolaisten Metadiabaasien Radiometrisia Jizconiikia, *Geologi*, 1971, vol. 23, nos. 9, 10, pp. 117 - 119.

Silvennoinen, A., On the Stratigraphic and Structural Geology of the Rukatunturi Area, Northeastern Finland, *Bull. Geol. Surv. Finl.*, 1972, no. 257.

Stacey, J.S. and Kramers, J.D., Approximation of Terrestrial Lead Isotope Evolution by a Two-Stage Model, *Earth Planet. Sci. Lett.*, 1975, vol. 26, no. 2, pp. 207 - 221.

Sudovikov, N.G., On Metamorphic Facies of the Yatulian Rocks in the Shuezero-Pebozero Area, *Tr. Leningr. Obshch. Estestvoispyt.*, 1934, issue 2, pp. 179 - 209.

Svetov, A.P. and Sviridenko, L.P., New Data on Geology of the Early Lopian Rocks within the Conjunction Zone between the Karelian and Belomorian Geoblocks, *Geologiya Petrologiya, Operativno-Informatsionnye Materialy*, Petrozavodsk: Karelian Branch of the USSR Acad. Sci., 1989, pp. 3 - 6.

Wetherill, G.W., Discordant Uranium-Lead Ages, *Trans. Am. Geophys. Union*, 1956, vol. 37, no. 3, pp. 320 - 326.

Stratigraphy and Geological Correlation, Vol. 2, No. 1, 1994, pp. 7 - 18. Translated from Stratigrafiya. Geologicheskaya Korrelyatsiya, Vol. 2, No. 1, 1994, pp. 10 - 22.
Original Russian Text Copyright © 1994 by Gorokhov, Choi Won Cheng, Glebovitskii, Baskakov, Buiko, Bushmin, Kim Yong Muk, Kim Reh Soo, Kim Choo Ryol, Krylov, Kutyavin, Mel'nikov, Morozov, Sedova.
English Translation Copyright © 1994 by Interperiodica Publishing (Russia).

Rubidium-Strontium Geochronology of Proterozoic Metamorphic Rocks in North Korea

I. M. Gorokhov*, Choi Won Cheng, V. A. Glebovitskii*, A. V. Baskakov*, A. K. Buiko*, S. A. Bushmin*, Kim Yong Muk**, Kim Reh Soo**, Kim Choo Ryol**, I. N. Krylov*, E. P. Kutyavin*, N. N. Mel'nikov*, N. E. Morozov*, and I. S. Sedova***

**Institute of Precambrian Geology and Geochronology, Russian Academy of Sciences, nab. Makarova 2, St. Petersburg, 199034 Russia*
***Geological Institute, Academy of Sciences of the Democratic People's Republic of Korea, Pyongsong, Democratic People's Republic of Korea*

Received August 21, 1992

Abstract – The Rb-Sr method was applied to determine the age of metamorphic processes within the Machenrjon (Sannon and Kimchaek blocks) and Chungsan (Nampo tectonic window) metamorphic belts in North Korea. Early Proterozoic pegmatite formation, related to regional amphibolite-facies metamorphism of supracrustal rocks, terminated by forming muscovite (acid leaching stage) in the Sannon block 1810 ± 14 Ma ago. The metasomatism during the retrograde stage of regional metamorphism in the rocks of the Namdechon Formation was close in time to the terminal pegmatite crystallization stage. The rocks of the Sondgey Formation in the Kimchaek block were migmatized during the final stage of granulite-facies metamorphism, 1640 ± 200 Ma ago. Within the Nampo uplift, the Rb-Sr isochron age of paragneisses estimated for all the rock samples is 1970 ± 25 Ma, corresponding to the retrograde stage of granulite metamorphism. The superimposed low-temperature greenschist-facies metamorphism of the rocks in the Machenrjon and Chungsan belts is 0.8 - 1.0 Ga old.

INTRODUCTION

A considerable area in North Korea is underlain by old metamorphic rocks (*Geologiya ...*, 1964; Marakushev *et al.*, 1966) (Fig. 1). Early Precambrian metamorphic rocks compose fragments of the North China granulite belt (the Nangnim block) and the Anshan granite–greenstone area (the Musan block) (Zhang, 1985). The Machenrjon and Chungsan metamorphic belts that formed over this crust (Glebovitskii *et al.*, 1993) can be traced into North and Middle China. A pronounced zonation of the andalusite–sillimanite and kyanite–sillimanite types, reaching the granulite-facies level is characteristic of them. According to North Korean structural schemes, these belts belong to eastern areas of the epi-early Proterozoic Sino-Korean craton and the epi-Riphean South China craton (the Yangtze craton), respectively.

The results of isotopic dating of the North Korean Precambrian rocks were adduced in a number of publications (Polevaya *et al.*, 1961; Marakushev *et al.*, 1966; Kropotkin, 1969; Yanagi and Yamaguchi, 1970; Litsarev *et al.*, 1983). However, the succession of metamorphic processes, both within the entire distribution area of Precambrian rocks and within individual structures, having in many cases their specific metamorphic history, is still insufficiently proven by isotope geochronological methods.

The present paper is the first attempt to systematically approach the isotopic dating of the metamorphic processes in the North Korean areas underlain by early Proterozoic metamorphic rocks. It is a part of the joint studies being conducted by the Institute of Precambrian Geology and Geochronology, Russian Academy of Sciences, and the Geological Institute, Academy of Sciences of the Democratic People's Republic of Korea according to the research project: "Study of the evolution of geological processes and ore formation in the Proterozoic." The age of metamorphic processes was determined by the Rb-Sr method.

ANALYTICAL TECHNIQUE

The Rb and Sr contents and the Rb to Sr ratio were determined in most of the whole-rock samples using X-ray fluorescence analysis with a VRA-30 X-ray fluorescence analyser for individual series of experiments. The contents were estimated to within ±10%, and the analytical error in determining the Rb/Sr ratio by the procedure described earlier (Krylov, 1979) was ±1.5%. Minerals and some whole-rock samples were analyzed using the isotope dilution technique (Varshavskaya *et al.*, 1975), and in this case the error of the Rb/Sr determination was ±0.5%.

The isotopic composition of strontium extracted by the ion-exchange method after the chemical decomposition of the samples was measured using the MI 1320 mass-spectrometer. The $^{87}Sr/^{86}Sr$ ratio in the SRM-987 interlaboratory standard during the work was 0.71021 ± 0.00005. The analytical error of this ratio determinant in the samples was assumed to be ±0.05%. The age and the initial $^{87}Sr/^{86}Sr$ were calculated by means of the modified regression approach (McIntyre *et al.*, 1966;

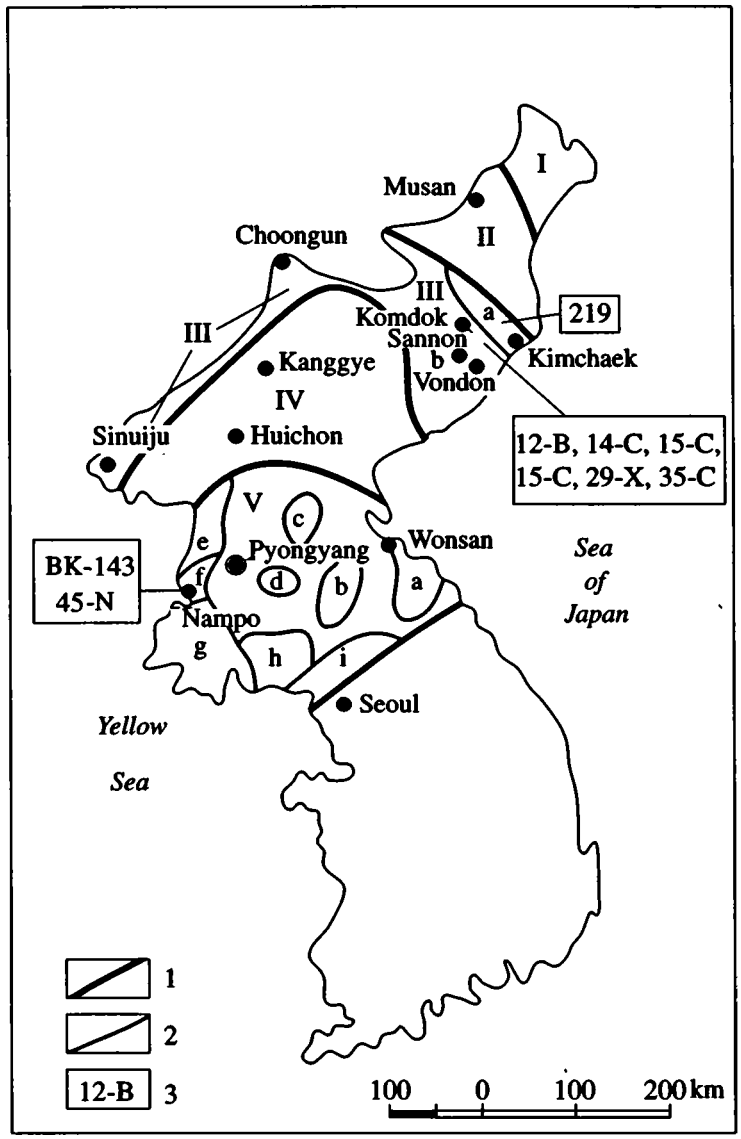

Fig. 1. Main tectonic structures and geographic regions of North Korea.

1 – Structure boundaries; 2 – boundaries of tectonic uplifts and regions; 3 – collection sites of sample series for isotopic dating. I – Tumangang belt; II – Kuanmon Basin; III – Machenrjon structural zone (a – Kimchaek and b – Sannon blocks); IV – Nangnim block; V – Pyongnam basin (a – Wonsan tectonic uplift, b – Ichon uplift, c – Yangdok uplift, d – Chemkol uplift, e – Chungsan uplift, f – Nampo uplift, g – Quail uplift, h – Haeju uplift, and i – Kaesong uplift).

Shukolyukov *et al.*, 1974), in which the relative errors on both coordinate axes were suggested. All the error values are expressed in the text and diagrams as a single standard deviation. The ^{87}Rb decay constant, used in the age calculation, is 1.42×10^{-11} year^{-1}.

MACHENRJON BELT

Geological setting. The Machenrjon belt metamorphic rocks compose the supposedly Archean–lower Proterozoic basement of the northeastern margin of the Sino-Korean craton, and its upper Proterozoic, weakly metamorphosed sedimentary cover. The stratified rocks of the Machenrjon area are traditionally united in the group of the same name, in which, according to the relative predominance of a given rock association, the generally amphibolitic Sondgey, carbonate Pucktechon, and aluminiferous Namdechon formations were identified (from the base upward) (Table 1). The Machenrjon belt is a natural eastward continuation of the early Proterozoic Liaoning structure of Northeastern China, where the Liaojitite Formation and the Liaohe Group are the stratigraphic and lithologic counterparts of the Machenrjon Group (Zhang, 1988). The "eugeosynclinal" rocks of the Liaojitite Formation are correlated with the amphibolites and basic schists of the Sondgey Formation. The high-magnesian marbles of the Dashiqiao Formation and the aluminiferous

metasediments of the Gaixian Formation, united in the "miogeosynclinal" Liaohe Group, are correlated with the Pucktechon and Namdechon formations of the Machenrjon Group, respectively. The Machenrjon belt, which is the continuation of the Northeastern China Liaoning structure, has a similar tectonic setting, separating the Musan block of the Anshan granite–greenstone area from the Nangnim granulite–gneiss block.

A distinct lateral inhomogeneity of lithostructural complexes is pronounced within the Machenrjon belt. The Pucktechon dolomitic marbles and the Namdechon migmatite–gneiss–schist rock association formed after highly differentiated sediments, compose the main part of the sequence in the western and southwestern belt parts (Sannon block). Subordinate amphibolites correspond in their composition to the basalts and basaltic andesites of the calc-alkaline series. Characteristic of the supracrustal rocks in the eastern part of the Machenrjon belt (Kimchaek block) is the predominance of amphibolites and basic schists of the Sondgey Formation, whose composition varies from komatiites and basaltic komatiites to tholeiitic basalts and basaltic andesites. Less abundant are moderately aluminiferous gneisses, marbles, and calciphyres; migmatization is widely manifested. Attention should be paid to the similarity in composition between the Sondgey Formation volcanic rocks and the rocks of the Archean greenstone belts, which suggests that the Machenrjon belt basement is exposed in the Kimchaek block.

The above data suggests, through analogy with the Liaoning structure, that the segments of the "miogeosynclinal" (Sannon block) and "eugeosynclinal" (Kimchaek block) types exist within the Machenrjon belt. Their primary inhomogeneity, originated at the accumulation stage of volcano-sedimentary, terrigenous, and carbonate strata, was subsequently realized in specific features of geologic evolution (ore formation, magmatism, and, particularly, metamorphic transformations).

Metamorphism. The Machenrjon belt metamorphism is inhomogeneous in temperature and pressure parameters and belongs to the shallow-depth, low-pressure andalusite–sillimanite facial series. The western, Sannon block with zonal metamorphism ranging from amphibolite to greenschist facies and the eastern, Kimchaek block with predominantly granulite metamorphism are clearly discriminated within the belt.

The Sannon block is, in the lateral direction, sharply inhomogeneous with regard to the temperature regime of regional metamorphism. Zones of high-temperature subfacies of an amphibolite facies, staurolite subfacies, and greenschist facies can be identified within it.

In the southern and central parts of the block, in the area of the Komdok, Sannon, Hotchon, and Wondon ore deposits, the garnet–cordierite–sillimanite subfacies of an amphibolite facies are most widespread and have a typical paragenesis, which is represented in the aluminiferous rocks of the Namdechon Formation as quartz + potassium feldspar + garnet + cordierite + sillimanite + muscovite + biotite. The maximum temperature in the amphibolite-facies zone (T = 630 - 650°C under P = 4 kbar) was determined in the area of the Wondon corund deposit in the migmatized gneisses. In the central part of the block, in the area of the Komdok and Hotchon ore deposits, the revealed parageneses of the staurolite subfacies zones of the Namdechon Formation are: quartz + biotite + andalusite + muscovite, quartz + biotite + muscovite + garnet + andalusite, quartz + chlorite + biotite + muscovite + staurolite, and quartz + chlorite + biotite + muscovite + staurolite + garnet. Such low-temperature greenschist-facies parageneses as quartz + chlorite + muscovite + biotite, quartz + chlorite + muscovite, quartz + biotite + garnet, quartz + sericite + garnet, and quartz + biotite + sericite in the north (the Hyesan area) seem to be the members of early Proterozoic metamorphic zonation. However, in the middle part of the Sannon block, in particular in the Hotchon and Komdok areas, they belong to the local zones of superimposed retrograde metamorphism.

Table 1. Correlation of the Proterozoic formations of the Sino-Korean craton

Northeastern China: Liaoning structure		North Korea: Machenrjon structure	
Group	Formation	Group	Formation
Liaohe	Gaixian	Machenrjon	Namdechon
	Dashiqiao		Pucktechon
Liaojitite			Sondgey

A pronounced retrograde stage of regional metamorphism is a characteristic feature of the Sannon block. In the areas of the Wondon, Hotchon, and Sannon mineral deposits, a clear retrograde drop in the metamorphism parameters was determined using mineral thermometers and barometers: the temperature decreased from 630 to 400°C, and the pressure, from 4 to 1 kbar. The ore-forming metasomatic processes related to acid leaching and conjugate alkalic metasomatism of the retrograde stage of regional metamorphism are intensely pronounced in these deposits. A general time succession of metamorphic and metasomatic processes in the moderately and highly aluminiferous gneisses of the Namdechon Formation at the Sannon chalcopyrite deposit is as follows: (1) migmatization and pegmatite formation, (2) the early alkalic stage of formation of microcline metasomatites with sillimanite, muscovite, and tourmaline, (3) acid leaching and conjugate iron-magnesian metasomatism resulting in the formation of quartz–sillimanite–muscovite–tourmaline and garnet–cordierite–biotite metasomatites and, perhaps, quartz veins with scheelite and sulfide ores, and (4) the late alkalic stage of the formation of albite metasomatites with quartz, muscovite, and tourmaline.

The data on the thermodynamic parameters of metamorphism in the Kimchaek block of supracrustal rocks is rather limited. In addition to carbonate rocks, which give no exact information on the P–T-parameters, the monoto-

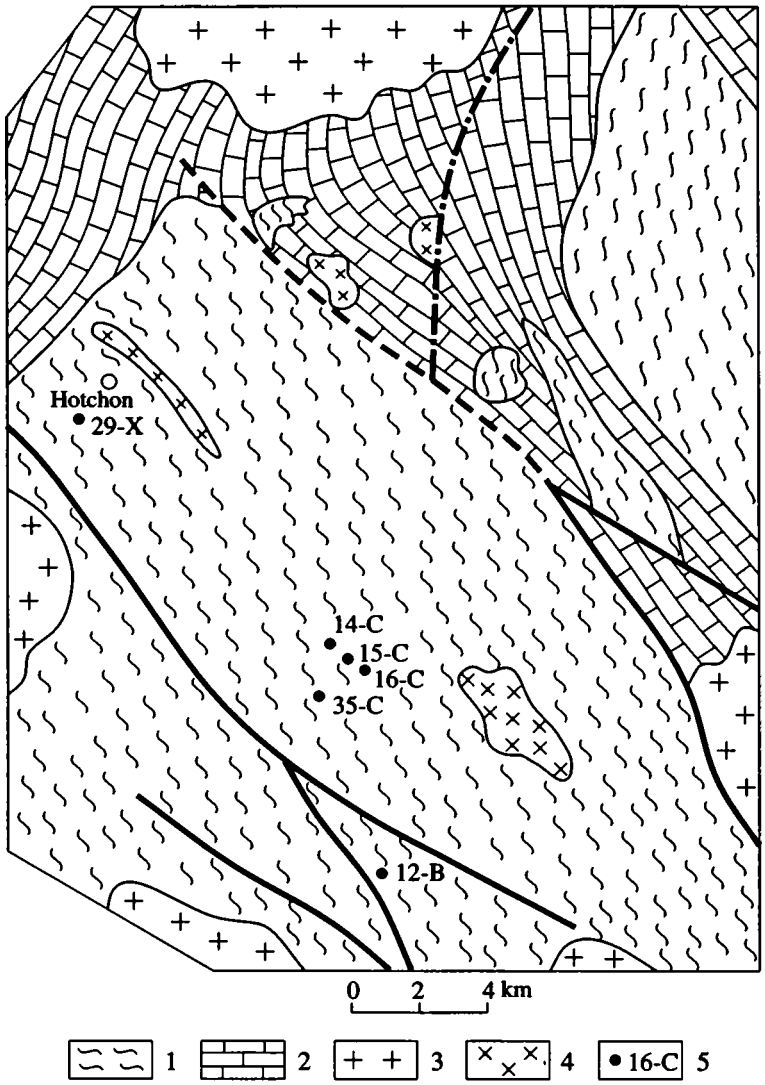

Fig. 2. Locations of the geochronological samples within the Sannon block area.

1 – Namdechon Formation; 2 – Pucktechon Formation; 3 – Mesozoic granites; 4 – Proterozoic granites; 5 – sample series for isotopic dating.

nous two-pyroxene schists, containing garnet only occasionally, are abundant there. The estimated pressure values range from 6.2 to 7.0 kbar, and the temperature values, from 750 to 860°C (Glebovitsky *et al.*, in press).

Geochronology of the Sannon block. The geochronological sampling was carried out in the Southern Hamgyong Province (Fig. 2), in the areas of the Sannon and Hotchon villages and in the Wondon River valley. All the sampled rocks belong or are spatially confined to the Namdechon Formation of the Machenrgon Group.

At the Sannon ore field, in the area of the Chegadon Mine, samples 15-C-1 and 15-C-2 were collected from a pegmatite, deformed together with the country rocks – the Namdechon aluminiferous gneisses. The pegmatite initially consisted of microcline, tourmaline (schorl), quartz, and a small amount of plagioclase. The paragenesis of sillimanite + muscovite + tourmaline was formed in it during the acid leaching stage.

The feldspar (an undivided mixture of microcline and plagioclase), microcline, and muscovite from samples 15-C-1 and 15-C-2 were analyzed using the Rb-Sr method (Table 2). The points of minerals in the Rb-Sr evolution diagram have a fair linear array (Fig. 3). The approximating straight line has an inclination which corresponds to the age of 1810 ± 14 Ma, with the initial $^{87}Sr/^{86}Sr = 0.726 \pm 0.028$ and MSWD[1] = 9.0 (model 3, McIntyre *et al.*, 1966).

Application of the isochron model to a given totality of rocks or minerals requires their simultaneous formation (in this case, crystallization) and the uniformity of their initial $^{87}Sr/^{86}Sr$ ratios. The MSWD value signifi-

[1] Mean square of weighted deviations.

cantly exceeds unity, indicating that the pegmatite minerals incompletely correspond to the isochron model (McIntyre *et al.*, 1966; Shukolyukov *et al.*, 1974); this may indicate that any of these conditions is invalid. First, the early stage of pegmatite crystallization, when the feldspars were formed, may be separated by a considerable time span from the acid leaching stage, when the muscovite was formed. Second, even if these processes were close in time, the minerals of the later stage could have another initial $^{87}Sr/^{86}Sr$ ratio, as has been shown in a number of publications (Yashchenko *et al.*, 1961; Brookins *et al.*, 1969; Riley, 1970). Of course, the combined influence of both these factors is also possible. Unfortunately, a small number of minerals, representing the successive stages of pegmatite crystallization, makes the statistical selection (McIntyre *et al.*, 1966; Shukolyukov *et al.*, 1974) between these possibilities rather difficult, and the ages and initial $^{87}Sr/^{86}Sr$ characteristic of individual crystallization stages cannot be calculated with sufficient precision. Therefore, it is impossible to establish the cause of the surplus spread of points relative to the approximating straight line with any confidence. It is clear, however, that under the circumstances the age value, calculated using the isochron method, cannot be considered the crystallization time of the entire association of the minerals studied. Nevertheless, the very high Rb/Sr values in muscovite do not make it, in relative terms, very dependent on the choice of the initial $^{87}Sr/^{86}Sr$ ratio. Consequently, we can suggest that the value of 1810 ± 14 Ma is fairly close to the muscovite crystallization time, even if the muscovite was formed at the acid leaching stage considerably later than the formation of the early pegmatite minerals.

In the area of the Chegadon orebody, the country rocks first underwent potassium metasomatism with the formation of microcline porphyroblastic rocks, and then, sodium metasomatism with the formation of ore tourmaline-bearing albitite. As the Rb contents in the latter are very low, samples of microcline metasomatites with sillimanite, muscovite, and tourmaline (14-C series) were collected for dating. The samples of this series weighed 1 - 1.5 kg each. A sample of basic garnet-cordierite-biotite-tourmaline metasomatite from the area adjacent to the acid leaching zone of the Pongkhwa orebody at the Sannon deposit (sample 35-C-2b), with a weight of about 10 kg, was also analyzed.

Another series of samples collected from biotite-sillimanite augen schist, which enclose the Sannon deposit, was taken along a 25 m section at a road cut between the Sannon village and the Chegadon Mine (16-C series). The samples weighed 1 to 2 kg (small samples), and only a single sample, 16-C-3b, weighed ca. 10 kg. Five small samples were schists, which had underwent acid leaching and were characterized by a high sillimanite content and a mineral association of biotite ± potassium feldspar ± garnet + quartz + sillimanite. The sixth sample (16-C-15) was a microcline–tourmaline–sillimanite–muscovite acid-leached metasomatite with biotite relicts.

Table 2. Analytical data on Rb-Sr in pegmatite from the Sannon mineral deposit area

No.	Sample no.	Mineral	Rb, ppm	Sr, ppm	$^{87}Rb/^{86}Sr$	$^{87}Sr/^{86}Sr$
1	15-C-1	Feldspar	444	62.1	21.91	1.2974
2	15-C-1	Microcline	495	47.8	32.45	1.5417
3	15-C-1	Muscovite	732	7.37	1045	27.651
4	15-C-2	Microcline	459	50.8	28.14	1.4851
5	15-C-2	Muscovite	893	9.48	918.9	24.918

Note: The Rb and Sr contents were determined using isotope dilution.

The analytical data for the mentioned metasomatite samples is given in Table 3. All these rocks were formed at the retrograde stage of regional metamorphism, but are undoubtedly related to different steps of this process. Even if the total duration of the retrograde metamorphism stage was not too great, and the rocks were considered to be of the same age, the step by step change in the fluid phase chemical composition should result in a variation of the Sr isotopic composition in this phase and, consequently, in the corresponding differences between the initial $^{87}Sr/^{86}Sr$ ratios in metasomatites. Therefore, applying the isochron approach to all series of analyzed samples would hardly be correct. Besides, because of the substantial differences of the Rb/Sr ratios in the samples of the 14-C and 16-C series, there is a real danger of obtaining a pseudochron dependence that would unite the two incogenetic series. And an attempt to calculate the age using the isochron method for individual sample groups would result in high MSWD values and hence in a considerable uncertainty concerning the results obtained. The position of the data points of the studied metasomatites relative to the reference isochron with an age of 1810 Ma, which corresponds to the time of muscovite formation in peg-

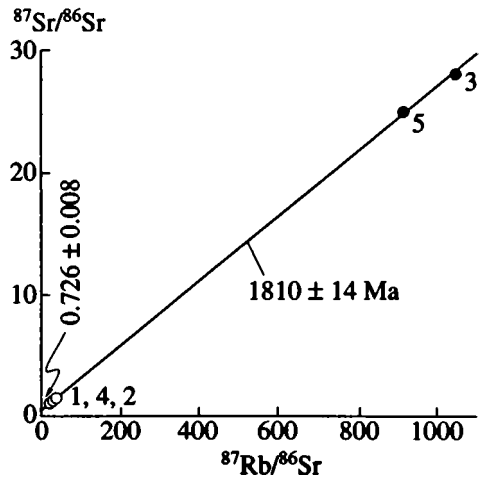

Fig. 3. Rb-Sr evolution diagram for the pegmatite minerals from the Sannon block. Open circles are feldspars, solid circles are muscovite. Sample nos. in the figure correspond to the nos. in Table 2.

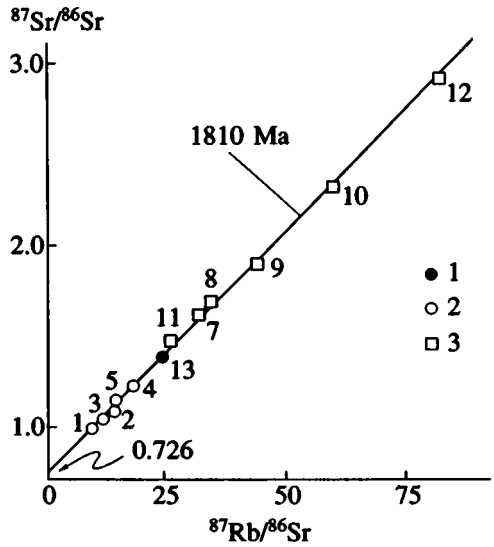

Fig. 4. Rb-Sr evolution diagram for the metasomatites from the Sannon block.

1 – microcline metasomatite with sillimanite, muscovite, and tourmaline; 2 – garnet–cordierite–biotite–tourmaline metasomatite; 3 – biotite–sillimanite augen schist. Sample nos. in the figure correspond to the nos. in Table 3. The sample point positions are given relative to the reference isochron with the age of 1810 Ma.

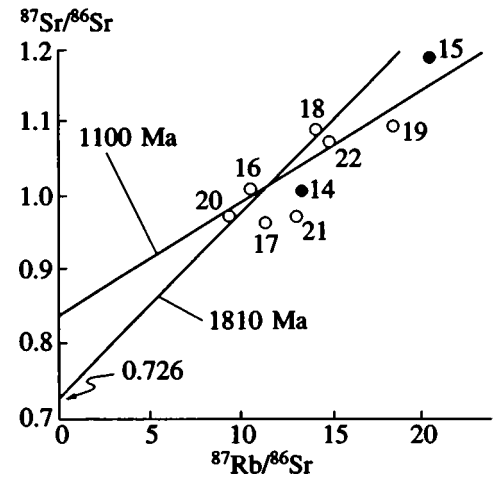

Fig. 5. Rb-Sr evolution diagram for the diaphtorites in the Sannon block.

Open circles are diaphtorites from the Hotchon village area, solid circles are diaphtorites from the Wondon River valley. Sample nos. in the figure correspond to the nos. in Table 3. The sample point positions are given relative to the reference isochrons with the ages of 1810 and 1100 Ma.

matite (samples 15-C-1 and 15-C-2) does, however, deserve attention. It can be seen in Fig. 4 that if a line with the same inclination equal to the inclination of the line for pegmatites intersects the ordinate axis at the point where $^{87}Sr/^{86}Sr = 0.726$, the points of all the rocks analyzed plot well along this line. This indicates that the metasomatic processes of the metamorphic retrograde stage were not too far removed in time from the terminal stage of pegmatite crystallization. Thus, the Rb-Sr data show that regional metamorphic processes within the Sannon area terminated close to 1810 Ma ago.

An attempt to date the superimposed retrograde metamorphism in the region under consideration was made in the Hotchon village area. Samples 1 - 1.5 kg in weight were collected across the strike of the rocks of the upper part of the Namdechon Formation (29-X series) from the road cut near the Mandok River, 1 km northwest of the Hotchon village, in an area 25 × 6 m. The rocks here are greenschist-facies diaphtorites after biotite–andalusite schist of the metamorphic staurolite zone. Diaphtorites compose an east-west striking stripe, about 10 km long and 1 - 2 km wide. The biotite–chlorite–sericite schist distributed there contains andalusite and staurolite relics. The greenschist-facies retrograde metamorphism of the Namdechon Formation rocks was, apparently, synchronous with the progressive metamorphism of the overlying upper Proterozoic sedimentary strata (Sangwon Group), which in this area consist mainly of quartzite and sericite–chloritoid schists.

In addition to the samples of the 29-X series, two samples of the Namdechon rocks, weighing about 10 kg each, were collected in the Wondon River valley, northwest of Tanchon. Samples 12-B-1b and 12-B-3b are retrogradely metamorphosed (greenschist facies) gneiss from the sillimanite metamorphic zone with a mineral paragenesis of quartz + potassium feldspar + biotite + garnet + cordierite + sillimanite + muscovite, also containing chlorite and sericite.

The Rb-Sr evolution diagram (Table 3, Fig. 5) demonstrates a considerable spread of points. Evidently, this is a result of the disturbance of the Rb-Sr systems somewhat later than when the timing of progressive metamorphism. As there is no linear arrangement of points in the diagram, it is impossible to determine the age of this process, but the points grouping near the reference isochron with an age of ca. 1100 Ma suggests that this value may be assumed to be the maximum age of the event, which resulted in the formation of low-temperature minerals when the Rb-Sr system components were redistributed. An incomplete homogenization of Sr isotopes is often observed in retrograde metamorphic processes when the geochronological sampling was beyond the zones of intense secondary schistosity, and the samples were collected in places situated several dozens of meters apart (Smalley *et al.*, 1983; Hickman and Glassley, 1984). The position of the points of samples 12-B-1b and 12-B-3b in Fig. 5 suggests that sillimanite–biotite gneiss from the Wondon River underwent a greenschist-facies retrograde metamorphism simultaneously with an andalusite–staurolite–biotite schist from the vicinity of the Hotchon village.

Thus, the data obtained indicate that the metamorphic events transforming the Machenrjon Group rocks within the Sannon block were separated by a time span of ca. 0.7 Ga.

Geochronology of the Kimchaek block granulites. The geochronological sampling was carried out near the Limdon village (North Hamgyong Province, Kilchu District), south of the Pkhosu phlogopite deposit. Various gneisses, marbles, and calciphyres of the Machenrjon Group lower unit (the Sondgey Formation) are exposed here. The rocks are migmatized and injected by leucocratic granite and pegmatite of the Rivon Complex.

The samples of migmatized biotite–garnet gneiss, sometimes containing sillimanite, were collected from an area 2 × 3 m in size; each sample weighed about 5 kg. At least two varieties of leucosome were noted in the sampled outcrop: one scattered lit-par-lit, thin, and discontinuous because of first-generation isoclinal folding, and another, thicker, forming branchy migmatites crumpled into second-generation folds. Both leucosome varieties are cut by leucocratic granite veins. The migmatite paleosome contains an association of garnet + biotite ± potassium feldspar + plagioclase + quartz (occasionally sillimanite). The secondary alterations are weak: plagioclase is inconsiderably sericitized, and sillimanite, possibly, is partially formed anew.

The *P–T*-parameters of metamorphism, determined in five studied migmatite samples, are within 750 - 800°C and 6.5 - 7.0 kbar (Glebovitsky *et al.*, in press), which corresponds to a granulite facies of moderate pressure. The migmatite chemical composition is rather monotonous, and the differences between the paleosomes and leucosomes are likewise insignificant. As the latter are enriched in garnet and impoverished in biotite, they contain more Fe and less K and Ti in comparison to the melanosomes, their silica contents being rather similar.

The points of four melanosomes, separated from samples 219-1, 219-2, 219-4, and 219-5 (Table 3), form a linear succession in the Rb-Sr evolution diagram (Fig. 6), though the points deviating from the approximating straight line somewhat exceed the experimental error (MSWD = 7.9). The errorchron inclination corresponds to the age of 1640 ± 200 Ma, with an initial $^{87}Sr/^{86}Sr$ = 0.724 + 0.014 (model 2, McIntyre *et al.*, 1966). The interpretation of this date depends on the process, which resulted in the last Sr isotopic equilibration in the analyzed rocks, and on its scale. The metamorphic event, which resulted in the biotite–garnet gneiss formation, and two subsequent migmatization stages with deformations corresponding to each of them, may be considered possible reasons for the equilibration.

It seems extremely unlikely that the age of 1640 ± 200 Ma corresponds to the premigmatite stage of rock formation, as the chemical composition of the analyzed melanosomes is not representative of garnet-biotite gneiss. Evidently, it should be the age of one of the migmatization stages, as the melanosomes became chemically separate at these stages in particular, and the Sr mobility was explained by the melt presence. Although the cases of isotopic disequilibrium between melanosomes and leucosomes are known (Grauert, 1974; Treloar and Kramers, 1989) and can be explained by a melt migration, most investigators determined that Sr isotopic exchange between melanosomes and leucosomes may be expected during the entire migmatization process (Pidgeon and Compston, 1965; Gorokhov *et al.*, 1970; Ferrara *et al.*, 1978; Skjernaa and Pedersen, 1982). The study of the Proterozoic migmatites in Southern Norway (Versteeve, 1975; Wielens *et al.*, 1980) showed that in such an exchange the Sr isotopic equilibration occurs on a scale from a few centimeters to a few meters.

The aforesaid suggests that the age of 1640 ± 200 Ma corresponds, most probably, to the final stage of ultrametamorphism, i.e., to the second migmatization stage,

Table 3. Analytical data on Rb-Sr for the metamorphic rocks from the Machenrjon belt

No.	Sample no.	Rb, ppm	Sr, ppm	$^{87}Rb/^{86}Sr$	$^{87}Sr/^{86}Sr$
Metasomatites from the Sannon block					
1	14-C-4	171	54	9.375	0.9740
2	14-C-6	211	49	14.01	1.0666
3	14-C-7	217	57	11.55	1.0299
4	14-C-8	262	45	18.05	1.2054
5	14-C-9	252	55	14.31	1.1273
6	16-C-2	200	24	44.05	1.8782
7	16-C-3	267	27	31.91	1.5958
8	16-C-3b	279	26	34.17	1.6666
9	16-C-7	251*	14.0*	59.93*	2.2906
10	16-C-8	284*	13.1*	73.78*	2.5311
11	16-C-11	309*	37.1*	25.90*	1.4474
12	16-C-15	220*	9.36*	82.61*	2.8798
13	35-C-2b	259	34	23.82	1.3757
Greenschist-facies diaphtorites from the Sannon block					
14	12-B-1b	257	60	13.05	1.0103
15	12-B-3b	274	43	20.21	1.1984
16	29-X-1	252	75	10.29	1.0101
17	29-X-7	274	71	11.20	0.9652
18	29-X-9	241	54	13.97	1.0935
19	29-X-10	252	45	18.20	1.1009
20	29-X-12	265	88	9.152	0.9745
21	29-X-13	269	95	12.88	0.9723
22	29-X-15	263	54	14.61	1.0863
Migmatites from the Kimchaek block					
23	219-1-M	203	113	5.526	0.8479
24	219-2-M	251	115	6.504	0.8799
25	219-4-M	172	108	4.748	0.8396
26	219-5-M	166	126	3.914	0.8154

* Analyzed using isotope dilution.

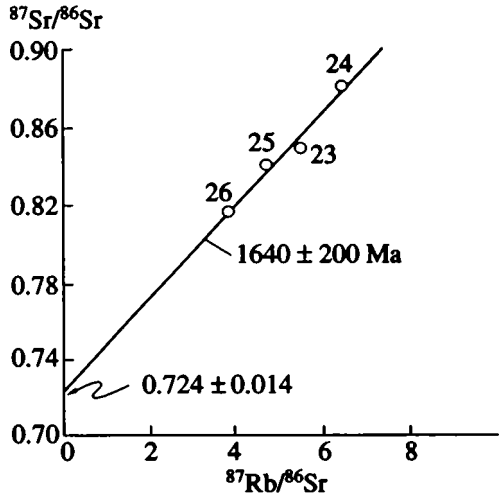

Fig. 6. Rb-Sr evolution diagram for the migmatized biotite-garnet gneisses from the Limdon village area.
Sample nos. in the figure correspond to the nos. in Table 3.

which occurs under conditions of the granulite facies. Within the experimental error, this value corresponds to the K-Ar and $^{40}Ar/^{39}Ar$ datings of phlogopite from the Pkhosu deposit (Marakushev *et al.*, 1966; Litsarev *et al.*, 1983), which gives us reason to suggest the time relation of phlogopite formation to the metamorphic processes dated in this study.

CHUNGSAN BELT

Geological setting. Precambrian rocks of the South China (Yangtze) craton basement are exposed in a number of tectonic uplifts; they compose both the intensely folded and highly metamorphosed pre-Riphean formations of the Chungsan belt and the gently dipping, weakly metamorphosed Riphean strata. A specific feature of the craton basement's geological history is its polymetamorphic nature, manifested in the early and late Proterozoic activations (Ren *et al.*, 1987). The largest tectonic uplifts exposing the basement are situated along the Yellow Sea coast. The rocks exposed in them are characterized by a low-gradient metamorphism and the formation of a kyanite–sillimanite facial series. The associations of tonalite and granite gneisses of a metamorphic amphibolite facies are predominant. The paragneiss complex of the Nampo uplift, bounded by the Taedong River mouth on the south and by the Haeju–Songnim–Katchkhon fault on the east is a peculiar exclusion. The rocks of the paragneiss complex crop out in the Nampo area. Aluminiferous gneisses and schists predominate among them, as well as amphibolites, carbonate rocks, and quartzites.

Metamorphism of the Nampo uplift. The metamorphic complex in this area underwent at least two stages of transformation: the early, of granulite and amphibolite facies, and the late, of amphibolite and greenschist facies.

The most high-temperature mineral association in the Nampo aluminiferous gneisses (granulites) consists of the paragenesis of garnet + cordierite + hypersthene + orthoclase + plagioclase + quartz. However, the parageneses of garnet + biotite + cordierite + orthoclase + quartz and garnet + hypersthene + biotite + orthoclase + quartz, characteristic of the medium-temperature subfacies of a granulite facies, are more widespread. The subsequent formation of schistosity resulted in associations of the low-temperature garnet–biotite–sillimanite–orthoclase subfacies, which are superimposed on the migmatites of granulite facies. Pegmatitic granite veins cut through all the generations of leucosomes. The next acid leaching processes caused the redistribution of biotite, garnet, and cordierite. The granulite metamorphism conditions in the Nampo area corresponded to T = 730 - 860°C and P = 6.0 - 7.2 kbar (Glebovitsky *et al.*, in press).

The subparallel zones of repeated schistosity with low-temperature associations of chlorite, muscovite, and brown-green biotite, replacing hypersthene, garnet, cordierite, and hornblende, developed in all the rocks, including pegmatite veins. This late stage of metamorphic alterations corresponded, probably, to the late Proterozoic activation of the South China craton basement.

Geochronology of the Nampo window rocks. Geochronological sampling was conducted 12 km from Nampo, in the area of the Sokhe dam (BK143 series), and 3 km to the east, in Vau Island (45-N series). The samples weighed 1 - 1.5 kg. Those of the BK143 series were collected in the bedrock outcrops in the floor of the channel under construction, for a distance of 0.5 to 0.6 km (BK143-2 and BK143-3), and in the small individual outcrops near the dam (BK143-5, BK143-6, BK143-7, and BK143-8). They are moderately and highly aluminiferous gneisses with parageneses of quartz + plagioclase + potassium feldspar + biotite + hypersthene + garnet + cordierite (samples BK143-2 and BK143-3), quartz + plagioclase + potassium feldspar + biotite + garnet + cordierite (sample BK143-5), and quartz + plagioclase + potassium feldspar + biotite + garnet + cordierite + sillimanite (sample BK143-8) (Table 4).

These samples, having no pronounced superimposed low-temperature alterations, contain a well preserved paragenesis of potassium feldspar with cordierite and hypersthene, which is critical for the granulite-facies zones. Only an insignificant chloritization of cordierite and garnet can be observed in some samples of the BK143 series. The most altered sample was the aluminiferous gneiss, not only chloritized but also sericitized (BK143-7), with an association of quartz + potassium feldspar + plagioclase + biotite + garnet + cordierite + sillimanite + muscovite + chlorite + sericite.

The samples collected in Vau Island (45-N series) from an outcrop about 70 m long have varying petrologic characteristics, differing from those of the aluminiferous gneisses of the BK143 series. Samples 45-N-3 and 45-N-9 are low-temperature gneisses with parageneses of quartz + plagioclase + biotite + muscovite +

chlorite + tourmaline (45-N-3) and quartz + plagioclase + muscovite + biotite (45-N-9). Geological observations in the outcrops unambiguously show their secondary blastomylonitic nature, and so they may have been formed either at the retrograde stage of granulite metamorphism or at the subsequent metamorphic cycle. On the other hand, samples 45-N-2 and 45-N-8 are the late metasomatic products of a superimposed schistosity (biotite–garnet blastomylonites).

Analytical data are presented in Table 4. In the Rb-Sr evolution diagram (Fig. 7), the points of six samples lie on the isochron with an age of 1970 ± 25 Ma, an initial $^{87}Sr/^{86}Sr$ ratio 0.7116 ± 0.0005, and MSWD = 1.0. In dating nonmigmatized rocks of the granulite facies, the restricted mobility of Sr and nearly unattainable homogenization of its isotopic composition in a dehydrated material should be taken into account (Gray and Compston, 1978). In some cases, especially for orthorocks, the Rb-Sr isochronous dates may be even regarded as the age of the protolith (Bingen *et al.*, 1990). However, most of the Rb-Sr isochrons for the rocks metamorphosed under conditions of a granulite facies were thought to determine the age of the corresponding metamorphic event (Versteeve, 1975; Clark and Schledewitz, 1988; Finn, 1989). Homogenization of the Sr isotopic composition is more probable for silicic granulites, which are the metamorphic products of volcano-sedimentary rocks (Iyer *et al.*, 1976). In this case, homogenization may be reached not only within individual outcrops (Versteeve, 1975; Gray and Compston, 1978), but sometimes on a wider scale (Pidgeon, 1967; Gorokhov *et al.*, 1976).

The good linear arrangement of the points of six paragneiss samples from the Nampo area in the Rb-Sr evolution diagram (Fig. 7) testifies to the Sr isotopic equilibration in these rocks 1970 ± 25 Ma ago. The process that resulted in this equilibration, was, evidently, regional metamorphism, as the preservation of premetamorphic Rb-Sr systems in the small samples of metasedimentary rocks can hardly be expected under conditions accompanying the complete transformation of mineral associations. The parameters of metamorphism (sample BK143-2) were estimated to be T = 800 - 850°C and P = 6.9 - 7.2 kbar (Glebovitsky *et al.*, in press). It should be noted that the homogenization of the Sr isotopic composition in the rocks situated hundreds of meters and several kilometers apart does not require a real mobilization of the rock substance over such distances. If the entire volume of protolith can be divided into a number of evenly distributed representative subvolumes, each with the same Rb/Sr ratio, corresponding to the average ratio in the entire protolith, then, as the radiogenic ^{87}Sr accumulates, these subvolumes will have similar $^{87}Sr/^{86}Sr$ mean values. And so, in order to obtain the homogeneous $^{87}Sr/^{86}Sr$ ratio of the entire rock mass over the course of metamorphism, the Sr isotopic equilibration only within the subvolumes is sufficient (Krogh and Hurley, 1968; Roddick and Compston, 1977). This case creates the impression of a regional homogenization, which requires that the Sr migrate for many kilometers, but in fact the physical equilibration is restricted to the only subvolume size. This mechanism is very effective in bedded sediments and volcanic rocks.

Table 4. Analytical data on Rb-Sr for the metamorphic rocks from the Chungsan belt

No.	Sample no.	Rb, ppm	Sr, ppm	$^{87}Rb/^{86}Sr$	$^{87}Sr/^{86}Sr$
1	45-N-2	77	257	0.8711	0.7495
2	45-N-3	18	125	0.4265	0.7236
3	45-N-8	159	178	2.652	0.7722
4	45-N-9	188	188	2.930	0.7936
5	45-N-10	143	254	1.656	0.7614
6	45-N-13	136	38	11.41	0.8700
7	BK143-2	88	160	1.552	0.7558
8	BK143-3	97	168	1.772	0.7615
9	BK143-5	96	132	2.149	0.7742
10	BK143-6	145	112	3.800	0.7951
11	BK143-7	121	115	3.203	0.7799
12	BK143-8	103	147	1.992	0.7675

It should be noted that, along with samples BK143-2, BK143-3, BK143-5, and BK143-8, which undoubtedly correspond to the metamorphism of granulite facies, two samples with low-temperature mineral association (45-N-3 and 45-N-9) also plot onto the isochron, having an age of 1970 ± 25 Ma. Therefore, these mineral parageneses seem to correspond to the retrograde stages of granulite metamorphism, which were not too far away in time from its culmination, rather than to a later superimposed metamorphic event. In this case, the value of 1970 ± 25 Ma may be interpreted as the minimum age of the metamorphism under conditions of granulite facies. The rather high value of the initial $^{87}Sr/^{86}Sr$ ratio (0.7116 ± 0.0005) characterizes the crustal prehistory of sedimentary protoliths.

The points of the other six paragneiss samples do not lie on this isochron, forming a clearly pronounced tendency towards linear arrangement with considerably less inclination, corresponding to the age of ca. 900 Ma. Both the samples which were clearly affected by the low-temperature greenschist metamorphism (45-N-2, 45-N-8, and BK143-7) and those with the high-temperature mineral parageneses (BK143-6 and 45-N-13) correspond to this "secondary" line. The disturbance of Rb-Sr systems by retrograde metamorphic transformations of highly metamorphosed rocks was observed earlier (Black *et al.*, 1979; Field and Råheim, 1979, 1980; Gorokhov *et al.*, 1981; Smalley *et al.*, 1983; Black, 1988; Finn, 1989). In such a case, a partial or even complete Sr isotopic equilibration may occur, especially within individual outcrops. The resetting of Rb-Sr systems is facilitated considerably by the accompanying deformation, which opens the way for the migration of solutions, transferring, among other components, Sr (Black *et al.*, 1979; Gorokhov *et al.*,

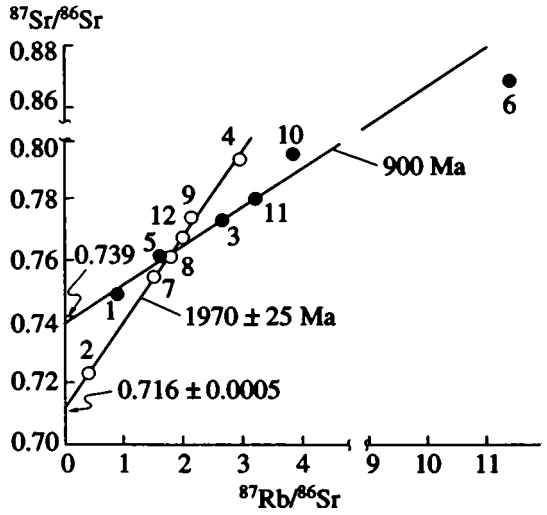

Fig. 7. Rb-Sr evolution diagram for the aluminiferous gneisses from the Nampo tectonic window.

Open circles are points of the samples for which the isochron with the age of 1970 ± 25 Ma was calculated, solid circles are sample points grouping along the reference isochron with the age of 900 Ma. Sample nos. in the figure correspond to the nos. in Table 4.

1981; Black, 1988). However, there are cases when such a resetting occurs without any obvious structural (Finn, 1989) or mineral (Black, 1988) transformations. The degree of disturbance of the Rb-Sr systems may depend on the Rb/Sr value in the sample (the presence or absence of strontium-containing mineral-acceptors that are the traps for the migrating radiogenic ^{87}Sr) (Bell and Blenkinsop, 1978; Smalley *et al.*, 1983). This explains a substantial disturbance of the Rb-Sr system in sample 45-N-13, which is characterized by a high Rb/Sr ratio and a low Sr content. Thus, the appearance of the linear dependence with an age of ca. 900 Ma (Fig. 7) can most likely be explained by low-temperature greenschist-facies metamorphism during the late Proterozoic activation of the South China craton basement.

The resetting of Rb-Sr systems throughout the paragneiss complex at the level of the whole-rock samples, resulting in the secondary isochron relations, can be considered in terms of either open or closed systems. The supply of Sr and Rb from the outside, or their loss in the course of superimposed metamorphism is, apparently, implied in the case of an open system. The closed system requires that the homogenization of the Sr isotopic composition take place in a considerable volume of rock (e.g., within the entire complex as a lithostructural unit) without an addition or loss of Rb and Sr. In such a system, the secondary isochron corresponds to the age of the superimposed metamorphism and intersects the ordinate at the point whose position is the function of the average Rb/Sr value in the rocks and the age difference between primary and superimposed metamorphic events. As was said above, the mechanism of the Sr isotopic homogenization does not require that Sr migrate a considerable distance.

The data available suggest that in the course of superimposed low-temperature metamorphism the rocks in the scale of the entire sampled paragneiss complex remained closed geochemical systems, at least with respect to Rb and Sr. In fact, using the mean Rb and Sr contents in the paragneiss samples, defining the isochron with an age of 1970 ± 25 Ma and an initial $^{87}Sr/^{86}Sr$ = 0.7116, the mean $^{87}Sr/^{86}Sr$ ratio in these rocks during the secondary Sr isotopic equilibration, about 900 Ma ago, can be calculated. The calculated ratio of 0.740 coincides well with the value determined by the intersection of the secondary isochron with the ordinate (Fig. 7) and confirms the absence of any noticeable supply or loss of Rb and Sr about 900 Ma ago for the entire sampled volume of paragneisses. Actually, the isochron with the age of 1970 Ma seems to be "turned" relative to its center of gravity. A similar situation was observed in the retrograde transformations of magmatic and metamorphic rocks in Southern Norway and Northern Wales (Smalley *et al.*, 1983; Evans, 1991).

Existence of a closed Rb-Sr system in the paragneiss complex during the superimposed metamorphism means that the process went on under conditions of a low water to rock ratio, i.e., with a rather small content of fluid phase. The same is indicated by the presence of inequilibrated mineral associations. Hence, it follows either that the retrograde transformations were induced by the mobilization of small amounts of H_2O and CO_2 contained in highly metamorphosed rocks and dissolved, for example, in quartz (Spear and Selverstone, 1983), or that they occurred with the absorbtion of a restricted amount of fluid with low Rb and Sr contents by dehydrated rocks from outside sources (Morrison and Valley, 1991). Taking into account the low-temperature metamorphic associations being confined to the zones of secondary schistosity, which facilitated the supply of the fluid from without, the second possibility seems more probable.

CONCLUSION

The work carried out demonstrates that the geologic history of the North Korean early Proterozoic complexes was lengthy and complicated.

The main metamorphic events occurred during the time interval of 1.7 - 2.0 Ga ago within the simultaneously evolving Machenrjon and Chungsan belts, which surrounded the Nangnim granulite block and differ substantially in their thermodynamic regimes of metamorphism. A noticeable discrepancy in ages calculated for them attracts attention. The high-temperature and high-pressure metamorphism in the Chungsan belt (granulite facies) was manifested no later than 1970 Ma ago, whereas the metasomatism directly following the regional metamorphism in the Machenrjon belt in the highest temperature zone was 1810 Ma old. The migmatites of the granulite facies in the Kimchaek block proved to be even younger. These data may tes-

tify to the true asynchronous nature of the studied metamorphic belts.

The low-temperature superimposed retrograde metamorphism, pronounced within the entire region under study, cannot be reliably dated, though, using the results obtained, one may suggest that its probable age is 0.8 - 1.0 Ga. Apparently, the retrograde metamorphism was manifested simultaneously and was related to the progressive metamorphism of the overlying Riphean strata.

REFERENCES

Bell, K. and Blenkinsop, J., Reset Rb/Sr Whole-Rock Systems and Chemical Control, *Nature*, 1978, vol. 273, no. 5663, pp. 532 - 534.

Bingen, B., Demaiffe, D., and Hertogen, J., Evolution of Feldspars at the Amphibolite–Granulite Facies Transition in Augen Gneisses (SW Norway): Geochemistry and Sr-Isotopes, *Contrib. Mineral. and Petrol.*, 1990, vol. 105, no. 3, pp. 275 - 288.

Black, L.P., Isotopic Resetting of U-Pb Zircon and Rb-Sr and Sm-Nd Whole-Rock Systems in Enderby Land, Antarctica: Implications for the Interpretation of Isotopic Data from Polymetamorphic and Multiply Deformed Terrains, *Precambrian Res.*, 1988, vol. 38, no. 4, pp. 355 - 365.

Black, L.P., Bell, T.H., Rubenach, M.J., and Withnall, I.W., Geochronology of Discrete Structural-Metamorphic Events in a Multiply Deformed Precambrian Terrain, *Tectonophysics*, 1979, vol. 54, no. 1/2, pp. 103 - 137.

Brookins, D.G., Fairbairn, H.W., Hurley, P.M., and Pinson, W.H., A Rb-Sr Geochronologic Study of the Pegmatites of the Middletown Area, Connecticut, *Contrib. Mineral. and Petrol.*, 1969, vol. 22, no. 2, pp. 157 - 168.

Clark, G.S. and Schledewitz, D.C.P., Rubidium–Strontium Ages of Archean and Proterozoic Rocks in the Nejanilini and Great Island Domains: Churchill Province, Northern Manitoba, Canada, *Can. J. Earth Sci.*, 1988, vol. 25, no. 2, pp. 246 - 254.

Evans, J.A., Resetting of Rb-Sr Whole-Rock Ages during Acadian Low-Grade Metamorphism in North Wales, *J. Geol. Soc. London*, 1991, vol. 148, no. 4, pp. 703 - 710.

Ferrara, G., Ricci, C.A., and Rita, F., Isotopic Ages and Tectono-Metamorphic History of the Metamorphic Basement of North-Eastern Sardinia, *Contrib. Mineral. and Petrol.*, 1978, vol. 68, no. 1, pp. 99 - 106.

Field, D., and Råheim, A., Rb-Sr Total Rock Isotope Studies on Precambrian Charnockitic Gneisses from South Norway: Evidence for Isochron Resetting during a Low-Grade Metamorphic-Deformational Event, *Earth Planet. Sci. Lett.*, 1979, vol. 45, no. 1, pp. 32 - 44.

Field, D. and Råheim, A., Secondary Geologically Meaningless Rb-Sr Isochrons, Low $^{87}Sr/^{86}Sr$ Initial Ratios and Crustal Residence Times of High-Grade Gneisses, *Lithos*, 1980, vol. 13, no. 4, pp. 295 - 304.

Finn, G.C., Rb-Sr Geochronology of the Archean Maggo Gneiss from the Hopedale Block, Nain Province, Labrador, *Can. J. Earth Sci.*, 1989, vol. 26, no. 12, pp. 2512 - 2522.

Geologiya Korei (Geology of Korea), Masaitis, V.L., Ed., Moscow: Nedra, 1964.

Glebovitsky, V.A., Tsoi, V.-Ch., Bushmin, S.A., Buyiko, A.K., Vapnik, E.A., Kim, R.-S., Kim, C.-A., and Sedova, I.S., Facies of Metamorphism and Metamorphic Evolution of Precambrian Complexes of North Korea, *J. Geol. Soc. Korea*, (in press).

Gorokhov, I.M., Varshavskaya, E.S., Kutyavin, E.P., and Lobach-Zhuchenko, S.B., Preliminary Rb-Sr Geochronology of the North Ladoga Region, Soviet Karelia, *Eclogae Geol. Helv.*, 1970, vol. 63, no. 1, pp. 95 - 104.

Gorokhov, I.M., Krylov, I.N., Baikova, V.S., *et al.*, Geochronological Study of the Kola Group Polymetamorphic Rock Complex, *Razvitie i Primenenie Metodov Yadernoi Geokhronologii* (Development and Application of the Nuclear Geochronology Technique), Leningrad: Nauka, 1976, pp. 177 - 192.

Gorokhov, I.M., Duk, V.L., Kitsul, V.I., *et al.*, Rb-Sr Systems of the Polymetamorphic Complexes in the Central Part of the Aldan Crystalline Massif, *Izv. Akad. Nauk SSSR, Ser. Geol.*, 1981, no. 8, pp. 5 - 17.

Gorokhov, I.M., Kutyavin, E.P., Volodichev, O.A., *et al.*, Rb-Sr Age of Magmatic and Metamorphic Rocks of the White Sea Complex (Western White Sea Region), *Sov. Geol.*, 1981, no. 3, pp. 67 - 75.

Grauert, B., Rb-Sr Isotopic Study on Whole Rocks and Minerals from the Baltimore Gneiss of the Phoenix Dome, Baltimore County, Maryland, *Carnegie Inst. Wash. Year Book*, 1974, vol. 73, pp. 1003 - 1007.

Gray, C.M. and Compston, W., A Rubidium-Strontium Chronology of the Metamorphism and Prehistory of Central Australian Granulites, *Geochim. Cosmochim. Acta*, 1978, vol. 42, no. 11, pp. 1735 - 1747.

Hickman, M.H. and Glassley, W.E., The Role of Metamorphic Fluid Transport in the Rb-Sr Isotopic Resetting of Shear Zones: Evidence from Nordre Strømfjord, West Greenland, *Contrib. Mineral. and Petrol.*, 1984, vol. 87, no. 3, pp. 265 - 281.

Iyer, S.S., Woodford, P.J., and Wilson, A.F., Rb-Sr Isotopic Studies of a Polymetamorphic Granulite Terrane, Strangways Range, Central Australia, *Lithos*, 1976, vol. 9, no. 3, pp. 211 - 224.

Krogh, T.E. and Hurley, P.M., Strontium Isotope Variation and Whole-Rock Isochron Studies, Grenville Province of Ontario, *J. Geophys. Res.*, 1968, vol. 73, no. 22, pp. 7107 - 7125.

Kropotkin, P.N., Absolute Age of Some Granites in Korea, *Izv. Akad. Nauk SSSR, Ser. Geol.*, 1969, no. 6, pp. 115 - 117.

Krylov, I.N., Application of the X-Ray Fluorescence Analysis for the Exact Quantitative Determination of the Rb/Sr in Isochron Dating, *Izotopnye Metody Izmereniya Vozrasta v Geologii* (Isotope Methods of Age Measuring in Geology), Moscow: Nauka, 1979, pp. 125 - 131.

Litsarev, M.A., Arakelyants, M.M., and Ivanenko, V.V., Application of the ^{39}Ar-^{40}Ar and K-Ar Methods for Determining the Phlogopite Formation Age (with Reference to a Deposit in the Democratic People's Republic of Korea), *Mass-Spektrometriya i Izotopnaya Geologiya* (Mass-Spectrometry and Isotopic Geology), Moscow: Nauka, 1983, pp. 125 - 137.

McIntyre, G.A., Brooks, C., Compston, W., and Turek, A., The Statistical Assessment of Rb-Sr Isochrons, *J. Geophys. Res.*, 1966, vol. 71, no. 22, pp. 5459 - 5468.

Marakushev, A.A., Kim Hak Jeh, Kim Hensyu, and Mishkin, M.A., Precambrian Metamorphic Complexes in Northeastern Korea and Southwestern Primor'e and Mineral Resources Related to Them, *Geologicheskoe Stroenie Severo-Vostochnoi Korei i Yuga Primor'ya* (Geological Structures of Northeastern Korea and Southern Primor'e), Moscow: Nauka, 1966, pp. 9 - 123.

Morrison, J. and Valley, J.W., Retrograde Fluids in Granulites: Stable Isotope Evidence of Fluid Migration, *J. Geol.*, 1991, vol. 99, no. 4, pp. 559 - 570.

Pidgeon, R.T., A Rubidium-Strontium Geochronological Study of the Willyama Complex, Broken Hill, Australia, *J. Petrol.*, 1967, vol. 8, no. 2, pp. 283 - 324.

Pidgeon, R.T. and Compston, W., The Age and Origin of the Cooma Granite and Its Associated Metamorphic Zones, New South Wales, *J. Petrol.*, 1965, vol. 6, no. 2, pp. 193 - 222.

Polevaya, N.I., Putintsev, V.K., and Sprintsson, V.D., Absolute Age of Some Magmatic and Metamorphic Rocks in North Korea, *Sov. Geol.*, 1961, no. 6, pp. 119 - 124.

Ren, T., Tiang, C., Zhang, Z., and Qin, D., *Geotectonic Evolution of China*, Beijing: Science, 1987.

Riley, G.H., Isotopic Discrepancies in Zoned Pegmatites, Black Hills, South Dakota, *Geochim. Cosmochim. Acta*, 1970, vol. 34, no. 6, pp. 713 - 725.

Roddick, J.C. and Compston, W., Strontium Isotopic Equilibration: A Solution to a Paradox, *Earth Planet. Sci. Lett.*, 1977, vol. 34, no. 2, pp. 238 - 246.

Shukolyukov, Yu.A., Gorokhov, I.M., and Levchenkov, O.A., *Graficheskie Metody Izotopnoi Geologii* (Graphic Methods of Isotope Geology), Moscow: Nedra, 1974.

Skjernaa, L. and Pedersen, S., The Effect of Penetrative Sveconorwegian Deformations on Rb-Sr Isotope Systems in the Römskog-Aurskog Höland Area, SE Norway, *Precambrian Res.*, 1982, vol. 17, no. 3/4, pp. 215 - 243.

Smalley, P.C., Field, D., and Råheim, A., Resetting of Rb-Sr Whole-Rock Isochrons during Sveconorwegian Low-Grade Events in the Gjerstad Augen Gneiss, Telemark, Southern Norway, *Chem. Geol.*, 1983, vol. 41, no. 3, pp. 269 - 282.

Spear, F.S. and Selverstone, J., Water Exsolution from Quartz: Implications for the Generation of Retrograde Metamorphic Fluids, *Geology*, 1983, vol. 11, no. 2, pp. 82 - 85.

Treloar, P.J. and Kramers, J.D., Metamorphism and Geochronology of Granulites and Migmatitic Granulites from the Magondi Mobile Belt, Zimbabwe, *Precambrian Res.*, 1989, vol. 45, no. 4, pp. 277 - 289.

Varshavskaya, E.S., Gorokhov, I.M., Krylov, I.N., *et al.*, Methods of Rubidium and Strontium Determination for Geochronological Investigations, *Sostoyanie Metodicheskikh Issledovanii v Oblasti Absolyutnoi Geokhronologii* (The State of Methodological Investigations in Absolute Geochronology), Moscow: Nauka, 1975, pp. 30 - 36.

Versteeve, A.J., Isotope Geochronology in the High-Grade Metamorphic Precambrian of Southwestern Norway, *Nor. Geol. Unders.*, 1975, no. 318, pp. 1 - 50.

Wielens, J.B.W., Andriessen, P.A.M., Boelrijk, N.A.I.M., Hebeda, E.H., Priem, H.N.A., Verdurmen, E.A.Th., and Verschure, R.H., Isotope Geochronology in the High-Grade Metamorphic Precambrian of Southwestern Norway: New Data and Reinterpretations, *Nor. Geol. Unders.*, 1980, no. 359, pp. 1 - 30.

Yanagi, T. and Yamaguchi, M., Ages of Some Precambrian Metamorphic Rocks in North China, *Mem. Fac. Sci. Kyushu Univ.*, 1970, vol. D20, no. 2, pp. 177 - 189.

Yashchenko, M.L., Varshavskaya, E.S., and Gorokhov, I.M., On the Anomalous Isotopic Composition of Strontium in Minerals from Metamorphosed Rocks, *Geokhimiya*, 1961, no. 5, pp. 420 - 425.

Zhang, Q., General Features of the Early Precambrian Geology and Metallogeny of Liaodong Peninsula, *Field Excursion Guidebook on the Ore Deposition Liaodong Peninsula, Int. Symp. on Metallogeny of the Early Precambrian*, Changchung, China, 1985, pp. 1 - 9.

Zhang, Q., Early Proterozoic Tectonic Styles and Associated Mineral Deposits of the North China Platform, *Precambrian Res.*, 1988, vol. 39, no. 1/2, pp. 1 - 29.

Stratigraphy and Geological Correlation, Vol. 2, No. 1, 1994, pp. 19 - 33. Translated from Stratigrafiya. Geologicheskaya Korrelyatsiya, Vol. 2, No. 1, 1994, pp. 23 - 38.
Original Russian Text Copyright © 1994 by Sergeev, Knoll, Kolosova, Kolosov.
English Translation Copyright © 1994 by Interperiodica Publishing (Russia).

Microfossils in Cherts from the Mesoproterozoic (Middle Riphean) Debengda Formation, the Olenek Uplift, Northeastern Siberia

V. N. Sergeev*, A. H. Knoll, S. P. Kolosova***, and P. N. Kolosov*****

**Geological Institute, Russian Academy of Sciences, Pyzhevskii per. 7, Moscow, 109017 Russia*
***Harvard University, Cambridge, Oxford St. 26, Massachusetts, 02138 USA*
****Institute of Geology, Yakut Scientific Center, Russian Academy of Sciences, pr. Lenina 31, Yakutsk, 677891 Russia*

Received March 10, 1993

Abstract – Silicified shallow-water marine carbonate deposits of the Proterozoic Debengda Formation (the Olenek Uplift, northeastern Siberia) contain well preserved microfossils. One of two distinct assemblages consists only of filamentous *Siphonophycus* microfossils, which are presumably the extracellular sheaths of hormogonium cyanobacteria. The other is dominated by coccoidal microfossils, first by the entophysalidacean cyanobacterium *Eoentophysalis*. The coccoidal assemblage was recognized in the layered carbonate precipitate structures of a superficially stromatolite appearance. Despite its simple composition, the microfossil assemblage supports the generally accepted Mesoproterozoic (middle Riphean) age of the Debengda Formation. This conclusion corresponds to the available data on isotopic geochronology, and to the composition of columnar stromatolites from the Debengda Formation. Both the structural features and carbon isotopic composition of its rocks are comparable to those of rocks of known Mesoproterozoic age, but differ from the characteristics of definitely Neoproterozoic deposits.

INTRODUCTION

Microfossils preserved in cherts allow us to form a representation of those living organisms that existed prior to the appearance of multicellular animals. In many Proterozoic sedimentary sequences, the silicified microfossils are abundant, diverse, and well preserved. Despite the wide range of this record, the silicified microfossils are still generally considered to be inadequate for biostratigraphic correlation. Acritarchs definitely useful for biostratigraphy are sometimes preserved in cherts of subtidal facies (Knoll, 1984, 1992; Awramik *et al.*, 1985; Sergeev, 1992; and others), but most Proterozoic cherts contain the remnants of evolutionary conservative prokaryotic microorganisms that lived in isolated peritidal environments (Knoll, 1985).

In this paper, we will argue that even silicified prokaryotic assemblages inhabiting restricted shallow-water settings can provide useful biostratigraphic information. This is possible because modern or ancient cyanobacteria and other prokaryotes are ecologically dependent, and their individual species have particular places of residence (see Knoll and Bauld, 1989 for a comprehensive discussion of the problem). Therefore, simultaneous with the change in coastal environments, there were transformations in the prokaryotic assemblages characteristic of this setting.

To illustrate this regularity, a new microbiota from the Debengda Formation of the Olenek Uplift, northeastern Siberia, is described below. The Debengda microfossils comprise two distinct assemblages that inhabited different ecological niches on a tidal flat. Most of the recovered taxa have wide stratigraphic ranges, which came into being as early as the Paleoproterozoic. Still, the Debengda microfossils have, in general, an evident Mesoproterozoic character. This corresponds to previous data on the middle Riphean age of the formation based upon stromatolites (Komar, 1966; Semikhatov and Serebryakov, 1983; Semikhatov, 1991). Its carbonate rock structures and data on its carbon isotopic composition are also characteristic of the Mesoproterozoic deposits.

GEOLOGY AND AGE OF THE DEBENGDA FORMATION

The Olenek uplift is in the northeastern part of the Anabar anteclise of the Siberian Platform (Fig. 1). The uplift, about 150 km across, is nearly isometric in shape. The Proterozoic (Riphean and Vendian) sedimentary rocks crop out in the central part of the structure, and are overlain by Paleozoic and Mesozoic rocks on the limbs.

The fossiliferous Debengda Formation occurs in the upper part of the Solooli Group section, which consists of an unmetamorphosed sedimentary sequence widespread throughout the Olenek uplift.

As much as 1500 m thick, the Solooli Group includes quartz sandstone, shale, and carbonate rocks and is subdivided into five units (from the base upwards): the Sygynakhtakh, Kyutingda, Arymas, Debengda, and Khaipakh formations (Komar, 1966; Semikhatov and Serebryakov, 1983; Semikhatov, 1976;

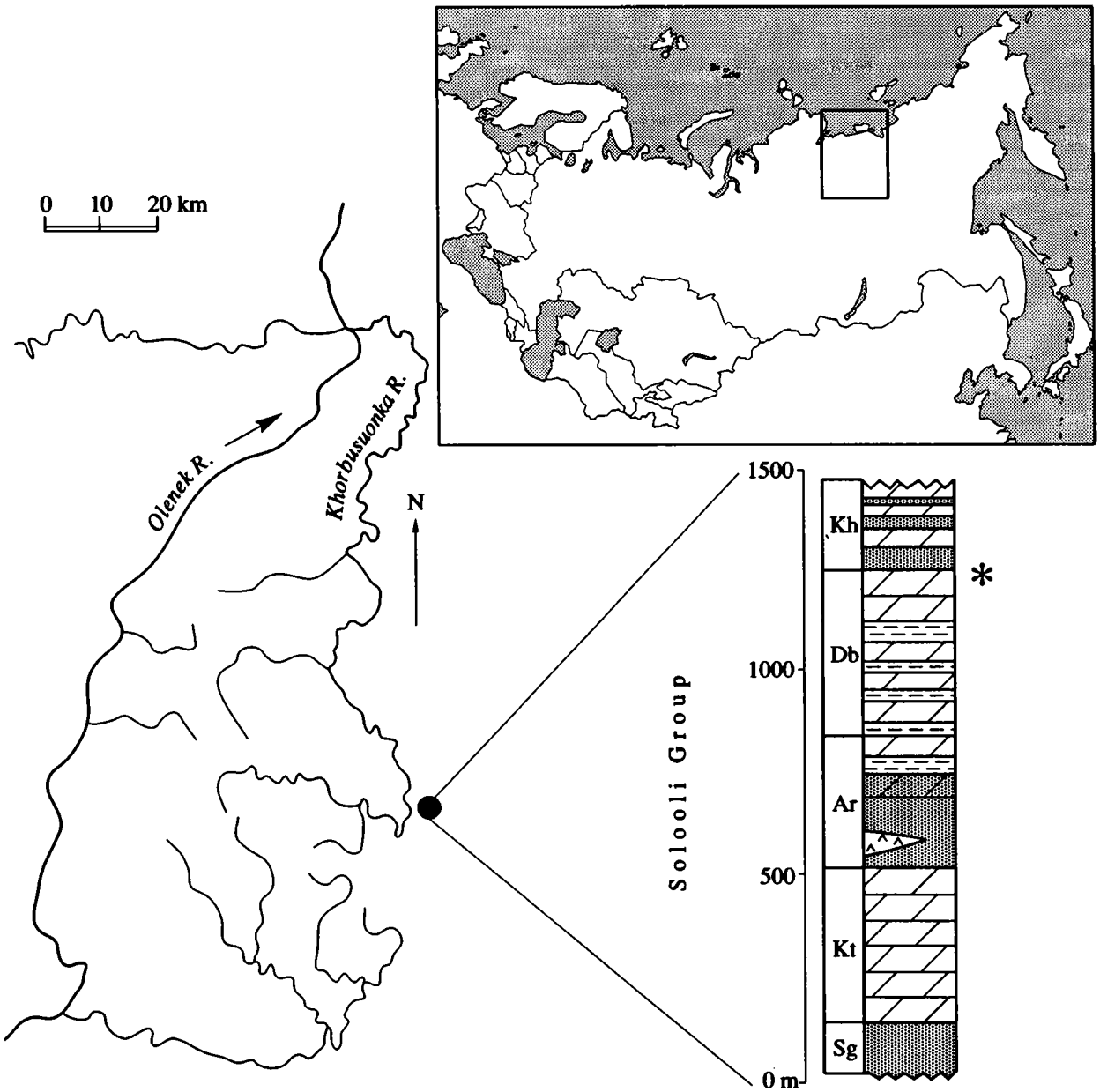

Fig. 1. Locality map and schematic stratigraphic column of the Solooli Group, the Olenek uplift, northeastern Siberia (modified after Semikhatov and Serebryakov, 1983).

The stratigraphic position of microfossils described in the text (samples 1-91 - 4-91, KG-91-11, and 1763) is marked by the asterisk. Abbreviations of the formation names: Sg – Sygynakhtakh, Kt – Kyutingda, Ar – Arymas, Db – Debengda, and Kh – Khaipakh.

Shpunt *et al.*, 1979). The group unconformably overlies the Archean, or Paleoproterozoic metamorphic rocks of the Eekit Group. It is discordantly overlain by the Vendian deposits of the Maastakh Formation of the Khorbusuonka Group.

The Debengda Formation lies conformably over the Arymas Formation, and is overlain, again conformably, by the Khaipakh Formation. The unit is subdivided into five subformations[1]. Two of them (the first and third) consist predominantly of sandstones alternating with siltstones and claystones. The second and fourth subformations are mostly composed of stromatolite limestones with sandstone and siltstone interbeds. The fifth consists of stromatolitic dolomite with lenses and interlayers of black cherts (mostly near the top of the unit), and thin siltstone interbeds. The total thickness of the Debengda Formation is between 470 and 520 m, and its fifth unit is 140 - 150 m thick (Shenfil', 1991).

Cherts bearing microfossils were sampled from an outcrop situated on the northern valley side of the Atyrdzhakh Creek (a small tributary of the Khorbusuonka River), about 1 km upstream of its mouth (Fig. 1).

[1] There are several approaches to the stratigraphic subdivision of the Debengda Formation. For example, Komar (1966) divided the formation into three units. Here, we follow the Shenfil's subdivision into five subformations (Shenfil' *et al.*, 1988; Shenfil', 1991).

At this locality, the uppermost 15 m of the fifth unit of the Debengda Formation is discordantly overlain by the arkose granular gravelstones and conglomerates of the basal beds of the Maastakh Formation. Near the Atyrdzhakh Creek mouth, these beds completely truncate the underlying Khaipakh Formation. The gray dolomite member with an orange-colored weathered surface is about 3 m below the top of the Debengda Formation being underlain by the fine siltstone and claystone; the upper portion of the formation is not exposed. The dolomite member consists of beds 1 to 10 cm thick, some of which are flaggy. The dolosiltite and dolarenite beds show rare desiccation cracks and ripples with an amplitude of 2 - 4 mm, and crest intervals of about 1 cm. These rocks alternate with dolomite showing laminae of a mm-scale. A finelly laminated chert bed is about 10 - 15 cm thick, and its abundant voids are filled with light-colored silica. The thin sections of the chert reveal its stromatolite origin. It is apparent that the lamination is formed by mats consisting of filamentous cyanobacteria (*Siphonophycus* spp.). The voids appear to be original features, which appeared as a result of gas bubbles produced by microbial decay and later filled by early diagenetic chalcedony. Their linear distribution seems to result from the laminated structure of mats formed by filamentous cyanobacteria. Even though some parts of the samples lack preserved microfossils because of their decay, the mats show a peculiar fabric produced by wavy, 300 - 500 μm thick laminae, which bend sinusoidally over the former voids. Any traces of the original carbonate fabric preceding the silicification are absent, though late diagenetic rhombohedrons of dolomite occur quite often (Plate III, Fig. 1).

The next member of silicified carbonate is about 5 m below in the sequence. These cherts are petrographically distinct from those described above. Their flat laminae and minute nodules (up to a few hundred microns thick) contain abundant dolomite rhombohedrons. The silicified rock parts have a persistent microlamination with a lamina thickness of 2 μm on average (Plate III, Fig. 5). These fabrics are almost fossil-free; instead the microfossils occur in amorphous patches between them (Plate III, Fig. 5). These are mostly the coccoidal forms, primarily *Eoentophysalis* spp. There are also rare intercalated mats of filamentous *Siphonophycus*, which indicate the paleoecological proximity of both facies dominated by different assemblages of microorganisms.

In colonies of *Eoentophysalis dismallakesensis*, as is common among forms of this genus, interior cells are absent. It is noteworthy that the cell disappearance is the result of neither colony compression nor destruction. It resulted rather from cell decay, when the voids left were later filled by diagenetic silica (Plate II, Fig. 3). This could occur only if the enclosing sediments were lithified prior to the cell decay. This feature of the *Eoentophysalis* colonies along with the layered fabric of surrounding sediments indicates the rapid process of carbonate precipitation and lithification in these facies. Yakshin (1990) recognized similar features in the underlying Kyutingda Formation, and interpreted them as stromatolites formed by cyanobacteria of the *Eoentophysalis* genus. However, *Eoentophysalis* could not have built these flat or domed structures, since they do not occur here; these structures are most probably of nonstromatolite origin. It is likely that, to a certain degree, the carbonate precipitation was the result of bacteria metabolism. But the cyanobacterial mats were definitely not a part of the process forming the above sedimentary structures.

The age of the Solooli Group is poorly constrained by radiometric data. Most determinations were made more than 25 years ago by the K-Ar method using insufficiently studied layered silicates from the glauconite group; they need the legitimacy of modern analytical techniques (*Resheniya* ..., 1993; Bibikova *et al.*, 1989). The early data on the Debengda Formation age is within the range of 1120 - 1040 Ma (Kazakov *et al.*, 1965). Data on the second unit of the Debengda Formation obtained recently by the isochronous Rb-Sr and K-Ar methods determines the age of its Al-glanconite as 1245 and 1265 Ma, respectively (Gorokhov *et al.*, 1992), confirming thus the middle Riphean age of the deposits.

Stromatolites of the Debengda Formation are represented mainly by endemic forms including *Colonnella cormosa* Kom., *Anabaria radialis* Kom., *Conophyton garganicum* Kor., *C. lituum* Masl., *C. metula* Kirich, and *Gongylina zonata* Kom. Most researchers believe that this assemblage is characteristic of the middle Riphean (Mesoproterozoic) age (Komar, 1966; Semikhatov and Serebryakov, 1983; Semikhatov, 1976, 1991). In fact, these taxa allow us to correlate sequences of the North Siberia province, yet the assemblage differs from those of the middle-upper Riphean stratotypes in the southern Urals and central and southern Siberia (Semikhatov, 1991). Some researchers suggest that the Debengda and overlying Khaipakh formations are late Riphean in age (Shenfil', 1991). But when evaluating this idea one should keep in mind that it is based upon the local "Siberian" opinion on the boundary position between the middle and late Riphean, which does not correspond to the boundary level adopted in the standard scale of the Precambrian in Russia (Semikhatov *et al.*, 1991). Below, we will consider the paleontological data that, in our opinion, favors the middle Riphean (Mesoproterozoic) age of the Debengda Formation.

Materials for this study were mainly collected by A.H. Knoll, J.P. Grotzinger, P.N. Kolosov, and S.P. Kolosova during the joint expedition to northeastern Siberia in 1991 (samples 1-91 - 4-91 and KG-91-11). In addition, we studied one sample (1734) from T.A. Ivanovskaya's 1989 collection kindly given to V.N. Sergeev. Sample localities are shown in Fig. 1.

MICROBIOTA COMPOSITION

As noted above, cherts of the upper Debengda Subformation contain two distinct assemblages of microfossils. Mats of filamentous microfossils contain

mainly *Siphonophycus inornatum* Zhang and much less abundant *Siphonophycus robustum* Schopf emend. Knoll et Golubic comb. Knoll *et al.* The more diverse assemblage associates with the above-described sedimentary fabrics, which resemble stromatolites. It is dominated by two distinct species of the *Eoentophysalis* genus: *E. dismallakesensis* Horodyski et Donaldson and *E. belcherensis* Hofmann. These microfossils occur mainly as colonies of several to several hundreds of cells scattered along the bedding surfaces, yet the contiguous populations forming thin mats rarely occur. Besides, there are the following microfossil taxa: *Gloeodiniopsis* aff. *lamellosa* Schopf emend. Knoll et Golubic, *G. gregaria* Knoll et Golubic, *Eosynechococcus medius* Hofmann, *Archaeoellipsoides grandis* Horodyski et Donaldson, *Siphonophycus robustum* Schopf emend. Knoll et Golubic, *Palaeolyngbya maxima* Zhang, *Clonophycus* sp., and *Myxococcoides* sp. (Fig. 2). *Gloeodiniopsis* aff. *lamellosa* and *Clonophycus* sp. occur as loose colonies between the filaments of *Siphonophycus robustum*, or in close association with *Eoentophysalis*. The ellipsoidal microfossils *Eosynechococcus medius* and coccoidal forms *Gloeodiniopsis gregaria* are subordinate elements of the assemblage, constituting 3% or less of all the present individuals. *Palaeolyngbya maxima* and *Archaeoellipsoides grandis* are extremely rare.

TAXONOMIC INTERPRETATION

Nearly all Debengda microfossils are the remnants of cyanobacteria or morphologically similar microorganisms. The mat-forming *Siphonophycus* species can be most reasonably interpreted as preserved extracellular empty sheaths of the so-called LPP-type (*Lyngbya–Phormidium–Plectonema*). Two species of the *Eoentophysalis* genus are convincingly similar to the modern entophysalidalean cyanobacteria, which thrive in peritidal environments. *Palaeolyngbya maxima* does not differ much from its modern analog, the blue-green alga *Lyngbya* (Schopf, 1968; Zhang, 1981). *Gloeodiniopsis* aff. *lamellosa* and *G. gregaria* are morphologically similar to some species of existing chroococcacean cyanobacteria of the *Gloeocapsa* Kütz and *Chroococcus* Nägell genera. As for *Clonophycus* sp., it also seems to be a remnant of the chroococcacean cyanobacteria, but its simple morphology precludes a confident taxonomic interpretation. Similarly, the botryoidal colonies of *Eosynechococcus medius* are usually referred to the chroococcacean cyanobacteria compared to such genera as *Synechococcus* and *Gloeothece*, but their simple rodlike shape is shared by many other bacteria.

The nature of *Archaeoellipsoides grandis* and *Myxococcoides* sp. is less evident. The ellipsoid forms of *A. grandis* may be the akinetes left by nostocalean cyanobacteria, or the remnants of eukaryotic organisms (Horodyski and Donaldson, 1980). Nonetheless, we do not agree that these ellipsoidal microfossils are the remnants of giant unicellular cyanobacteria resembling *Synechococcus* species, as suggested by Golovenok and Belova (1984). The clusters of *Myxococcoides* sp. seem to be empty envelopes of the chroococcacean cyanobacteria, or the remnants of unicellular protists.

PALEOENVIRONMENTAL INTERPRETATION

Conclusions concerning the habitat environment of the Debengda microbiota are based on both lithological data and microfossil composition. The stratiform lamination in the Debengda rocks, as well as their fine-grained flaggy clastic carbonates, minute symmetrical ripples, desiccation cracks, and large voids permit us to suggest that microfossiliferous sediments were deposited on a tidal flat (Green *et al.*, 1989).

This interpretation is supported by the silicified microfossil composition, as many of their modern counterparts inhabit the intertidal zone. For example, the modern species of the *Entophysalis* genus, analogs of the Debengda *Eoentophysalis* spp., are widespread in the tidal flats of the Shark Bay in Australia, Persian Gulf, and Bahama Bank (Golubic, 1976). The brown pigment, colored surface of *Eoentophysalis dismallakesensis* and *E. belcherensis* colonies (Plate I, Fig. 10; Plate II, Figs. 1, 2, and 10), is comparable with the yellow-brown coloring agent (scytonemine) produced by cells of the modern *Entophysalis* in response to the intensive sun radiation under subaerial conditions (Golubic and Hofmann, 1976; Hofmann, 1976; D. Oehler, 1978; Zhang, 1981). The morphology of the sheaths of *Siphonophycus*, which form mats of filamentous microfossils, does not in itself indicate a particular environment, but such assemblages of filamentous microorganisms of high density and low diversity occur in deposits of the upper intertidal and supratidal zones (Green *et al.*, 1989; Knoll *et al.*, 1991). Abundant plankton remains, which characterize many Proterozoic and Cambrian microfossil assemblages, preserved in cherts of the subtidal origin (Knoll, 1984; Yin, 1987; Sergeev, 1991; Knoll *et al.*, 1991), were not found among the Debengda microbiota.

The apparent environmental proximity of the two microfossil assemblages from the Debengda Formation is consistent with the data on other Proterozoic microbiota and on modern tidal flats, where taxonomically distinct assemblages of microorganisms inhabit adjacent ecological niches throughout the entire range of peritidal settings (Knoll and Golubic, 1979; Knoll *et al.*, 1991; Sergeev, 1993). In fact, one of our samples contains mixed microfossil taxa that occur in two distinct Debengda assemblages, thus underscoring their close paleoenvironmental relations.

AGE OF THE DEBENGDA MICROBIOTA

Like other microbiotas from cherts, the assemblage of the Debengda Formation includes morphologically simple microfossils of filamentous and coccoidal shape. Mendelson and Schopf (1982) classified such assemblages as "typical" Proterozoic. Of course, the term

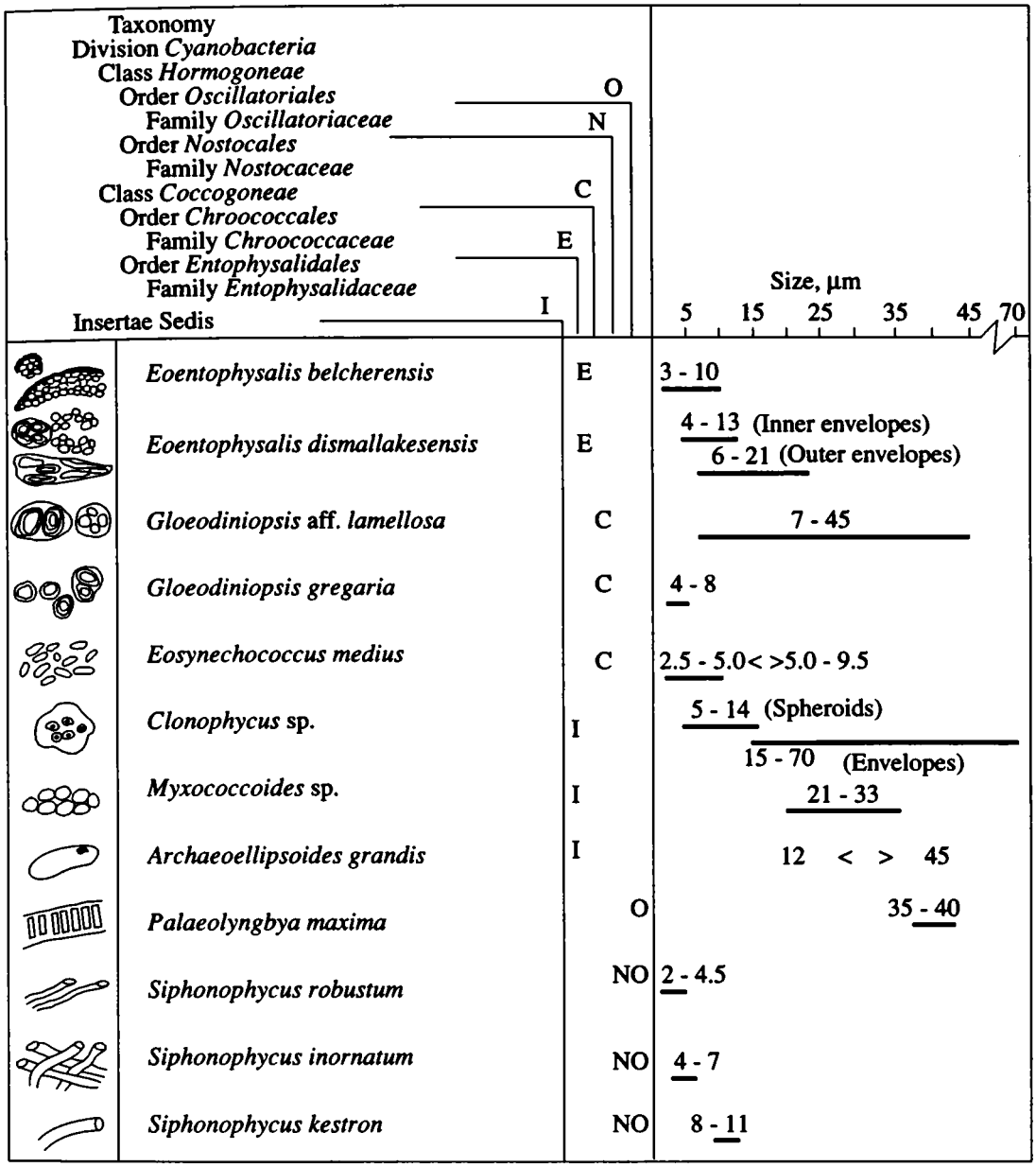

Fig. 2. Synopsis of the Debengda microbiota.

"typical" encompasses variations from one Proterozoic era to another. Silicified microfossils from the Neoproterozoic (late Riphean and Vendian) marine sediments usually include acanthomorphic acritarchs (Lo, 1980; Knoll, 1984, 1992; Awramik *et al.*, 1985; Zang and Walter, 1989; Allison and Awramik, 1989; Knoll *et al.*, 1991; and others). Microfossil assemblages from Paleoproterozoic iron formations or subtidal silicified carbonates have their own peculiarities (Barghoorn and Tyler, 1965; Hofmann and Schopf, 1983; Knoll *et al.*, 1988).

The microfossil assemblages with the dominant *Eoentophysalis* species also warn against the uncritical usage of the term "typical." Such assemblages occur throughout the Paleo- and Mesoproterozoic strata (Hofmann, 1976; Muir, 1976; D. Oehler, 1978; Zhang, 1981; Strother *et al.*, 1983; Yakshin, 1990; Sergeev, 1993), yet were not found in the Neoproterozoic marine rocks, where other microorganisms dominate in the microbiotas, with *Eoentophysalis* occurring only as isolated colonies amid them (Knoll *et al.*, 1991; Sergeev, 1992). This seems abnormal, because the entophysalidalean cyanobacteria are the abundant mat-forming organisms in the intertidal zones of Recent oceans (Golubic and Hofmann, 1976). We believe, still, that the distinct environments of Paleo- and Mesoproterozoic basins with chemical precipitation of carbonates in the peritidal zones explain why the microfossil

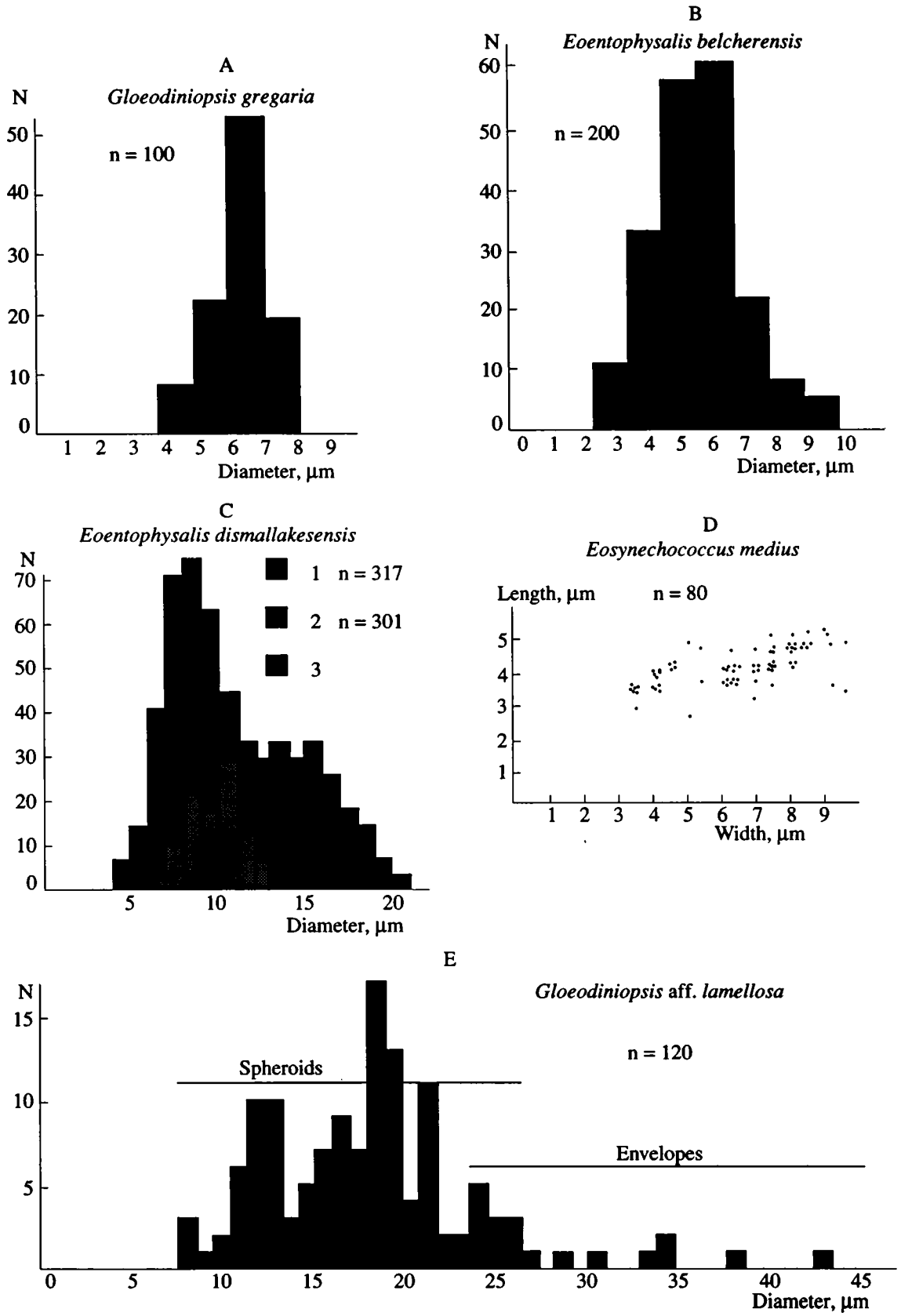

Fig. 3. Size of the coccoidal microfossils of the Debengda microbiota. A - C and E – frequency distribution of diameter size of the spheroidal microfossils. D – length to width ratios of the ellipsoidal microfossils.

1 – Inner diameter of spheroids; 2 – outer diameter of spheroids; 3 – overlapping parts of two previous histograms; N – number of measurements.

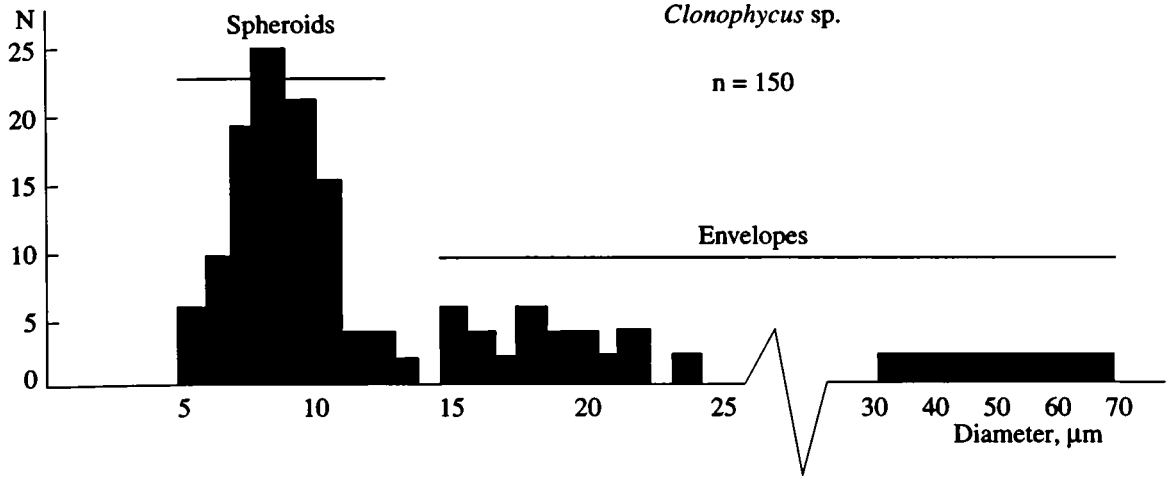

Fig. 4. Frequency distribution of diameter size of spheroids and outer envelopes for the coccoidal microfossil *Clonophycus* sp. N is number of measurements.

assemblages with clearly dominating *Eoentophysalis* are nearly absent in the Neoproterozoic deposits. The entophysalidalean cyanobacteria were, most likely, thriving in those tidal environments with intensive carbonate precipitation. When at the end of the Mesoproterozoic this process ceased, the microorganism assemblages rich in *Eoentophysalis* disappeared as well. The small number of Phanerozoic finds additionally reflects a decrease in the abundance of the early diagenetic cherts (Maliva *et al.*, 1989).

The presence of the ellipsoid microfossil *Archaeoellipsoides grandis* Horodyski et Donaldson is one of the characteristic features of the Debengda microbiota (Plate I, Fig. 1). This species occurs in several microbiotas from the Mesoproterozoic cherts, e.g., in the Dismal Lakes Group, Canada (Horodyski and Donaldson, 1980), the Wimishan Formation, China (Zhang, 1985), the Billyakh Group of the Anabar uplift, Siberia (Golovenok and Belova, 1984; Yakshin, 1991; Sergeev, 1993), and the Bylot Supergroup, Baffin Island, Canada (Hofmann and Jackson, 1991), yet they were not found in cherts of a reliable Neoproterozoic age.

So, despite their simple composition, the Debengda microbiota supports the Mesoproterozoic (middle Riphean) age of the host deposits. The estimated age is consistent with the peculiar sedimentary fabrics of the Debengda rocks untypical of the Neoproterozoic carbonates. Measurements of the carbon isotopic composition in four samples of the Debengda dolomite provided the values: $\delta^{13}C = -0.65, -1.00, -0.60,$ and $-0.70‰$ PDB. The data is comparable to the carbon isotopic ratios in the Billyakh Group and other Mesoproterozoic carbonates, whereas a noticeable enrichment in the $\delta^{13}C$ isotope characteristic of many Neoproterozoic dolomites and limestones (especially of those younger than 850 Ma) (Knoll *et al.*, 1986) was not found. Thus, data on micropaleontology, sedimentology, and isotopic geochemistry are consistent with the Mesoproterozoic age of the Debengda Formation that was earlier suggested using stromatolite study and radiometric dating.

DESCRIPTION OF MICROFOSSILS

Microfossils described in the paper were studied in thin sections of black cherts. All microfossils were photographed in a transmitted light through a blue filter; measurements were made using the eyepiece reticle, and taking the nearest micrometer readings. The described specimens are supplemented with the "English Finder" coordinates. All specimens are deposited in the paleobotanical collections of the Harvard University Herbaria (Cambridge, USA) in the paleontological collection of the Yakutian Institute of Geosciences, Russian Academy of Sciences (Yakutsk, Russia), and paleontological Collection No. 4689 of the Geological Institute, Russian Academy of Sciences (Moscow, Russia).

Kingdom Eubacteria

Division Cyanobacteria

Class Coccogoneae

Order Chroococcales

Family Chroococcaceae Nägeli, 1849

Genus *Gloeodiniopsis* Schopf emend. Knoll et Golubic, 1979

Type species *G. lamellosa* Schopf emend. Knoll et Golubic, 1979

Gloeodiniopsis aff. *lamellosa*

Plate I, Figs. 2, 3, 6, 7

Description. The single, double to multilamellated spheroids and ellipsoids occurring as solitary unicells, or their dyads, triads, tetrads (cross and planar), and octads surrounded by common single- or multilamellated envelopes. The outer layers of spheroid and ellipsoid envelopes are nearly transparent, and usually have a regular concentric structure; their walls, ca. 0.5 μm thick, are fine-grained. The inner layers are translucent

and more irregular in configuration; their walls are coarse-grained, and ca. 1.0 μm thick. An opaque, spheroidal inclusion, 2.0 - 3.0 μm in diameter, is sometimes attached to the innermost layer of the envelope. The outer diameter of the spheroids varies between 7 and 32 μm. The resicles around the spheroid groups are monolayerd, transparent, 22 - 45 μm in diameter; their walls are medium-grained, ca. 1 μm thick.

Gloeodiniopsis aff. *lamellosa* occurs mainly as loose colonies of a few dozen spheroids situated between tubular forms of *S. inornatum* and *S. robustum*, or in close association with *E. belcherensis* and *E. dismallakesensis*.

Discussion. The microfossils described here differ from the type populations of *G. lamellosa* (Schopf, 1968; Knoll and Golubic, 1979) in a wider range of spheroid diameters. So, we classify the Debengda population as *Gloeodiniopsis* aff. *lamellosa*.

Being amended, the *Gloeodiniopsis* genus was interpreted as the fossil counterpart of modern chroococcacean cyanobacteria *Gloeocapsa*, or *Chroococcus*[2] (Schopf and Blacic, 1971; Knoll and Golubic, 1979). The new diagnosis concerns not only single spheroids, but also their dyads, triads, tetrads, and octads surrounded by a common envelope (Knoll and Golubic, 1979). Earlier, similar spheroid groups with the common envelope were described as *Clonophycus* genus (J. Oehler, 1977; D. Oehler, 1978), and later as *Eogloeocapsa* genus (Golovenok and Belova, 1984). In their latest work, Golovenok and Belova (1992, Fig. 2) reconstructed the cycle of life and decay of *Eogloeocapsa arcata* Mendelson et Schopf comb. Golovenok et Belova from the Riphean Sukhaya Tunguska Formation of the Turukhansk uplift. The reconstruction does not differ essentially from the life cycle suggested previously for *Gloeodiniopsis lamellosa* (Knoll and Golubic, 1979; Fig. 9). Therefore, we propose to use the name of the *Gloeodiniopsis* genus to classify fossil forms similar in morphology to modern cyanobacteria of the *Gloeocapsa–Chroococcus* type, and the name of the *Clonophycus* genus for the coccoidal microfossils of an unclear biological affinities surrounded by a common vesicle.

Materials. Several dozen specimens in the thin sections of cherts from the Debengda Formation.

Gloeodiniopsis gregaria Knoll et Golubic, 1979

Plate III, Fig. 4

Gloeodiniopsis gregaria: Knoll and Golubic, 1979, pp. 147, 148, Fig. 10; Knoll, 1982, p. 782, Pl. 7, Figs. 1 - 5.

Holotype. The Harvard University paleobotanical collection, no. 60301; Australia, Ellery Creek locality, 80 km west of the Alice Springs; Neoproterozoic (late Riphean), Bitter Springs Formation.

[2] Many researchers do not separate the *Gloeocapsa* and *Chroococcus* genera (Elenkin, 1938; Komarek and Anagnostides, 1986), as the difference between them is minor, and consists in different sheath thickness and coloring (Desikachary, 1959; Golubic, 1976). It is impossible, evidently, to distinguish the original color of fossil sheaths of cyanobacteria.

Description. Spheroids with single to multilamellated envelopes occurring as unicells, or dyads, triads, and tetrads. The spheroids form colonies of several to hundreds of loose or sometimes contiguous individuals. The spheroid envelopes are translucent and irregular in shape; walls are fine-grained and less than 0.5 μm thick. A spot-like round inclusion up to 1 μm in diameter may sometimes be attached to the innermost layer of the envelope. The outer diameter of spheroids varies between 4 - 8 μm.

Comparison. The species differs in size from other species of the *Gloeodiniopsis* genus (see Sergeev, 1992, for the comparative size characteristics of the *Gloeodiniopsis* species).

Distribution. The Mesoproterozoic: Debengda Formation, northern Siberia; the Neoproterozoic (upper Riphean): the Bitter Springs Formation, Australia; the Draken Conglomerates, Svalbard (Knoll, 1982).

Materials. Several hundred spheroids in the thin sections of cherts from the Debengda Formation.

Genus *Eosynechococcus* Hofmann, 1976

Type species *Eosynechococcus moorei* Hofmann, 1976

Eosynechococcus medius Hofmann, 1976

Plate I, Fig. 5

Eosynechococcus medius: Hofmann, 1976, p. 1058, Pl. 2, Figs. 9 and 10; Mendelson and Schopf, 1982, pp. 72 - 74, Pl. 3, Figs. 1 and 2; Knoll, 1982, p. 780, Pl. 8, Figs. 11 - 13; Hofmann and Jackson, 1991, pp. 371, 372, Figs. 7.14 and 7.15.

Holotype. Geological Survey of Canada, No. 43588; Belcher Islands; a nameless island at the northern side of the Churchill Sound; Paleoproterozoic, the Belcher Supergroup, the Kasegalik Formation.

Description. Single lamellated, rodlike, empty, nonseptate ellipsoids occurring in dense, irregular colonies. The colonies associate with those of *E. belcherensis* and *E. dismallakensis*. The ellipsoid length varies from 5.0 to 9.5 μm, the width from 2.5 to 5.0 μm; the length to width ratio changes from 1 to 3. The spheroid envelopes are translucent; the medium-grained walls are ca. 0.5 μm thick.

Comparison. E. medius is intermediate in size range as compared to other species of the *Eosynechococcus* genus.

Distribution. Paleoproterozoic: the Belcher Supergroup, Canada; Mesoproterozoic: the Uluksan Group, Canada, the Sukhaya Tunguska Formation, the Turukhansk uplift and the Debengda Formation, the Olenek uplift in Siberia; Neoproterozoic: the Draken Conglomerates, Spitsbergen.

Materials. Several colonies in thin sections of the Debengda Formation cherts.

Family Entophysalidaceae Geitler, 1925

Genus *Eoentophysalis* Hofmann
emend. Mendelson et Schopf, 1982

Type species *Eoentophysalis belcherensis* Hofmann, 1976

Eoentophysalis belcherensis Hofmann, 1976
Plate I, Figs. 10 and 11

Eoentophysalis belcherensis: Hofmann, 1976, pp. 1070 - 1072, Pl. 4, Figs. 1 - 5, Pl. 5, Figs. 3 - 6, Pl. 6, Figs. 1 - 14;
(for the full synonymy see Sergeev, 1992).

Holotype. Geological Survey of Canada, No. 42770; Canada, Belcher Islands, a nameless island at the northern side of the Churchill Sound; Paleoproterozoic, Belcher Supergroup, Kasegalik Formation.

Description. Single- or multilamellated spheroids occurring as globular and botryoidal colonies, or in the pustulose stratiform laminae. The colonies of the two former types consist of several hundred spheroids, those of the third type contain up to several thousand individuals. The colony margins are almost always dark-brown in color. The spheroid morphology varies from the regular spheres to irregular subangular individuals. Spheroids with a single layered envelope are dominant. The envelopes are translucent; walls are fine-grained, and less than 0.5 μm thick. Opaque spot-like globular inclusions may be present inside the spheroids. The spheroid diameter is 3 - 10 μm.

Comparison. E. belcherensis differ from *E. yudomatica* Lo and *E. dismallakesensis* Horodyski et Donaldson mainly in their smaller size, yet they are larger and better preserved than *E. cumulus* Knoll et Golubic (see Sergeev, 1992, Table I, for a thorough comparative characterization of various *Eoentophysalis* species).

Discussion. E. belcherensis from the Debengda Formation differs from the species found in the type locality of the Belcher Supergroup mainly by the single layered envelopes. Yet the fossils from the Debengda Formation are identical to *E. belcherensis* from several Mesoproterozoic units: Gaoyuzhuang Formation in China (Zhang, 1981), Amelia and Balbirini formations in Australia (Muir, 1976; D. Oehler, 1978; Hofmann and Schopf, 1983), Kotuikan and Yusmastakh formations in the Anabar uplift (Sergeev, 1993).

Distribution. Paleoproterozoic: the Belcher Supergroup, Canada; Mesoproterozoic: Gaoyuzhuang Formation, China; the Amelia and Balbirini formations, Australia; the Avzyan Formation, the southern Urals, Kotuikan and Yusmastakh formations, the Anabar uplift; Neoproterozoic: the Draken Conglomerates, Spitsbergen, the Narssarssuk Formation and Eleonore Bay Group, Greenland.

Materials. Several hundred colonies of hundreds to thousands of spheroids in the thin sections of the Debengda Formation cherts.

Eoentophysalis dismallakesensis
Horodyski et Donaldson, 1980
Plate II, Figs. 1 - 10

Eoentophysalis dismallakesensis:
Horodyski and Donaldson, 1980, pp. 146 - 149, Figs. 10 A - 10D, 11 A - 11G, 12 A and 12B
(see Sergeev, 1992, for a full synonymy).

Holotype. Geological Survey of Canada, thin section No. 57987; Canada, 8 km west of the bay in the northeastern Dismal Lake; Mesoproterozoic, Dismal Lakes Group.

Description. Multilamellated spheroids and ellipsoids occurring as dyads, tetrads, and octads in the colonies of several specimens to thousands of them. The spheroid envelopes are concentric. The morphology of colonies varies from loose spheroid clusters to the palmelloid colonies of globular and semiglobular shape. Often, the spheroid envelopes are unidirectionally elongated, perhaps because of the polarized growth of cells in an attempt to escape burial. The margins of many colonies are pigmented dark-brown. Spheroids are usually distinguishable in the marginal parts surrounding the empty inner zones of the colonies. The outer layers of spheroid envelopes are translucent; the walls are fine-grained, and ca. 0.5 μm thick. The inner layers are medium- to coarse-grained, ca. 1.0 μm thick. An opaque inclusion about 2.0 - 2.5 μm in diameter is commonly attached to the inner side of the central envelope layer. The outer diameter of spheroids ranges from 6 to 21 μm, their inner diameter measured by the inner layers of envelopes is 4 - 13 μm.

Comparison. E. dismallakesensis differs from *E. cumulus* Knoll et Golubic and *E. belcherensis* Hofmann in its larger size. As compared to *E. yudomatica* Lo, it differs in the spherical and hemispherical shape of the colonies (see Sergeev, 1992, Table I, for the full comparative characteristics of the *Eoentophysalis* species).

Discussion. The microfossils assigned here to *E. dismallakesensis* differ from the population type in having a slightly larger size range (spheroids of *E. dismallakesensis* in the Dismal Lakes Group are 4 - 13 μm long and 3 - 10 μm wide). Yet in the population type of *E. dismallakesensis*, the outer sheaths became an amorphous mass, and in fact the diameters of the Dismal Lakes spheroids were the same as those in the Debengda populations. According to other morphological characteristics, the two populations are strikingly similar.

E. dismallakesensis from the Debengda and Dismal Lakes cherts do not form the pustulose stratiform mats resembling thus the chroococcacean cyanobacteria. Nonetheless, the Debengda forms show a polarized growth, the characteristic feature of Entophysalidaceae, which is absent in the Croococcaceae (Golubic, 1976). For this reason, the Debengda coccoidal microfossils are included in the *Eoentophysalis* genus.

Distribution. Mesoproterozoic: the Dismal Lakes Group, Canada; the Debengda Formation, Siberia; Neoproterozoic?–Vendian? (late Riphean? or Vendian?): the Chichkan Formation, southern Kazakhstan.

Materials. A few hundred colonies in the thin sections of the Debengda Formation cherts.

Class Hormogoneae

Order Oscillatoriales

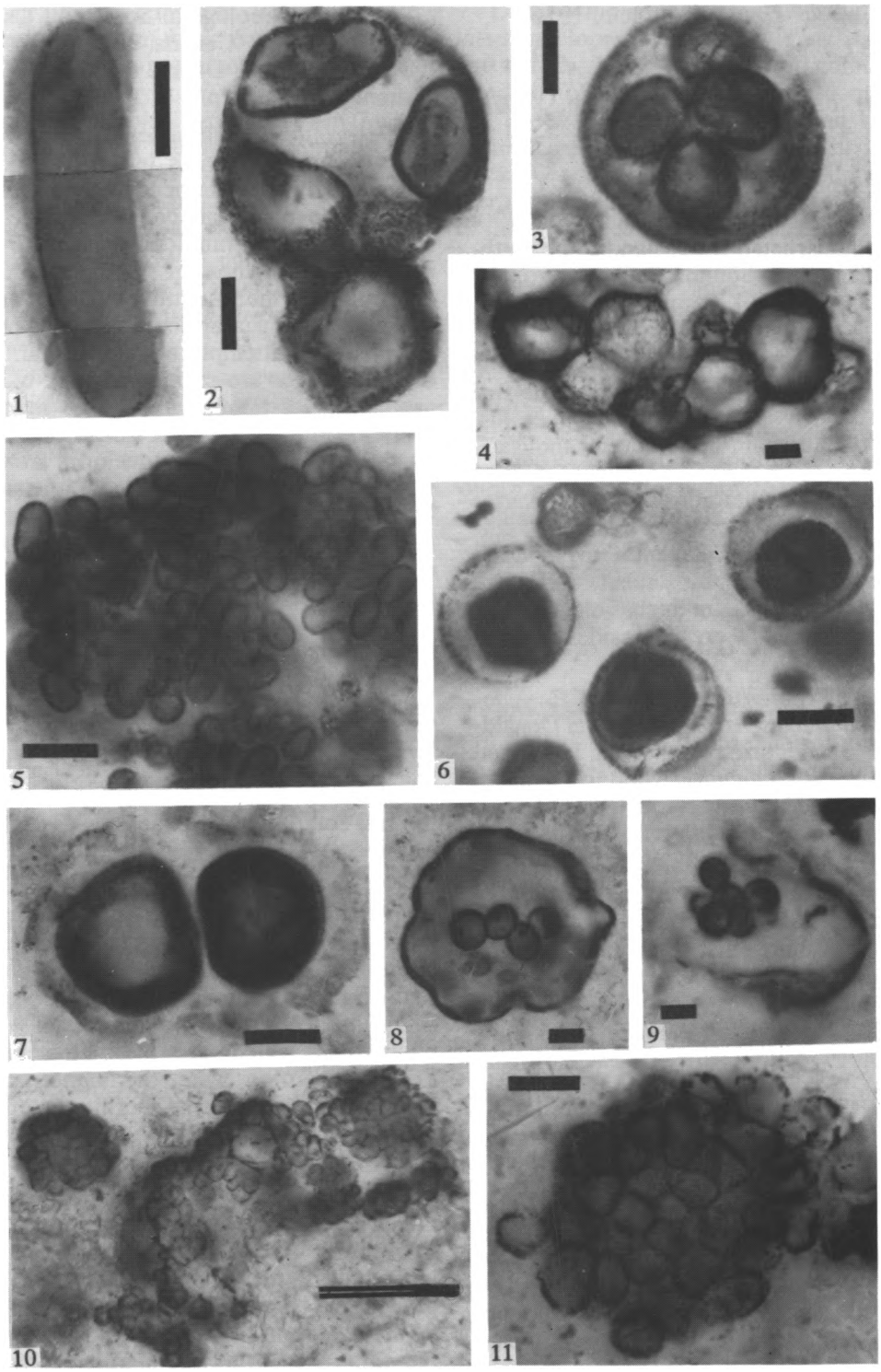

Plate I. Coccoidal and filamentous microfossils of the Debengda microbiota.

1 – *Archaeoellipsoides grandis* Horodyski et Donaldson, slide 2-91-3, coordinates Q-45-2; 2, 3, 6, 7 – *Gloeodiniopsis* aff. *lamellosa*: 2 – slide 3-91-2, coordinates M-43-3, 3 – slide 3-91-2, coordinates J-43-3, 6 – slide 548, coordinates N-47-3, and 7 – slide 2-91, coordinates R-48-2; 4 – *Myxococcoides* sp., slide 549, coordinates J-47-3; 5 – *Eosynechococcus medius* Hofmann, slide 2-91, coordinates L-56-1; 8, 9 – *Clonophycus* sp.: 8 – slide 546, coordinates Q-35-1 and 9 – slide 547, coordinates W-28-3; 10, 11 – *Eoentophysalis belcherensis* Hofmann: 10 – slide 2-91-3, coordinates N-50-4 and 11 – slide 3-91-3, coordinates J-55-3.

All specimens are from the Debengda Formation. Single bar scale equals 10 μm, double bar equals 50 μm.

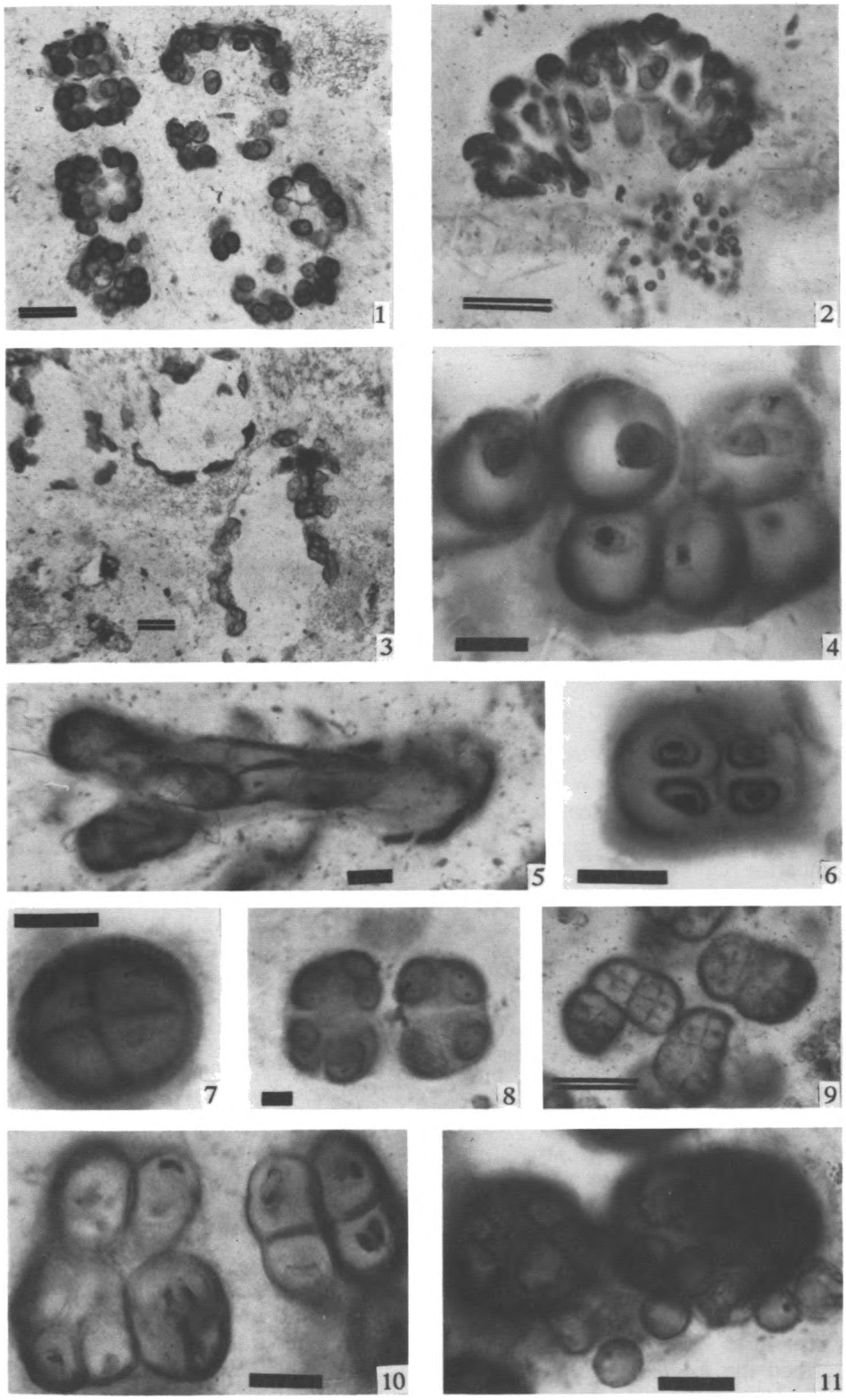

Plate II. Coccoidal microfossils of the Debengda microbiota.

1 - 10 – *Eoentophysalis dismallakesensis* Horodyski et Donaldson: 1 – slide 2-91-5, coordinates S-46-4, 2 – slide 2-91-3, coordinates L-54-2, 3 – slide 2-91-3, coordinates M-45-4, 4 – slide 2-91-3, coordinates K-55-2, 5 – slide 2-91-3, coordinates K-55-1, 6 – slide 2-91-3, coordinates J-48-1, 7 – slide 547, coordinates S-29-4, 8 – slide 549, coordinates J-32-3, 9 – slide 2-91-3, coordinates J-52-4, and 10 – slide 2-91-3, coordinates P-58-1; 11 – *Clonophycus* sp., slide 2-91-2, coordinates G-55-4.

All specimens are from the Debengda Formation. Single bar scale equals 10 μm, double bar equals 50 μm.

Family Oscillatoriaceae (S.F. Gray) Dumortier et Kirchner, 1898

Genus *Palaeolyngbya* Schopf, 1968

Type species *Palaeolyngbya barghoorniana* Schopf, 1968

Palaeolyngbya maxima Zhang, 1981, Plate III, Fig. 8

Palaeolyngbya maxima: Zhang, 1981, p. 495, Pl. 2, Figs. 4, 6, 7.

Holotype. Collection of the Paleontological Laboratory of Beijing University, China, thin section BGP No. 7822; China, Pangjapu Iron Mine, Hebei; Mesoproterozoic, the Gaoyuzhuang Formation.

Description. Uniseriate, unbranching trichomes within the well-defined extracellular sheath; filaments are 35 - 40 μm in diameter and ca. 160 μm long. An individual trichome consists of tablet translucent cells 22 - 26 μm wide and 5 - 6 μm long. Cross walls are distinct; the trichome cells are not in contact; side walls are also distinct, fine-grained, and less than 0.5 μm thick. The sheath is transparent, nonlaminated, hyaline, and less than 0.5 μm thick.

Comparison. P. maxima differs from other species of the *Palaeolyngbya* genus in a larger diameter of its cells.

Distribution. Mesoproterozoic: the Gaoyuzhuang Formation, China; the Debengda Formation, the Olenek uplift, northern Siberia.

Materials. One specimen in the thin section of the Debengda Formation chert.

Incertae Sedis

Clonophycus sp.

Pl. I, Figs. 8 and 9; Pl. II, Fig. 11.

Description. Groups of single lamellated spheroids surrounded by a common vesicle of spheroidal or irregular shape. The vesicles occur individually, or as groups of individuals. Their outer walls are sometimes broken, and spheroids are outside of them. The spheroids are thin-walled, and usually contain inner opaque inclusions less than 0.5 μm in diameter. The outer walls of the vesicles are translucent; they are medium-grained, and 1 - 2 μm thick. Inside the colonies, the spheroid diameters are from 5 to 14 μm; the diameter of the outer vesicles varies from 15 to 70 μm.

Discussion. The *Clonophycus* genus was described by J. Oehler (1977), and emended by D. Oehler (1978) as "cells contained within a psilate to finely granular, spherical sac-like structure." Later Golovenok and Belova (1984) described the *Eogloeocapsa* genus as "cells usually forming in isolated colonies of two to eight, sometimes many more cells, surrounded by a common sheath." Evidently both taxa were referred to the same type of microfossils, and so *Eogloeocapsa* is the junior synonym of *Clonophycus*.

Golovenok and Belova (1984) compared *Eogloeocapsa* with the modern cyanobacterium *Gloeocapsa* Kütz. Neither J. Oehler nor D. Oehler suggested a definite biological interpretation for the *Clonophycus* species, only mentioning that they could be the remnants of either procaryotic or eucaryotic organisms.

According to the size range of spheroids, *Clonophycus* sp. resembles *C. vulgaris* from the Paleo- or Mesoproterozoic (pre-Riphean or lower Riphean) Balbirini Formation in Australia, but has a much larger outer envelope diameter, which is why we describe this form as *Clonophycus* sp.

Materials. About 50 specimens in the thin sections of the black cherts from the Debengda Formation.

Genus *Archaeoellipsoides* Horodyski et Donaldson, 1980

Type species *Archaeoellipsoides grandis* Horodyski et Donaldson, 1980

Archaeoellipsoides grandis Horodyski et Donaldson, 1980

Plate I, Fig. 1

Archaeoellipsoides grandis: Horodyski and Donaldson, 1980, pp. 154 - 156, Figs. 16A - 16H; Schopf, 1992, Pl. 9, Figs. 1K and 1L.

Holotype. Geological Survey of Canada, thin section No. 57988; Canada, 8 km west of the northeastern bay of the Dismal Lakes; Mesoproterozoic, the Dismal Lakes Group.

Description. A solitary, single lamellated, slightly curved ellipsoid with rounded ends, found between the colonies of *E. belcherensis* and *E. dismallakesensis*. The ellipsoid is nonseptate, and nearly empty inside except for several small blobs of the amorphous dark material. The ellipsoid is 45 μm long and 12 μm wide; the length to width ratio is nearly 4. The ellipsoid envelope is translucent; the wall is medium-grained, and of variable thickness, from less than 0.5 μm to more than 1.0 μm.

Comparison. A. grandis Horodyski et Donaldson differs from *A. obesus* Zhang in its larger size, and from *A. longus* Sergeev in its single lamellated envelope.

Discussion. Golovenok and Belova (1984) described the ellipsoid bodies of *A. grandis* from the Mesoproterozoic Kotuikan and Yusmastakh formations of the Anabar uplift as the new species of the *Eosynechococcus* genus. As already noted, we doubt that these microfossils are the remnants of the giant ellipsoid cyanobacteria similar to the *Eosynechococcus* genus, therefore we left them classified as *Archaeoellipsoides*. According to the description by Horodyski and Donaldson (1980), the size of *A. grandis* is highly variable, and it seems possible to recognize several species of the taxon (Zhang, 1985). Yet limited material from the Debengda Formation (only one specimen was found) precludes a more precise taxonomic definition.

Distribution. Mesoproterozoic: the Dismal Lakes Group, Canada; the Kotuikan and Yusmastakh formations, Anabar uplift, and the Debengda Formation, Olenek uplift, northern Siberia.

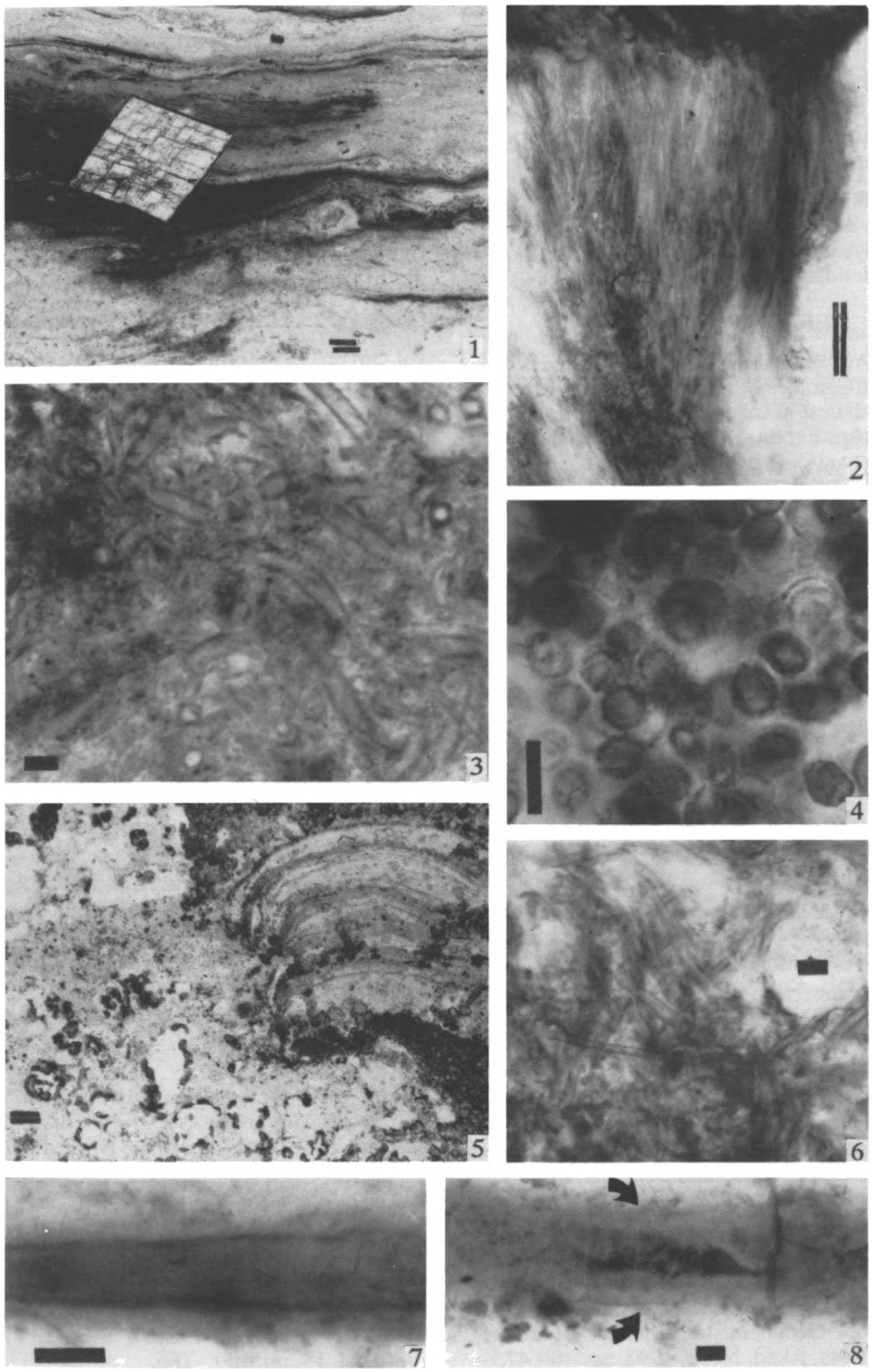

Plate III. Filamentous and coccoidal microfossils of the Debengda microbiota.

1 – Low magnification view of the *Siphonophycus inornatum* Zhang mats illustrating their characteristic fabric. Note the euhedral dolomite crystal grown after silicification, slide KG-91-11-FL, coordinates U-46; 2 – vertically oriented filament bundles of *Siphonophycus inornatum* Zhang, slide KG-91-11-2A, coordinates L-46-3; 3 – tangled sheaths of *Siphonophycus inornatum*, slide 1-91-2, coordinates Q-51-4; 4 – *Gloeodiniopsis gregaria* Knoll et Golubic, slide 2-91-2, coordinates M-45-1; 5 – laminated pseudostromatolitic structures characteristic of the *Eoentophysalis* assemblages; note that colonies of *Eoentophysalis dismallakesensis* are present only between these structural elements; slide 2-91-3, coordinates N-44-0; 6 – tangled sheaths of the *Siphonophycus inornatum* and *Siphonophycus robustum* (Schopf) emend. Knoll et Golubic emend. Knoll *et al.*, slide 548, coordinates V-32-1; 7 – *Siphonophycus inornatum*, slide 549, coordinates L-42-2; 8 – a poorly preserved filament of *Palaeolyngbya maxima* Zhang; arrows point to the sheath, slide 2-91, coordinates S-55-4.

All specimens are from the Debengda Formation. Single bar scale equals 10 μm, double bar equals 100 μm.

ACKNOWLEDGMENTS

We are grateful to S. Golubic (Boston University) for his helpful discussion, and to T.A. Ivanovskaya (Geological Institute, Russian Academy of Sciences) for providing a sample used in this study. Our special thanks to M.A. Semikhatov for his helpful comments.

This study was supported by the Russian Science Foundation grant 93-05-9403 (V.N. Sergeev's work), and partly by NASA grant NAGW-873 to A.H. Knoll.

REFERENCES

Allison, C.W. and Awramik, S.M., Organic-Walled Microfossils from Earliest Cambrian or Latest Proterozoic Tinder Group Rocks, Northwest Canada, *Precambr. Res.*, 1989, vol. 43, pp. 253 - 294.

Awramik, S.M. *et al.*, Prokaryotic and Eukaryotic Microfossils from a Proterozoic/Phanerozoic Transition in China, *Nature*, 1985, vol. 315, pp. 655 - 658.

Barghoorn, E.S. and Tyler, S.A., Microorganisms from the Gunflint Cherts, *Science*, 1965, vol. 147, pp. 563 - 577.

Bibikova, E.V., Lobach-Zhuchenko, S.V., Semikhatov, M.A., Shurkin, K.A., and Shcherbak, K.A., Geochronological Scale of Precambrian of the East European Craton and Its Surroundings, *Izv. Akad. Nauk SSSR, Ser. Geol.*, 1989, no. 4, pp. 3 - 21.

Desikachary, T.V., *Cyanophyta: Indian Council of Agricultural Research, Monographs on Algae*, New Delhi, 1959.

Elenkin, A.A., *Sine-Zelenye Vodorosli SSSR* (Blue-Green Algae of the USSR), Moscow: Akad. Nauk SSSR, 1938, vol. 1.

Golovenok, V.K. and Belova, M.Yu., Riphean Microbiotas in Cherts of the Billyakh Group in the Anabar Uplift, *Paleontol. Zh.*, 1984, no. 4, pp. 20 - 30.

Golovenok, V.K. and Belova, M.Yu., Microfossils in Cherts from the Sukhaya Tunguska Formation of the Riphean in the Turukhansk Uplift, *Dokl. Ross. Akad. Nauk*, 1992, vol. 323, no. 1, pp. 114 - 118.

Golubic, S., Taxonomy of Extant Stromatolite-Building Cyanophytes, *Stromatolites*, Walter, M.R., Ed., Amsterdam: Elsevier, 1976, pp. 113 - 126.

Golubic, S. and Hofmann, H.J., Comparison of Holocene and Mid-Precambrian Entophysalidaceae (Cyanophyta) in Stromatolitic Algal Mats: Cell Division and Degradation, *J. Paleontol.*, 1976, vol. 50, pp. 1074 - 1082.

Gorokhov, I.M., Baskakov, A.V., Semikhatov, M.A., Kutyavin, E.P., Mel'nikov, N.N., and Turchenko, T.L., Rb-Sr Systems in the Middle Riphean Siltstones of the Olenek Uplift, *XIII Simposium po Geokhimii Isotopov, Tez. Dokl.* (XIII Symp. on Isotope Geochemistry, Abstracts of Papers), Moscow: GEOKHI Ross. Akad. Nauk, 1992, pp. 46 - 47.

Green, J.W., Knoll, A.H., and Swett, K., Microfossils from Silicified Stromatolitic Carbonates of the Upper Proterozoic Limestone–Dolomite "Series," Central East Greenland, *Geol. Mag.*, 1989, vol. 119, pp. 527 - 551.

Hofmann, H.J., Precambrian Microflora, Belcher Island, Canada: Significance and Systematics, *J. Paleontol.*, 1976, vol. 50, pp. 1040 - 1073.

Hofmann, H.J. and Jackson, C.D., Shelf-Facies Microfossils from the Uluksan Group (Proterozoic Bylot Supergroup), Baffin Island, Canada, *J. Paleontol.*, 1991, vol. 65, pp. 361 - 382.

Hofmann, H.J. and Schopf, J.W., Early Proterozoic Microfossils, *Earth's Earliest Biosphere: Its Origin and Evolution*, Schopf, J.W., Ed., Princeton: Princeton Univ., 1983, pp. 321 - 360.

Horodyski, R.J. and Donaldson, J.A., Microfossils from the Middle Proterozoic Dismal Lakes Group, Arctic Canada, *Precambrian Res.*, 1980, vol. 11, pp. 125 - 159.

Kasakov, G.A., Knorre, G.K., and Prokof'eva, L.N., The Absolute Age of Precambrian Sedimentary Rocks of the Olenek Uplift, East Siberia, *Geokhimiya*, 1965, no. 11, pp. 1313 - 1317.

Knoll, A.H., Microfossils from the Late Precambrian Draken Conglomerate, NY Friesland, Svalbard, *J. Paleontol.*, 1982, vol. 56, pp. 755 - 790.

Knoll, A.H., Microorganisms of the Late Precambrian Hunnberg Formation, Nordaustlanded, Svalbard, *J. Paleontol.*, 1984, vol. 58, pp. 131 - 162.

Knoll, A.H., A Paleobiological Perspective on Sabkhas, *Ecological Studies*, Friedman, G.M. and Krumbein, W.E., Eds., 1985, vol. 53, pp. 407 - 485.

Knoll, A.H., The Early Evolution of Eukaryotes: A Geological Perspective, *Science*, 1992, vol. 256, pp. 622 - 627.

Knoll, A.H. and Bauld, J., The Evolution of Ecological Tolerance in Prokaryotes, *Trans. R. Soc. Edinburgh: Earth Sci.*, 1989, vol. 80, pp. 209 - 223.

Knoll, A.H. and Golubic, S., Anatomy and Taphonomy of a Precambrian Algal Stromatolite, *Precambrian Res.*, 1979, vol. 10, pp. 115 - 151.

Knoll, A.H., Hayes, J.M., Kayfman, A.J., Swett, K., and Lambert, I.B., Secular Variation in Carbon Isotope Ratios from Upper Proterozoic Succession of Svalbard and East Greenland, *Nature*, 1986, vol. 321, pp. 832 - 838.

Knoll, A.H., Strother, R.K., and Rossi, S., Distribution and Diagenesis of Microfossils from the Lower Proterozoic Duck Creek Dolomite, Western Australia, *Precambrian Res.*, 1988, vol. 38, pp. 257 - 279.

Knoll, A.H., Swett, K., and Mark, J., Paleobiology of a Neoproterozoic Tidal Flat/Lagoonal Complex: the Draken Conglomerate Formation, Spitsbergen, *J. Paleontol.*, 1991, vol. 65, pp. 531 - 570.

Komar, V.A., *Stromatolity Verkhnedokembriiskikh Otlozhenii Severa Sibirskoi Platformy i Ikh Stratigraficheskoe Znachenie* (Stromatolites in the Upper Precambrian Deposits of the North Siberian Craton, and Their Stratigraphic Significance), Moscow: Nauka, 1966.

Komarek, J. and Anagnostidis, K., Modern Approach to the Classification System of Cyanophytes, *Archiv für Hydrobyol.* 1986, Supplement to vol. 73(2), pp. 157 - 226.

Lo, S.C., Microbial Fossils from the Lower Yudoma Suite, Earliest Phanerozoic, Eastern Siberia, *Precambrian Res.*, 1980, vol. 13, pp. 109 - 166.

Maliva, R.G., Knoll, A.H., and Siever, R., Secular Change in Cherts Distribution: A Reflection of Evolving Biological Participation in the Silica Cycle, *Palaios.*, 1989, vol. 4, pp. 519 - 532.

Mendelson, C.V. and Schopf, J.W., Proterozoic Microfossils from the Sukhaya Tunguska, Shorikha, and Yudoma Formations of the Siberian Platform, USSR, *J. Paleontol.*, 1982, vol. 56, pp. 42 - 83.

Muir, M.D., Proterozoic Microfossils from the Amelia Dolomite, McArthur Basin, Northern Territory, *Alcheringa*, 1976, vol. 1, pp. 143 - 158.

Oehler, D.Z., Microflora of the Middle Proterozoic Balbirini Dolomite (McArthur Group) of Australia, *Alcheringa*, 1978, vol. 2, pp. 269 - 310.

Oehler, J.H., Precambrian Microfossils and Associated Mineralization in the McArthur Deposit, Northern Territory, Australia, *Alcheringa*, 1977, vol. 1, pp. 315 - 349.

Resheniya Vsesoyuznogo Stratigraficheskogo Soveshchaniya po Dokembriyu, Paleozoyu i Chetvertichnoi Sisteme Sibiri (Resolutions of the All-Union Conference on the Precambrian, Paleozoic, and the Quaternary System of Siberia), Novosibirsk: Nauka, 1983.

Schopf, J.W., Microflora of the Bitter Springs Formation, Late Precambrian, Central Australia, *J. Paleontol.*, 1968, vol. 42, pp. 651 - 688.

Schopf, J.W. and Blacic, J.M., New Microorganisms from the Bitter Springs Formation (Late Precambrian) of the North-Central Amadeus Basin, Central Australia, *J. Paleontol.*, 1971, vol. 45, pp. 925 - 960.

Semikhatov, M.A., Experience in Stromatolite Studies in the USSR, *Stromatolites*, Walter, M.R., Ed., Amsterdam: Elsevier, 1976, pp. 337 - 357.

Semikhatov, M.A., General Problems of Proterozoic Stratigraphy in the USSR, *Soviet Sci. Rev., General Geol.*, 1991, vol. 1, pp. 1 - 192.

Semikhatov, M.A. and Serebryakov, S.N., *Sibirskii Gipostratotip Rifeya* (Siberian Hypostratotype of the Riphean), Moscow: Nauka, 1983.

Semikhatov, M.A., Shurkin, K.A., Aksenov, E.M., *et al.*, New Stratigraphic Scale of the Precambrian in USSR, *Izv. Akad. Nauk SSSR, Ser. Geol.*, 1991, no. 4, pp. 3 - 16.

Sergeev, V.N., Silicified Microfossils of the Precambrian in the Urals and Kazakhstan, and Their Biostratigraphic Implication, *Izv. Akad. Nauk SSSR, Ser. Geol.*, 1991, no. 11, pp. 87 - 97.

Sergeev, V.N., *Okremnennye Mikrofossilii Dokembriya i Kembriya Urala i Srednei Asii* (Silicified Microfossils of the Precambrian and Cambrian in the Urals and Central Asia), Moscow: Nauka, 1992.

Sergeev, V.N., Silicified Ripfean Microfossils of the Anabar Uplift, *Strat. and Geol. Correlation*, 1993, vol. 1, no. 3, pp. 264 - 278.

Shenfil', V.Yu., *Pozdnii Dokembrii Sibirskoi Platformy* (Late Precambrian of the Siberian Craton), Novosibirsk: Nauka, 1991.

Shenfil', V.Yu., Yakshin, M.S., Kats, A.G., and Frolova, Z.B., Detailing of the Upper Part of the Riphean Sequence in the Olenek Uplift, *Pozdnii Dokembrii i Rannii Paleozoi Sibiri. Vend i Rifei* (Late Precambrian and Early Paleozoic in Siberia: Vendian and Riphean), Novosibirsk: IGIG SO Akad. Nauk SSSR, 1988, pp. 20 - 36.

Shpunt, B.R., Shapovalova, I.G., Shashkina, E.A., *et al.*, *Proterozoi Severo-Vostochnoi Okrainy Sibirskoi Platformy* (Proterozoic of the Northeastern Margin of the Siberian Craton), Novosibirsk: Nauka, 1979.

Strother, P.K., Knoll, A.H., and Barghoorn, E.S., Microorganisms from the Late Precambrian Narssärssuk Formation, North-Western Greenland, *J. Paleontol.*, 1983, vol. 26, pp. 1 - 32.

Yakshin, M.S., On the Problem of the Microfabric Origin in the Early Riphean Stratified Stromatolites, *Iskopaemye Problematiki SSSR* (Fossil Problematics in the USSR), Moscow: Nauka, 1990, pp. 5 - 13.

Yakshin, M.S., *Vodoroslevaya Mikrobiota Nizhnego Rifeya Anabarskogo Podnyatiya* (The Lower Riphean Algal Microbiota from the Anabar Uplift), Novosibirsk: Nauka, 1991.

Yin Leiming, Microbiotas of Latest Precambrian Sequences, *Stratigraphy and Paleontology of the Systemic Boundaries in China: Precambrian-Cambrian Boundary I*, Nanjing: Nanjing Univ., 1987, pp. 415 - 494.

Zang, W. and Walter, M.R., Latest Proterozoic Plankton from the Amadeus Basin in Central Australia, *Nature*, 1989, vol. 337, pp. 642 - 645.

Zhang, Y., Proterozoic Stromatolite Microfloras of the Gaoyuzhuang Formation (Early Sinian: Riphean), Hebei, China, *J. Paleontol.*, 1981, vol. 55, pp. 485 - 506.

Zhang, Y., Coccoid Microfossils from the Doushantou Formation (Late Sinian) of Southern China, *Precambrian Res.*, 1985, vol. 28, pp. 163 - 173.

Stratigraphy and Geological Correlation, Vol. 2, No. 1, 1994, pp. 34 - 39. Translated from Stratigrafiya. Geologicheskaya Korrelyatsiya, Vol. 2, No. 1, 1994, pp. 39 - 45.
Original Russian Text Copyright © 1994 by Koren'.
English Translation Copyright © 1994 by Interperiodica Publishing (Russia).

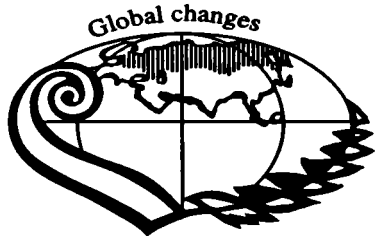

Evolution of the biosphere

Dynamics of Graptolite Diversity across the Wenlock–Ludlow Boundary

T. N. Koren'

All-Russian Institute of Geology, Srednii pr. 74, St. Petersburg, 199026 Russia

Received December 23, 1992

Abstract – Developmental dynamics of graptolites from the Tyan'-Shan' pelagic facies crossing the Wenlock–Ludlow boundary seem to display their global taxonomic and morphological changes thoroughly. This is caused by the cosmopolitan distribution of many taxa, and is evident as a result of the exceptional thoroughness of biostratigraphic material. A final stage of the mass extinction, the crisis state of the group, and its subsequent recovery period were particularly well-documented within the time interval between the *dubius/nassa* and the *nilssoni/colonus* zones. The *lundgreni* extinction event eliminated the taxonomically and morphologically diverse monograptid and plectograptid fauna, which had evolved since the end of the Llandovery. During the post-crisis period, the taxonomic composition of Homerian graptolites and trends in their morphological changes varied considerably. As a whole, this time interval was characterized by the survival of conservative taxa followed by their population growth. Later, begining with the *sherrardae* zone, they gave rise to a new, more specialized species of a limited time range. Several phyletic lines of morphologically monotonous monograptids evolved simultaneously during the late Homerian time, when the plectograptid fauna reached its maximum morphologic and taxonomic diversity. The evolution of these taxonomic or morphoecological groups during the early Ludlow also displayed opposite tendencies. The diversity of the monograptid species increased at the expense of the plectograptid species. It is likely that graptolites with continuous and reticular periderms adopted differently to environmental changes during the ecological crisis.

Among the Silurian plankton fauna, graptolites are of primary value in the reconstruction of the main taxonomic and morphological diversity through time. Their high evolutionary rate, extensive distribution areas, and comprehensive paleontological material, as well as detailed zonal subdivision and correlation of the enclosing rocks, help to determine the range and trends of specific and inter-regional changes.

An analysis of the taxonomic composition of successive zonal assemblages shows that the evolution of Silurian graptolites was interrupted by several biotic crises of various scales. These crises resulted in sharp or critical falls in diversity, altering the further development of graptolites. Extinction events differed from each other in their character (sudden or step wise) and in the degree of pre-crisis fauna diversity, and could be selective in respect to any taxon or ecological group. Every extinction event was followed by subsequent recovery stages having different recovery rates. In general, from the late Llandovery to the end of the Silurian the diversity of the graptolite genera and species decreased (Koren', 1987; Koren' and Rickards, 1979).

The most informative models of the diversity of graptolite dynamics can be reconstructed for the periods when the group underwent the whole development cycle, from mass extinction and the subsequent crisis (Walliser, 1988) to a new diversity maximum. The Homerian–Gorstian interval yields the most complete information concerning the succession and character of biological events in graptolite evolution. We were able to recognize synchronous extinction events, morphological innovations, adaptive radiation, and speciation stages in several simultaneously developing phylogenetic lines on a global scale.

The graptolite crisis at the end of the *lundgreni* zone was recognized in the earliest period of study of the late Wenlockian graptolites, when the *lundgreni* and the *ludensis* zones were established in Great Britain. Respectively, the base of the *ludensis* / = *vulgaris*, (Wood, 1900) zone was suggested to be the Wenlock–Ludlow boundary, and thus also the upper-lower Silurian boundary. The event at the top of the *lundgreni* zone was confirmed by later studies of many sections in Eurasia, North Africa and North America, where the detailed zonal subdivision of the upper Wenlockian and the lower Ludlowian beds was established (Koren' *et al.*, 1986; Koren' and Rinenberg, 1988; Jaeger, 1989, 1991; Koren', 1992; Lenz, 1980). New biostratigraphical data

concerning the composition and distribution of the Homerian graptolites were recently obtained from the pelagic deposits of the Alai ridge, Central Asia. This data enables us to estimate general regularities in the evolution of cyrthograptid, monograptid, and plectograptid forming cosmopolitian graptolite fauna at the Wenlock–Ludlow boundary (Koren', 1991, 1992). In comparison with those known in other regions, the Alaian graptolites of the *sherrardae–ludensis* zonal interval are extremely diverse. Their assemblages include not only new species, but also monograptids characteristic of the European, Arctic, and Australian sequences. This fauna provides the best opportunity for interregional correlations.

The upper Wenlockian–lower Ludlowian graptolite-bearing beds in the Southern Tyan'-Shan' consist of different calcareous and clastic rock facies. Black claystones with calcarenite lenses comprise continuous sequences in the lower parts of the Kursala and Irdzhilga formations occurring on the northern and southern slopes of the Alai ridge and have the most complete faunal characteristics (Fig. 1). The most complete graptolite sequence was studied in the Kursala Formation exposed along the Peshkaut and Yangiaryk streams and near the Tul' settlement. The diversity of graptolites collected from seven measured sections was analyzed at a species level. The Homerian fauna includes more than 35 species, 14 among them belong to the *Monograptus* genus. The sections within the studied area (about 100 km east to west) were correlated using the biostratigraphic data combined with the results of detailed structural mapping.

Detailed collections of graptolites from the condensed sections enabled us to obtain a succession of the upper Wenlockian graptolite comparable to that of the European sequences (Jaeger, 1991). The *lundgreni/testis*, *dubius/nassa*, *sherrardae* (*praedeubeli*), *deubeli*, and *ludensis* zones were recognized with their boundaries defined according to the diagnostic species appearance, extinction events, and population bursts of some transit species.

A comparison of the mass extinction event at the top of the *lundgreni/testis* zone with other Silurian events of sharp diversity falls established the former event as one of the most significant biotic crises (Koren', 1987; Jaeger, 1991). It divides the late Wenlockian graptolites into two distinct assemblages, the early and late Homerian, which are different in taxonomic composition and morphological diversity. The early Homerian monograptid fauna of the *lundgreni/testis* zone contain the last representatives of the *Monoclimacis vomerina*, *Monograptus priodon*, and *Pristiograptus dubius*

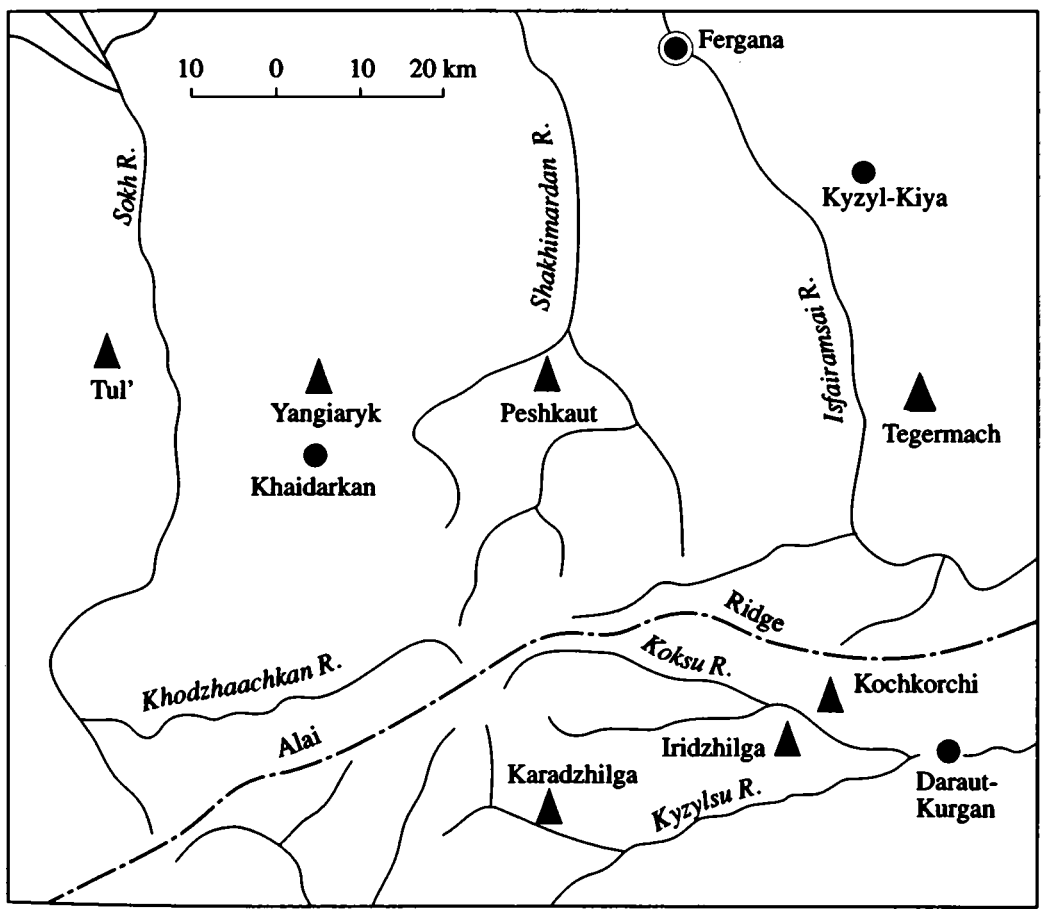

Fig. 1. Localities of the Wenlockian–Ludlowian boundary sections on the northern and southern slopes of the Alai Ridge.

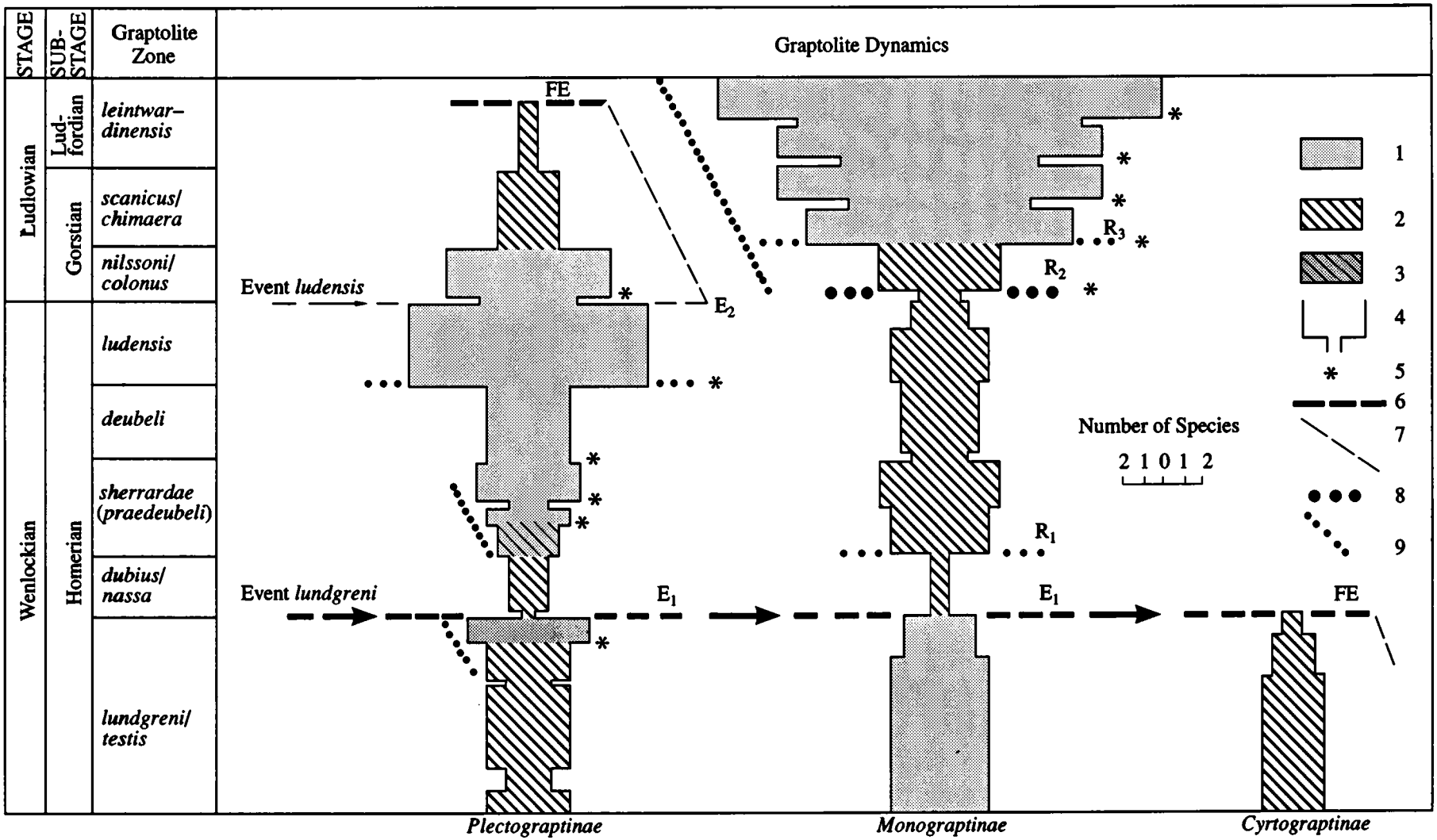

Fig. 2. Dynamics of the graptolite morphological and taxonomic diversity in the Homerian and Gorstian times.

1, 2, 3 – maximum, minimum, and average morphological diversity; 4 – taxonomic diversity; 5 – introduction of new morphological features; 6 – mass extinction event; 7 – phase of gradually declining diversity; 8 – radiation event; 9 – phase of gradually increasing diversity; E – extinction; R – radiation; FE – final extinction.

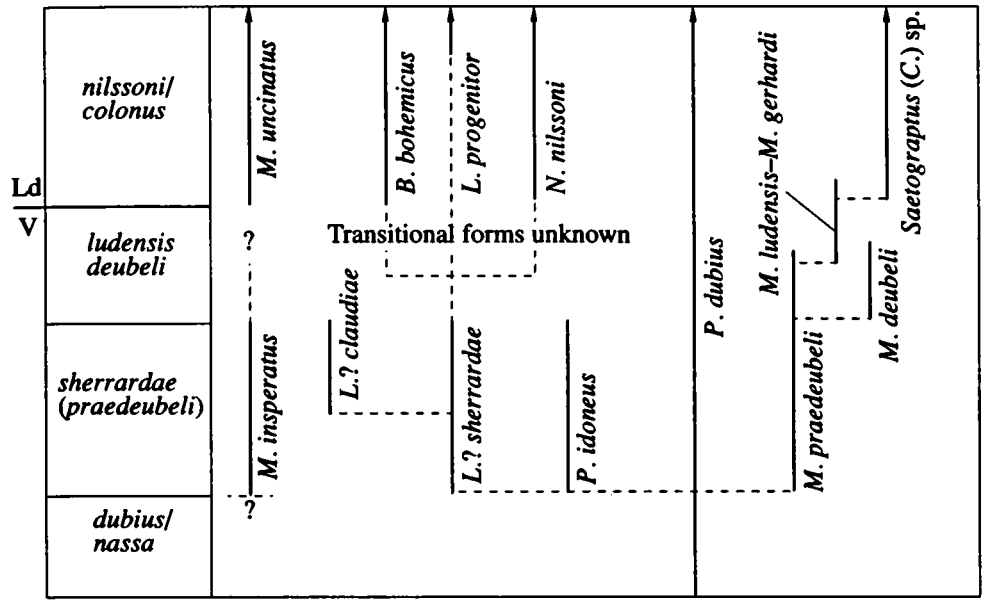

Fig. 3. Stratigraphic distribution of the Homerian and lower Gorstian diagnostic taxa of monograptids in the lower part of the Kursala Formation, northern slopes of the Alai Ridge.

groups, which were widespread and known since the end of Llanodovery and the beginning of Wenlock. Some of them were characteristic only of this time interval (*Monoclimacis flumendosae* and *Monograptus testis*), others are also known from the underlying Sheinwoodian deposits (*Monograptus flemingii* and *Pristograptus dubius*). They were associated with short-ranging cyrtograptids and plectograptids characteristic of the *lundgreni/testis* zone. In general, the structure and forms of rhabdosome, theca, and aperture apparatus vary within the fauna. Nevertheless, only several taxa of cyrthograptids may be considered specialized forms.

The biotic crisis at the end of the *lundgreni/testis* zone affected all morphological and morphoecological groups of the Wenlockian graptolids (Fig. 2). During this short time interval the last colonies of multibranched, complicated cyrthograptids disappeared. This event also eliminated nearly all simple monograptid morphotypes, save the most primitive *Pristiograptus dubius* group. Later this group formed the main ancestral stock, which gave rise to the more specialized late Homerian–early Gorstian lines. The diverse and specialized plectograptid fauna also became extinct, with only one taxon (*Plectograptus praemacilentus*) passing into the upper Homerian beds. As a whole, the *lundgreni* extinction event was massive and sudden. The morphologically diverse and specialized taxa became extinct on a global scale.

Taxonomic composition and morphologic evolution changed significantly in the post-crisis period. In all the known localities, an assemblage of the *dubius/nassa* zone (Fig. 2) is the least diverse (2 - 3 species). Other characteristic features of the post-crisis period were manifested at a population level and expressed in sharp increasing of abundance of the transit *Pristiograptus dubius* and newly appeared *Gothograptus nassa* species. The first speciation events at the base of the *sherrardae* zone indicate the beginning of the new diversification stage. A relatively frequent appearance of new short-lived taxa resulting from adaptive radiation and phyletic evolution was common within this zone.

The plectograptyd and monograptid evolution in the post-crisis time (*sherrardae–ludensis* zones) had different trends. Only preliminary data on the late Homerian plectograptyd taxonomic composition are available, though this group was the most abundant and diverse within the *sherrardae* and *ludensis* zones. In studied sections, this group is represented by numerous, but flattened imprints. It requires a detailed study of the morphologically complicated reticular rhabdosomes, which includes a comparative paleontological analysis of volumetric plectograptid specimens. Using determinations of more than twenty new species from the Kursala Formation, it is only possible to outline the general trends in the evolution and dynamics of diversity of the *Gothograptus*, *Agastograptus*, and *Plectograptus* genera. At the beginning of the *sherrardae* zone, the plectograptid stock split, and a diverse plectograptid fauna was formed as a result of the introduction of several new morphological characteristics. This fauna was mainly represented by specialized, short-ranged taxa of several phyletic lines. Another stage of plectograptid diversity, at which the group reached its last maximum diversification, occurred within the late Homerian *ludensis* zone. This group was prevalent in the graptolite assemblages of the latest zone of the Homerian, being the most abundant and taxonomically diverse. Unlike plectograptids, the contemporaneous post-crisis

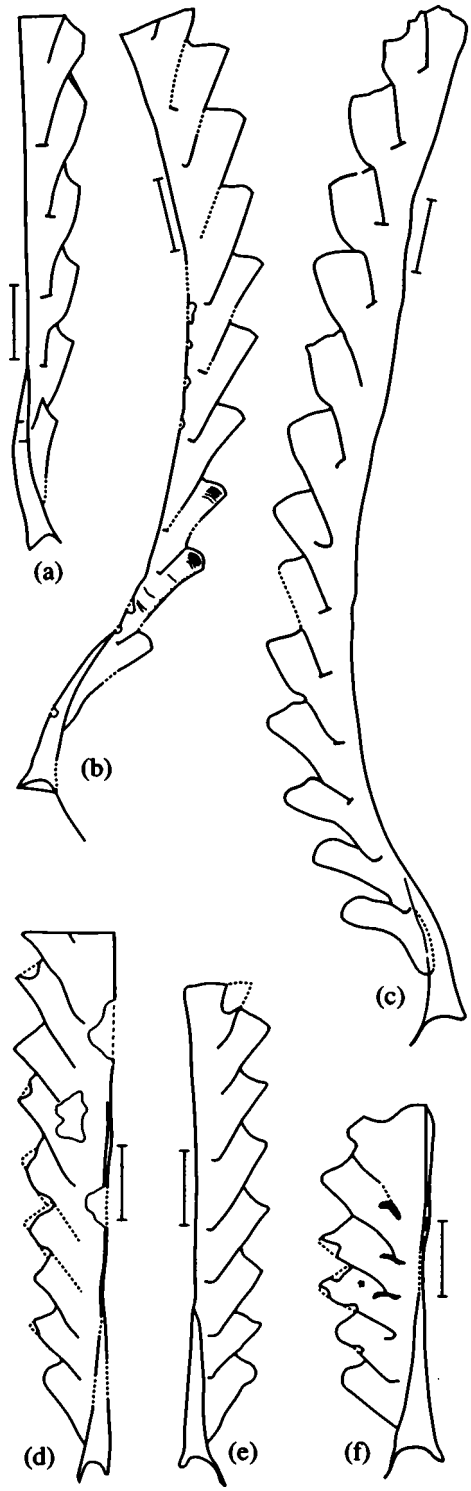

Fig. 4. (a) *Pristiograptus idoneus* Koren; (b) *Lobograptus*? *sherrardae* (Shevrin); (c) *L.*? *claudiae* Koren; (a), (b), (c) Peshkaut stream, Kursala Formation, *sherrardae* zone; (a), (b) section 26 A; (c) section 24; ×10; (d) *Monograptus praedeubeli* Jaeger, an extreme form with a relatively straight sikula; (e) *Monograptus deubeli* Jaeger, the extreme form with a sikula slightly widening near the aparture, Nura-Tau ridge, Mershikor beds, specimen 713/2 and 614/9, *deubeli* zone, ×10; (f) *M. deubeli* Jaeger, Tul' settlement, Kursala Formation, *deubeli* zone, specimen 10-7, ×10.

monograptids were morphologically uniform, having introduced into their evolution only one morphological feature, the paired lateral eminences on the theca apertures. The species differs only by the degree of the prominence and persistence of this feature in the astogeny. Originally, these species seem related to the long-lived, conservative *Pristiograptus dubius*. The late Homerian monograptid assemblages of the Southern Tyan'-Shan' include species of phyletic lines that evolved in local basins, and only a small admixture of immigrants.

Morphological changes seen in the available paleontologic material allows us to reconstruct at least three evolutionary lines, which appeared nearly simultaneously close to the base of the *sherrardae* zone, as indicated by biostratigraphic data (Fig. 3).

The first line corresponds to the stratigraphic and morphological succession of three species: *Pristiograptus idoneus*, *Lobograptus*? *sherrardae*, and *L.*? *claudiae* found in the lower part of the Kursala Formation (Fig. 4). The morphological transformations occur as follows:

(1) A transition from *P. dubius* to *P. idoneus* was accompanied by a narrowing and appearing of smooth dorso-ventral bending of the extreme proximal combined with the ventral bend of the sikula.

(2) The transformation of *P. idoneus* into *L.*? *sherrardae* was characterized by a sharp enlargement of the metasikula aparture along with the appearance of dorsal rhabdosome bend and minor dorsal eminences on the theka apertures. According to theka and rhabdosome structure, *L.*? *sherrardae* resembles the early Ludlowian *Neodiversograptus nilssoni* and *Lobograptus progenitor*, thus suggesting possible genetic relations.

(3) At its appearance, *L.*? *claudiae* did not differ from its ancestral form *L.*? *sherrardae* in sikula and rhabdosome structures, but its extreme proximal thekas was of an uncommon rastrit-like form. *L.*? *claudiae* is considered to be a lateral terminal branch of the described line. The distinct specialization of the first thekas and a narrow stratigraphic range of the taxon coexisting with the late *L. sherrardae* (Fig. 3) verified this conclusion.

The second filogenetic line originating from the same conservative *P. dubius* stock is inferred from the succession of *Monograptus praedubelli*, *M. deubelli* (lateral branch), *M. ludensis*, and *M. gerhardi* species. It was recognized for the first time in the european and north-african sections (Jaeger, 1959; Barka and Jaeger, 1989; Koren', 1991), and later, in the sections of Arctic Canada, Russia and southern Tyan'-Shan'. Main variations are expressed in the introduction of new morphological features, paired lateral lobes on the aparture of the extreme proximal thekas, and then by their subsequent size variations and the degree of penetration in the colony. The sikula form also changed considerably, from a straight to the ventrally curved one, or one sharply expanding near the aparture (Fig. 4).

Thus far, the third phylogenetic line of the late Homerian monograptids is represented by the *Monograptus*

insperatus species known only from the Kursala Formation of the northern slope of the Alai ridge. It is characterized by well-developed lateral aperture lobes in all rhabdosome thekas. This feature was unknown in monograptid evolution until the late Ludlowian–early Przhidolian.

First and second phylogenetic lines had high evolution potential, being ancestral for main stocks of the early Ludlowian monograptids, linograptids, cucullograptids, and neocucullograptids. The third line has a cryptogenic origin. Its relations with the morphologically similar monograptid fauna of the Ludlowian and Przhidolian are unknown.

The evolutionary dynamics of monograptids and plectograptids during the late Homerian had opposite tendencies (Fig. 2). At the beginning of the *deubeli* zone, monograptid diversity was reduced to 2 to 3 species and remained at that level till the end of the *ludensis* zone. At the same time, plectograptids attained their maximum morphological and taxonomic variability within the *ludensis* zone, being the most abundant members of populations of that time interval as well. Mono- and plectograptid evolutionary bio-events contrasted extremely across the *ludensis–nilssoni/colonus* zones boundary and during the early and late Ludlow times. Recent data obtained in the Southern Tyan'-Shan' provided evidence that at the end of the *ludensis* zone, the ancestral stock of Homerian monograptids (*M. ludensis* and *L.? sherrardae*) split, giving rise to a new progressive monograptid fauna (Urbanek, 1966, 1970, 1992). It reached its maximum morphological and taxonomic diversity at the beginning of the *leintwardinensis* zone. In addition, the top of the *ludensis* zone was marked by an evident extinction of various short-lived plectograptids, which lost their dominant role among the early Ludlowian graptolite assemblages. Since the start of the *nilssoni/colonus* zone they gradually declined and finally became extinct at the time of the *leintwardinensis* zone. The revealed differences suggest that the Monograptinae and Plectograptinae subfamilies were morphological groups, which ecologically replaced each other in the graptolite habitats. The decrease of monograptids species was compensated by an increase in the abundance of plectograptid species in the late Homerian; while in the early Ludlowian the situation was opposite. It seems that graptolites with solid and reticular periderms had different abilities to adapt to environmental changes in the course of ecological crises.

Graptolites from the Tyan'-Shan' pelagic sediments show that the dynamics of their evolution across the Wenlock-Ludlow boundary reflects rather completely global changes in taxonomic and morphological graptolite diversity on species and zonal levels. This is caused by the cosmopolitan distribution of many taxa and comprehensive biostratigraphic material.

REFERENCES

Barca, S. and Jaeger, H., New Geological and Biostratigraphical Data on the Silurian in SE-Sardinia. Close affinity with Thuringia, *Bull. Soc. Geol. Ital.*, 1989, vol. 108, pp. 565 - 580.

Jaeger, H., *Graptoliten und Stratigraphie des Jungsten Thuringer Siluris*, Berlin: Abh. Dtsch. Akad. Wiss., 1959, no. 2.

Jaeger, H., Graptolite Fauna Turnover and the Revised Graptolite Zonation across the Wenlock–Ludlow Boundary, *The Murchison Symp.: An Int. Symp. on the Silurian System, Programme and Abstracts*, Univ. of Keele, UK, 1989, pp. 49 - 50.

Jaeger, H., Neue Standard-Graptolithenzonenfolge nach der "Grossen Krise" an der Wenlock/Ludlow Grenze (Silur), *Neueg. Jaurb. Geol. Palaont. Abhandl.*, 1991, vol. 182, no. 3, pp. 303 - 354.

Koren', T.N., Graptolite Dynamics in Silurian and Devonian Time, *Bull. Geol. Soc. Denmark*, 1987, vol. 35, pp. 149 - 159.

Koren', T.N., The Lundgreni Extinction Event in Central Asia and Its Bearing on Graptolite Biochronology within the Homerian, *Proc. Estonian Acad. Sci., Geol.*, 1991, vol. 40, pp. 74 - 78.

Koren', T.N., Extinctions and Recoveries of Graptolite Faunas in Late Wenlock through Ludlow, *Phanerozoic Global Bio-Events and Event-Stratigraphy: 5th Int. Conf. on Bio-Events*, Göttingen, 1992.

Koren', T.N., Klishevich, V.L., and Rinenberg, R.E., Reference Section of the Upper Silurian and the Lower Devonian Beds in the Southern Fergana, *Sov. Geol.*, 1986, no. 11, pp. 62 - 74.

Koren', T.N. and Rickards, R.B., Extinction of the Graptolites, *The Caledonides of the British Isles – Reviewed*, Harris, A.L., Holland, C.H., and Leake, B.E., Eds., Edinburgh: Scottish Acad., 1979, pp. 457 - 466.

Koren', T.N. and Rinenberg, R.E., Lundgreni Event in the Late Wenlock Pelagic Beds of the Southern Tyan'-Shan', *Graptolity v Istorii Zemli: Tezisy Dokladov V Simpoziuma po Izucheniyu Graptolitov v SSSR* (Graptolites in the Earth's History: Abstacts of the V Symp. on Graptolite Study in USSR), Vil'nyus, 1988, pp. 11 - 14.

Lenz, A.C., Wenlockian Graptolite Reference Section, Clear-Water Creek, Nahanni National Park, Northwest Territories, Canada, *Canad. Earth. Sci.*, 1980, vol. 17, no. 8, pp. 1075 - 1086.

Urbanek, A., On the Morphology and Evolution of the *Cucullograptinae* (*Monograptidae*, *Graptolithina*), *Acta Palaeontol. Polon.*, 1966, vol. 11, nos. 3, 4.

Urbanek, A., *Neocucullograptinae* n. Subfam. (Graptolithina) – Their Evolutionary and Stratigraphic Bearing, *Acta Palaeontol. Polon.*, 1970, vol. 15, nos. 2, 3.

Urbanek, A., The Biotic Crisis in the History of Upper Silurian Graptolites, *Phanerozoic Global Bio-Events and Event-Stratigraphy: 5th Int. Conf. on Bio-Events*, Göttingen, 1992.

Walliser, O.H., The Bilbao Conference "Palaeontology and Evolution: Extinction Events": A Big Step Forvard in Understanding Exceptional Global Changes, *Rev. Esp. Paleontologia*, 1988, no Extraordinario, pp. 5, 6.

Wood, E.M.R., The Lower Ludlow Formation and Its Graptolite Fauna, *Quart. J. Geol. Soc. London*, 1900, vol. 56, pp. 415 - 492.

Stratigraphy and Geological Correlation, Vol. 2, No. 1, 1994, pp. 40 - 48. Translated from Stratigrafiya. Geologicheskaya Korrelyatsiya, Vol. 2, No. 1, 1994, pp. 46 - 54.
Original Russian Text Copyright © 1994 by Bol'shakova, Gekker, Goryunova, Dubatolov, Ivanovskii, Kosmynin, Luchinina, Sokolov, Tesakov.
English Translation Copyright © 1994 by Interperiodica Publishing (Russia).

Evolution of the biosphere

Paleozoic Coral Reefs in Russia

L. N. Bol'shakova*, M. R. Gekker*, R. V. Goryunova*, V. N. Dubatolov, A. B. Ivanovskii*, V. N. Kosmynin*, V. A. Luchinina**, B. S. Sokolov*, and Yu. I. Tesakov****

**Paleontological Institute, Russian Academy of Sciences, ul. Profsoyuznaya 123, Moscow, 117647 Russia*
***United Institute of Geology, Geophysics, and Mineralogy, Siberian Branch of Russian Academy of Sciences, Universitetskii pr. 3, Novosibirsk, 630090 Russia*

Received January 26, 1993

Abstract – The earliest reef ecosystems were primitive and were insignificant in the relief formation. A change in the reef building occurred in the Phanerozoic, when organisms secreting or accumulating $CaCO_3$ appeared. The first structures were frameless, having been formed by algae and spongiomorphids. Framework structures, which appeared in the middle Ordovician, characterized the most complicated ecosystems. In the Paleozoic, the principal skeleton-building organisms were algae, stromatoporoids, corals, and bryozoans.

Using both our own and other available data, this paper presents general characteristics of principal organisms building the Paleozoic biogenic carbonate structures: algae, stromatoporoids, corals, and bryozoans.

The earliest ecosystems were primitive and played a minor role in relief formation. The corresponding $CaCO_3$ accumulation was maintained only in narrow-ranged environmental conditions. Nevertheless, this was sufficient for the compensated accumulation of significant carbonate deposits.

In the Phanerozoic, the marine biogenic relief-forming process changed after the appearance of many organisms secreting or accumulating $CaCO_3$. The first carbonate structures were frameless and formed with organisms such as algae and spongiomorphids. Both groups were responsible for the sedimentation of suspended and transported (predominantly pelitomorphic) material and the accumulation of their skeletal $CaCO_3$. Muddy mounds formed by these organisms were not more than a few meters in height. These ecosystems were zoned, and successive in the vertical section, which made them similar to the later "reefs." So, as they grew toward the sea surface, the biogenic structures first formed by algae may pass finally to the shallow-water stromatolitic sedimentation (Ahr, 1971).

The frameless structures of the early Paleozoic were located in the shallow shelf areas affected by low-energy waves. The range of conditions under which these structures were formed was considerably narrower than that for recent framework structures, but much wider than that for stromatolites. In addition to the "relief builders," the early Paleozoic frameless ecosystems were inhabited by echinoderms, trilobites, brachiopods, and other organisms. This also indicates complications in the ecosystem. The corresponding structures can be traced up to recent times and show a replacement of one algal taxa by others, up to the presently existing geniculate chlorophites and rodophites inclusive, and of one faunal group by others.

Framework structures, which appeared in the middle Ordovician, characterize the most complicated and highly ordered ecosystems and, thus, the most intensive accumulation of $CaCO_3$. This may be related to the diversification of colonial organisms such as stromatoporoids, corals, and bryozoans present at that time. Along with other advantages, colonial life provides a high rate of skeletal organism formation owing to more complete systems of nutrition, reproduction, and regeneration of organisms as well as their ability to adapt environments transforming them into more hospitable conditions. This ability is more evident after framework building and relief formation, i.e., at the level of a reef ecosystem or a similar biogenic structure. The adaptation trends toward a conditional differentiation and an increase in environmental gradients. This results in a compound system of highly stratified ecological niches and numerous feedbacks, and subsequently a stable ecosystem. The framework building can affect the physical and chemical environmental parameters: illumination intensity, hydrodynamics, ground inclination, water saturation with $CaCO_3$, etc. Reefs and other biogenic structures most clearly dem-

onstrate the Gaia hypothesis (Lovelock and Margulis, 1973), which occurs at an ecosystem level lower than the biosphere as a whole. One of the principal reef-builders, the lime-producing colonial cnidarians, are characterized by an extremely low biomass per surface unit. Considering the energy required for organism activity and the intensification of its life processes, particularly the secretion of $CaCO_3$, this is advantageous.

We are, at present, unaware of what radical, environmental changes caused the near synchronous appearance of all the principal Paleozoic reefbuilders. However, this is considered to be one of the most important problems concerning biosphere evolution, equivalent to that of the appearance of Vendian multicellular and ancient skeletal organisms.

From the middle Ordovician, and continuing through the Phanerozoic, different skeleton-forming organisms played, alternately, major and minor roles in the formation of the biogenic structure, as indicated by some of the groups discussed below. But the functioning principle of a reef ecosystem remained unchanged owing to the ecosystem efficiency and peculiarities of colonial organisms.

Calcareous algae. Blue-green, green and red algae become calcified in their lifetime. Their representatives are known to have existed both in the Precambrian and in the Paleozoic.

The blue-green algae include calcibionts, which have no recent analogues. Their calcareous sheaths were formed around filaments, cells, and colonies. Only the outer envelope of the alga remains preserved, reflecting a filament form without traces of cellular texture. Fossil green algae are representatives of the Siphonophyceae class. They have calcified sheaths of siphons, peripherical ramifications, utricules, and sporangia as well as voids between these elements. Outer thalline parts are mineralized higher than inner ones. Red algae display calcified outer parts of the thallome; the structural details are preserved perfectly. The earliest calcibionts were found in the upper Vendian strata. Widespread in the Cambrian, they built abundant biogenic structures, usually without animal participation. The first *Solenopora* appeared in the late Cambrian. Together with *Parachaetetes*, which appeared later, they were the only representatives of red algae during the Ordovician, Silurian, and Devonian. Rare green algae Seletonellaceae and Dasyporellaceae also occur first in the Cambrian strata.

Scarce algal flora of the early Ordovician had an inherited character. Calcibionts *Garwoodia*, *Hedstroemia*, *Ortonella*, and others. occurred universally in the middle and late Ordovician. Since that time, the green algae *Vermiporella*, *Dasyporella*, *Apidium*, *Mastopora*, and others became abundant.

The Silurian biogenic structures were formed mainly by the calcibionts *Renalcis* and *Fistuella.* In the late Silurian, the reef-forming process abated. The algal assemblage includes only calcibionts (*Girvanella* and *Rothpletzella*) and less abundant red algae (*Solenopora*). The early Devonian shows the same trend of predominant calcibionts and a poor diversity of Siphonophyceae. In the middle of the early Devonian the situation changed and an unprecedented diversity of Siphonophyceae (Lanciculaceae, Dimorphosiphonaceae, and Dasycladaceae) is evident against the background of conservative Cyanobacteriae.

The Siphonophyceae orders – Siphonales, Dasycladales, and Siphonocladales diversified during the middle and late Devonian – Lanciculaceae disappeared almost completely.

The Carboniferous is characterized by abundant green (particularly Palaeoberesellaceae) and red algae. The latter included, besides *Solenopora* and *Parachaetetes*, some representatives of *Katavella*. The calcibionts were of minor importance.

The early Permian marks the peak in the evolution of the green and red algae. The calcibionts *Tubiphytes* also played a major role in the reef formation.

Thus, the calcareous algae played a crucial role in Paleozoic reef-formation; the calcibionts dominated in the early Paleozoic, and the green algae in the late Paleozoic. The red algae became increasingly important in the late Paleozoic.

Stromatoporoids. The possibility that stromatoporoids began to occur in the middle Ordovician is supported by reliable evidence. At this time, they contributed actively to the formation of biogenic structures (variably-shaped bioherms up to several tens of meters in size). Together with the algae, they built frameworks by producing massive, semispherical, tabloid, domal, nodular, or platy colonies. In these cases, corals were repressed. In other bioherms, the stromatoporoids had a subordinate role, while the corals were principal reefbuilders. When the biogenic structures are only composed by stromatoporoids, their genus and species composition is extremely uniform. Molluscan shells and dead polyparia coral were commonly used by the stromatoporoids as a substratum. The Ordovician shows vesicular (*Cystostroma*, *Stromatocerium*, *Plumatalinia*, *Pachystylostroma*, *Forolinia*, *Rosenella*, and *Aulacera*) and laminar (*Ecclimadictyon* and *Clathrodictyon*) morphological types of caenostea. The stromatoporoids were accompanied by crinoids, bryozoans, brachiopods, and other organisms.

In the Silurian, the stromatoporoids became increasingly important reefbuilders. Sometimes they composed bioherms up to several hundred meters in diameter, which existed for a long time. As shown by Lecompte (1952), a structure may be built by different organisms whose activity varies among different stages of reef growth. At an early stage, the stromatoporoids were subordinate, the corals and algae dominated. Growing gradually in importance, the stromatoporoids became predominant at the terminal stages, superseding all the other organisms. Species of genera *Densastroma*, *Clathrodictyon*, *Pseudolabechia*, *Plumatalinia*, *Plectostroma*, *Labechia*, *Simplexodictyon*, and *Plexodictyon* were most abundant.

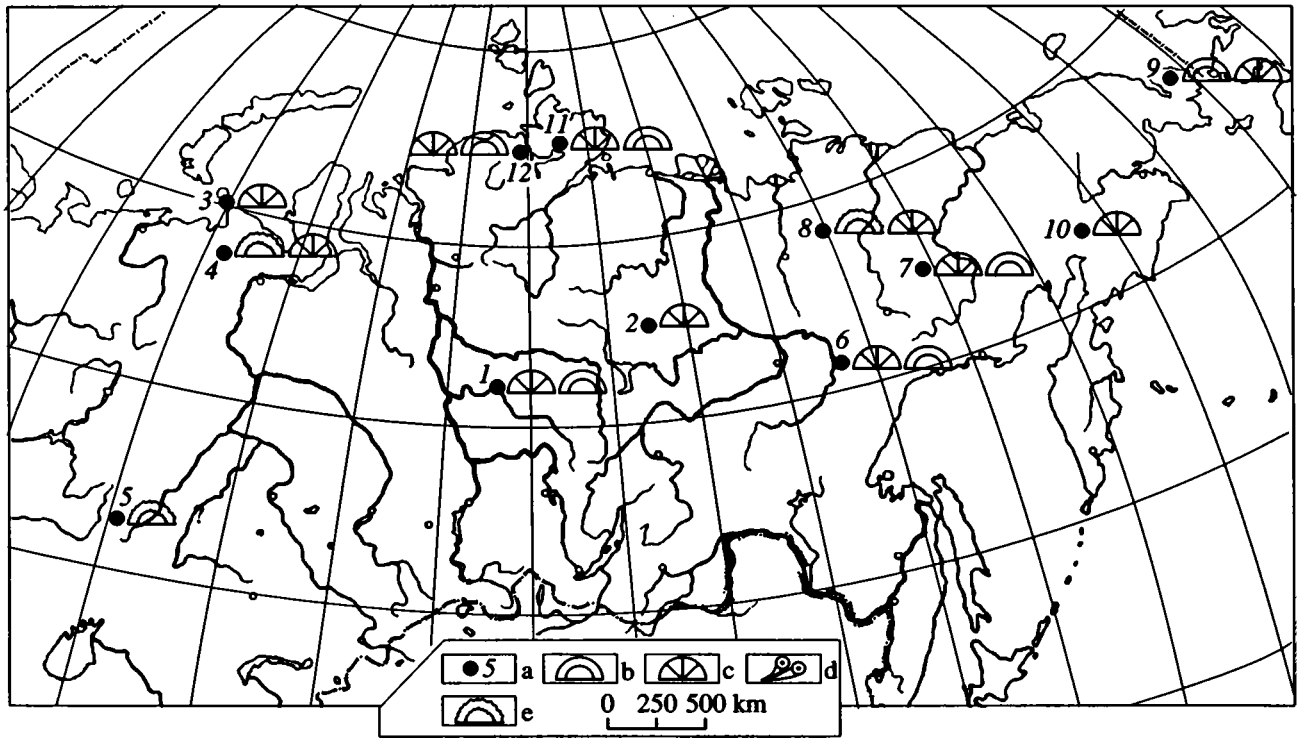

Fig. 1. Localities of the Ashgillian biogenic structures.

1, 2 – the Siberian platform: *1* – the Bol'shaya Nirunda and Nizhnyaya Chunku rivers and *2* – the Morkoka River; *3* – Vaigach Island; *4* – the Pai-Khoi Range, the Kozhim River basin; *5* – Southern Trans-Urals; *6* – the Sette-Daban Range; *7* – the Omulevka River basin, eastern Cherskii Range; *8* – the Tas-Khayakhtakh Range; *9* – the Chukotka Peninsula; *10* – the Koryak Upland, the Penzhinskii Range; *11* – the Taimyr Peninsula, the Parnaya River; *12* – the Nizhnyaya Taimyra River; a – localities; b – stromatoporoids; c – tabulates; d – rugoses; e – algae.

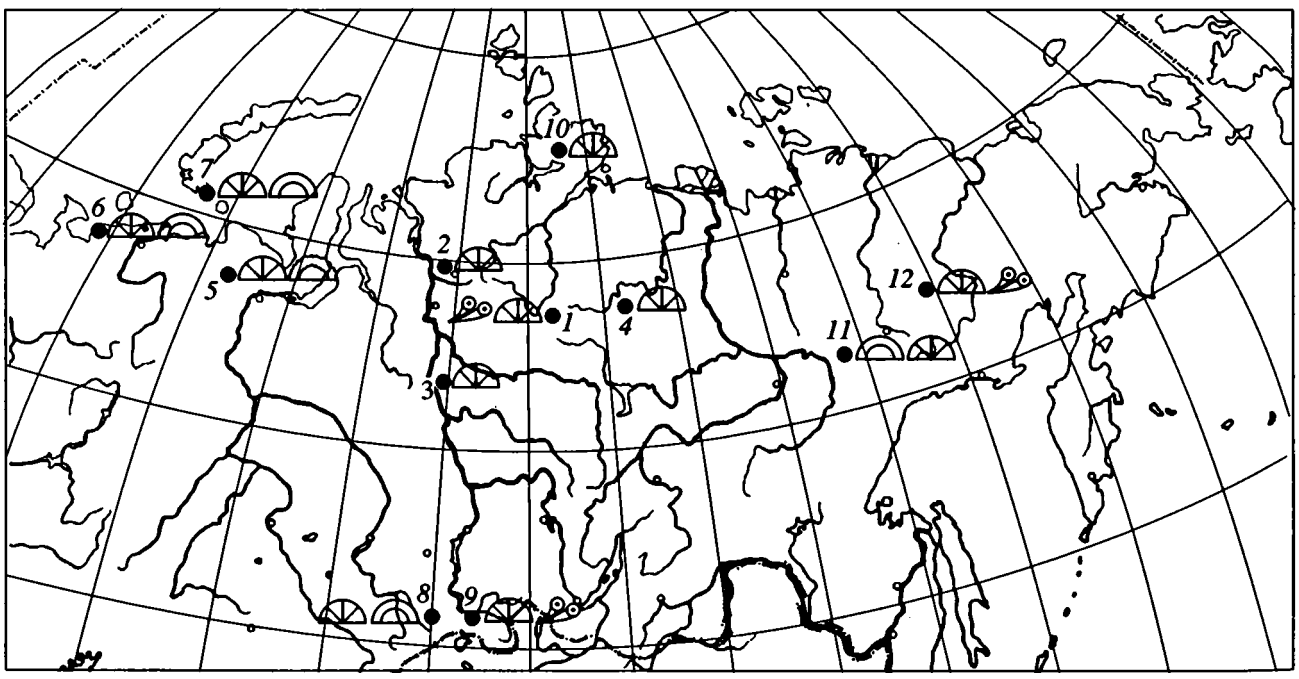

Fig. 2. Localities of the Llandoverian biogenic structures.

1 - 4 – the Siberian platform: *1* – the Moiero River, *2* – the Noril'sk region, *3* – the Bakhta River, and *4* – the Nizhnyaya Bol'shaya Kuonda River; *5* – the Pechora syneclise; *6* – Timan; *7* – Novaya Zemlya, the Khatanzeya Peninsula; *8* – Western Sayan; *9* – Tuva, a lower course of the Elegest River; *10* – the Taimyr Peninsula, the Parnaya River; *11* – the Sette-Daban Range, the Tompo–Vostochnaya Khandyga Interfluve; *12* – the Omulevka Mountains. For other symbols see Fig. 1.

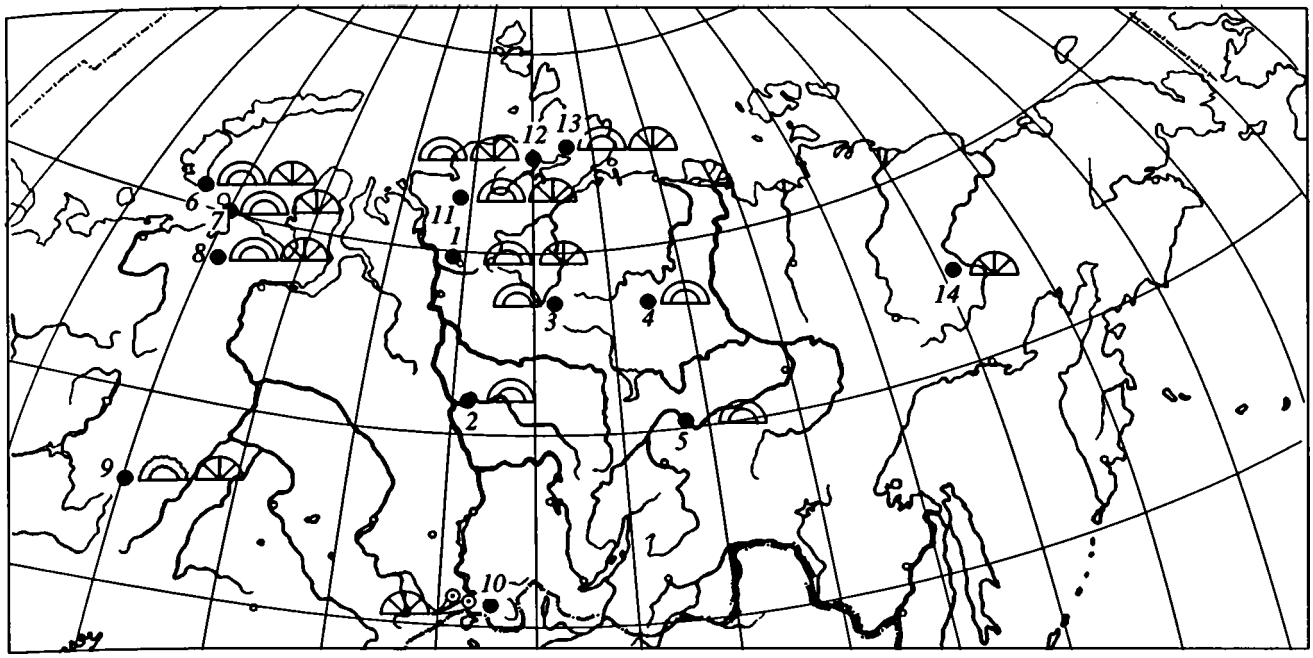

Fig. 3. Localities of the Wenlockian biogenic structures.

1 - 5 – the Siberian platform: *1* – the Noril'sk region, the Levyi Omnutakh River, *2* – the Kureika River, *3* – the Moiero River, *4* – the Nizhnyaya Bol'shaya Kuonda River, and *5* – the Lena River, 2 km upstream from the mouth of the Nyuya River; *6* – Novaya Zemlya, the Khatanzeya Peninsula; *7* – Vaigach Island; *8* – Western Urals, the Belaya–Elets zone; *9* – Eastern Urals, the Tagil–Magnitogorsk synclinorium; *10* – Tuva, a lower course of the Elegest River; *11* – the Taimyr Peninsula, the Tareya River; *12* – the Nizhnyaya Taimyra River, the Pryanaya River basin; *13* – the Parnaya River; *14* – the Omulevka Mountains, the Iryudi River basin. For other symbols see Fig. 1.

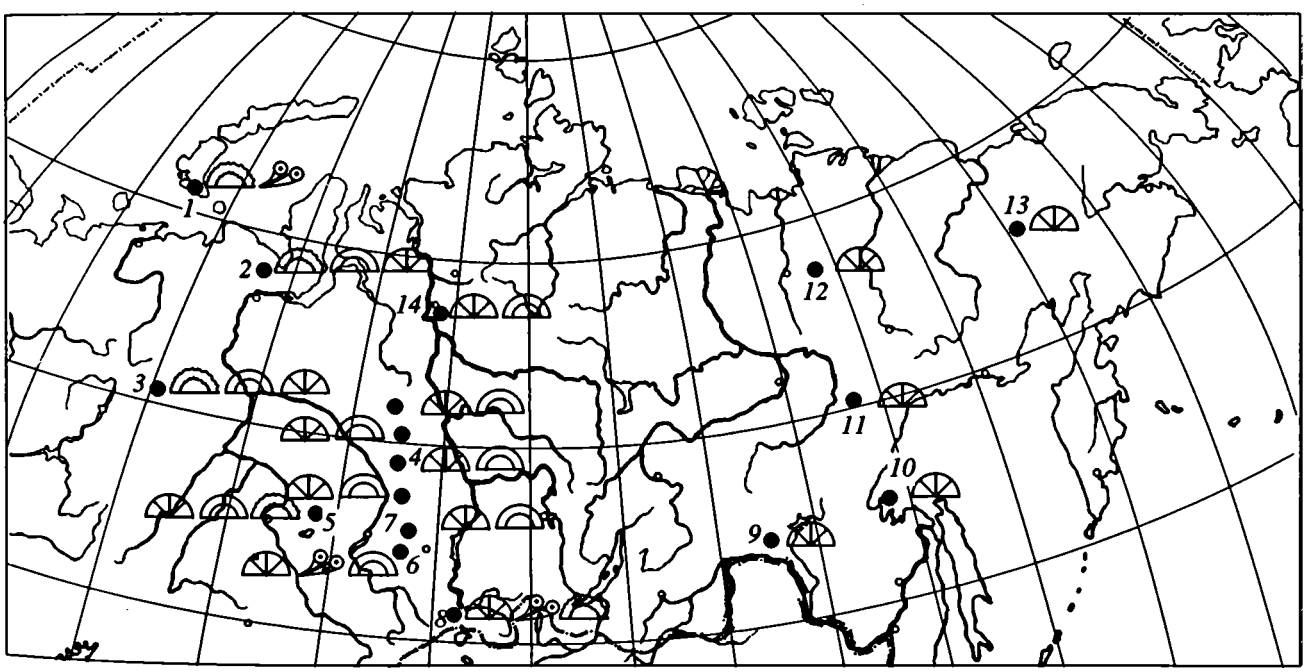

Fig. 4. Localities of the Givetian reefs and other biogenic structures.

1 – Novaya Zemlya, Yuzhnyi Island; *2* – the Polar Urals, the Usa, Bol'shaya Usa and Lek–Elets River basins; *3* – Northern Urals, the Central Tagil synclinorium, the Sos'va–Petropavlovsk zone; *4* – the jointing area of the Kolyvan'–Tom' trough and the Salair basin; *5* – the southeastern West Siberian plate, the Nyurol'ka basin; *6* – the northeastern Salair, the southwestern margin of the Kuzbass; *7* – the northern margin of the Kuzbass, the Anzhero-Sudzhensk region; *8* – the Minusinsk depression; *9* – the Amur–Okhotsk area, the Bol'shoi Ol'doi River basin; *10* – the Shantar Isles; *11 - 13* – the northeastern Asia, the Verkhoyan–Kolyma system: *11* – the Sette-Daban Range, *12* – the Tas-Khayakhtakh Range, and *13* – the Omolon massif, the Ush-Urakchan Range, the Talalakh River basin; *14* – the Siberian platform, the Noril'sk region. For other symbols see Fig. 1.

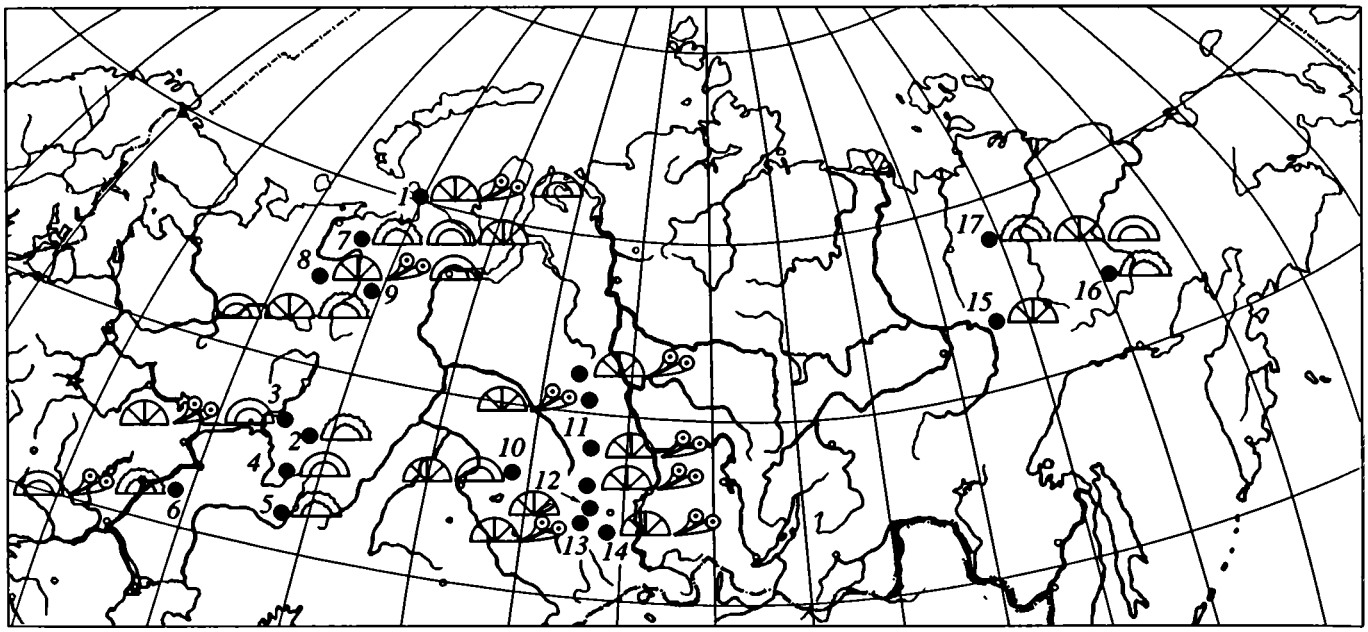

Fig. 5. Localities of the Frasnian reefs and other biogenic structures.

1 – Vaigach Island; *2* – the Middle Urals, the Chusovaya River basin; *3* – the eastern Urals–Volga region; *4* – Southern Urals, the Malyi Ik, Inzer, and Askyn River basins; *5* – the eastern slope of Southern Urals, western limb of the Magnitogorsk synclinorium; *6* – the Caspian syneclise (the Uimet–Linevo, Teplovka, and Buzuluk depressions, southern end of the Kama–Kinel' trough system; *7* – the Pechora syneclise; *8* – Southern Timan; *9* – Southern Urals; *10* – Western Siberia, the Nyurol'ka basin; *11* – Kolyvan'–Tom' trough; *12* – the northern margin of the Kuzbass, the Anzhero-Sudzhensk region; *13* – the western margin of the Kuzbass, the Bol'shie Izyly River; *14* – the southern margin of the Kuzbass, the Kondoma River; *15* - *17* – the northeastern Asia: *15* – Southern Verkhoyan'e, the Sette-Daban Range, *16* – the Omulevka zone, the Bol'shoi Tuonnakh Range, lower course of the Yasachnaya River, and *17* – the Tas-Khayakhtakh Range. For other symbols see Fig. 1.

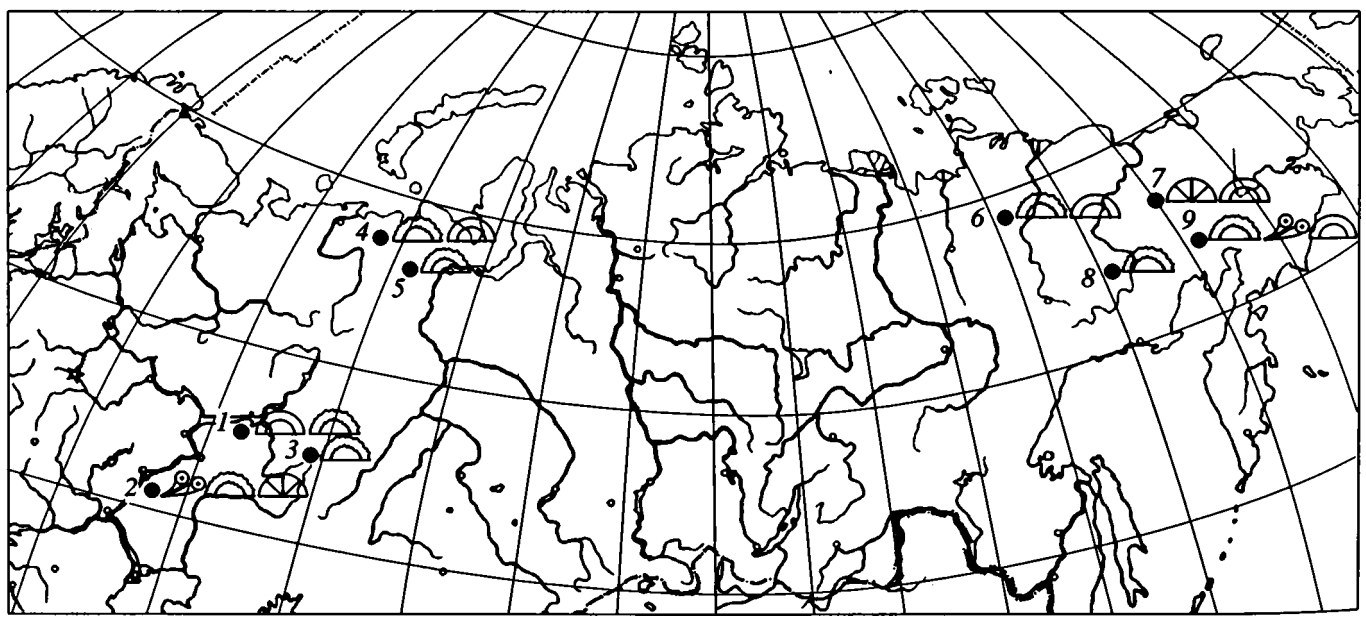

Fig. 6. Localities of the Famennian reefs and other biogenic structures.

1 – the Cis-Urals trough; *2* – the Saratov region, western and northern edges of the Caspian syneclise; *3* – the western slope of the middle Urals and southern North Urals; *4* – the Pechora syneclise; *5* – the Polar Urals; *6* - *9* – northeastern Asia: *6* – the Verkhoyansk–Kolyma zone, the Selennyakhskii Range, *7* – the Omolon massif, the Ush-Urakchan Range, *8* – the Bol'shoi Tuonnakh Range, upper course of the Yasachnaya River, and *9* – the Alazeya folded zone, the Omolon River basin. For other symbols see Fig. 1.

Fig. 7. Localities of the Gzhelian reefs and other biogenic structures.

1 – Northern Timan, algal-coral bioherms and banks; *2* – the Chernyshev Range, algal bioherms; *3* – the Shugor River, algal bioherms; *4* – the Pripyat'–Donets avlakogene, algal bioherms and biostromes; *5* – the Karasala monocline (to the south of the Volgograd City), algal-bryozoan bioherms; *6* – the eastern edge of the Caspian syneclise, algal biostromes; *7* – the Karachaganak–Koblanda Uplift zone, algal-bryozoan reefs; *8* – the northern and western Caspian syneclise, algal-bryozoan bioherms and reefs; *9* – the southern and eastern Caspian syneclise, algal-bryozoan bioherms and reefs; *10* – Northern Pamir, the Darvaz–Transalai zone, algal reefs; *11* – Northern Pamir, the Karakul' zone, algal reefs; *12* – the eastern Koryak Upland, algal reefs; *13* – the southeastern slope of the Sikhote-Alin' Range, algal-coral-bryozoan reefs and bioherms; a – localities; b – bryozoans; c – algae.

Fig. 8. Localities of the Asselian reefs and other biogenic structures. For other symbols see Fig. 7.

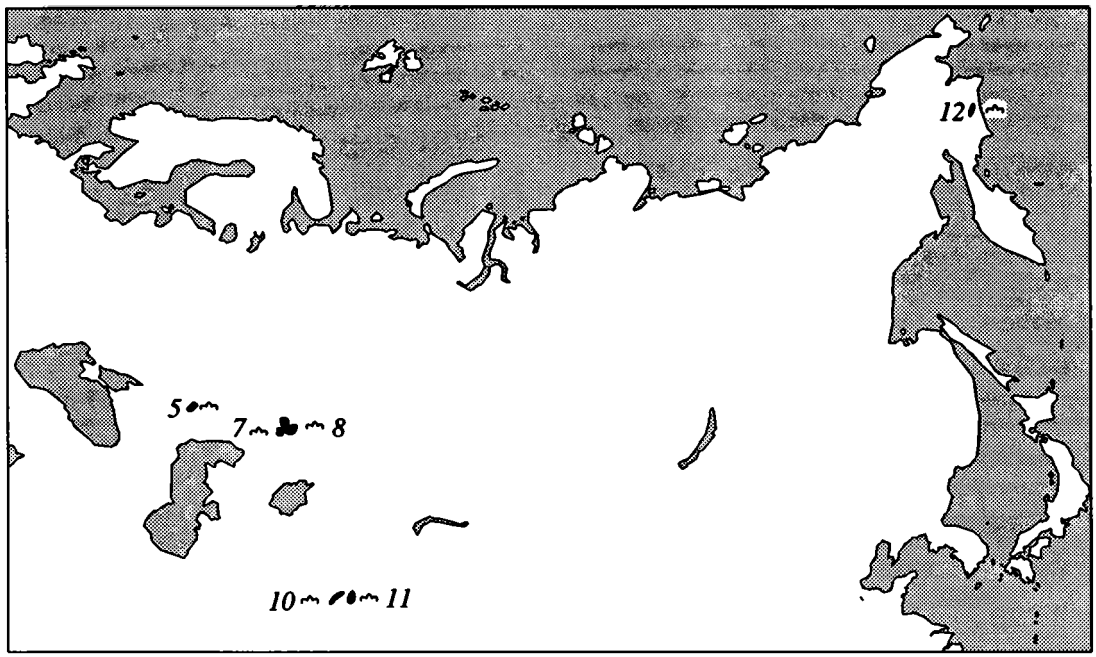

Fig. 9. Localities of the Artinskian reefs and other biogenic structures. For other symbols see Fig. 7.

At this stage of development, a single bioherm exhibits colonies of various shapes: flattened, diskoid, cylindric, or nodular. Colony shapes characterize a family. But the colony shape has a very plastic feature developing only under optimal conditions: abundance of food, absence of strong current, normal salinity, and pure water. Under unfavorable conditions, the colonies, regardless of their specific composition, varied in appearance and form.

The Devonian stromatoporoids were active in the reef building. They were dominated by forms with well differentiated laminas and columns as well as with thick, often united horizontal and vertical skeletal elements: *Stromatopora*, *Parallelostroma*, *Gerronostroma*, *Hermatostroma*, *Atelodictyon*, *Trupetostroma*, *Plexiostroma*, *Styloporella*, *Idiostroma*, and *Parallelopora*. Stromatoporoids with massive colonies, inhabiting shallow rough basins of the euphotic zone, played a major role.

Primarily, the stromatoporoids formed the stable frontal framework of a reef. Layers of massive colonies are often underlain by lamellar forms, which need deep and quiet environments. However, lamellar colonies inhabited the bedrocks near the water's edge as well, and often comprised muddy interlayers. Such populations were likely to inhabit quiet bottom areas with a muddy ground. The colony forms varied so as to survive silting. In contrast to massive and lamellar stromatoporoids, which mainly inhabited the margins of the biogenic structures, nodular ones preferred its inner parts. They also occurred in amphiporitic-stromatoporitic layers. If the intact nodular colonies are presently in the position occupied during their life, they may have been formed in a quiet basin, which had limited links with the open sea, e.g., in a vast shelf lagoon deeper than the optimal depth for the massive stromatoporoids.

Corals (tabulatomorphs and rugoses). Among the Paleozoic reef-forming organisms, tabulates, heliolitoids, and rugoses are of great importance. Since their evolutionary appearance (the early Ordovician) they contributed to the formation of biogenic structures, but only since the middle Ordovician have these abundant and diverse corals spread throughout the shallow shelf. The Ordovician reef corals include representatives of the Agetolitidae, Lichenariidae, Sarcinulidae, Tetradiidae, and Halysitidae (tabulates), Cyctophyllidae, Plasmoporellidae (heliolitoids), Streptelasmatidae (solitary rugoses), and Cyathophylloidae (colonial rugoses) families.

Near the Ordovician–Silurian boundary a sharp change in coral assemblages occurred: three orders of the tabulates and four families of the heliolitoids became extinct; the rugose assemblages were more or less renewed. This is related to a wide regression in the late Ordovician, which resulted in the disappearance of many favorable habitats in the shallow shelfs, where banks, biostromes, and bioherms were formed on vast shallow platforms. Frequent biohermal banks were also restricted to edges of the shallow shelf. The early Silurian transgression destroyed the relatively deep-water ecological niches of corals, which had been stabilized by the end of the Ordovician. As a result, at the beginning of the Silurian those populations whose habitats were not affected or who did not subside too deep survived. These are the tabulates families Favosilidae, Syringoporidae, Auloporidae, and Halysitidae; heliolitoid families Protaraeidae, Heliolitidae, and Proporidae;

the rugoses families Streptelasmatidae and Cyathophylloidae.

Most of the earliest Silurian cnidarian taxa were represented by a solitary species. The corals diversified in the second half of the Llandoverian, when they became the real reefbuilders. The early Llandoverian and late Silurian corals were either typical or sometimes dominant members of such communities. The most characteristic Silurian reef-forming corals are Favositidae, Multisoleniidae, Striatoporidae, Heliolitidae (tabulatomorphs), Arachnophyllidae, Ptychophyllidae, and Cystiphyllidae (rugoses).

During the early and middle Devonian the Paleozoic corals became the most important organisms in the reef formation. Many biogenic structures of this period are composed completely of tabulate remains (favositids, alveolitids, especially their squamulate forms, and pachiporids). The role of the rugoses increased in importance. Typical reef-forming specimens were colonial Columnariidae, Disphyllidae, Cyathophyllidae, and Phillipsastraeidae. Representatives of these families correspond to the Holocene scleractinians in their reef-forming role. The end of the middle Devonian is characterized by extinction of favositids and an increasingly prominent role of less massive dendroporids, alveolitids, and caenitids. The Frasnian coral assemblage is less diverse. Sharp ecological changes in the Famennian caused the disappearance of many coral groups among both the tabulates and rugoses. Earlier, the heliolitoids and cystiphyllids became extinct. Syringoporids, auloporids, aulocystids, myshleniids, rare dendroporids and rugoses evolved into Carboniferous forms. The Tournaisian–Visean time is marked by an evolutionary diversification of the tabulates and rugoses. However, they played only a minor role in the reef formation though their remains frequently occur in biogenic structures of the late Paleozoic.

Though it is unlikely that the early corals (particularly rugoses) were hermatypic, they did become capable of symbiosis with zooxantellas in the Devonian. Biogenic structures similar to the recent coral reefs are known to have existed since the Devonian.

Birenheide (1962) and others suggest zoning in the distribution of coral was present in the Devonian reef. Its coastal part was inhabited mainly by tabulates with rare rugoses; further towards the open sea the rugoses gradually increased in abundance, becoming as important as the tabulates. The rugoses were dominated by species forming both branching and massive polyparia. The same coral groups occurred near the reef edge, in an area with a wide distribution of crinoids. Generally, solitary rugoses with crinoids inhabited the deepest zone of the reef.

Bryozoans. Bryozoan bioherms and reefs are known from several Paleozoic stratigraphic levels (Cuffey, 1985 and others).

The bryozoans are thought to play a dual role in the biogenic structures: primarily, their involvement in framework building, and in addition, their support, together with other organisms, of reef growth.

Distribution and functions of the bryozoans in bioherms and reefs are strictly controlled by their trophic links. The Paleozoic bryozoans flourished in the algae and crinoid communities, but were less compatible with the stromatoporoids and tabulates. Evidently, rugoses were serious rivals of the Devonian reef bryozoans. The bryozoans are able to adapt to various substratums, preferring either a firm and stable, or a supple and mobile one.

The role of the bryozoans in reef formation depends on their colonial forms. Among highly variable forms, the lamellar and massive colonies were prevalent at the beginning of bryozoan evolution. Branching or reticular species later became dominant. Rodlike, ramificated, and reticular colonies appeared to be the most plastic and advanced. The middle Ordovician reticula were generally large-looped and consisted of thin light (Phylloporininae) or thick flattened rods (Ptylodictyinae) united only by the anastomoses. Later, reticular forms were small-looped, consisting of thin rods with crossbars (Fenestellidae). Taxonomic criterium serves as a good indicator of bryozoan structural evolution.

The early Ordovician (Arenigian) bryozoans are represented by massive and platy zoaria of the Ceramoporina and Esthonioporin suborders. At that time they did not form bioherms, but grew as bushes inhabited by brachiopods and crinoids, and spread over the areas of firm ground. The true bryozoan bioherms appeared in the middle Ordovician. These were small domal mounds, whose framework was built by bryozoans, e.g., by *Esthoniopora* forming massive colonies with numerous growth layers. In the Caradocian, Ceramoporina, and Esthonioporina were replaced by Phylloporinina and Ptylodictylina with anastomose reticula, and by thin-branched Goldfussitrypina. The Silurian structures were also small in size. Resembling in shape the Ordovician structures, they differ from them by the presence of Halloporina, Stictoporellina, and Nikiforovellina.

The Devonian bryozoan bioherms and reefs were built by branching trepostomids of the Anplexoporina suborder and by encrusting and branching forms of Fistuliporina. Fenestellina species were of great importance in the construction of the Devonian reef.

In the Carboniferous reefs, the bryozoans played a subordinate role, trapping and accumulating sediments. Among these bryozoans are thin neat colonies of Rhabdomesina, feathered and reticular Fenestellina, and thick-branched trepostomids (Amplexoporina).

The Permian reefs were mainly built by bryozoans of the suborders Fenestellina, Fistuliporina, and Timanodictyina. The Paleozoic bryozoans were extinct by the end of the Permian.

The maps (Figs. 1 - 9) show major localities of reef structures in Russia: the Ordovician-Silurian (Figs. 1 - 3), Devonian (Figs. 4 - 6), and the late Carboniferous and early Permian (Figs. 7 - 9). For symbols indicating

dominant reefbuilders see Fig. 1. The algae were of prime importance during all the intervals discussed, while the stromatoporoids and corals played a significant role only in the Silurian and Devonian. Figures 1 - 3 (the Ashgillian–Llandoverian–Wenlockian) show an increase in the importance of the cnidarians as framework forming organisms during the transgression, which caused the appearance of numerous shallow shelf platforms, i.e., ecological niches that favor corals. An opposite pattern is observed in the middle Paleozoic (Givetian–Frasnian–Famennian) (Figs. 4 - 6), when regression resulted in an almost complete disappearance of such areas. In the Devonian, when warm and shallow epicontinental seas were the most widespread, the cnidarians played a crucial role in reef formation. No similar trends were traced in the late Paleozoic, when the reefbuilders were algae and, to a lesser extent, bryozoans. We compiled maps using the materials from the anthology "Phanerozoic reef and sulfate-bearing formations of the USSR" (1990).

We thank N.V. Bochkareva and E.V. Zlokazova for their help in our study.

REFERENCES

Ahr, W.M., Paleoenvironment, Algae Structures and Fossil Algae in the Upper Cambrian of Central Texas, *J. Sediment., Petrol.*, 1971, vol. 71, pp. 205 - 216.

Birenheide, R., Siedlungs- und Wuchsformen mitteldevonischer Korallen aus der Eifel, *Natur. und Museum*, 1962, vol. 52, no. 1, pp. 21 - 28.

Cuffey, K.J., Expanded Reef-Rock Textural Classification and the Geologic History of Bryozoans Reefs, *Geology*, 1985, vol. 13, pp. 307 - 310.

Lecompte, M., Les stromatoporoids du dévonien moyen et supérieur du bassin de Dinant, *Mém. Inst. Roy. Sci. Natur. Belge*, 1952, vol. 117, pp. 216 - 359.

Lovelock, F.E. and Margulis, L., Athmospheric Homeostasis by and for the Biosphere: the Gaia Hypothesis, *Tellus*, 1973, no. 26, pp. 1 - 10.

Rifogennye i Sul'fatonosnye Formatsii Fanerozoya SSSR (Phanerozoic Reef and Sulfate-Bearing Formations of the USSR), Moscow: Nedra, 1990.

Stratigraphy and Geological Correlation, Vol. 2, No. 1, 1994, pp. 49 - 55. Translated from Stratigrafiya. Geologicheskaya Korrelyatsiya, Vol. 2, No. 1, 1994, pp. 55 - 61.
Original Russian Text Copyright © 1994 by Barskov, Bogoslovskaya, Zhuravleva, Kiselev, Kuzina, Leonova, Shimanskii, Yatskov.
English Translation Copyright © 1994 by Interperiodica Publishing (Russia).

Main Morphological Events in the Evolution of Paleozoic Cephalopods

I. S. Barskov*, M. F. Bogoslovskaya*, F. A. Zhuravleva*, G. N. Kiselev, L. F. Kuzina*, T. B. Leonova*, V. N. Shimanskii*, and S. V. Yatskov***

**Institute of Paleontology, Russian Academy of Sciences, Profsoyuznaya ul. 123, Moscow, 117647 Russia*
***Department of Paleontology, St. Petersburg State University, 16-ya Liniya 29, St. Petersburg, 199178 Russia*

Received January 26, 1993

Abstract – New morphological features in shell structure, which were the starting points of cephalopod diversification into taxa of high ranks (subclasses, orders, superfamilies), are considered as phylogenetic events. Main morphological innovations in the evolution of nautiloid cephalopods; the formation of endosiphuncular and cameral deposits, shell coiling, truncation of the phragmocone's apical end, and contracted aperture, which originated to make the relative shell positioning in the water more efficient. Changes in the lobe line structure and various types of complications in the primary lobes (ventral, umbonal, and lateral) were the most important morphological innovations in convolute ammonoids. The functional significance of these changes remains unclear, but recognition of equally significant changes in primary lobes requires a review of the Paleozoic Ammonoidea taxonomy at the suborder level.

This paper is a continuation of a study whose first results have been published (Barskov *et al.*, 1993). The original materials are supplemented by T.B. Leonova's revised data on the Permian Ammonoidea and data of V.N. Shimanskii, F.A. Zhuravleva, and G.N. Kiselev on Carboniferous, Devonian, and Silurian non-ammonoid cephalopods (Fig. 1). General conclusions from the previous paper on the dynamics of generic diversity and interpretation of relevant changes remain valid. The evolution of non-ammonoid cephalopods was analyzed in a number of works (Barskov, 1989; Zhuravleva, 1972; *Osnovy Paleontologii*, 1962; Shimanskii, 1989; Shimanskii and Zhuravleva, 1961; *Treatise on Invertebrate Paleontology*, 1964; Teichert, 1967).

This paper presents an analysis of morphological innovations, which were the starting points of new trends in the evolution of the group (phylogenetic events). This is reflected in the taxonomy of high ranking fauna groups, from superfamilies to subclasses.

The events of primary importance are: (1) the appearance of the Cephalopoda as an independent molluscan class; (2) the appearance of the Ammonoidea; (3) the acquisition of an internal shell, which probably occurred more than once and is most likely characteristic of various taxa ranks. This problem is not considered here.

Formation of the cephalopod structural style began when primary benthic and creeping forms, similar in organization to monoplacophoran molluscs, acquired a phragmocone, which is a functional adaptation to regulate buoyancy. This provided for their transition into new pelagic zone environments. At the first stage, before appearance of the Ammonoidea, main morphological innovations were intended to improve the regulation of the buoyancy process and to support in various ways its relative position in the water. Only indirect evidence to judge how the buoyancy was intensified exists. Morphological changes such as the thinning of the siphuncle hard envelope and decrease of its diameter seem to reflect the specialization of the posterior phragmocone-related part of the animal body, which was transformed into a special organ, supporting the phragmocone function as a gas-liquid float. This morphological trend is clearly seen in all cephalopod groups when their early and late forms are compared. It is likely that there was another, extensive way of improving the siphuncle pumping activity at the expense of increasing its epithelium surface. Morphologically, it was the formation of a radial structure of the siphuncle. This adaptation was repeatedly used in cephalopod history (orders Oncocerida, Discosorida, and others).

Various morphological features, supporting the shell's relative position in the water, became the starting points that really determined cephalopod diversification at a high taxonomic rank. One can distinguish several ways of shell and body stabilization in orientated position: (1) formation of deposits inside the siphuncle envelope; (2) formation of deposits inside the phragmocone camerae. Both ways are especially effective for those forms with an orthocone shell, though they are also favorable for endogastric and, to a lesser degree, for exogastric forms. (3) Coiling of the shell into flat spiral, which is one of the most effective solutions to the problem of shell stabilization. It occurs through the convergence of buoyancy and gravity centers, when an animal is constantly under indifferent equilibrium and occupy any position relative to the bottom or water surface with minimal energy loss;

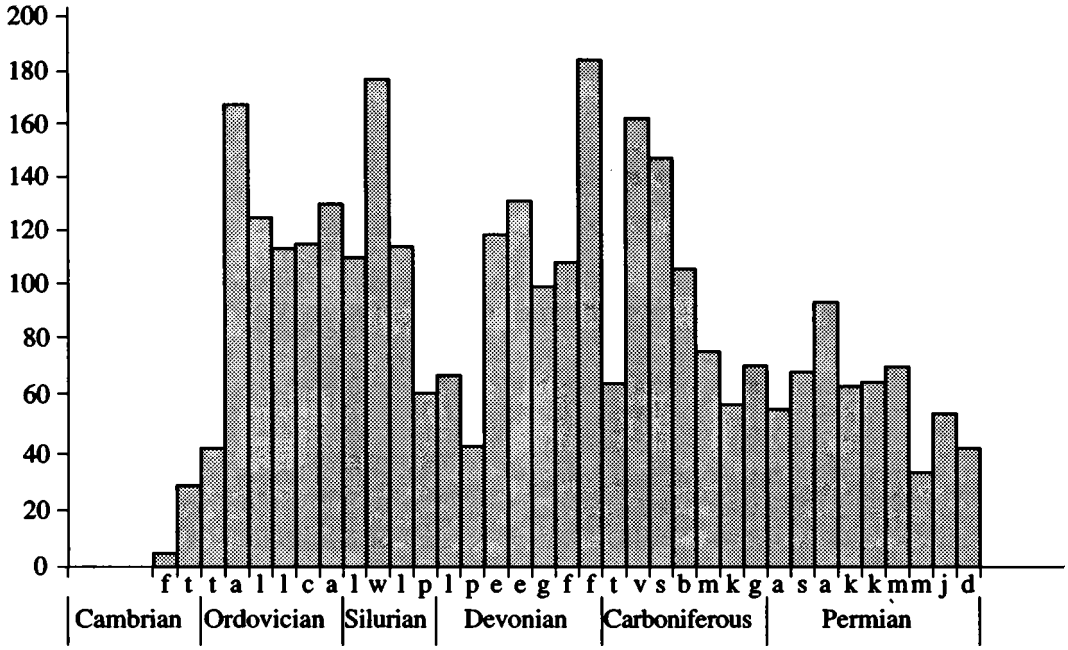

Fig. 1. Generic diversity of the Paleozoic Cephalopoda.

Y-axis – number of genera; X-axis – stages. Cambrian: f – Franconian and t – Trempealeanuan; Ordovician: t – Tremadocian, a – Arenigian, l – Llanvirnian, l – Llandeilian, c – Caradocian, and a – Ashgillian; Silurian: l – Llandoverian, w – Wenlockian, l – Ludlovian, and p – Przidolian; Devonian: l – Lochkovian, p – Pragian, e – Emsian, e – Eifelian, g – Givetian, f – Frasnian, and f – Famennian; Carboniferous: t – Tournaisian, v – Visean, s – Serpukhovian, b – Bashkirian, m – Moscowian, k – Kasimovian, and g – Gzelian; Permian: a – Asselian, s – Sakmarian, a – Artinskian, k – Kungurian, k – Kubergandian, m – Murgabian, m – Midian, j – Julfian, and d – Dorashamian.

(4) truncation of the back part of the phragmocone, which brings together the gravity and buoyancy centers; and (5) formation of a contracted or constricted aperture, an adaptation of forms that orientate in a hypostome position and use their shell as a passive float. The various ways of shell stabilization are shown on Fig. 2. One more feature of shell stabilization in different representatives of the ancestral order Ellesmerocerida (cephalopods) resulted in diversification of taxa at the order rank.

The first morphological event was the formation of the order Endocerida, characterized by the appearance of endosiphuncular deposits (endocones) equilibrated to the back end of the long-cone straight shell, providing buoyancy in a horizontal position with the ventral side directed downward.

The second morphological event resulted in the shell coiling into spiral plane and the formation of the order Tarphycerida.

The third event was the near simultaneous diversification of Ellesmerocerida into a number of high-rank taxa, each of which realized its own type of shell stabilization. The appearance of the order Actinocerida is related to the formation of endosiphuncular deposits. This was a new stage in siphuncle specialization as a buoyancy regulator as compared to Endocerida. It was expressed morphologically in different structures of the siphuncular envelope, namely, in its thinner and convex connective rings. Actinocerida also produced the cameral deposits, but the main function of stabilization was undoubtedly controlled by endosiphuncular deposits.

The stabilization function of cameral deposits is more evident in forms of the order Orthocerida, though some its families also had minor deposits inside the siphuncle. Yet it is precisely the cameral deposits that define the morphological peculiarity of the Orthocerida.

Endosiphuncular and cameral deposits are also typical of two other orders: Pseudorthocerida and Dissidocerida. The first, according to its morphology, is intermediate between the Actinocerida and Orthocerida, possessing (1) more evolved endosiphuncular deposits than in orthocerids, but comparable with those in actinocerids, and (2) a siphuncular envelope structure resembling that of the orthocerids. The shape of endosiphuncular deposits in the order Dissidocerida resembles, to a limited extent, the endocerids. However, the structure of its siphuncular envelope renders it more similar to pseudorthocerids.

Thus, at least four large taxa of a rank not lower than the order (actinocerids and endocerids are distinguished as subclasses) independently used the endosiphuncular deposits as the main regulator of shell stabilization. At the same time or somewhat later, we observe the first truncation of the posterior shell edge. The truncated apical end of the phragmocone in forms with a orthocone shell is a very effective way to converge the buoyancy and gravity centers. This resulted in

the separation of the order Ascocerida from the orthocerids. A trend to be free of the phragmocone apical end occurs in the development of the orthocerids at least twice. However, the taxonomic rank of these transformations is considered to be lower (Sphooceratidae family in the Silurian and the Brachycycloceratidae family in the Carboniferous).

Another group of morphologically similar taxa consists of the Oncocerida and Discosorida orders, which appeared simultaneously. Initially, these forms are, having curved cyrtoceracone shell, exogastric in the first and endogastric in the second case. The curved shell is able to constructively support a positioning, which is close to the hypostome one, limiting the shell function of a more or less passive float. The development of additional mechanisms of shell orientation are rendered unnecessary, though they are present as endosiphuncular and cameral deposits in some forms of the discocerids, and as very rare cameral deposits in the oncocerids. However, it appears that the principle of shell morphology in these orders reveals their rejection of additional stabilization mechanisms. As a natural consequence, their shell had a predominantly hypostome orientation and their formation consisted of contracted and constricted apertures. This morphological tendency in both orders (more evident in oncocerids) was already realized in the Silurian, and may be considered independently as a *fourth morphological event.*

The *fifth morphological event* of the pre-ammonoid stage in cephalopod evolution is a recurring tendency of the shell coiling. This tendency was realized simultaneously in two phylogenetic branches and resulted in the formation of the Nautilida order from the exogastric cyrtoceracone oncocerids and the Ammonoidea subclass from the orthocone bactritids. This ends the search for an optimal shell shape, as regards its use as a gas-liquid hydrostatic apparatus.

Summarizing the pre-ammonoid evolutionary stage, the following should be emphasized. Practically all the morphological innovations were realized at the early stages of class evolution, i.e., in the early Ordovician or at the beginning of the middle Ordovician (Fig. 3). At that time, nine of the eleven generally accepted orders of non-ammonoid cephalopods; Endocerida, Orthocerida, Tarphycerida, Actinocerida, Discocerida, Pseudorthocerida, Dissidocerida, Oncocerida, and Ascocerida, came in to existence. The initial Ellesmerocerida order originated in the late Cambrian, and the Nautilida is the only post-Ordovican order. The Bactritida order is an ancestor of Ammonoidea, apparently having also originated in the early Ordovician.

The independent taxonomic status of the ammonoids is caused only by morphological acquisition, i.e., the formation of a planispiral shell. This was the third attempt in the evolution of cephalopods to use a morphological innovation favorable from the viewpoint of hydrostatics. But only this attempt became the most important event in the evolution of cephalopods, and resulted in the appearance of a group that outgrew all the earlier and later groups in its diversity. Significant phylogenetic success was predetermined, apparently, by ancestoral structural peculiarities and, probably, by their ecological specialization. The main feature of the bactritids is a thin siphuncle contiguous to the shell wall. As a result, the suture on the ventral side was interrupted, forming the neck lobe (termed the ventral lobe in the ammonoids), and an omnilateral lobe formed on the lateral sides of the shell. From here on,

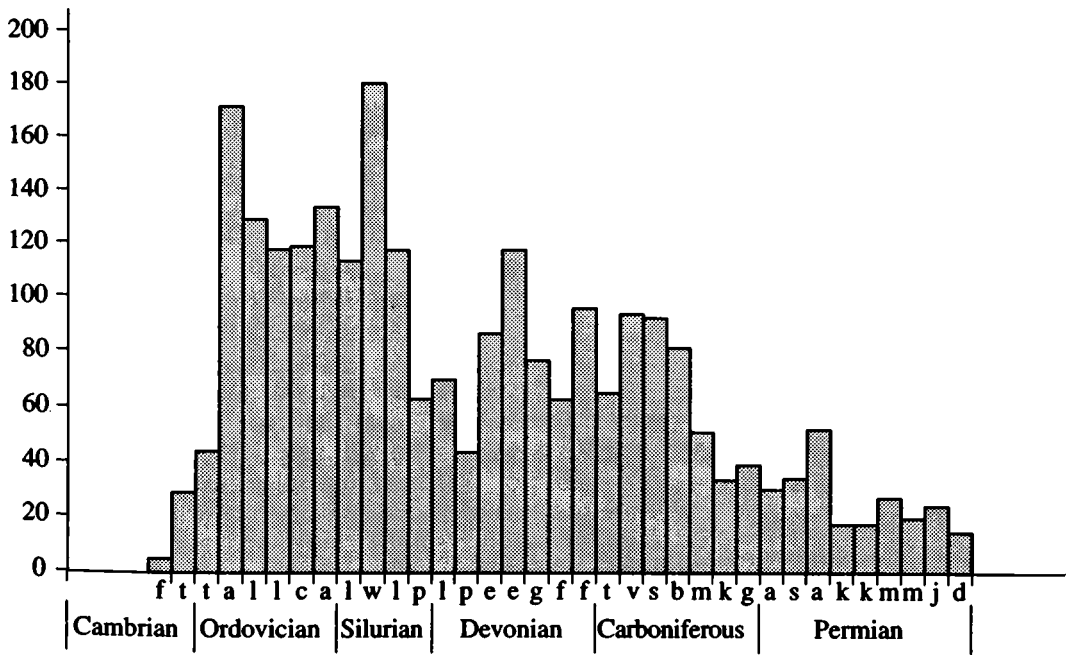

Fig. 2. Generic diversity of nautiloid cephalopods in the Paleozoic. See Fig. 1 for symbols.

we will use the terminology of elements of the lobe line and its formula after V.E. Ruzhentsev (1960).

Shell morphology of the Paleozoic Ammonoidea is quite diverse; encompassing practically all variants of the whorl expansion rate and the degree of overlapping discovered by D. Raup (1966, 1967). However, the main transformations, which provided for the rapid evolution and unusual diversity of the Ammonoidea in the Paleozoic, took place in the septum. The initial tendency of lobe line complication, namely the increasing number of lobes and their dismembering, formed the main evolutionary trend. Key moments of this tendency, which lead to principally new morphological changes and to important phylogenetic consequences (the genesis of high rank taxa of the modern Ammonoidea taxonomy), we term as morphological events. Their types (U-event, L-event, and so on) are defined with regard to those parts of the septum where changes occurred (Fig. 4).

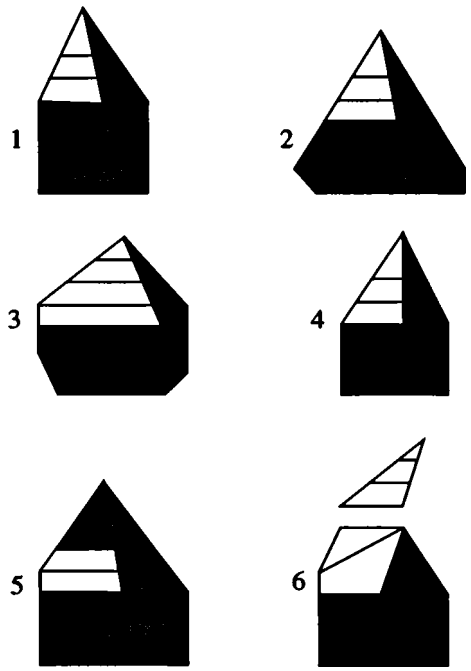

Fig. 3. Sketch images of main morphological events among nautiloid cephalopods.

1 – formation of endosiphuncular deposits; 2 – formation of short-conic shell (passive float); 3 – formation of contracted aperture; 4 – formation of phragmocone; 5 – formation of cameral deposits; 6 – truncation of shell apical end.

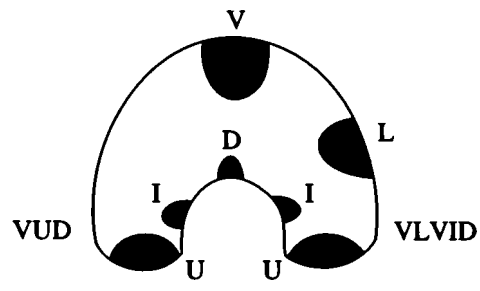

Fig. 4. Sketch image of the transverse section of a shell whorl of the Ammonoidea.

Symbols of main primary lobes: D – dorsal, I – inner, L – lateral, U – umbonal, and V – ventral. Locality of lobes and formula of the primary lobe line of L-branch (to the right), U-branch (to the left).

During their formation, the Ammonoidea inherited from their ancestors a lobe line with simple ventral and omnilateral lobes; according to accepted terminology their conditional formula is VO. The dorsal lobe (D) formed almost simultaneously because of contacting whorls, and the formula became VO : D. This was *the first event*, which resulted in the formation of the Agoniatitina suborder, the oldest in the Anarcestida order. Another new feature, apparently of the same time, the three-merous ventral lobe used as a diagnostic feature of the Auguritina suborder whose initial formula was $(V_2V_1V_2)O : D)$, did not result in significant phylogenetic consequences and did not develop further.

The second event (U-event) is a transformation of the wide omnilateral lobe of the Agoniatitina into an umbonal one, which gave rise to the Anarcestina suborder with the initial formula VU : D. Thus the U-branch, one of two main Paleozoic phyletic lines, came into being. Principle septum changes, which took place many times during evolution, formed various trends complicating the lobe line, which were used to distinguish large taxa (Fig. 5).

The third event (L-event) is the formation of the lateral lobe between the ventral and umbonal lobes. Taxonomically, this is used to define the Tornoceratina suborder, the most ancient in the Goniatitida order, with the primary formula VLU : D. If we accept the modern classification of the Ammonoidea, it starts the second phylogenetic line (L-branch) corresponding to the Goniatitida order. The septum transformations in this branch did not cause phylogenetic consequences as large as those in the U-branch, despite the fact that observed complications in the lobe line are sometimes more complex than in the latter branch.

Further, the septum complications in each of two main philogenetic lines (U-branch and L-branch) were rather similar, but occurred at different times and did not always cause equivalent taxonomic consequences.

The fourth event (3V-event) depicts the appearance of triseptate ventral lobe and separation of the Gephuroceratina suborder with the primary formula $(V_2V_1V_2)U : D)$. This disarticulation of the V-lobe gave rise to new elements in the lobe line: an inner lateral lobe (I) first, and subsequent umbonal lobes. Despite the high rate of evolution, which increased the number of lobes to 54, this trend was not continued.

The fifth event followed, notable in the U-branch as the 2V-event that generated the very limited Timanoceratina suborder with the formula $(V_1V_1)U : ID$; this suborder existed briefly and disappeared without a trace.

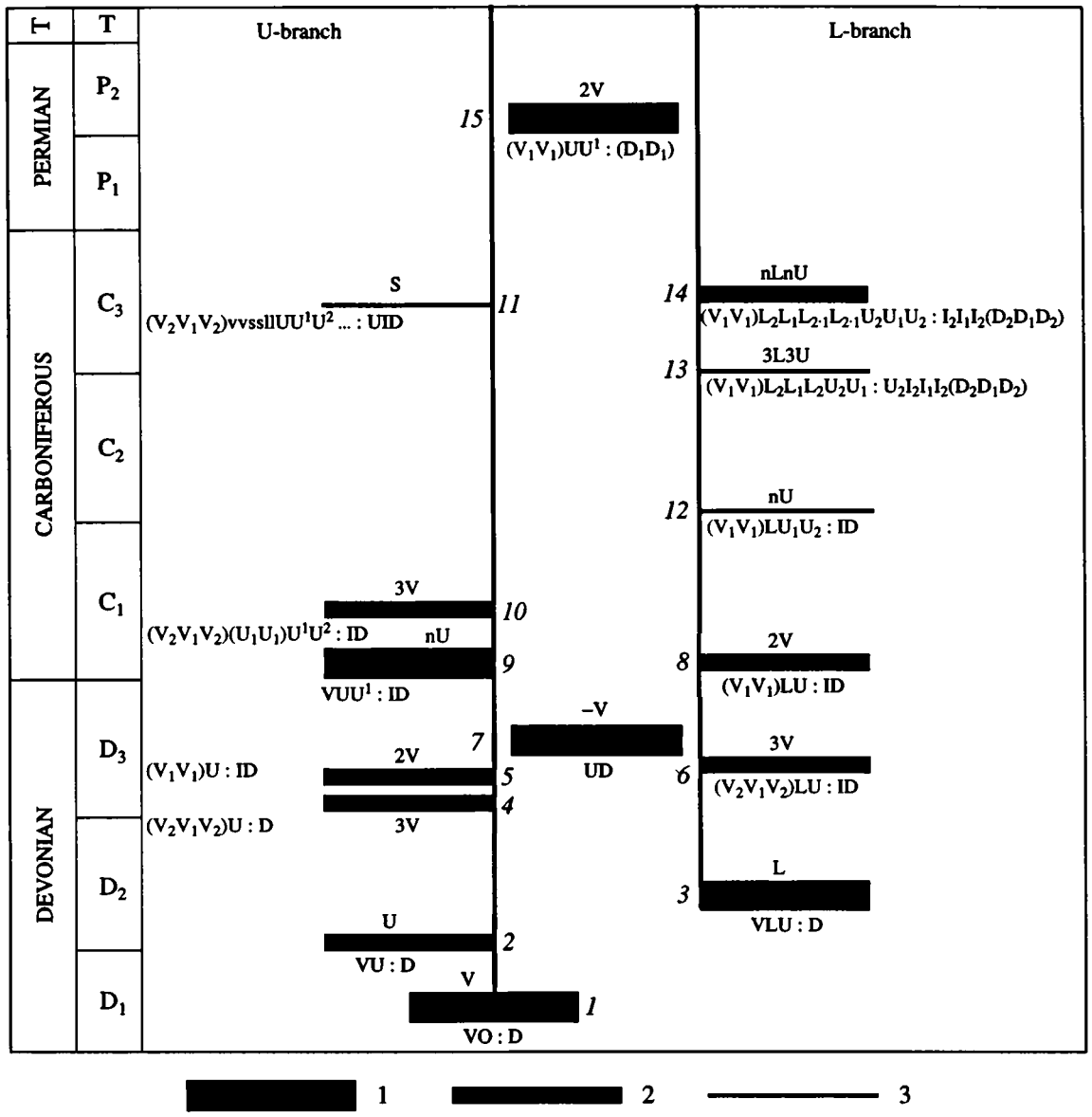

Fig. 5. Main morphological events in the history of the Paleozoic Ammonoidea.

1 – orders, 2 – suborders, and 3 – superfamilies; *1 - 15* – ordinal numbers of events.

The sixth event (3V-event) took place in the L-branch, and is characterized by the appearance of a triseptate ventral lobe. This event was similar to the fourth one in the U-branch, but did not develop further. The resultant Praeglyphioceratina suborder with the initial formula $(V_2V_1V_2)LU : ID$ developed slowly over a very short period.

The seventh event (V-event) was unprecedented. Morphologically, it manifested itself in the displacement of the siphuncle from the ventral to the dorsal side, and in a general reorganization of its septum. Taxonomically, this event resulted in the creation of the Clymeniida order. The ventral lobe disappeared first, and the lobe line formula became UD (Clymeniina suborde). Later, the V-lobe appeared again, but this time unrelated to the ventral position of siphuncle. It appears to be a resetting of the original lobe line of the Ammonoidea with the formula VU : D (Gonioclymenina suborder). All the previously mentioned ways of V- and U-lobe complication occurred in this lobe line during a short period. Morphological simplifications of the ventral and dorsal lobes, including their full disappearance, also occurred. The clymeniids had a large diversity "boom" during the short period of their existence (the Famennian) and became extinct without descendants (Bogoslovskii, 1969).

The eighth event (2V-event) observed in the L-branch was one of the most important. The origin of the Goniatitina suborder with the initial formula $(V_1V_1)LU : ID$ is the key moment of this event. The double partition of the ventral lobe caused many changes in the septum, which at the first stage took

place only in the initial eight lobes, and did not change the original formula. More principal changes resulted in the formation of additional lobes. Their partition occurred during subsequent events (Ruzhentsev and Bogoslovskaya, 1978; Kulmann, 1981).

The ninth event (nU-event) in the U-branch was nearly simultaneous with the eighth one in the L-branch. This was the origin of the Prolecanitida order with the initial formula VUU^1 : ID. The appearance of the second umbonal lobe in the initial lobe line determined, apparently, the main septum complication trend of, the increasing number of simple umbonal lobes, which migrated first, towards the outer side, and further towards the inner side.

The tenth event (3V/2V-event) in the U-branch gave rise to the Medlicottiina suborder with the primary formula $(V_2V_1V_2)(U_1U_1)U^1U^2$: ID. The simultaneous appearance of a triseptate ventral lobe and a biseptate first umbonal lobe in the lobe line determined the suborder separation. The biseptate first umbonal lobe is typical of all specimens of this suborder, but sometimes only at the early stages of ontogenesis. In the first stage, the complication included an increase in the amount of umbonal lobe and the dissection of their base. The beginning of the second stage is indicated by *the eleventh event* (s-event), when principally new and earlier unknown ways of septum complication were recognized in the development of adventive lobes in the outer saddle. This gave rise to the successfully developed Medlicottiidae family, which has the primary formula $(V_2V_1V_2)$ vvssllUU^{1}U^2 ... : ... UID.

The twelfth event (nU-event) is seen in the L-branch. For the first time in the history of the Goniatitina, changes in the septum went beyond the limits of eight lobes. The lobe multiplication occurred with the addition of umbonal lobes, a diagnostic feature of the Schistocerataceae superfamily, which has the initial formula $(V_1V_1)LU_1U_2$: ID. Later, the Goniatitina multiplied their lobe number many times and in various ways. This occurred at various stages of general evolution, even being repeated sometimes. Relevant features were used to distinguish taxa lower than the suborder rank. It is reasonable to emphasize that among the variety of ways, the two ways of septum complication after the nU-event resulted in the creation of forms with the most complex lobe lines known for the Paleozoic Ammonoidea.

One of them, defined here as *the thirteenth event* (3L3U-event), determined a separation of the Maratonitaceae superfamily having the initial formula $(V_1V_1)(L_2L_1L_2)U_2U_1$: $U_2(I_2I_1I_2)D$. A triple partition of the primary L-, U-, and I-lobes caused the complication of the lobe line via the significant dissection of all lobes without the appearance of new elements. *The fourteenth event* (nLnU-event) was morphologically similar. As a result, the Cyclolobaceae superfamily having the primary formula $(V_1V_1)L_2L_1L_{2\cdot1}L_{2\cdot1}U_2U_1U_2 : I_2I_1I_2(D_2D_1D_2)$ came into existence. In contrast to the thirteenth event, the last one tended to multiply all of the lobes. This resulted in the creation of new forms with 58 - 60 lobes with a degree of dissection equal to that of the complex-lobed Mesozoic Ammonoidea (Bogoslovskaya, 1990).

Finally, the appearance of the biseptate ventral lobe and the crenulated base of V- and U-lobes in the lobe line typical of the ancient prolecanitids was the *fifteenth event* in the Paleozoic history of the Ammonoidea. Taxonomically, it is a ramification of the most ancient Paraceltina suborder having the primary formula $(V_1V_1)UU^1$: (D_1D_1) from the Ceratitida order.

The most important morphological events in the Ammonoidea history are related to the appearance and transformation of primary V, U, and L outer lobes. Frequency and times of these transformations in primary lobes were directly dependant on the events of their appearance. Changes in the most ancient ventral lobe started before those in other types and were most frequent, having a recurrent character. The U-lobe begins to multiply soon after its appearance. Changes in the latest L-lobe, which was very conservative for a long time, characterize the beginning of the second stage in this evolutionary line. The taxonomic significance of the primary phylogenetic events under consideration as compared to the modern taxonomy of the Ammonoidea (Bogoslovskaya *et al.*, 1990) varies. Following the logic of the above distinguished phylogenetic events, providing them with a corresponding taxonomic significance, it is necessary to review the Ammonoidea classification at the order and suborder ranks. For example, the ramification of the Paleozoic Ammonoidea into the U- and L-branches must be reflected in the taxonomy. The events transformating the lateral lobe of the Goniatitina and the outer saddle of the Medlicottiina also seem to rate a higher taxonomic value.

REFERENCES

Barskov, I.S., *Morfogenez i Ekogenez Paleozoiskikh Tsefalopod* (Morphogenesis and Ecogenesis of Paleozoic Cephalopods), Moscow: Mosk. Gos. Univ., 1989.

Barskov, I.S., Bogoslovskaya, M.F., Kuzina, L.F., Zhuravleva, F.A., Shimanskii, V.N., and Yatskov, S.V., Dynamics of Changes in Generic Diversity and Ecological Structure of Cephalopods (Cambrian–Carboniferous), *Ekosistemnye Perestroiki i Evolyutsiya Biosfery* (Ecosystem Reorganizations and Biosphere Evolution), Moscow: Nedra, 1993, issue 1, (in press).

Bogoslovskii, B.I., *Devonskie Ammonoidei: 1. Agoniatity* (The Devonian Ammonoidea: 1. Agoniatites), Moscow: Nauka, 1969.

Bogoslovskaya, M.F., Main Development Trends and Classification of the Late Paleozoic Ammonoids Marathonitaceae and Cyclolobacaeae, *Iskopaemye Tsefalopody* (Fossil Cephalopods), Moscow: Nauka, 1990, pp. 70 - 86.

Bogoslovskaya, M.F., Mikhailova, I.A., and Shevyrev, A.A., Taxonomy of the Ammonoidea, *Sistematika i Filogeniya Bespozvonochnykh* (Invertebrate Classification and Phylogeny), Moscow: Nauka, 1990, pp. 69 - 98.

Kullmann, J., Carboniferous Goniatites, *The Ammonoidea*, London: Academic, 1981, pp. 37 - 48.

Osnovy Paleontologii, Spravochnik dlya Paleontologov i Geologov SSSR, Mollyuski, Golovonogie, 1 (Treatise on

Paleontology, a Guide for Paleontologists and Geologists of the USSR, Mollusks, Cephalopoda, 1), Moscow: Akad. Nauk SSSR, 1962.

Raup, D.M., Geometric Analysis of Shell Coiling: General Problems, *J. Paleontol.*, 1966, vol. 40, no. 6, pp. 1178 - 1190.

Raup, D.M., Geometric Analysis of Shell Coiling: Coiling in Ammonoids, *J. Paleontol.*, 1967, vol. 41, no. 1, pp. 43 - 65.

Ruzhentsev, V.E., *Printsipy Sistematiki, Sistema i Filogeniya Paleozoiskikh Ammonoidei* (Principles of Classification, System, and Phylogeny of the Paleozoic Ammonoidea), Moscow: Akad. Nauk SSSR, 1960.

Ruzhentsev, V.E. and Bogoslovskaya, M.F., *Namyurskii Etap v Evolyutsii Ammonoidei, Pozdnenamyurskie Ammonoidei* (The Namurian Stage in Evolution of Ammonoidea, the Late Namurian Ammonoidea), Moscow: Nauka, 1978.

Shimanskii, V.N., Events in Evolution of the Cephalopoda, *Osnovnye Sobytiya Istoricheskogo Razvitiya Tsefalopod* (Main Events in Cephalopoda Evolution), Available from VINITI, 1989, no. 2042-B89, pp. 2 - 38.

Shimanskii, V.N. and Zhuravleva, F.A., *Osnovnye Voprosy Systematiki Nautiloidei i Rodstvennykh im Grupp* (Main Problems of Nautiloidea and Related Groups Classification), Moscow: Akad. Nauk SSSR, 1961.

Teichert, C., Major Features of Cephalopod Evolution, Essays in Paleontology and Stratigraphy, *Raymond C. Moore Commemorative Volume*, Univ. Kansas, Dept. Geol. Spec. Publ. 2, 1967, pp. 162 - 210.

Treatise on Invertebrate Paleontology, Pt. K. Geol. Soc. Amer. Univ. Kansas, 1964.

Zhuravleva, F.A., *Devonskie Nautiloidei, Otryad Discosorida* (The Devonian Nautiloidea, the Order Discosorida), Moscow: Nauka, 1972.

Stratigraphy and Geological Correlation, Vol. 2, No. 1, 1994, pp. 56 - 67. Translated from Stratigrafiya. Geologicheskaya Korrelyatsiya, Vol. 2, No. 1, 1994, pp. 62 - 73.
Original Russian Text Copyright © 1994 by Yaroshenko, Bach Imam.
English Translation Copyright © 1994 by Interperiodica Publishing (Russia).

Global changes

Evolution of the biosphere

Palynology of the Lower Permian Deposits in Northeastern Syria

O. P. Yaroshenko* and I. Bach Imam**

** Geological Institute, Russian Academy of Sciences, Pyzhevskii per. 7, Moscow, 109017 Russia*
*** The Syrian Petroleum Company, Damascus, Syria*

Received October 10, 1992

Abstract – The assemblage of miospores, discovered in the sections from the oil wells Ode-107, Ode-116, and Rumelan-6 in northeastern Syria, is tentatively dated back to the early Permian according to characteristic forms typical of the Permo-Carboniferous and the lower Permian of western Europe, the lower Permian of China, Australia, Turkey and Israel, and the Permian of Iraq. In the studied sections, the early Triassic is not recorded for lack of diagnostic forms. Taxa from different paleogeographic zones (Euramerian, Cathaysian, Gondwanian) make up the mixed composition of the Syrian palynoflora, and reveal its ecotonic nature and close relations between these areas of the early Permian. The striking similarity between the assemblages from the sections of Northeastern Syria and Southern Turkey (the Hazro section) implies that the Syrian localities probably belong to southern parts of the Tethys located between Eurasia and the African continent.

The Paleozoic deposits in Syria are nearly omnipresent. Their total thickness grows from the southwest to the northeast toward the Mesopotamia marginal trough, reaching 3 - 5 km.

On this territory, Jankauskas and Talli (1978) subdivided and identified the Ordovician, Silurian, and Carboniferous deposits studying the assemblages of acritarchs, chitinozoan, graptolites, spores, and other organic remains. Khoga (1985) used miospores to determine the age of the Permo-Carboniferous deposits; earlier, he found the first Triassic miospores in northeastern Syria (Khoga, 1972).

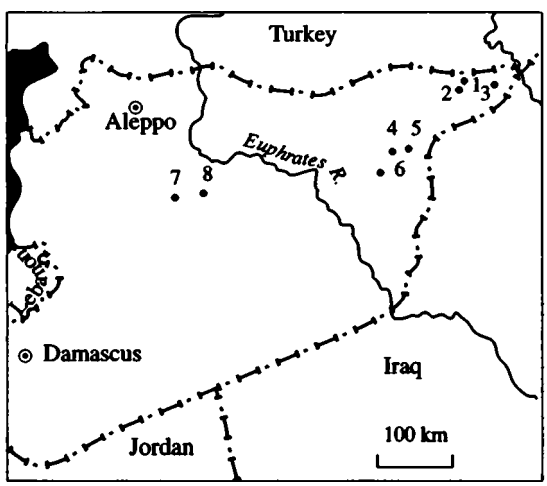

Fig. 1. Location scheme of oil wells.
1 – Ode-107; 2 – Ode-116; 3 – Rumelan-6; 4 – Jbissa; 5 – Tichrin; 6 – Maaza; 7 – Habari-1; 8 – Zidan.

In the course of later studies, Yaroshenko *et al.* (1982) recorded several assemblages of miospores in the Triassic deposits recovered by oil wells in the central and northeastern regions of Syria. As a result of subsequent palynological research in these areas (Yaroshenko and Bach Imam, 1989), the pollen assemblages from the deposits were correlated with the miospores typical of the following stratigraphic units: the upper lower Triassic, the lower middle Triassic, the Anisian, the Ladinian, the Carnian, and probably the Norian and Rhaetian–Liassic; the latter two units were also observed in the northwestern sections. The oldest are the uppermost beds of the lower Triassic and the lower beds of the middle Triassic in the central region (the oil well Wahab-I). Later research discovered the lower Triassic deposits in both the central and the northwestern regions (Bebeshev *et al.*, 1988).

Of the evidence supporting the early Triassic age of the studied deposits, primary is the presence of pollen assemblages containing the early Triassic and paleophytic forms. Palynological, lithological, and other data, analyzed by Bebeshev *et al.* (1988), allowed them to refute the alleged absence of lower Triassic deposits in the northeastern area, as indicated in the stratigraphic scheme of the Syrian Petroleum Company.

Apparently, the presence of the lower Triassic in northeastern Syria cannot be entirely dismissed, but it does require more convincing palynological data from other wells to support insufficient evidence from the

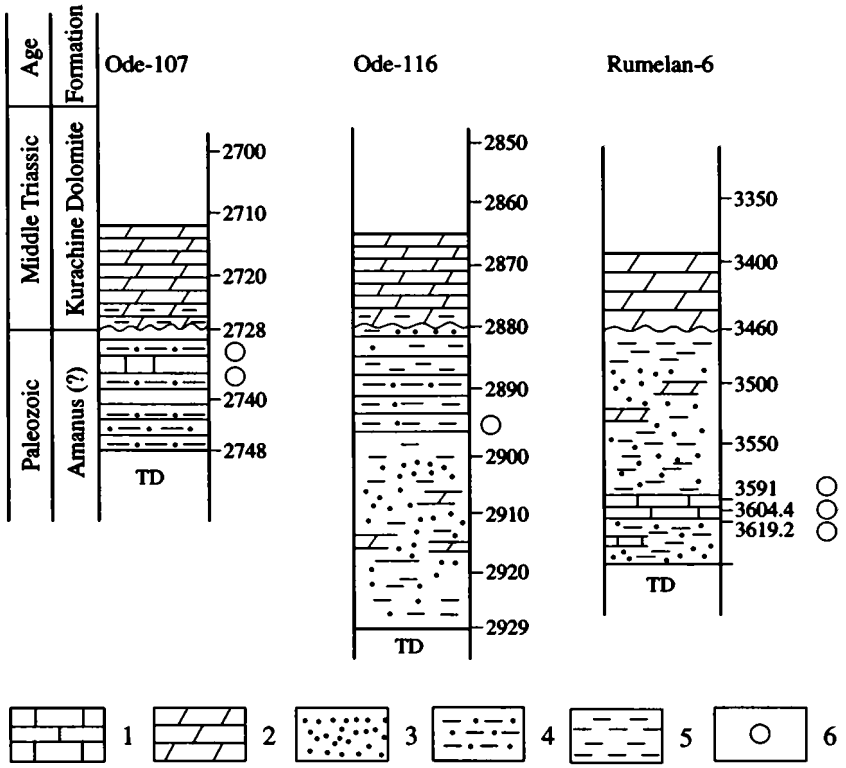

Fig. 2. Correlation chart of lower Permian deposits in Northeastern Syria; Amanus Formation; Kurachine Dolomite Formation.
1 – limestone; 2 – dolomite; 3 – sandstone; 4 – silty claystone; 5 – clay shale; 6 – samples with miospores.
Scale: Ode-107, Ode-116, 10 m : 1 cm; Rumelan-6, 50 m in 1 cm.

Ode-107 and Ode-116 sections gathered by Bebeshev *et al.* (1988). This is confirmed by the data that we received using samples of the same intervals recovered from these two wells and Rumelan-6, which showed the presence of forms typical of the Permo-Carboniferous and Permian pollen assemblages. The purpose of this paper is to present adequate evidence dating the analyzed deposits as the Permian–Carboniferous, or more likely the early Permian.

The miospores we studied in the sections of the indicated wells (Fig. 1) are from beds of grey sandstone alternating with silty claystone that become more calcareous higher in the section (Fig. 2). The taxonomic compositions of the miospores of the six studied samples are very similar and, therefore, they are described as one assemblage; the samples were obtained from Ode-107 (at depths of 2735 and 2737 m), Ode-116 (at the interval 2896 - 2897.4 m), and Rumelan-6 (at depths of 3591, 3604.4, and 3619.2 m). The list of taxa and their distribution by samples is given in the table. The most typical microspores are shown on six Plates. Depending on their congestion, 250 - 700 microspores were counted in every sample.

In all samples, the spores (59.5 - 92) are more prevalent than the pollen (8 - 50.5)[1]; the spores being present as trilete (21.5 - 66.5) and monolete (24.5 - 43.5) forms. The identified pollen forms are bisaccate non-taeniate (0.5 - 32.0), striatiti (1.5 - 15.5), and monosaccate (1.5 - 15). Along with genera forms of extensive stratigraphic range, such as *Leiotriletes*, *Punctatisporites*, *Calamospora*, *Verrucosisporites*, *Punctatosporites*, *Alisporites*, and *Vitreisporites*; diagnostic taxa of the Permian and Permo-Carbon iferous deposits of various regions are present. Among them are *Triquitrites iraqiensis*, *Stellisporites inflatus*, *Schopfites lateralis*, *Polymorphisporites ornatus*, *Knoxisporites* sp., *Laevigatosporites vulgaris*, *Torispora* spp., *Thymospora* spp., *Striatoabieites multistriatus*, *Hamiapollenites insolitus*, *Potonieisporites novicus*, etc. Most of these taxa are typical of the Carboniferous and Permian deposits in western Europe (Alpern, 1959; Venkatachala and Bharadwaj, 1962 - 1964; Doubinger, 1974; Visscher *et al.*, 1974; Clayton *et al.*, 1977; Doubinger and Elsass, 1979; Paquette *et al.*, 1980), Algiers (Doubinger and Fabre, 1983), and Canada (Barss, 1967). Some of the taxa mentioned above are noted in the Permo-Carboniferous deposits of Syria (Khoga, 1985). In the lower Permian deposits of China, Kaiser (1976) recognized *Concavissimisporites*, *Triquitrites*, *Radiizonates*, *Laevigatosporites*, *Columnisporites*, *Punctatosporites granifer*, and also *Torispora laevigata*, *T. securis*. The following miospores were studied in the lower Permian deposits of Australia (Segroves, 1970; Foster, 1979): *Acanthotriletes tereteangulatus*, *Concavissimisporites grumulus*, *Tubercu-*

[1] The numerals in parentheses indicate the spore content in % of the total amount of miospores.

Distribution of miospores (in %) in the lower Permian deposits of northeastern Syria

Miospores / Oil well, interval, depth in m	Ode-107		Ode-116	Rumelan-6		
	2735	2737	2896 - 2897.4	3591	3604.4	3619.2
Leiotriletes sp.	18	7.5	2.5	2	4	2
Iragispora labrata	2	8	+		4	
Iragispora sp.		2	+	0.5		3
Calamospora sp.	0.5	0.5	+	7	1	+
Punctatisporites spp.	2	0.5		14	10.5	5
Cyclogranisporites spp.	+	0.5	1.5	1	5.5	8.5
Verrucosisporites sp.	+	+	+			1
Schopfites lateralis	3	5.5	5			
Lophptriletes sp.		+	0.5	0.5	2	2.5
Concavissimisporites grumulus	20	19.5	3		1	
Acanthotriletes tereteangulatus	+	0.5		1		
Acanthotriletes sp.	+		+			
Triguitrites iragiensis	4	3	1.5			
Triguitrites sp.	3	+	+			1.5
Stellisporites inflatus	2	2.5			1	
Stellisporites sp.		+	+			
Polymorphisporites ornatus	6	5	3			2
Polymorphisporites sp.	0.5					
Reticulatisporites sp.			+	+	+	
Convolutisporites spp.	1	1.5	0.5	+		
Foveosporites sp.	+					
Stenozonosporites sp.	1.5	+				
Radiizonates cf. *R. solaris*			0.5			
Radiizonates sp.		+	+	2		
Knaxisporites sp.	4	4.5	1	1.5	1	3.5
Laevigatosporites vulgaris	2	2.5	+		1	2
Punctatosporites spp.	6.5	10	2	1.5	1	8
Tuberculatosporites modikus	3	+	4	14	1	10
Spinosporites sp.	2	2				
Thymostopa cicatricosa	1.5	1.5				1
T. pseudothiessenii	1	2	21			
Thymostopa sp.	+					
Torispopa laevigata	4	5.5	10	2	4	2.5
T. securis	3.5	4	3.5	11.5	6.5	
T. verricosa	1	3.5		1	19.5	20
Columnisporites sp.	+	+	+			
Vitreisporites sp.	0.5			0.5	0.5	0.5
Alisporites sp.	0.5	0.5	1			
Pinuspollenites thoracatus	0.5	+				
Platysaccus sp.	+		1	5.5		2
Sulcatisporites sp.	+	+	+			
Scheringipollenites ovatus			1	+	1.5	
Klausipollenites schaubergeri			1		1	

(Contd.)

Miospores / Oil well, interval, depth in m	Ode-107		Ode-116	Rumelan-6		
	2735	2737	2896 - 2897.4	3591	3604.4	3619.2
Falcisporites sp.			+			
Pteruchipollenites sp. cf. *P. gracilis*			1	2		
Disaccites sp.		+	3	24	8	17
Distriatites cf. *D. dettmannae*			1.5			
Protohaploxypinus sp.	+			+		2
Limitisporites sp.			+			0.5
Lueckisporites sp.				0.5	1	
Striatoabieites multistriatus	4.0	1.5	1			
Hamiapollenites insolitus			5	+	0.5	
Hamiapollenites sp.			4			
Striatites sp.				12	+	
Praecolpatites sinuosus	1.0		+	+		
Pretricolpipollenites bharadwaji				+	+	1
Potonieisporites novicus	1.5	2	7	3.5	8	2
Potonieisporites sp.	+		5	0.5	2	+
Florinites cf. *eremus*						1
Monosaccites sp.	+	+	3	+	2	
Cycadopites sp.		1	+			
Unidentified	+	3	+	2	7.5	1.5
Pyramidosporites cf. *racemosus*		+	3	+		
Number of forms	626	700	530	450	250	400
Spores:	91	92	62	59.5	67	72.5
Trilete	66.5	61	21.5	29.5	34	29
Monolete	24.5	31	40.5	30	33	43.5
Pollen:	8	8	37.5	50.5	32.5	27
Disaccites (nontaeniate)	1.5	0.5	10.5	32	11	19.5
Disaccites (striatiti)	4	1.5	12	14.5	3.5	2.5
Monosaccites	1.5	2	15	4	12	3
Monocolpates, etc.	1	3.5	+	+	6	1

latosporites modicus, *Laevigatosporites vulgaris*, *Thymospora cicatricosa*, *Praecolpatites sinuosus*, *Striatoabieites multistriatus*, *Potonieisporites* spp., *Distriatites dettmannae*, *Pretricolpipollenites bharadwaji*, *Scheuringipollenites ovatus*, and *Pyramidosporites* sp. Several of the taxa from this list are noted as typical for the Permian of Pakistan (Balme, 1970): *A. tereteangulatus* and *L. novicus*, and representatives of *Punctatosporites*, *P. novicus*, *Hamiapollenites insolitus*, *Pinuspollenites thoracatus*, and *P. bharadwaji*.

A comparison of the assemblages from the Permian sections in the nearby Iraq, Turkey, and Israel is of considerable importance. The Syrian assemblage is distinguished by the presence of *Hamiapollenites insolitus*, *Potonieisporites novicus*, i.e., the taxa that were used to establish the palynozonation in the lower Permian deposits of Israel (Eshet and Cousminer, 1986). This zone, however, has a predominant amount of striatiti pollen, contains representatives of the genus *Vittatina*, but lacks the *Torispora* and *Thymospora* forms typical of the Syrian assemblage. A comparison with the Permian assemblage from a locality near Mosul in northern Iraq (Singh, 1964) shows that the common forms are *Iraqispora labrata*, *Triquitrites iraqiensis*, *Punctatosporites* (*Punctatosporites marrattiodes*), *Thymospora pseudothiessenii* (*Thymospora opaqua*), *Schopfites lateralis*, representatives of genera

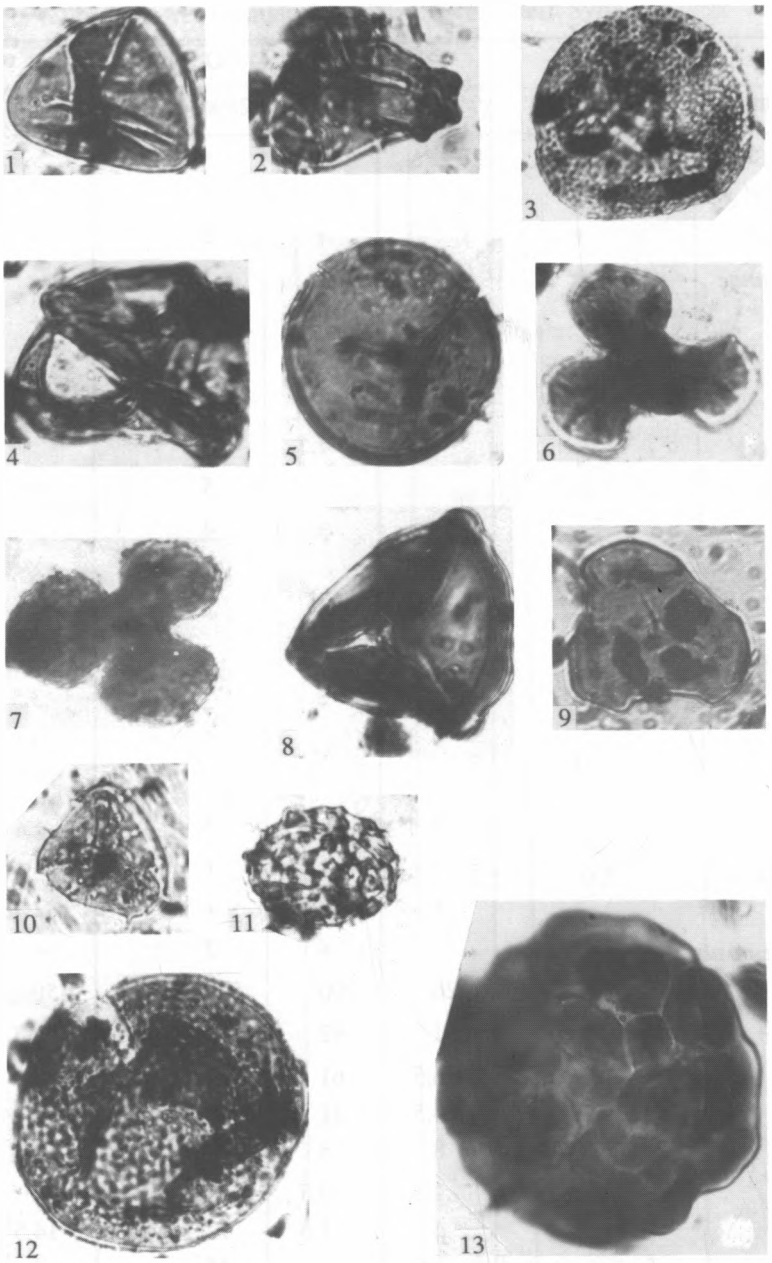

Palynomorphs from the lower Permian deposits of northeastern Syria.

Plate I.

1 – *Leiotriletes* sp. *L.* cf. *gulaferus* Alpern, 1959, Ode-107, 2737 m.
2 – *Triquitrites iraqiensis* Singh, 1964, Ode-116, int. 2896 - 2897.4 m.
3, 12 – *Cyclogranisporites* sp. cf. *C. unctus* Kaiser, 1976, Ode-116, int. 2896 - 2897.4 m.
4 – *Knoxisporites* sp., Ode-107, 2735 m.
5 – *Punctatisporites* sp., Ode-116, int. 2896 - 2897.4 m.
6, 7 – *Stellisporites* spp., 6 – *S. inflatus* Alpern, 1959, Ode-107, 2737 m.
8 – *Iraqispora labrata* Singh, 1964, Ode-107, 2737 m.
9 – *Triquitrites* sp., Ode-107, 2737 m.
10 – *Acanthotriletes tereteangulatus* Balme et Hennelly, 1956, Ode-107, 2737 m.
11 – *Thymospora pseudothiessenii* (Kosanke) Alpern et Doubinger, 1973, Ode-116, int. 2896 - 2897.4 m.
13 – *Verrucosisporites* sp., Ode-107, 2737 m.
×750 for all figures.

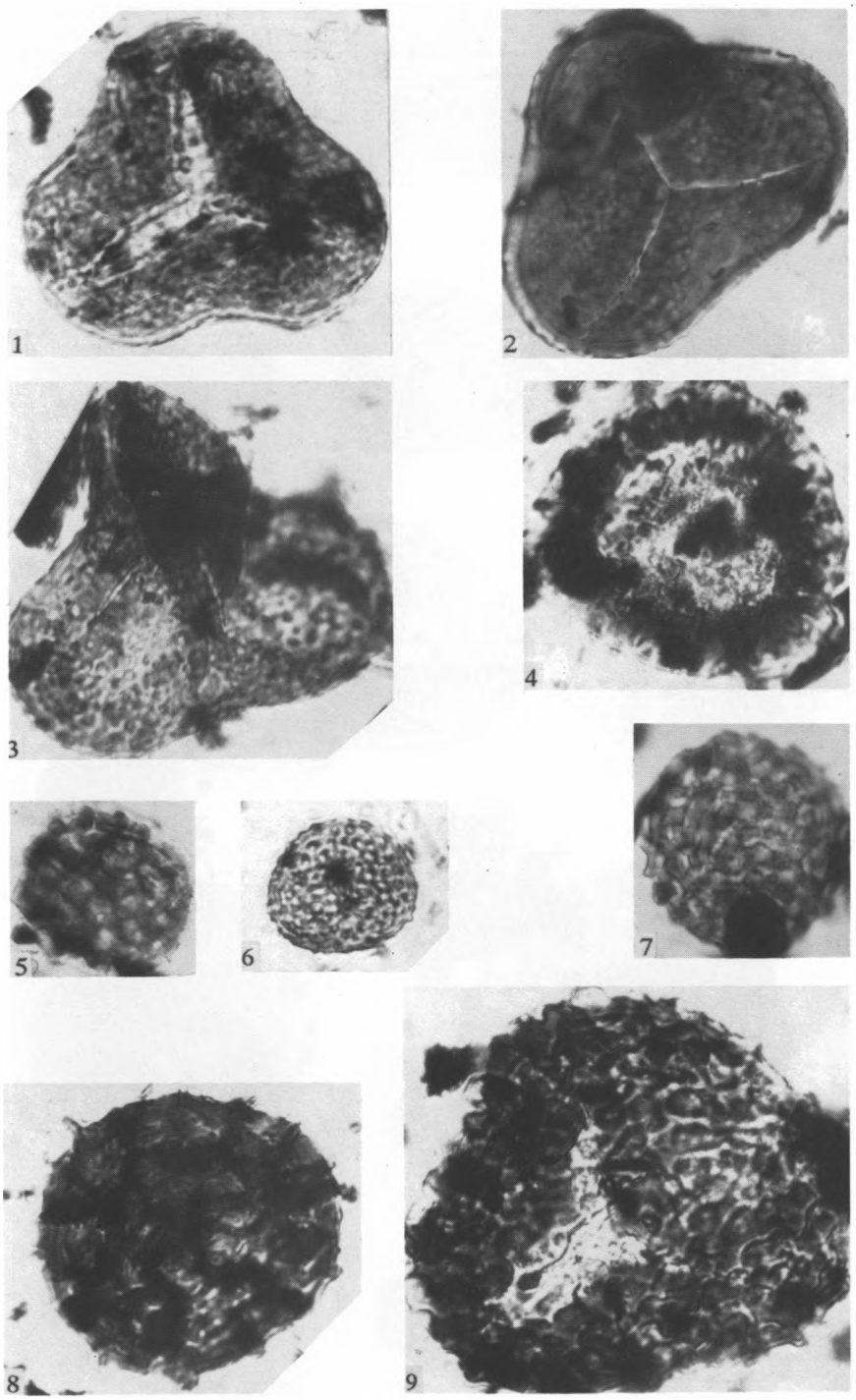

Plate II.

1 - 3 – *Concavissimisporites grumulus* Foster, 1979, Ode-107, 2737 m.
4 – *Radiizonates solaris* Kaiser, 1976, Ode-116, int. 2896 - 2897.4 m.
5, 7 – *Convolutispora* spp., Ode-107, 2737 m.
6 – *Punctatosporites granifer* Potonie et Kremp, 1956, Ode-107, 2735 m.
8 – *Reticulatisporites* sp., Rumelan-6, 3604.4 m.
9 – *Polymorphisporites ornatus* Alpern, 1959, Ode-107, 2737 m.
×750 for all figures.

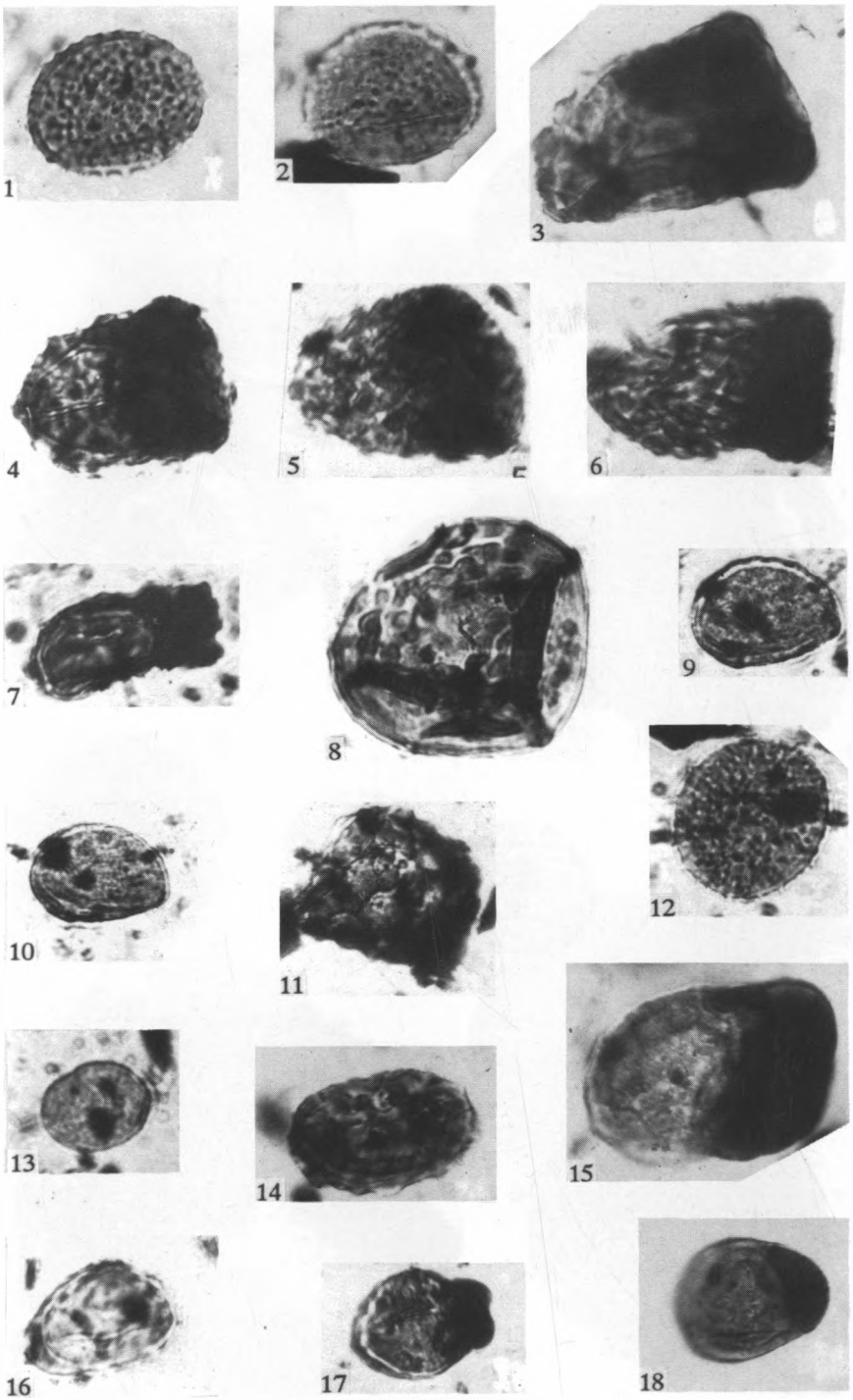

Plate III.

1, 2 – *Tuberculatosporites modicus* Balme et Hennelly, 1956, Ode-107, 2735 m.
3 - 7 – *Torispora verrucosa* Alpern, 1959. 3, 4, 6 – Ode-107, 2737 m; 5 – Ode-116, int. 2896 - 2897.4 m; 7 – Ode-107, 2735 m.
8 – *Schopfites lateralis* Singh, 1964, Ode-107, 2735 m.
9, 10 – *Torispora securis* (Balme) Alpern, Doubinger et Horst, 1965, Ode-107, 2735 m.
11 – *Thymospora* sp., Ode-107, 2735 m.
12 – *Spinosporites* sp., Ode-107, 2737 m.
13 – *Punctatosporites minutus* (Ibr.) Alpern et Doubinger, 1973, Ode-107, 2737 m.
14 – *Thymospora cicatricosa* (Balme et Hennelly) Hart, 1965, Ode-107, 2735 m.
15 - 18 – *Torispora laevigata* Bharadwaj, 1957, Ode-107, 2737 m.
×750 for 1, 2, 8, 11, 13, and14; ×1000 for 15 - 18.

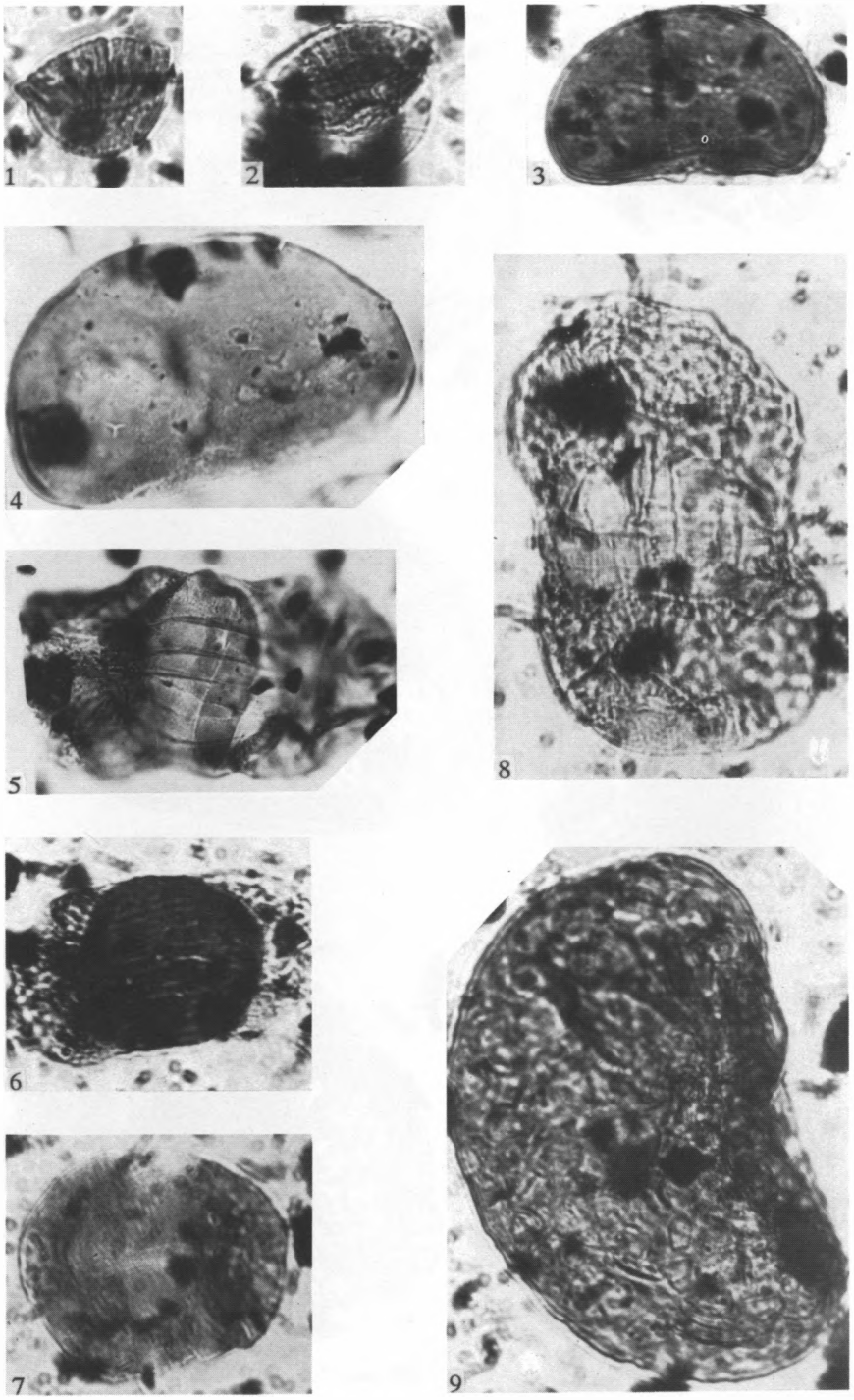

Plate IV.

1, 2 – *Striatoabieites multistriatus* (Balme et Hennelly) Hart, 1964, Ode-107, 2737 m.
3, 4 – *Laevigatosporites vulgaris* (Ibr.) Alpern et Doubinger, 1973, Ode-107, 2737 m.
5 – *Hamiapollenites insolitus* (Bharadwaj et Salujha) Balme, 1970, Ode-116, int. 2896 - 2897.4 m.
6 – *Protohaploxypinus* spp., Rumelan-6, 3619.2 m.
7 – *Lueckisporites* sp., Rumelan-6, 3604 m.
8 – *Distriatites* sp. cf. *D. dettmannae* (Segroves) Foster, 1979, Ode-116, int. 2896 - 2897.4 m.
9 – *Columnisporites* sp., Ode-107, 2737 m.
×750 for all figures.

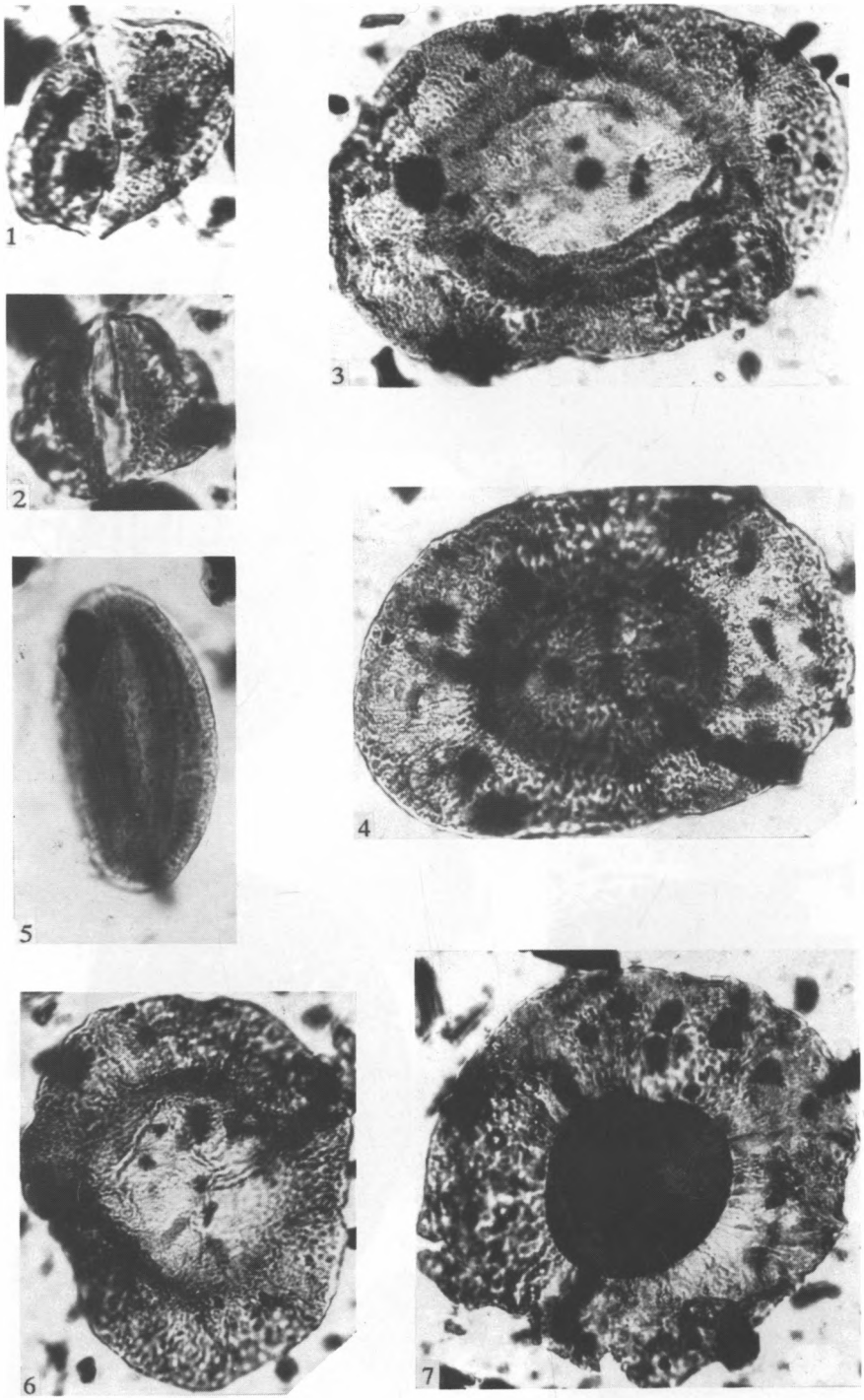

Plate V.

1, 2 – *Scheuringipollenites ovatus* (Balme et Hennelly) Foster, 1975, Ode-116, int. 2896 - 2897.4 m.

3, 4 – *Potonieisporites novicus* Bharadwaj: 3 – Ode-116, int. 2896 - 2897.4 m and 4 – Ode-107, 2735 m.

5 – *Praecolpatites sinuosus* (Balme et Hennelly) Bharadwaj et Srivastava, 1969, Ode-107, 2735 m.

6 – *Potonieisporites* sp., Ode-116, int. 2896 - 2897.4 m.

7 – *Florinites* sp., cf. *F. eremus* Balme et Hennelly, 1956, Rumelan-6, 3619.2 m.

×750 for 1, 2, and 5; ×600 for 3, 4, 6, and 7.

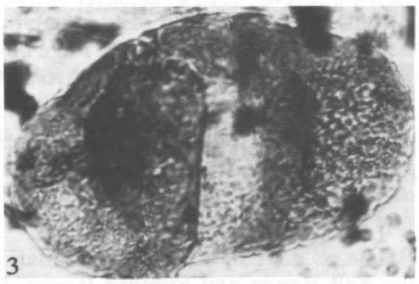
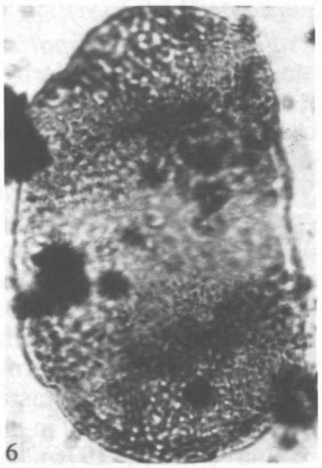
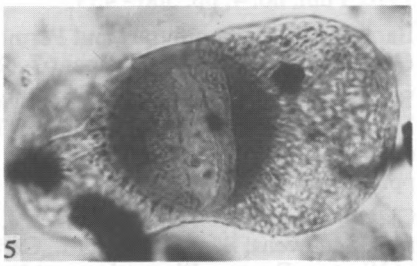
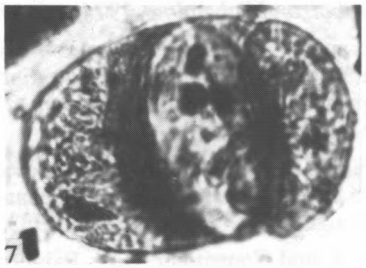

Plate VI.

1 – *Pinuspollenites thoracatus* Balme, Ode-107, 2735 m.
2 – *Klausipollenites schaubergeri* (Potonie et Klaus) Balme, 1970, Ode-116, int. 2896 - 2897.4 m.
3, 7 – *Falcisporites* sp., Ode-116, int. 2896 - 2897.4 m.
4 – *Pretricolpipollenites bharadwaji* Balme, 1970, Rumelan-6, 3619.2 m.
5 – *Platysaccus* spp., Ode-107, 2735 m.
6 – *Pteruchipollenites* sp. cf. *P. gracilis* (Segroves) Foster, 1979, Ode-116, int. 2896 - 2897.4 m.
8 – *Pyramidosporites* cf. *racemosus* Balme, 1970, Ode-116, int. 2896 - 2897.4 m.
×750 for 1 - 7; ×600 for 8.

Cyclogranisporites, *Laevigatosporites*, *Potonieisporites*, and a number of other taxa. The assemblage from Iraq, however, does not have the *Torispora* forms characteristic of the Syrian assemblage, implying its older age.

The assemblage we studied is most similar to the assemblages observed in the deposits of two lacustrine horizons of the Hazro section near Diyarbakir in southern Turkey (Agrali and Akyol, 1967); the horizons were dated back to the Artinskian–Kungurian time. Similarities between these assemblages, particularly with the assemblage of the upper horizon, is evident in the taxonomic composition and quantitative contents of the major groups of miospores. Forms common to the assemblages of northeastern Syria and Hazro section are *Concavissimisporites grumulus* (*Concavisporites trilobatus*, *C. crassus*, *C. granulatus*), *Iraqispora labrata* (*Kyrtomisporis*), and *Tuberculatosporites modicus*; representatives of the genera *Knoxisporites*, *Alisporites*, *Hamiapollenites*, *Lueckisporites*; and forms of monosaccate pollen. The similarity is best emphasized by the presence of an appreciable amount of monolete spores: *Punctatosporites*, *Thymospora*, and *Torispora*; moreover, the latter two genera are represented by variously ornamented forms ranging from smooth to intricately sculptured. These forms are also significant in the assemblage from the upper horizon of the Hazro section (Agrali and Akyol, 1967). The correlation of our assemblage with the Permo-Carboniferous and lower Permian assemblages from the remote and nearby regions seems to indicate its early Permian age. A similar group of taxa observed in the assemblage from northeastern Syria and also recorded in the nearly coeval deposits in China (Kaiser, 1976), Australia (Segroves, 1970; Foster, 1979), and western Europe (Alpern, 1959; Doubinger, 1974; Visscher, 1974) indicates the mixed composition of the studied palynoflora.

The generalized conclusions are:

(1) The assemblage of miospores from the sections of the oil wells Ode-107, Ode-116, and Rumelan-6 located in northeastern Syria contains forms typical of the Permo-Carboniferous deposits in western Europe, of the lower Permian in China, Australia, and Pakistan, and of the Permian in Turkey, Iraq, and Israel. This similarity allows us to tentatively date the assemblage back to the early Permian time.

(2) The absence of the early Triassic diagnostic forms persuades us to dismiss the age determination suggested by Bebeshev *et al.* (1988) for sections of the oil wells Ode-107 and Ode-116.

(3) The mixed composition of Syrian palynoflora containing taxa known to exist in different paleogeographical regions (Euramerian, Cathaysian, Gondwanian) indicates its transitional, ecotonic character and close relations between these regions in the early Permian.

(4) A close similarity of assemblages from the sections of northeastern Syria and southern Turkey (the Hazro section) implies that the Syrian sections may be located in a southern part of the Tethys between the Eurasian and the African continents (Güvenc, 1985).

ACKNOWLEDGMENTS

The authors wish to extend their sincere thanks to M.A. Akhmet'ev and N.A. Volkova for their review of the manuscript and valuable advice. We are particularly grateful to Dr. C.B. Foster of Canberra for his helpful comments on our determination of certain taxa of miospores in the course of discussion during his visit to Moscow in August 1991.

REFERENCES

Agrali, B. and Akyol, E., Etude palynologique des charbons de Hazro et considerations sur l'age des horizons lacustres du Permo-Carbonifére, *Bull. Miner. Res. and Explor. Inst. Turk.*, 1967, no. 68, pp. 1 - 26.

Alpern, B., *Contribution à l'étude palynologique et pétrographique des Chàrbons Francais, Thèses de docteur des sciences naturelles*, Paris: Faculté des Sciences de l'Univ. de Paris, 1959.

Balme, B.E., Palynology of Permian and Triassic Strata in the Salt Range and Surghar Range, West Pakistan, *Stratigraphic Boundary Problems: Permian and Triassic of West Pakistan*, Kansas: Univ. Press Kansas, Dep. Geol. Spec., 1970, Publ. no. 4, pp. 306 - 453.

Barss, M.S., Carboniferous and Permian Spores of Canada, *Geol. Surv. Canada*, 1967, Paper 67-11, pp. 1 - 94.

Bebeshev, I.I., Dzhalilov, Yu.M., Portnyagin, L.A., Yudin, G.T., Muolla, A., Zaza, T., and Yuzef, A., The Triassic Deposits of Syria, *Izv. Akad. Nauk SSSR, Ser. Geol.*, 1988, no. 11, pp. 43 - 53.

Clayton, G., Coquel, R., Doubinger, J., Gueinn, K.J., Loboziak, S., Qwens, B., and Streel, M., Carboniferous Miospores of Western Europe: Illustration and Zonation, *Meded. Rijks. Geol. Dienst. Nieuwe Ser.*, 1977, vol. 29, pp. 1 - 71.

Doubinger, J., Etudes Palynologiques dans Autunien, *Rev. Palaeobot. and Palynolog.*, 1974, vol. 17, nos. 1, 2, pp. 21 - 38.

Doubinger, J. and Elsass, Ph., Le bassin Permo-Carbonifere d'Autun, Nouvelles données stratigraphiques et palynologiques, *Bull. Soc. Histoire Natur. d'Autun*, 1979, no. 91, pp. 9 - 25.

Doubinger, J. and Fabre, J., Mise en évidence d'un Autunien à "Flore mixte" dans le bassin de Béchar-Abadlia (Sahara occidental algerien), *Pollen et Spores*, 1983, no. 1, pp. 91 - 116.

Eshet, Y. and Cousminer, H.L., Palynozonation and Correlation of the Permo-Triassic Succession in the Negev, Israel, *Micropaleontol.*, 1986, vol. 32, no. 3, pp. 193 - 214.

Foster, C.B., Permian Plant Microfossils of the Blair Athol Coal Measures and Basal Rewan Formation of Queensland, *Publ. Geol. Surv. B*, 1979, nos. 372, 244.

Güvenc, T., Permian of Turkey, *6th Colloquium on Geology of the Aegean Region, Piri Reis International Contribution*, Izdar, E. and Nakoman, E., Eds., Izmir: Dokuz Eylul Univ., 1985, no. 2, pp. 263 - 282.

Jankauskas, T.V. and Talli, S., The Paleozoic Period in the Territory of the Syrian Arab Republic, *Izv. Akad. Nauk SSSR, Ser. Geol.*, 1978, no. 11, pp. 92 - 97.

Kaiser, H., Die Permische Mikroflora der Cathaysia-Schichten von Nordwest Schansi, China, *Palaeontographica B*, 1976, vol. 159, Parts 4 - 6, pp. 83 - 157.

Khoga, I., Palynological Investigation on Upper Triassic (Kurachine Dolomite) Deposits in the Northeastern Part of Syria, *Jahrb. Geol. Bundesanst (Oesterreich)*, 1972, Sonderbd. 19.

Khoga, I., The Use of Palynology in Permo-Carbon Stratigraphy of the Syrian Oil Wells, *6th Colloquium on Geology of the Aegean Region, Piri Reis International Contribution*, Izdar, E. and Nakoman, E., Eds., Izmir: Dokuz Eylul Univ., 1985, no. 2, pp. 375 - 384.

Paquette, Y., Doubinger, J., and Courel, L., Étude palynologique de la couche du toit du bassin Autunien de l'Aumance (Assise de buxières): Liaison avec les milieux sédimentaires, *Bull. Soc. Histoire Natur. d'Autun*, 1980, no. 95, pp. 85 - 101.

Segroves, K.L., Permian Spores and Pollen Grains from the Perth Basin, Western Australia, *Grana*, 1970, vol. 10, no. 1, pp. 43 - 73.

Singh, H.P., A Miospore Assemblage from the Permian of Iraq, *Paleontology*, 1964, vol. 7, Part 2, pp. 240 - 265.

Venkatachala, B.S. and Bharadwaj, D.C., Sporological Study of the Coals from Falkenberg (Faulquemont) Colliery, Lothringen (Lorraine, France), *Palaeobotanist*, 1962 - 1964, vol. 11, no. 3, pp. 159 - 207.

Visscher, H., Huddleston Slater-Offerhaus, M.G., and Wong, T.E., Palynological Assemblages from "Saxonian" Deposits of the Saar-Nahe Basin (Germany) and the Dome de Barrot (France): An Approach to Chronostratigraphy, *Rev. Palaeobot. and Palynolog.*, 1974, vol. 17, nos. 1, 2, pp. 39 - 56.

Yaroshenko, O.P., Bach Imam, I., and Nassri, S., Palynological Assemblages of the Triassic in Syria and Their Stratigraphic Significance, *Izv. Akad. Nauk SSSR, Ser. Geol.*, 1982, no. 9, pp. 72 - 77.

Yaroshenko, O.P. and Bach Imam, I., Palynoflora and Stratigraphy of Deposits of the Middle and Upper Triassic in Syria, *Paleofloristika i Stratigrafiya Fanerozoya* (Paleoflora and Stratigraphy of the Phanerozoic), Moscow: GIN Akad. Nauk SSSR, 1989, pp. 32 - 65.

Stratigraphy and Geological Correlation, Vol. 2, No. 1, 1994, pp. 68 - 74. Translated from Stratigrafiya. Geologicheskaya Korrelyatsiya, Vol. 2, No. 1, 1994, pp. 74 - 80.
Original Russian Text Copyright © 1994 by Nevesskaya.
English Translation Copyright © 1994 by Interperiodica Publishing (Russia).

Evolution of the biosphere

Changes in the Taxonomic and Ecologic Composition of Shelf Benthic Assemblages at the Permian–Triassic Boundary

L. A. Nevesskaya

Paleontological Institute, Russian Academy of Sciences, Profsoyuznaya ul. 123, Moscow, 117868 Russia

Received January 26, 1993

Abstract – Changes in the taxonomic and ecologic composition of shelf benthic assemblages at the Permian–Triassic boundary and their possible causes were studied. Analysis of the data available showed that though the mass extinction and general crisis of the biota at this boundary were among the most considerable of Phanerozoic events, they were, among benthic groups, neither synchronous nor similar in scale. Ethological and trophic compositions were stable in most shelf zones; only reef assemblages composed of sessile sestonophagi disappeared.

At the beginning of the Permian the following benthic groups dominated the shelves: foraminifers, tetracorals, tabulates, brachiopods (Spiriferida and Productida), typical Paleozoic bryozoans, namely Trepostomida, Cystoporida, Fenestellida, Cryptostomida, Rhabdomesida, crinoids, and ostracodes. Bivalve mollusks, gastropods, and sponges also occurred, as well as hyolithids, echinoderms (Blastoidea, Echinida, Holothurioidea, Asteroidea, and Ophiuroidea), hydroids, rostroconchs, trilobites, and other rare groups.

In the second half of the Permian, the extinction of some groups began (Fig. 1), and by the end of the Permian it resulted in the disappearance of fusulinids, hyolithids, blastoids, edrioasteroids, trilobites, and brachiopods, namely Orthida, Strophomenida, and Productida. However, athyrids, rhynchonellids, and terebratulids became dominant. The Bryozoan orders Fenestellida, Cryptostomida, and Rhabdomesida disappeared, and only four trepostomid genera survived into the Triassic. Paleozoic crinoids Flexibilia, Camerata, and most of Inadunata, as well as echinoid orders Palaechinoida and Echinocystitoida became extinct, conularians and tabulates almost disappeared (Morozova, 1970; Dobruskina, 1976; Krasilova, 1979; Raup, 1979; Shimanskii, 1987; Stanley, 1988; Kotlyar and Rostovtsev, 1989; and others).

The late Permian extinction maximum, the same as that of the Maestrichtian, was one of the greatest in the Phanerozoic: more than 90% of species, 65 - 76% of genera, and 52 - 57% of families became extinct (Raup, 1978, 1979; Sepkoski, 1978, 1979, 1986). However, the extinction was not catastrophic. Rather, it had a selective character.

Among the extinct forms, the polyhaline thermophilic groups, especially representatives of reef assemblages, dominated (Fisher, 1968; Dagys and Ustritsky, 1973; Gobbett, 1973; Kozur, 1980; Ross and Ross, 1982; Flügel and Stanley, 1984; and others). Before their disappearance, the latter usually occurred in basins of the tropical region, including the Paleotethys (Kozur, 1980; Stanley, 1988). Such forms were fusulinids (Foraminifera), tetracorals, and many bryozoans. Late Permian reefs were mainly formed by sponges and calcareous algae (Flügel and Stanley, 1984).

Different authors suggested the following causes of the late Permian extinction: (1) a decrease in ocean water salinity, up to 30 or 31.5‰, as a result of regression and brine concentration in the abyssal areas (Fischer, 1964, 1968, 1986; Lantzy *et al.*, 1977; Stevens, 1977; Zharkov, 1981); (2) reduction of the area of epicontinental seas because of regression (Valentine and Moore, 1972; Schopf, 1974; Simberloff, 1974; Kozur, 1980; Hallam, 1989), which resulted in the disappearance of certain ecologic niches, including reef knolls (*Razvitie i Smena* ..., 1965; Boukot, 1975); (3) "oxygen" water mixing after a cool period associated with upwelling (Wilde and Berry, 1986); (4) global cooling and glaciation in the southern polar region and, to a lesser extent, in North Siberia, as well as a 125 - 225 m drop in the eustatic sea level, which caused the disappearance of warm shallow seas (Hallam, 1984; Stanley, 1988); (5) an increase in nutrient deficiency in sea water because of the accumulation

of sediments rich in organic matter that, in turn, resulted in a lowering of the oxygen content in the atmosphere and the extinction of land plants and animals (Hoffman, 1989); (6) a decrease in phytoplankton (Tappan, 1982); or (7) combinations of the above-mentioned factors (Astaf'eva-Urbaitis and Yasamanov, 1986). Other hypotheses have also been suggested, e.g., a cosmic one (Schindewolf, 1954; McLaren, 1970), a reduction of genetic variability (Bretsky and Lorenz, 1970), change in the oxygen content (McAlester, 1970, 1971), and an increase of arid and continental areas (Nakazawa, 1985).

Most of these hypotheses are common nowadays, and there is no consensus on the causes of extinction.

The duration and rate of the late Permian extinction are also open to discussion. According to S. Stanley (1988), the extinction occurred throughout the late Permian, i.e., during the Guadalupian and Dzhulfian (about 10 Ma), whereas, according to G.V. Kotlyar and K.O. Rostovtsev (1989), extinction took place only in the second half of the late Permian, and in the first half – during the Kubergandian and Midian – all faunal groups, including higher fusulinids, flourished. The extinction rate was not catastrophic, but rather was gradual and irregular, so that some Permian relics still occurred in the early Triassic seas (*Razvitie i Smena* ..., 1965; Stepanov, 1972; Dagys, 1974; Kozur, 1980; Tappan, 1982; Kotlyar *et al.*, 1983; Clark *et al.*, 1986; Passini, 1988; Kotlyar and Rostovtsev, 1989).

The late Permian extinction considerably impoverished the benthos. At the beginning of the Triassic, only bivalve mollusks dominated, whereas small foraminifers, brachiopods, gastropods, bryozoans, sphinctozoans, echinoderms, and crustaceans were scarce. Rare corals, most likely, also occurred, and later became widespread (Fig. 1).

The early Triassic fauna was cosmopolitan and contained many relict Permian genera and species, which survived, within limited areas, the late Permian crisis (*Razvitie i Smena* ..., 1965; Fisher, 1968; Stepanov, 1972; Kummel, 1973; Dagys, 1974; Dobruskina, 1976; Boukot, 1975; Krasilova, 1979; Shimanskii, 1987; Kotlyar and Rostovtsev, 1989).

The diversity of benthos began to increase only during the second half of the early Triassic, during the Olenekian. In the middle Triassic, scleractinians appeared, as well as some new taxa of small foraminifers, brachiopods, gastropods, crinoids, and other groups. Part of the new faunal elements were formed from the Permian euryhaline fauna relics preserved in refugia, shallow semisea late Permian basins (Fischer, 1964, 1968; Stepanov, 1972; Kozur, 1980), and the other parts, from cosmopolitan early Triassic forms.

As for the Permian and Triassic benthic assemblages composition in different biogeographic areas, the assemblages of the tropical region, especially reefs, were characterized by the greatest taxonomic diversity.

In the Permian, brachiopods, bivalve mollusks, and bryozoans dominated in marginal sea areas (littoral and

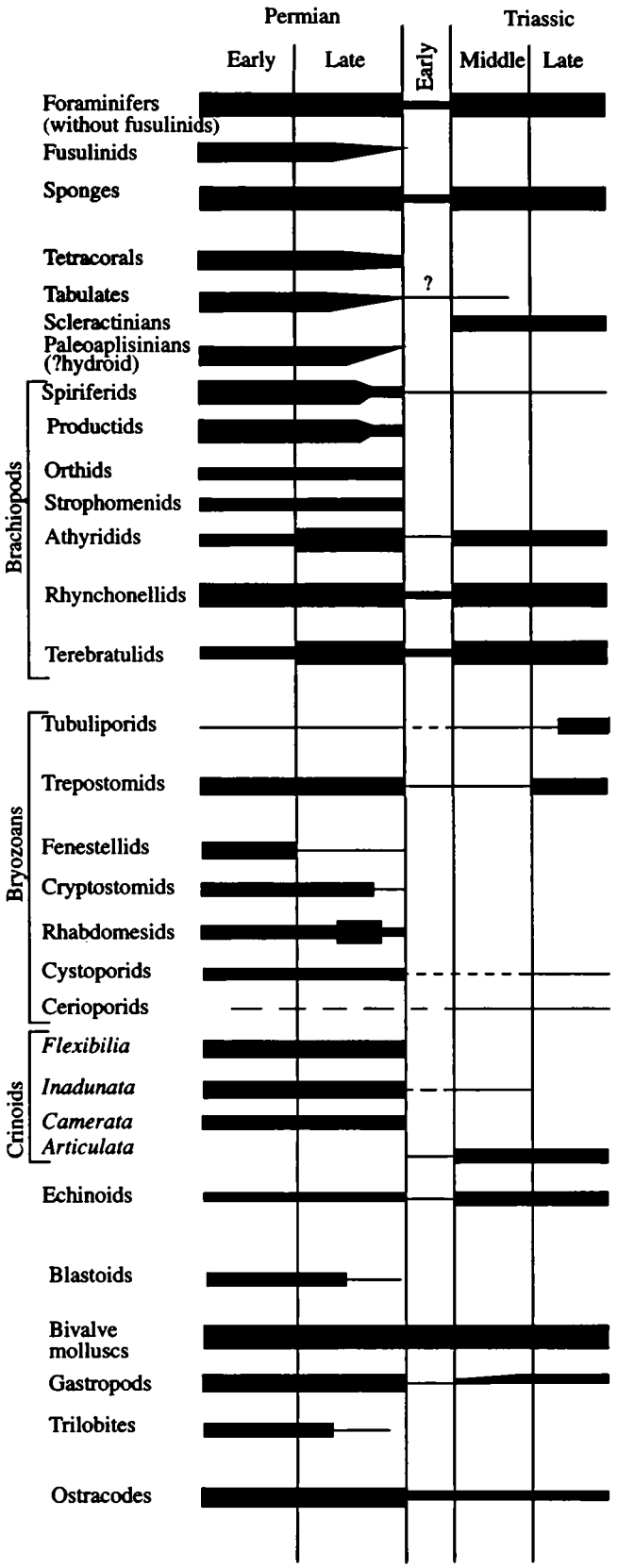

Fig. 1. Distribution of the main invertebrate groups that composed benthic shelf assemblages in the Permian and Triassic.

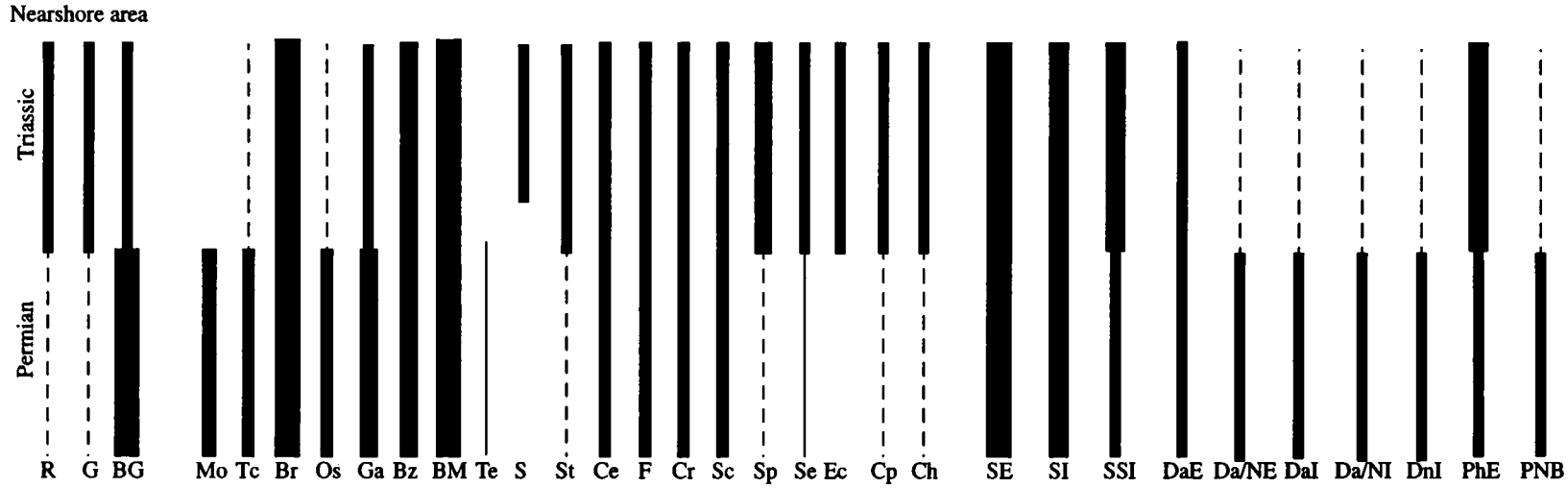

Fig. 2. Taxonomic and ethologotrophic composition of benthic assemblages from the nearshore areas of Permian and Triassic seas. Taxonomic groups: BG – blue-green algae; Bl –blastoids; BM – bivalve mollusks; Br – brachiopods; Bz – bryozoans; Ce – cephalopods; Ch – chaetetids; Co – conodonts; Con – conulariids; Cp – cirripeds and other crustaceans; Cr – crinoids; Ec – echinoids; F – foraminifers; G – green algae; Ga – gastropods; Hy – hydroids; Mo – monoplacophorans; Os – ostracodes; Pa – paleoaplisinians (? hydroid); Pr – problematics; R – red algae; S – scleractinians; Sc – scaphopods; Se – serpulids; Sp – sponges; St – stromatoporids; Ta – tabulates; Tc – traces; Te – tetracorals; Tr – trilobites. Ethologotrophic groups: DnI – infaunal nonassorting detritophagi; DaI – infaunal assorting detritophagi; Da/NI – infaunal assorting detritophagi/necrophagi; Da/NE – epifaunal assorting detritophagi/necrophagi; DaE – epifaunal assorting detritophagi; SI – infaunal sestonophagi; SSI – semi-infaunal; SE – epifaunal sestonophagi; PhE – epifaunal phytophagi; PNB – nektobenthic predators; PE – epifaunal predators.

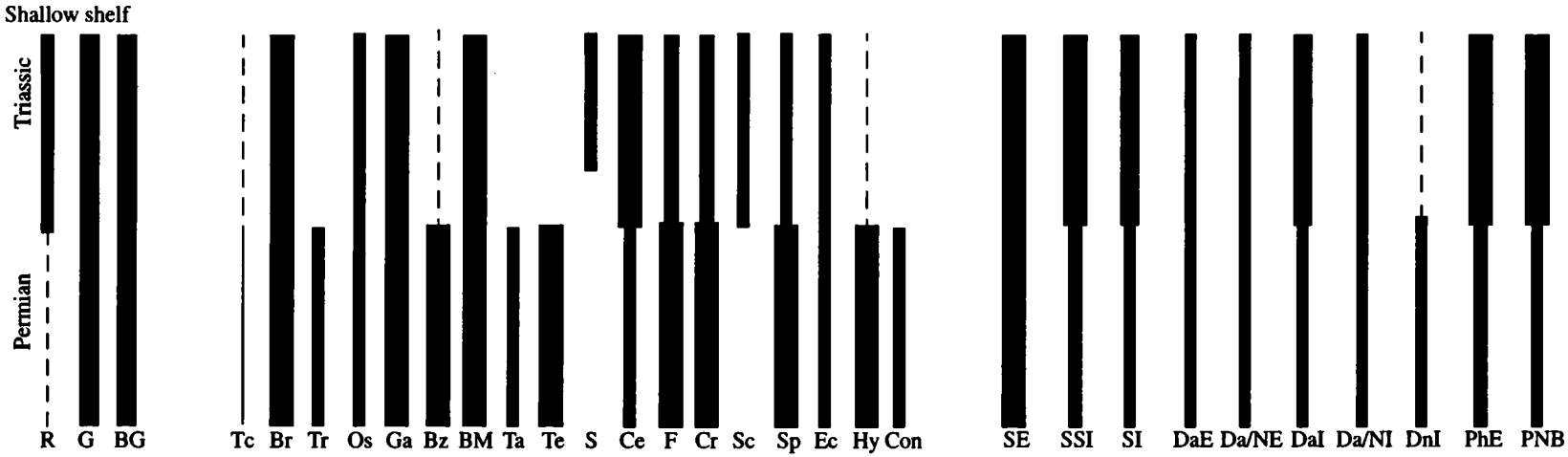

Fig. 3. Taxonomic and ethologotrophic composition of benthic assemblages from the shallow shelf of Permian and Triassic seas. Legend is the same as for Fig. 2.

lagoons) and in the nearshore shallow basins of this region. Foraminifers, gastropods, scaphopods, monoplacophorans, ostracodes, crinoids, ? worms, rare tetracorals, and nektobenthic cephalopods also occurred there. Epifaunal sestonophagi (vagile and sessile, and free-lying) dominated, whereas infaunal sestonophagi and detritophagi, epifaunal mobile phytophagi, detritophagi and necrophagi, as well as nektobenthic predators were of minor importance (Fig. 2).

On the open shallow shelf, the benthos was considerably more diverse. It included numerous brachiopods, bryozoans, foraminifers, tetracorals, hydroids, crinoids, sponges, gastropods, and bivalve mollusks, as well as rarer tabulates, trilobites, echinoids, ostracodes, and nektobenthic cephalopods. Among the ethologotrophic groups, the epifaunal sestonophagi were dominant, whereas semi-infaunal and infaunal sestonophagi, epifaunal mobile detritophagi, necrophagi, phytophagi, and nektobenthic predators were less important (Fig. 3).

Bioherms were formed on the shallow shelf sandbanks by bryozoans, tetracorals, hydroids, sphinctozoans and sclerosponges, some brachiopods, and bivalve mollusks, as well as by calcareous algae (green, blue-green, and red). Numerous foraminifers, crinoids, gastropods, common monoplacophorans, scaphopods, tabulates, ostracodes, blastoids, and serpulids were associated with the bioherms (Fig. 4).

On the deep-water shelf, benthic forms were less diverse and numerous. This sea zone was inhabited by foraminifers, bryozoans, sponges (usually siliceous), infaunal bivalve mollusks, gastropods, ostracodes, nektobenthic cephalopods, and, more seldom, by other groups. Ethologotrophic composition was rather mixed, but no one group prevailed. Some epifaunal sessile and free-lying sestonophagi, mobile detritophagi, and necrophagi, infaunal detritophagi, (?) planktobenthic sestonophagi, and nektobenthic predators were recorded there (Fig. 5).

In the marginal, nearshore shallow sea areas of the boreal and notal regions, bivalve mollusks were dominant. Gastropods, brachiopods, and bryozoans were common, whereas other groups were relatively few. Blue-green calcareous algae were widespread. Epifaunal sestonophagi prevailed. On the shallow shelf, brachiopods, bryozoans, crinoids, and foraminifers, which dominated in the assemblages of the tropical region, were supplemented with bivalve mollusks and gastropods. Tetracorals were scarcer than in the tropical region, whereas hydroids were absent. The same as in the above-mentioned zones, epifaunal sestonophagi, vagile and sessile, as well as free-lying, prevailed. Semi-infaunal and infaunal sestonophagi, epifaunal and infaunal mobile detritophagi, and necrophagi, phytophagi, and nektobenthic predators were rarer.

In both the Triassic and Permian, the greatest taxonomic diversity characterized assemblages of the tropical biogeographic region, especially reefs. Reefs and other bioherms were formed during the middle Triassic by scleractinians, calcisponges, hydroids, forms of obscure origin (*Tubiphytes*, *Thaumatoporella*, and *Ladinella*), and calcareous algae. Bivalve mollusks, brachiopods, bryozoans, foraminifers, and other groups occurred within the reefs. They were referred to different ethologotrophic groups, namely to epifaunal vagile and free-lying sestonophagi, epifaunal mobile detritophagi and necrophagi, phytophagi, nektobenthic predators and necrophagi, scarcer infaunal detritophagi and sestonophagi, and semi-infaunal sestonophagi (Fig. 4). At the same time, the epifaunal sessile sestonophagi were predominant in the reef assemblages.

Bivalve mollusks dominated in the rest of the shelf zones of the tropical and boreal regions. Brachiopods and gastropods were also widespread, especially in shallow water. Conchostracans usually inhabited nearshore areas, whereas other invertebrate groups, namely foraminifers, sponges, scleractinians, bryozoans, scaphopods, echinoderms, and serpulids were of secondary importance.

The shallow shelf and nearshore areas were dominated by epifaunal vagile (more seldom free-lying) sestonophagi. Numerous phytophagi and semi-infaunal sestonophagi were present, whereas infaunal sestonophagi, infaunal and epifaunal detritophagi and necrophagi, as well as nektobenthic predators and necrophagi were considerably less abundant (Figs. 2 and 3).

Bivalve mollusks were dominant in deep-water assemblages. Scleractinians, brachiopods, gastropods, scaphopods, crinoids, and echinoids were considerably rarer.

The deep-water shelf was inhabited equally by semi-infaunal (? or pseudoplanktonic) and epifaunal vagile sestonophagi, infaunal detritophagi, and nektobenthic predators and necrophagi. Infaunal sestonophagi, as well as epifaunal detritophagi and predators were scarce (Fig. 5).

Accordingly, though mass extinction and crisis of the biota at the Permian–Triassic boundary were among the major Phanerozoic events, they were not synchronous for all the organisms. Different groups became extinct at different times, and the number and diversity of some of them decreased throughout the late Permian or its second half. The dimensions of the extinction were also unequal among different groups.

The ethologotrophic composition was stable on most of the shelf. Only the taxa characteristic of different ecologic groups were replaced.

Only the areas with reef structures in the tropical biogeographic region were marked by considerable changes as a result of the extinction of main reef-constructing organisms, so that at the beginning of the Triassic, reef assemblages almost disappeared and were formed again only at the middle Triassic. As much as reef-constructing forms were represented mainly by sessile sestonophagi, just that ethologotrophic group suffered most from the crisis.

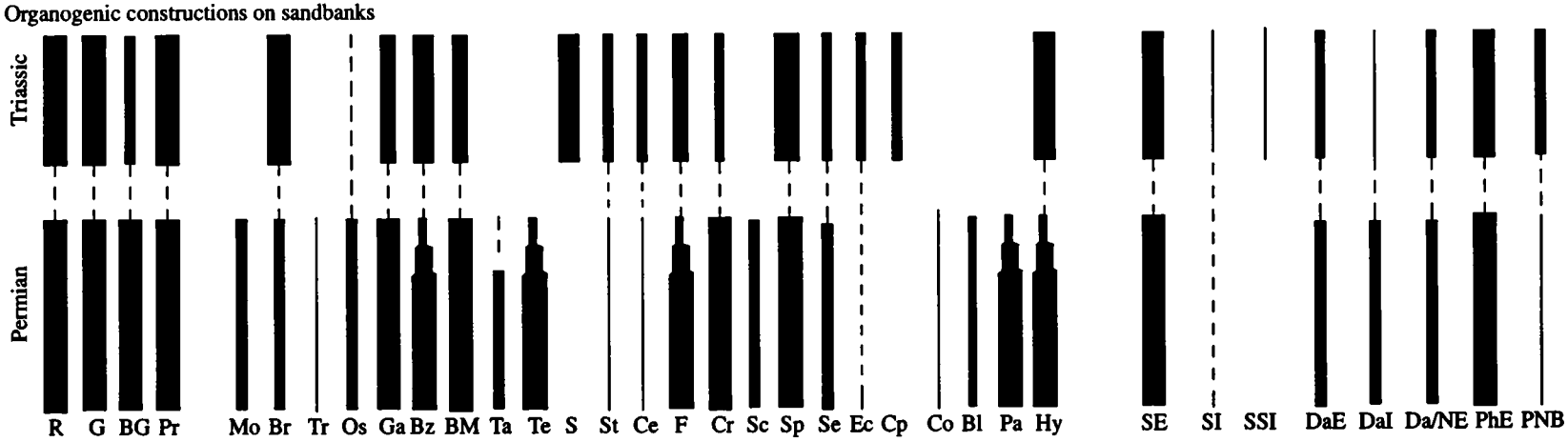
Organogenic constructions on sandbanks
Triassic
Permian
R G BG Pr Mo Br Tr Os Ga Bz BM Ta Te S St Ce F Cr Sc Sp Se Ec Cp Co Bl Pa Hy SE SI SSI DaE DaI Da/NE PhE PNB

Fig. 4. Taxonomic and ethologotrophic composition of benthic assemblages of organogenic constructions on sandbanks of the Permian and Triassic seas. Legend is the same as for Fig. 2.

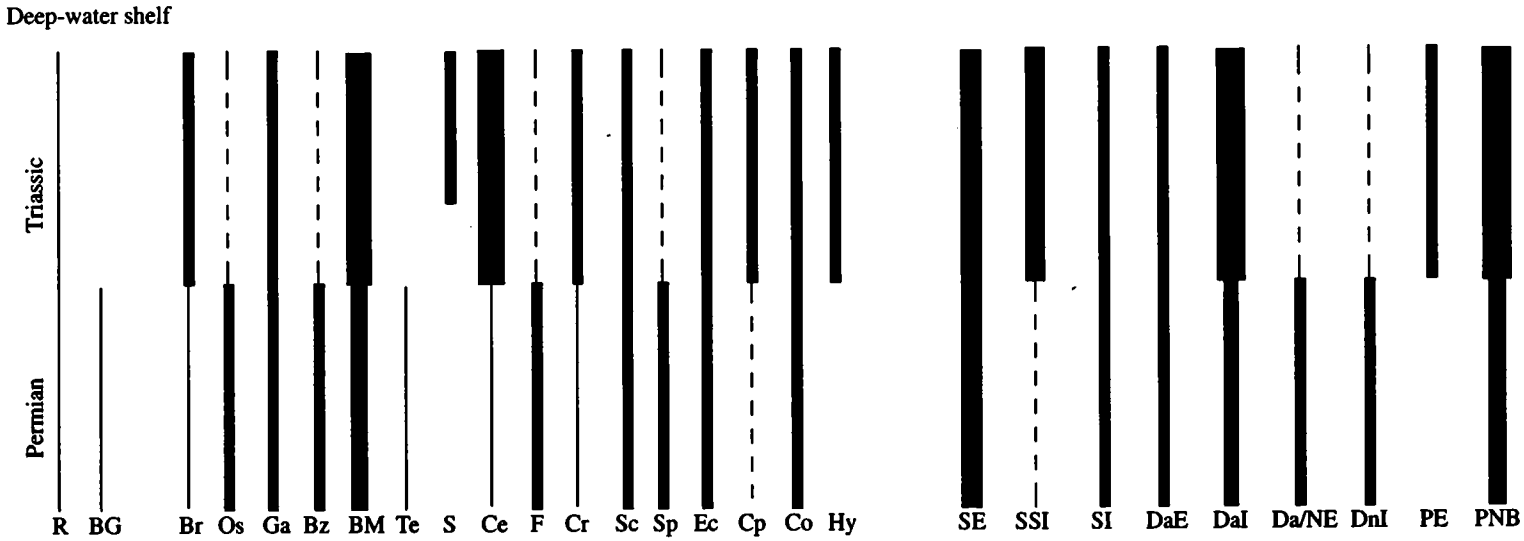

Fig. 5. Taxonomic and ethologotrophic composition of benthic assemblages from the deep-water shelf of the Permian and Triassic seas. Legend is the same as for Fig. 2.

REFERENCES

Astaf'eva-Urbaitis, K.A. and Yasamanov, N.A., Faunal Assemblages and Temperatures of the Northeastern USSR Marine Basins in the Permian, *Byull. MOIP, Otd. Geol.*, 1986, vol. 61, no. 4, pp. 101 - 109.

Boucot, A.J., *Evolution and Extinction Rate Control*, Amsterdam: Elsevier, 1975.

Bretsky, P.W. and Lorenz, D.M., An Essay on Genetic-Adaptive Strategies and Mass Extinctions, *Bull. Geol. Soc. Am.*, 1970, vol. 81, no. 8, pp. 2449 - 2456.

Clark, D.L., Cheng-Yuan, W., Orth, Ch.J., and Gilmore, J.S., Conodont Survival and Low Iridium Abundances across the Permian–Triassic Boundary in South China, *Science*, 1986, vol. 233, no. 4767, pp. 984 - 986.

Dagys, A.S., *Triasovye Brakhiopody. Morfologiya, Sistematika, Filogenez, Stratigraficheskoe Znachenie i Biogeografiya* (Triassic Brachiopods: Morphology, Systematics, Phylogeny, Stratigraphic Significance, and Biogeography), Novosibirsk: Nauka, 1974.

Dagys, A.S., Main Regularities in Geographic Differentiation of Triassic Brachiopods, *Paleobiogeografiya Severa Evrazii v Mezozoe* (Mesozoic Paleobiogeography of North Eurasia), Novosibirsk: Nauka, 1974, pp. 7 - 22.

Dagys, A.S. and Ustritsky, V.I., The Main Relationships between the Changes in Marine Fauna at the Close of the Permian and the Beginning of the Triassic, *Canad. Soc. Pet. Geol. Mem.*, 1973, no. 2, pp. 647 - 654.

Dobruskina, I.A., The Permian–Triassic Boundary, *Granitsy Geologicheskikh Sistem* (Boundaries of Geologic Systems), Moscow: Nauka, 1976, pp. 145 - 167.

Fischer, A.G., Brackish Oceans as the Cause of the Permo-Triassic Marine Faunal Crisis, *Problems in Paleoclimatology*, London: Interscience, 1964, pp. 566 - 577.

Fischer, A.G., The Two Phanerozoic Supercycles, *Catastrophes and Earth History: New Uniformitarianism*, Berggren, W.A. and van Couvering, J.A., Eds., Princeton: Princeton Univ., 1984, pp. 129 - 150.

Flügel, E. and Stanley, G.D., Reorganisation, Development, and Evolution of Post-Permian Reefs and Reef Organisms, *Paleontogr. Am.*, 1984, vol. 54, pp. 177 - 186.

Gobbett, D.J., Permian Fusulinacea, *Atlas of Palaeobiogeography*, Hallam, A., Ed., Amsterdam: Elsevier, 1973, pp. 152 - 158.

Hallam, A., Pre-Quaternary Sea-Level Changes, *Annu. Rev. Earth and Planet. Sci.*, 1984, vol. 12, pp. 205 - 243.

Hallam, A., The Case for Sea-Level Change as a Dominant Causal Factor in Mass Extinction of Marine Invertebrates, *Philos. Trans. R. Soc. London*, 1989, vol. B. 325, no. 1228, pp. 437 - 455.

Hoffman, A., What, if Anything, are Mass Extinctions?, *Philos. Trans. R. Soc. London*, 1989, vol. B. 325, no. 1228, pp. 253 - 261.

Kotlyar, G.V. and Rostovtsev, K.O., Late Permian–Early Triassic Evolution of the Tethian Marine Biota, *Osadochnaya Obolochka Zemli v Prostranstve i Vremeni: Stratigrafiya i Paleontologiya* (Earth Sedimentary Cover in Space and Time: Stratigraphy and Paleontology), Moscow: Nauka, 1989, pp. 55 - 62.

Kotlyar, G.V., Zakharov, Yu.D., Kochirkevich, B.V., *et al.*, *Pozdnepermskii Etap Evolyutsii Organicheskogo Mira. Dzhul'finskii i Dorashamskii Yarusy SSSR* (Late Permian Stage of the Organic World Evolution. Dzhulfian and Dorashamian Stages of the USSR), Leningrad: Nauka, 1983.

Kozur, H., Die Faunenänderungen Nahe der Perm/Trias– und Trias/Jura–Grenz und Ihre Möglichen Ursachen, *Freiberg. Forschungsh.*, 1980, no. 357, pp. 111 - 134.

Krasilova, I.N., Triassic Biogeography, *Itogi Nauki i Tekhniki: Stratigrafiya, Paleontologiya: Biogeografiya Mezozoya* (Science and Technics Results: Stratigraphy, Paleontology: Mesozoic Biogeography), Moscow: VINITI, 1979, vol. 9, pp. 6 - 28.

Kummel, B., Lower Triassic (Scythian) Molluscs, *Atlas of Paleobiogeography*, Hallam, A., Ed., Amsterdam: Elsevier, 1973, vol. 22, pp. 233 - 255.

Lantzy, R.J., Dacey, M.F., and Makenzie, F.T., Catastrophe Theory: Application to the Permian Mass Extinction, *Geology*, 1977, vol. 5, pp. 724 - 728.

McAlester, A.L., Animal Extinctions, Oxygen Consumption, and Atmospheric History, *J. Paleontol.*, 1970, vol. 44, pp. 405 - 409.

McAlester, A.L., Oxygen Consumption Rates and Their Paleontologic Significance Reply, *J. Paleontol.*, 1971, vol. 45.

McLaren, D.J., Presidental Adress: Time, Life, and Boundaries, *J. Paleontol.*, 1970, vol. 44, no. 5, pp. 801 - 815.

Morozova, I.P., *Mshanki Pozdnei Permi* (Late Permian Bryozoans), Moscow: Nauka, 1970.

Nakazawa, K., The Permian and Triassic Systems in the Tethys – Their Paleogeography, *The Tethys, Her Paleogeography and Paleobiogeography from Paleozoic to Mesozoic*, Nakazawa, K. and Dickins, J.M., Eds., Tokyo: Tokai Univ., 1985, pp. 93 - 111.

Passini, M., Un'Esperienza Diretta di Ricersa sulla Crisi Biologica al Limite fra Permiano e Trias nelle Dolomiti, *Boll. Soc. Paleontol. Ital.*, 1988, vol. 27, no. 1, pp. 109 - 114.

Raup, D.M., Cohort Analysis of Generic Survivorship, *Paleobiology*, 1978, vol. 4, no. 1, pp. 1 - 15.

Raup, D.M., Size of the Permo-Triassic Bottleneck and Its Evolutionary Implications, *Science*, 1979, vol. 206, no. 4415, pp. 217 - 218.

Razvitie i Smena Morskikh Organizmov na Rubezhe Paleozoya i Mezozoya (Evolution and Replacement of Marine Biota at the Paleozoic–Mesozoic Boundary), Moscow: Nauka, 1965.

Ross, C.A. and Ross, J.R.P., Biogeographic Influences on Late Palaeozoic Faunal Distributions, *Recent and Fossil Bryozoa*, Larwood, G.P. and Nielsen, C., Eds., Fredensborg: Olsen et Olsen, 1982, pp. 199 - 212.

Schindewolf, O.H., Über die Möglichen Ursachen der Grossen Erdgeschichtlichen Faunenschnitte, *N. Jahrb. Geol. Paläont.*, 1954, no. 10, pp. 457 - 465.

Schopf, Th.J.M., Permo-Triassic Extinctions: Relation to Sea-Floor Spreading, *J. Geol.*, 1974, vol. 82, no. 2, pp. 129 - 143.

Sepkoski, J.J., A Kinetic Model of Phanerozoic Taxonomic Diversity: 1. Analysis of Marine Orders, *Paleobiology*, 1978, vol. 4, no. 3, pp. 223 - 251.

Sepkoski, J.J., A Kinetic Model of Phanerozoic Taxonomic Diversity: 2. Early Phanerozoic Families and Multiple Equilibria, *Paleobiology*, 1979, vol. 5, no. 3, pp. 222 - 251.

Sepkoski, J.J., Global Bioevents and the Question of Periodicity, *Lect. Notes Earth Sci.*, 1986, vol. 8, pp. 47 - 61.

Shimanskii, V.N., Historic Development of the Biosphere, *Evolyutsiya i Biotsenoticheskie Krizisy* (Evolution and Biocoenotic Crises), Moscow: Nauka, 1987, pp. 5 - 45.

Simberloff, D.S., Permo-Triassic Extinctions: Effects of Area on Biotic Equilibrium, *J. Geol.*, 1974, vol. 82, no. 2, pp. 267 - 277.

Stanley, G.D., The History of Early Mesozoic Reef Communities: A Three-Step Process, *Palaios.*, 1988, vol. 3, no. 2, pp. 170 - 183.

Stanley, S.M., Paleozoic Mass Extinctions: Shared Patterns Suggest Global Cooling as a Common Cause, *Amer. J. Sci.*, 1988, vol. 288, no. 4, pp. 334 - 352.

Stepanov, D.L., Paleozoic–Mesozoic Boundary in the Light of the Recent Data, *Vestn. Lenin. Univ., Ser. Geol., Geogr.*, 1972, no. 24, issue 4, pp. 34 - 45.

Stevens, C.H., Was Development of Brackish Oceans a Factor in Permian Extinctions?, *Geol. Soc. Am. Bull.*, 1977, vol. 88, no. 1, pp. 133 - 138.

Tappan, H., Extinction or Survival: Selectivity and Causes of Phanerozoic Crises: Geological Implications of Impacts of Large Asteroids and Comets on the Earth, *Geol. Soc. Am.*, 1982, Spec. Pap. 190, pp. 265 - 275.

Valentine, J.W. and Moores, E.M., Global Tectonics and the Fossil Record, *J. Geol.*, 1972, vol. 80, pp. 167 - 184.

Wilde, P. and Berry, W.B.N., The Role of Oceanographic Factors in the Generation of Global Bioevents, *Lect. Notes Earth Sci.*, 1986, vol. 8, pp. 75 - 91.

Zharkov, M.A., Stages of Tremendous Evaporite Accumulation and Problem of the World Ocean Salinity Change in the Phanerozoic, *Problemy Evolyutsii Geologicheskikh Protsessov* (Problems of Geological Processes Evolution), Novosibirsk: Nauka, 1981, pp. 110 - 121.

Stratigraphy and Geological Correlation, Vol. 2, No. 1, 1994, pp. 75 - 79. Translated from Stratigrafiya. Geologicheskaya Korrelyatsiya, Vol. 2, No. 1, 1994, pp. 81 - 85.
Original Russian Text Copyright © 1994 by Bragin.
English Translation Copyright © 1994 by Interperiodica Publishing (Russia).

Evolution of the biosphere

Radiolarians as Indicators of Triassic Climate in Northeast Asia

N. Yu. Bragin

Institute of Geology, Russian Academy of Sciences, Pyzhevskii per. 7, Moscow, 109017 Russia

Received January 26, 1993

Abstract – Known assemblages of the Triassic radiolarians from different regions of the world are analyzed. A considerable geographic differentiation of radiolarian faunas in the middle and late Triassic is shown to result from their distribution throughout different climatic belts. Boreal faunas are known in northeast Asia (except the Koryak Upland) and north Alaska. Tropical faunas are distributed throughout the Mediterranean region and along the Asian and North American margins of the Pacific ocean. Owing to significant taxonomic differences between the boreal and tropical assemblages, the Triassic radiolarians can serve as biotic indicators of paleoclimates.

Various Triassic deposits, most of which contain radiolarians, are widespread in northeast Asia. The most abundant assemblages come from siliceous and volcanogenic-siliceous formations, which, in general, occur in areas adjacent to the Pacific ocean: the Koryak Upland, Sakhalin, the lower course of the Amur River, eastern Primor'e, and eastern Japan. The great similarity between the radiolarian assemblages of these regions allowed us to trace recognized biostratigraphic units from Japan to the Koryak Upland (Bragin, 1991). Triassic radiolarians were also studied in many regions of various paleogeographic and paleoclimatic belts: North America, the Mediterranean belt, the Philippines, and northeast Siberia. Therefore, it seems pertinent to compare radiolarian assemblages from northeast Asia with those from other regions in order to find out whether those assemblages can be confidently correlated with paleoclimate environments.

So far, radiolarians of the early Triassic and early-middle Anisian age have only been studied in a few localities of Japan and the Sikhote-Alin' area, and in many cases the data are incomplete. Therefore, the middle Triassic (late Anisian–early Ladinian) assemblages, which are the most thoroughly studied, should be analyzed first. Typical assemblages of this age are known from sequences of the Sikhote-Alin' area (the Dal'negorsk Settlement), Sakhalin (the Yunona Mountain), and Japan (Bragin, 1991, 1991; Blome, 1987; Nishizono *et al.*, 1982; Takashima and Koike, 1982; Yao, 1982). These assemblages are dominated by various species of the *Pseudostylosphaera* (*P. japonica*, *P. tenue*, *P. acrior*, *P. spinulosa*, and others) and *Triassocampe* (*T. deweveri*, *T. scalaris*, and others) genera. Representatives of the Eptingiidae (*Eptingium manfredi*) and Pentactinocarpidae (*Pentactinocarpus fusiformis*, *P. acanthicus*) families, and genus *Yeharaia* (*Y. japonica*, *Y. elegans*, *Y. annulata*) are typical. The assemblages from the above regions differ insignificantly in composition. An assemblage from the upper Anisian–lower Ladinian strata of the Koryak Upland (Bragin, 1991) is identical to them.

A comparative analysis of the Pacific and coeval Mediterranean assemblages of Italy (De Wever *et al.*, 1990; Dumitrica *et al.*, 1980; Martini *et al.*, 1989) and Slovenia (Gorican, 1990) shows that the latter are dominated by the same taxa, except for genus *Yeharaia*, which is rare in the Tethys area. In addition, members of the Oertlispongiidae family are common in the Mediterranean area (Dumitrica *et al.*, 1980), but sporadic in eastern Russia and Japan. This, however, can be explained by a better preservation of thin skeletal elements of Oertlispongiidae in the Tethyan carbonate rocks than jaspers and siliceous rocks of other regions. The northeast Asian genus *Yeharaia* is also present in the middle Triassic assemblages from the Philippines (Cheng, 1989; Yeh, 1990), similar to those from Japan, the Sikhote-Alin' area, and Sakhalin. So, in general, the late Anisian–early Ladinian assemblages from the Pacific margins and the Alpine region are very similar in composition.

Let us now consider the late Ladinian–early Karnian interval. An assemblage of this age dominated by diverse Muelleritortiidae (*Muelleritortis cochleata*, *Tritortis kretaensis*) and Pseudostylosphaera (*P. inaequata*, *P. imper-*

spicua) is known from sequences of the Dal'negorsk Settlement (the Primor'e), the Yunona Mountain (Sakhalin), the Koryak Upland (Bragin, 1991), and different regions of Japan (Nakaseko and Nishimura, 1979; Nishizono *et al.*, 1982). The assemblage contains also *Triassocampe* deweveri, *Yeharaia elegans*, and *Pentactinocarpus fusiformis* inherited from the underlying beds, and in addition the representatives of genus *Xiphotheca* (*X. dimidiata*, *X.* sp.). The above taxa (except *Xiphotheca*) are characteristic of the upper Ladinian–lower Carnian strata of the Alpine–Mediterranean area (De Wever, 1984; Kazintsova and Lozynyak, 1986; Kozur, 1988, 1988; Kozur and Krahl, 1984), where they occur together with abundant Oertlispongiidae and representatives of the genus *Ditortis*, unknown in the Pacific area. Finally, late Ladinian assemblages were recorded in western Canada and are similar in composition to those from northeastern Asia (Cordey *et al.*, 1988).

The late Carnian–early Norian assemblages were described from key sections of the Triassic siliceous strata in the Sikhote-Alin' area and Sakhalin (Bragin, 1991). Assemblages from the Koryak Upland (Bragin, 1991, 1991) and Japan (Nakaseko and Nishimura, 1970, Nishizono *et al.*, 1982; Takashima and Koike, 1982; Yao, 1982; Yoshida, 1986) are also well studied. The assemblages are dominated by Capnuchosphaeridae (*Capnuchosphaera triassica*, *C. theloides*, *C. lea*, and others) and Capnodocinae (*Capnodoce anapetes*, *C. antiqua*, and others). Representatives of the genera *Japonocampe*, *Xiphotheca*, and *Syringocapsa* are common in them. This composition of radiolarian assemblages is typical of most localities in northeast Asia. However, a more diverse assemblage was found in the eastern section of Koryak Upland (Bragin, 1991). In addition to the mentioned taxa, this assemblage contains the genera *Pentaspongodiscus*, *Orbiculiforma*, *Veghicyclia*, and *Karnospongella*. This assemblage is identical to the Tethyan assemblages of Sicily, Greece, Turkey, and Austria, and, having a more diverse composition, differs from most of the east Asian assemblages (De Wever *et al.*, 1979; Kozur and Mostler, 1972, 1979, 1981). The late Carnian–early Norian radiolarians also occur in many regions of North America: Oregon, California, and Mexico (Blome, 1984; Pessagno *et al.*, 1979). Similar in composition to the assemblages from Japan and east Russia, they are characterized by a particular abundance of Capnuchosphaeridae and Capnodocinae. The separate assemblages of north Alaska (Blome, 1987) have a taxonomic composition similar to the above assemblages, but show a relative scarcity of members from the Capnodocinae family. Thus, in the late Carnian–early Norian time interval, the Pacific and Tethyan radiolarian faunas differ mainly at the species level (Blome, 1987). Only the north Alaskan assemblages differ at the genus and family ranks.

The early Norian–Rhaetian (?) assemblages are known in the same regions and sequences of northeast Asia as the older ones (Bragin, 1991). Abundant representatives of the Saturnalidae family (*Praemesosaturnalis*, *Pseudoheliodiscus*, *Mesosaturnalis*, and others), the Pantanelliinae subfamily (*Betraccium* and *Pantanellium*), and the genera *Canoptum* (*C. rhaeticum*) and *Livarella* (*L. longus*, *L. gifuensis*, and *L. densiporata*) are typical of these assemblages. Their composition remains the same in localities from the Koryak Upland to Japan and the Philippines (Bragin, 1991; Yao, 1982; Yeh, 1992; Yoshida, 1986). The coeval Tethyan assemblages are known in the Alps (Kozur and Mostler, 1972, 1979, 1981). They are generally similar with a slight difference in the species composition, particularly members of the family Saturnalidae. In contrast, most of the North American assemblages differ notably from both the east Asian and Tethyan ones, having a greater abundance and diversity of the subfamilies Pantanelliinae (*Betraccium*, *Cantalum*, and *Pantanellium*) and multicyrtid nassellarians (*Laxtorum*). These assemblages are known in Mexico, Oregon, British Columbia, and south Alaska (Blome, 1984, 1987; Carter, 1990; Carter *et al.*, 1989; Pessagno *et al.*, 1979; Pessagno and Blome, 1980). At the same time, very poor assemblages with a low diversity of genera *Pantanellium* and *Ferresium* are found in the Brooks Range, north Alaska (Blome, 1987). A similar assemblage was discovered in the upper Norian strata of New Zealand (Blome *et al.*, 1987).

This analysis permits the following conclusions. The late Anisian–early Ladinian time is characterized by an extraordinary similarity between the east Asian, North American, and Tethyan radiolarian assemblages. The same is true for the late Ladinian–early Carnian. In the late Carnian–middle Norian, the assemblages of the different regions began to be diverge; the Brooks Range assemblage of Alaska being the most specific. The differences became more distinct in the late Norian–Rhaetian, when one can distinguish at least three groups of assemblages restricted to certain provinces: Tethys–east Asia, North America, and north Alaska (the figure). The New Zealand assemblage is referred to the last province. The regional distribution and fauna differentiation in the Triassic was already recognized using Ammonoidea, Nautiloidea, Bivalvia, and other fossils as examples (Dagys *et al.*, 1979). In the case of radiolarians this can be observed only in the late Triassic, and is characteristic of the north Alaskan and New Zealand faunas.

The rest of the regions are characterized by a great similarity in fauna, perhaps caused by their location in a single climatic belt, in this case, the tropical one. The especially strong similarity of east Asian and Tethyan assemblages has long attracted the attention of biostratigraphy, paleontology, and tectonics specialists. It should be emphasized that the middle and especially upper Triassic strata of the Koryak Upland and other regions of northeast Asia adjacent to the Pacific ocean are characterized by tropical associations of diverse organisms (not only radiolarians): cephalopods, bivalves, conodonts, corals, and foraminifers (Bragin, 1991). The occurrence of such faunas in these regions is

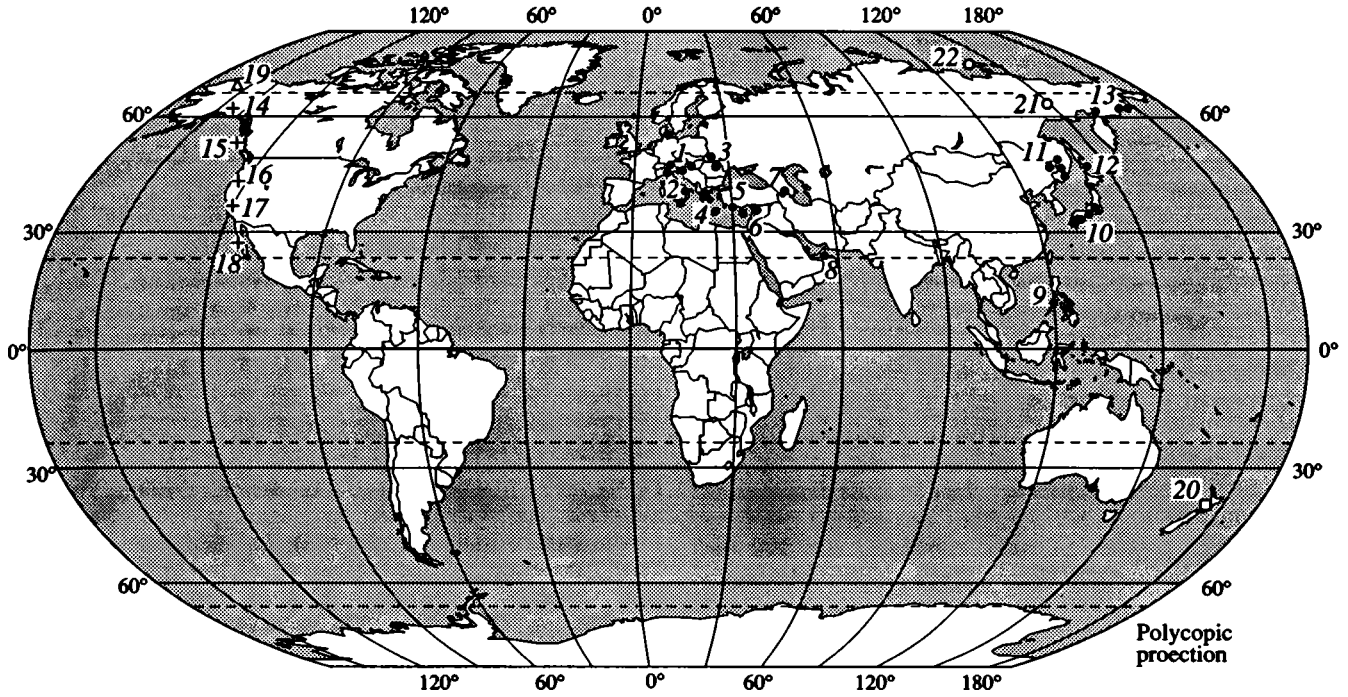

Localities of the middle and late Triassic radiolarians.

The Mediterranean and East Asian tropical provinces: *1* – the Alps and Hungary; *2* – Southern Italy and Sicily; *3* – the Carpathians; *4* – Greece and Crete; *5* – Turkey; *6* – Cyprus and Syria; *7* – Lesser Caucasus; *8* – Oman; *9* – the Philippines; *10* – Japan; *11* – Sikhote-Alin' and western Manchuanguan; *12* – Sakhalin; *13* – the Koryak Upland. The North American tropical-subtropical province: *14* – southern Alaska; *15* – British Columbia; *16* – Oregon; *17* – California; *18* – Mexico. The North American boreal province: *19* – the Brooks Range. The Notal province: *20* – New Zealand. The East Siberian boreal province: *21* – the Omolon massif; *22* – Kotel'nyi Island.

anomalous, as the polar area is thought to have existed in the Koryak–Kamchatka region at that time (Zakharov and Sokarev, 1990). The plate tectonics reconstructions discussed earlier (Bragin, 1991) were introduced into the discussion as a possible explanation of this phenomenon. Up to now, in spite of their evidently controversial character, there is no convincing alternative to these reconstructions.

Nevertheless, whether the composition of the Triassic radiolarian assemblage can indicate their climatic distribution, or, in other words, whether the radiolarians can serve as reliable climatic indicators is an issue that needs clarification. This is a question of the utmost importance because radiolarians are often the only group of organisms occurring in siliceous rocks unaccompanied by other fossils. The above analysis does not suggest considerable differences between radiolarian assemblages of different and very remote regions. These faunas do not seem promising as climatic indicators. Yet new radiolarian occurrences were recently discovered in the boreal Triassic strata of northeast Siberia (Bragin, 1990). The composition of these assemblages is essentially different from previously known assemblages, and requires special discussion.

The most diverse assemblages were distinguished from the upper Anisian–lower Ladinian beds of the Omolon massif. Contemporaneous faunas occur in Kotel'nyi Island. Poorly preserved and less diverse radiolarian assemblages of the early (Olenekian) and late (Carnian) Triassic also are known from this region. The upper Anisian–lower Ladinian strata contain spherical spumellarians with archaic skeletal spicula similar to Paleozoic Entactiniidae, spherical and diskoidal forms with spongy shells assigned to the subfamily Spongodiscoidea, various spherical spicula-free spumellarians with several lattice shells, as well as rare representatives of the genera *Pseudostylosphaera*, *Archaeothamnulus*, *Pentactinocarpus*, *Hozmadia*, and *Triassocampe*. The Omolon massif has no taxa characteristic of the deposits of the tropical Tethyan and Pacific regions, such as the Eptingiidae, Oertlispongiidae, and Foremanelliidae families, and the genera *Yeharaia*, *Anisicyrtis*, *Poulpus*, and others. The species composition of the genera *Pseudostylosphaera* and *Triassocampe* is considerably less diverse. The assemblage has a peculiar archaic character, and is, in general, impoverished. These features allow us to recognize the regions of its distribution as a special, boreal province (the figure). The boreal character of this province, as well as the north Alaska (the Brooks Range) region is indicated by both the composition of fossils (Ammnonoidea and other mollusks, see Dagys *et al.*, 1979), and the type of lithogenesis characterized by the intensive development of terrigenous deposits along with a minimum carbonate accumulation. Regions like

British Columbia show specific assemblages of ammonoids (and possibly radiolarians) including both tropical and boreal elements (Dagys *et al.*, 1979).

Thus, the great difference in high-level taxonomy between the boreal and tropical Triassic radiolarian assemblages confirms earlier conclusions that the similarity between the Mediterranean and Koryak Upland assemblages suggests a tropical origin of the latter. The wide geographical distribution of the tropical radiolarian assemblages supports the notion that a warm, glaciation-free climate existed during the Triassic, when there was only a small boreal area. Some of the dominant thermophilic assemblages are present, which can be interpreted to be transitional (subtropical, southern boreal, etc.); for example, those of north Alaska and New Zealand. Finally, from all that has been stated it is clear that the composition of the Triassic radiolarian assemblages is to a great extent dependent on their occurrence in a given climatic province, and that the Triassic radiolarians can be considered biotic indicators of climate.

REFERENCES

Blome, Ch.D., Upper Triassic Radiolaria and Radiolarian Zonation from Western North America, *Bull. Amer. Paleontol.*, 1984, vol. 85, pp. 1 - 88.

Blome, Ch.D., Paleogeographic Significance of Lower Mesozoic Radiolarians from the Brooks Range, Alaska, *Alaskan North Slope Geology*, Tailleur, I. and Weimer, P., Eds., Bakersfield: Calif. Soc. Econ. Paleont. and Miner., Pacific Sec., 1987, vol. 1, pp. 371 - 380.

Blome, Ch.D., Moore, P.R., Simes, J.E., and Watters, W.A., Late Triassic Radiolaria from Phosphatic Concretions in the Torlesse Terrane, Kapiti Island, Wellington, *Geol. Surv. New Zealand*, 1987, Rec. 18, pp. 103 - 109.

Bragin, N.Yu., *Radiolyarii i Nizhnemezozoiskie Tolshchi Vostoka SSSR* (Radiolarians and the Lower Mesozoic Units of the USSR East Regions), Moscow: Nauka, 1991.

Bragin, N.Yu., The Carnian Radiolarian Assemblage from Volcanogenous–Siliceous Formations of the Ekonai Zone, the Koryak Upland, *Izv. Akad. Nauk SSSR, Ser. Geol.*, 1991, no. 6, pp. 79 - 86.

Bragin, N.Yu., Triassic Radiolarians of the Omolon Massif, *Ispol'zovanie Radiolyarii v Stratigrafii i Paleobiologii: Tezisy Dokladov Devyatogo Vsesoyuznogo Seminara po Radiolyariyam* (Utilization of Radiolarians in Stratigraphy and Paleobiology: Abstracts of Papers of the 9th All-Union Seminar on Radiolarians), Ufa: Ufa Gos. Univ., 1990, pp. 15 - 16.

Carter, E.S., New Biostratigraphic Elements for Dating Upper Norian Strata from the Sandilands Formation, Queen Charlotte Island, British Columbia, Canada, *Marine Micropaleontol.*, 1990, no. 15, pp. 313 - 328.

Carter, E.S., Orchard, M.J., and Tozer, E.T., Integrated Ammonoid-Conodont-Radiolarian Biostratigraphy, Late Triassic Kunga Group, Queen Charlotte Islands, British Columbia, *Current Res., Pt. H, Geol. Surv. Canada*, 1989, Pap. 89-1H, pp. 23 - 30.

Cheng, Y.-N., Upper Paleozoic and Lower Mesozoic Radiolarian Assemblages from the Busuanga Island, North Palawan Block, Philippines, *Bull. Nat. Mus. Natur. Sci.*, 1989, no. 1, pp. 129 - 175.

Cordey, F., De Wever, P., Dumitrica, P., Danelian, T., Kito, N., and Vrielynck, B., Description of Some New Middle Triassic Radiolarians from the Camp Cove Formation, Southern British Columbia, Canada, *Rev. Micropaleontol.*, 1988, vol. 31, no. 1, pp. 30 - 37.

Dagys, A.S., Arkhipov, Yu.V., and Bychkov, Yu.M., *Stratigrafiya Triasovoi Sistemy Severo-Vostoka Azii* (Triassic Stratigraphy of Northeast Asia), Moscow: Nauka, 1979.

De Wever, P., Triassic Radiolarians from the Darno Area (Hungary), *Acta Geol. Acad. Sci. Hung.*, 1984, vol. 27, nos. 3, 4, pp. 295 - 306.

De Wever, P., Sanfilippo, A., Riedel, W.R., and Gruber, B., Triassic Radiolarians from Greece, Sicily and Turkey, *Micropaleontology*, 1979, vol. 25, no. 1, pp. 75 - 110.

De Wever, P., Martini, R., and Zaninetti, L., Datation Paleontologique des Radiolarites du Lagonegro (Formation du Monte Facito, Italie Meridionale): Individualization des le Trias Moyen de Bassins Pelagiques en Tethys Occidentale, *G.R. Acad. Sci.*, Paris, 1990, t. 310, ser. II, pp. 583 - 589.

Dumitrica, P., Kozur, H., and Mostler, H., Contribution to the Radiolarian Fauna of the Middle Triassic of the Southern Alps, *Geol. Palaeontol. Mitt.*, Innsbruck, 1980, vol. 10, no. 1, pp. 1 - 46.

Gorican, S., Middle Triassic Radiolarians from Slovenia (Yugoslavia), *Geologija*, 1990, nos. 31, 32, pp. 133 - 197.

Kazintsova, L.I. and Lozynyak, P.Yu., Stratigraphy of the Triassic Deposits of Soviet Carpatians and the Significance of Radiolarians, *Aus Sitzungberichten Osterr. Acad. Wissenschaften. Matem.-Naturw. Kl.*, 1986, Part 1, vol. 1, pp. 47 - 51.

Kozur, H., Muelleritortiidae N. Fam., Eine Charakteristische Longobardische (Oberladiniche) Radiolarienfamilie, *Freiberg. Forchungesh* – H., 1988, vol. 1, no. 419, pp. 51 - 61.

Kozur, H., Muelleritortiidae N. Fam., Eine Charakteristische Longobardische (Oberladiniche) Radiolarienfamilie, *ibid.*, 1988, vol. 2, no. 247, pp. 95 - 99.

Kozur, H. and Krahl, H., Erster Nachweis Triassischer Radiolaria in der Phyllit-Gruppe auf der Insel Kreta, *Neues Jb. Geol. Paläontol.*, 1984, no. 7, pp. 400 - 404.

Kozur, H. and Mostler, H., Beitrage zur Erforschung der Mesozoischen Radiolaria, vol. 1, *Geol. Paläeontol. Mitt.*, Innsbruck, 1972, vol. 2, no. 819, pp. 1 - 60.

Kozur, H. and Mostler, H., Beitrage zur Erforschung der Mesozoischen Radiolaria, vol. III: Die Oberfamilien Actinommacea Haeckel, 1862 Emend., Artiscacea Haeckel, 1982, Multiarcusellacea Nov, der Spumellaria und Triassiche Nassellaria, *ibid.*, 1979, vol. 9, no. 112, pp. 1 - 132.

Kozur, H. and Mostler, H., Beitrage zur Erforschung der Mesozoischen Radiolaria, vol. IV: Thalassosphaeracea Haeckel, 1962, Hexastylacea Haeckel, 1882 Emend Petrushevskaja, 1979, Sponguracea Haeckel, 1862, Emend und Weitere Triassische Lithocycliacea, Trematodiscacea, Actinommacea und Nassellaria, *ibid.*, 1981, vol. S, pp. 1 - 208.

Kozur, H. and Mostler, H., The Polyphyletic Origin and the Classification of the Mesozoic Saturnalids (Radiolaria), *ibid.*, 1983, vol. 13, no. 313, pp. 1 - 47.

Martini, R., De Wever, P., Zaninetti, L., Danelian, T., and Kito, N., Les radiolarites triasiques de la formation du Monte Facito Auct. (Bassin de lagonegro, Italie meridionale), *Rev. Paleobiolog.*, 1989, vol. 8, no. 1, pp. 143 - 161.

Nakaseko, K. and Nishimura, A., Upper Triassic Radiolaria from Southwest Japan, *Sci. Rep. Col. Gen. Educ. Osaka Univ.*, 1979, vol. 28, no. 2, pp. 61 - 109.

Nishizono, Y., Ohishi, A., Sato, T., and Murata, M., Radiolarian Fauna from the Paleozoic and Mesozoic Formations Distributed along the Mid-Stream of Kuma River, Kyushu, Japan, *News Osaka Micropaleontology, Spec. vol.*, 1982, no. 5, pp. 311 - 326.

Pessagno, E.A., Jr., Finch, W., and Abbott, P.L., Upper Triassic Radiolaria from the San Hipolito Formation, Baja California, *Micropaleontology*, 1979, vol. 25, no. 1, pp. 160 - 197.

Pessagno, E.A., Jr. and Blome, Ch.D., Upper Triassic and Jurassic Pantanelliinae from California, Oregon and British Columbia, *ibid*, 1980, vol. 26, no. 2, pp. 225 - 273.

Takashima, K. and Koike, T., Triassic Radiolarian Faunas in Chert from Some Areas in Japan, *News Osaka Micropaleontology, Spec. vol.*, 1982, no. 5, pp. 45 - 50.

Yao, A., Middle Triassic to Early Jurassic Radiolarians from the Inuyama Area, Central Japan, *J. Geosci. Osaka City Univ.*, 1982, vol. 25, pp. 53 - 70.

Yeh, K.-Y., Taxonomic Studies of Radiolaria from Busuanga Island, Philippines, *Bull. Nat. Muss. Natur. Sci.*, 1990, no. 2, pp. 1 - 63.

Yeh, K.-Y., Triassic Radiolaria from Uson Island, Philippines, *ibid.*, 1992, no. 3, pp. 51 - 91.

Yoshida, A., Upper Triassic to Lower Jurassic Radiolarian Biostratigraphy in Kagamigahara City, Gifu Prefecture, Central Japan, *J. Earth Sci. Nagoya Univ.*, 1986, vol. 34, pp. 1 - 21.

Zakharov, Yu.D. and Sokarev, A.N., Permian–Triassic Paleomagnetism of Eurasia, *Saito Ho-on Kai Spec. Pub.*, 1990, no. 3, pp. 313 - 323.

Stratigraphy and Geological Correlation, Vol. 2, No. 1, 1994, pp. 80 - 87. Translated from Stratigrafiya. Geologicheskaya Korrelyatsiya, Vol. 2, No. 1, 1994, pp. 86 - 94.
Original Russian Text Copyright © 1994 by Kuznetsova.
English Translation Copyright © 1994 by Interperiodica Publishing (Russia).

Evolution of the Jurassic Tethyan Foraminifera

K. I. Kuznetsova

Geological Institute, Russian Academy of Sciences, Pyzhevskii per. 7, Moscow, 109017 Russia

Received January 31, 1993

Abstract – The evolution of foraminiferal assemblages that inhabited the East Mediterranean basins during the Jurassic is discussed using the analysis of the material obtained during my work in Syria from 1986 to 1991 and of the Jurassic foraminifera collections from the adjacent countries, the Crimea, Caucasus, and southwestern Europe. Analysis of the taxonomic composition of the assemblages and their changes through time and space revealed stages of the foraminifera development related to sea basin dynamics in the Jurassic. Faunal assemblages differing in composition and structure are confined to different facies-ecological environments and structural zones. The time range of some stages is nearly equal to the stratigraphic unit of age (stage). According to the biological peculiarities of the fauna, i.e., the dominant morphotypes, rates of evolution, tolerance, intensity of speciation, distribution areas, degree of endemism, two large stages (megaphases) of the Tethyan foraminiferal evolution are recognized: the early-middle Jurassic and late Jurassic–early Cretaceous.

The evolution of foraminifera, like any other group of organisms, is a multicomponent process, rates and trends of which depend on a number of factors: biological peculiarities of a group under discussion, its dependence on a complex of abiotic factors, species migrations, and others.

Most of these factors are unstable during even the smallest stage in foraminiferal evolution, a zone, in this case. The wider the studied distribution area of the group and the longer the analyzed period of its evolution, the more complex and reliable its evolutionary patterns.

The vast areas of the Mesozoic Tethys ocean inhabited by the diverse and abundant Jurassic biota including foraminifera are of exceptional interest for such studies.

Using my own abundant materials, mostly from Syria, partly from Israel, Crimea, Caucasus, and Western Europe, as well as publications on the other Tethyan regions, such as the French-Spanish Pyrenees, Algeria, Morocco, Sinai, Saudi Arabia, Iran, and Iraq, I attempted to consider the Jurassic foraminiferal evolution in the Tethys.

Analysis of the foraminiferal assemblages included studies on their taxonomic composition, facies and ecological dependence, distribution area sizes of both the assemblages and principal components (mainly at the generic level), and morphological peculiarities of dominant groups.

According to the dominant groups, the Jurassic Tethyan foraminifera belong to the cyclamminid-pfenderinid type of Protozoa, (Gordon, 1970; Basov *et al.*, 1972; Basov, 1974; Kuznetsova and Gorbachik, 1985), which inhabited the tropical and subtropical basins.

Ecologically, these are benthic forms, i.e., facies-controlled organisms. Planktonic foraminifera, which appear in the Jurassic, are rare, but they occur in the deposits of three of the seven studied stages.

In a biogeographic sense, these assemblages contain tropical Tethyan endemics, widespread subtropical forms, and cosmopolites occurring outside of the Tethys in the Boreal realm (boreal-cosmopolitan elements) (Fig. 1).

Bearing in mind the foresaid, I have distinguished the main stages of the Jurassic foraminiferal evolution in Syria and the adjacent Mediterranean regions.

The first stage corresponding to the lower Jurassic, which cannot be divided into stages in Syria, is distinguishable in fauna from Morocco and southwestern France. The stage is characterized by the occurrence of representatives of the Orbitopsellidae family restricted in distribution by the tropical Tethyan area. Associated *Pseudocyclammina*, *Lituosepta*, *Haurania*, and *Pfenderina*, which are also endemics, have a wider stratigraphic distribution and are recorded in the middle and partly upper Jurassic of the East Mediterranean.

In Syria, the lower Jurassic sediments were deposited in shallow, sometimes brackish-water basins, as indicated by an impoverished composition of foraminiferal assemblages and by the presence of fresh-water ostracodes. In the Crimea, this time was characterized by a deposition of Tavriya Series lacking foraminifers.

The second stage spans the stratigraphic interval of the Aalenian–lower Bajocian and is characterized in Syria by a predominance of boreal-cosmopolitan elements (*Epistomina*, *Lenticulina*, and *Citharina*) and less abundant Tethyan endemics (*Timidonella*). In southwestern Syria, these assemblages were formed under conditions of the mid-littoral zone. In southwestern Europe, identical assemblages existed in similar settings (Pellissie *et al.*, 1984).

The third stage corresponds in time to the Bajocian. Secreting benthic foraminifera retain their predomi-

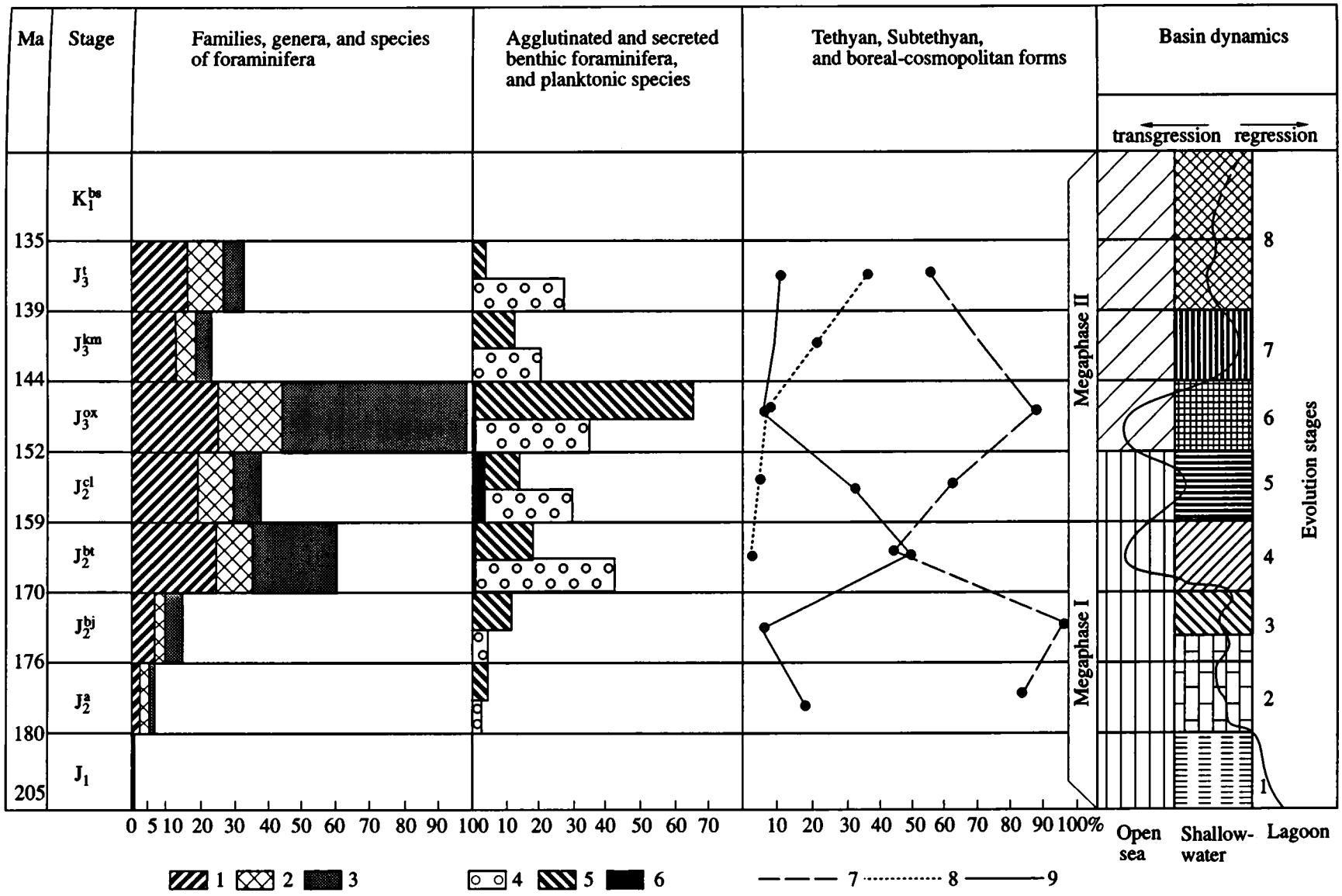

Fig. 1. Relations between different taxonomic, ecological, and paleobiogeographic components in the Jurassic foraminiferal thanatocoenoses of Syria and the basin dynamics.

1 – families; 2 – genera; 3 – species; 4 – agglutinated benthic foraminifera; 5 – secretory benthic foraminifera; 6 – planktonic foraminifera; 7 – boreal-cosmopolitan forms; 8 – Subtethyan forms; 9 – Tethyan forms.

nance in the assemblages, and the Tethyan elements are still of secondary importance. The wide distribution of these assemblages over the Mediterranean enables the correlation of the Bajocian deposits in Algeria, Morocco, Sinai, and southwestern Syria, revealing a common stage in fauna evolution.

The fourth (Bathonian) stage corresponds to a wide transgression. In the Mediterranean, it is marked by the occurrence of various foraminiferal assemblages, which evolved in different parts of the rapidly expanding basin. The boreal-cosmopolitan elements continue to predominate in southern and southwestern Syria, Sinai, and northern Africa, but in central and northwestern Syria, southwestern France, and Algeria they were of minor importance. Here the Tethyan endemics increase sharply in abundance and taxonomic diversity. The planktonic foraminifera (*Conoglobigerina* and *Globuligerina*) appear for the first time. The Syrian foraminiferal assemblages were renewed at the genus level. Eighteen genera originated at either the beginning, or in the middle of the Bathonian stage (Fig. 2).

The fifth stage of the foraminiferal development spans the Callovian, when there was some contraction of the marine transgression and an increased differentiation of facies-ecological environments in the East Mediterranean. Two types of assemblages, inheriting in general their composition from the Bathonian faunas, are typical of this stage. Southwestern Syria and the Sinai Peninsula were areas of terrigenous–carbonate sedimentation, which preserved assemblages dominated by the boreal-cosmopolitan elements. Here less abundant Tethyan forms inhabited the shallow-water mediolittoral zones and the carbonate platform areas. Northwestern Syria, the French-Spanish Pyrenes, and Morocco were occupied by the shallow-water Tethyan endemics. Transitional type assemblages with abundant boreal-cosmopolitan elements appeared in the Crimea and Caucasus. The planktonic foraminifera advanced in species diversity.

The sixth stage, marked by significant changes in the Mediterranean foraminiferal assemblages, is related to the expansion of the marine transgression in the Oxfordian. The taxonomic diversity of this group reaches its maximum; the secreting benthic forms increase sharply in importance; and the planktonic foraminifera continue to develop. The boreal-cosmopolitan to Tethyan elements ratio is 9 : 1, varying slightly in different parts of the basin. In the remote regions, the assemblages are characterized by a uniform composition. The environmental uniformity seems to be characteristic during the wide transgression that reaches the central part of Syria (the Palmyrides). New taxa (*Everticyclammina*, *Choffatella*, *Mesoendothyra*, and *Alveosepta*) appear and spread over the Crimea, Caucasus, Syria, and Israel. These taxa existed till the end

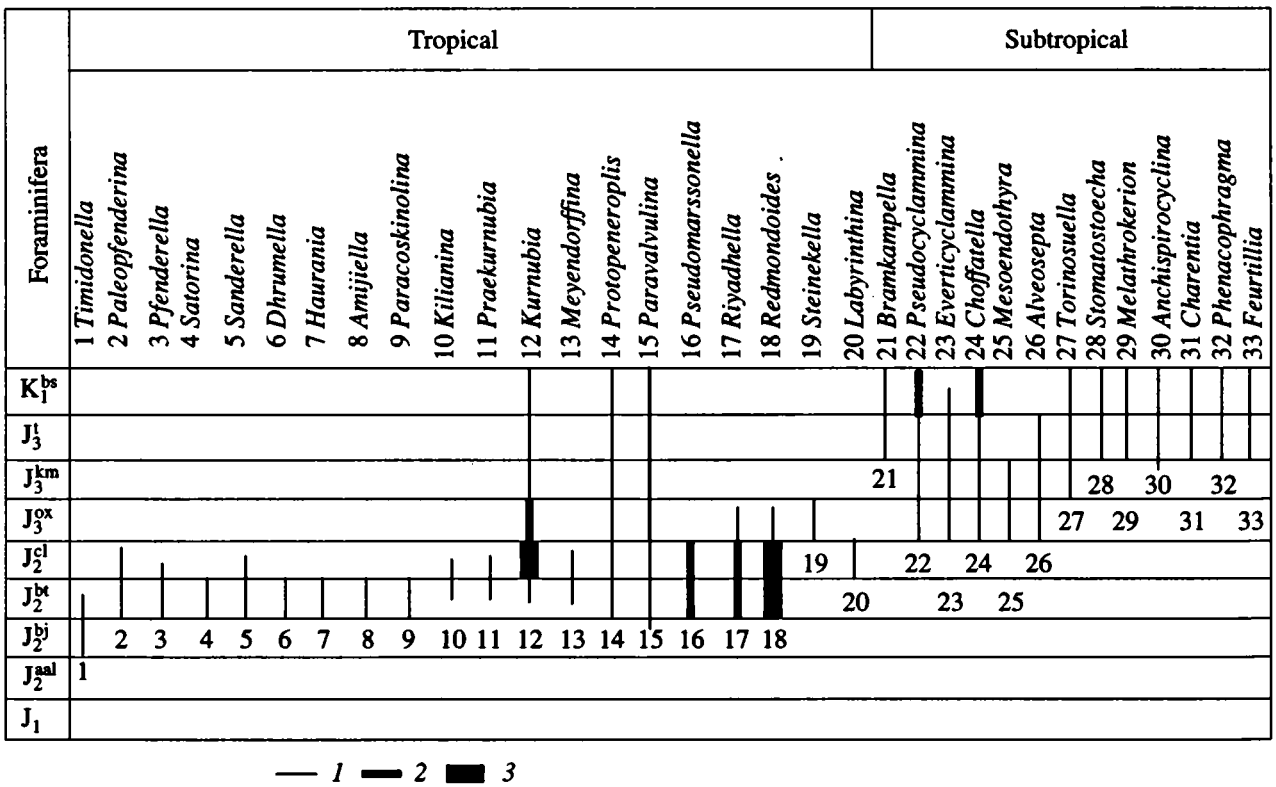

Fig. 2. Stratigraphic range of some foraminiferal genera (the tropical and subtropical types of the Tethyan fauna).

1 – one or two species; *2* – three - five species; *3* – more than five species.

of the Jurassic, and some of them occurred in the Cretaceous.

The beginning of *the seventh (Kimmeridgian) stage* is related to a regressive phase in the development of the East Mediterranean basins accompanied by a general structural reorganization of the region. This resulted in an improverished fauna composition and a mosaic pattern of the Kimmeridgian deposits in Syrian territory. The deposits occur mostly in its southwestern part and are very similar to the coeval deposits of Israel in composition and depositional environments. In the foraminiferal assemblages, the boreal-cosmopolitan elements predominate distinctly over the Tethyan forms. In northwestern Syria, the randomly preserved Kimmeridgian deposits yielded foraminiferal assemblages, which included Subtethyan elements (*Torinosuella*). The agglutinated benthic species dominated over the secreted forms. No planktonic foraminifera have been recovered in the coastal shallow-water sediments.

The eighth and final stage of the foraminiferal development spans the end of the Jurassic and the beginning of the Cretaceous, indicating that the Tithonian and Berriasian assemblages share a common evolutionary stage. The deposits of this age have a limited and mosaic distribution in the Near East. The assemblages show high taxonomic diversity and retain the previous relationships between the Tethyan, Subtethyan and boreal-cosmopolitan groups, amid which the Subtethyan and cosmopolitan elements dominate, while the Tethyan endemics are less abundant. At the beginning of the stage, the generic composition of the Tethyan fauna was renewed: six new genera appeared and were then distributed widely in the Cretaceous. These genera belong to the subtropical fauna widespread in the Near East, Crimea, Caucasus, southwestern Europe, and northern Africa. It is characteristic that the modifications in the foraminiferal composition occurring near the Jurassic–Cretaceous boundary are as adynamic in the Tethys area as they are in the Boreal province. The fauna was renewed only at the species level. New Cretaceous elements appeared at the beginning and in the middle of the late Tithonian.

When analyzing changes in the foraminiferal assemblages in the context of their close relations to the development of the Jurassic Tethyan basins, I refrained from discussing such important factors as biological peculiarities, rates of evolution, and the spatial distribution of this group.

Since a rate of evolution of a taxon (a genus in our case, because we deal with the generic categories as far as evolution is concerned) varies inversely in relation to the duration of its existence, I attempted to define the moments of the rate changes, the relationships between the Tethyan foraminifera during the Jurassic, and some morphological trends in their evolution.

The Jurassic evolution of the Tethyan foraminifers in the Mediterranean can be divided into two large stages, or megaphases, differing in the morphotypes of their dominants, rates of evolution, area of distribution, and intensity of speciations.

The first megaphase spans the long interval from the early Jurassic (Pliensbachian–Toarcian) to the end of the middle Jurassic (Callovian). Foraminiferal assemblages of this megaphase are characterized by: (1) the occurrence of highly specialized forms with complex exo- and endoskeletal structures, a particular morphotype, (2) a high degree of fauna endemism at the family level, (3) a reduced tolerance as a result of the high specialization of the fauna, (4) limited distribution areas of genera and families, (5) high rates of genus evolution; genus life-intervals are 5.5 - 11 Ma, those for species are, accordingly, 1 - 3 Ma, which corresponds to one or two ammonite zones, and (6) highly intensive speciation.

The second megaphase of the Tethyan foraminiferal evolution occurs from the late Jurassic to the beginning of the early Cretaceous, having such characteristics as: (1) the occurrence of highly specialized forms along with more adapted, competitive groups, mainly of the family Lituolidae, which became dominants, (2) a different morphotype of dominants, (3) a lesser degree of endemism of the assemblages (at the genus level), (4) moderate tolerance, (5) broader distribution areas covering the tropical and subtropical Tethyan regions (the East Mediterranean, Crimea, Caucasus, North Africa, Central Europe), and (6) moderate rates of evolution. Generic taxa existed for 17 - 21 Ma. Worth noting, the rates of species evolution did not decrease in comparison to the previous stage, and the species life-periods are 1 - 3 Ma.

So, these are the peculiarities of evolution of the foraminifera, which inhabited the Mediterranean in the Jurassic.

The evolutionary trends discussed were revealed by thorough studies of the foraminiferal assemblages from Syria.

Analysis of the composition, structure, and stratigraphic range of the Syrian assemblages suggests the following conclusions.

The most abundant and diverse assemblages are confined to the deposits of the Bathonian, Callovian, Oxfordian, and Tithonian stages. The Liassic, Aalenian(?), Bajocian, and Kimmeridgian strata, which have limited distribution in Syria, are characterized by less abundant, although locally rather diverse and copious assemblages. The quantitative relationship between the benthic forms with secreted and agglutinated tests is variable. Most of the stages show a predominance of arenaceous over calcareous forms, and only in the Bajocian and Oxfordian did the calcareous foraminifera become dominant in the benthic thanatocoenoses. This is related to the occasional invasions of the boreal-cosmopolitan forms, mainly of the Lenticulinidae and Vaginulinidae families, dominant in the assemblages from the Boreal provinces, Madagascar, western Indostan, and the Atlantic shelf of Canada. As was previously noted, the planktonic foraminifers are scarce

and represented by single specimens of *Globuligerina bathoniana* (Pazdro), *G. calloviensis* K. Kuzn., *G. meganomica* K. Kuzn., and *G. oxfordiana* (Grigelis). But these species are of great stratigraphic and correlative importance, being zonal index species for the foraminiferal zones of the Bathonian, Callovian, and Oxfordian. They subglobally distributed and can be used to correlate sections from different paleobiochores: provinces, areas, and belts.

ASSEMBLAGE ANALYSIS

The earliest Jurassic strata in Syria are of Liassic age and contain ostracodes and rare foraminifera. They are exposed in two sections, in the Anti-Lebanon, near the village of Arneh and in the Coastal Mountains, near the village of Jdaida. The first section yielded rare specimens of *Trochammina nana* Brady known from the Liassic of western Europe and an ostracode assemblage including *Procytheridea magnicoutensis* Apostolescu, *P. sermoisensis* Apostolescu, *P. triebel* Klingler, *P. vermiculata* Apostolescu, *Procytheridea* sp., *Progonocythere strilla* Sylvester-Bradley, *Aphelocythere kuhni* Triebelel et Klinger, *Isobythocypris ovalis* Bate and Coleman, *Cytherelloidea* sp., *Limnocythere* sp. nov. A, and *Limnocythere* sp. nov. B. The Jdaida section yielded tests of *Involutina liassica* (Jones), typical of the Liassic strata in Europe and North America.

The middle Jurassic strata are represented by deposits of all four stages and contain abundant and diverse foraminiferal thanatocoenoses.

The oldest assemblages include *Timidonella sarda* Bassoulet, Chabrier et Fourcade, *Ammobaculites cobbani* Loeblish et Tappan, *Lenticulina protracta* (Bornemann), *Citharina chlatrata* (Terquem), *C. pauperata* (Terquem), and *Praelamarckina humilis* Kaptarenko, which are characteristic of the Aalenian and Aalenian–Bajocian. The species list shows the presence of both typical Tethyan forms (*Timidonella sarda*) and boreal-cosmopolitan elements represented by the genera *Lenticulina*, *Astacolus*, and *Citharina*, which occur in abundance in western Europe, Madagascar, the Sinai Peninsula, and Morocco. This assemblage was found for the first time, present only in the sections of the Jurassic strata in southwestern Anti-Lebanon, Syria (the village of Arneh, the Hermon Mountains, and the foothills of the Jebel Sheikh Range). The assemblage is characterized by a high diversity of abundant species. For example, forms of *Timidonella sarda* Bassoulet, Chabrier et Fourcade are represented in some beds by dozens of tests of micro- and megalospherical generation. The same is true for the Lituolidae family, especially for abundant tests of some species of *Ammobaculites*. *Praelamarckina humilis* Kapt., known from the Aalenian in the platform part of the Ukraine and northwestern margins of the Donets basis, is represented by sporadically occurring small-sized specimens.

The Bajocian assemblages inherit particular features from their predecessors. They also include abundant boreal-cosmopolitan forms of Lenticulinidae and Vaginulidae, but no Tethyan endemics. The assemblages show more diverse taxonomic composition and include up to 30 species of 11 genera and 7 families. Noteworthy, the appearance of some Ceratobuliminidae (*Praelamarckina*, *Lamarckella*, and *Reincholdella*) and Epistominidae (*Epistomina*) in the Bajocian. These forms have a broad geographical distribution. However, being benthic organisms, they are indicative of facies-ecological environments and are related, generally, to shallow shelf sediments. Quite a different assemblage was recovered from the Bajocian deposits of the Coastal Mountains. It is less diverse than that from the Anti-Lebanon and consists mainly of rare lenticulins (*Lenticulina polymorpha* (Terq.), *L. veta* Hoffman), marginulins (*Marginulina solida* Terq.), and nodosariids.

No fossiliferous Bajocian strata have been found in the region of Kurd-Dag and Palmyrides.

The Bathonian is marked by a wide marine transgression in the East Mediterranean and many other regions of the world. Deposits of this age are recorded in all the Jurassic sequences of Syria, and contain abundant and diverse foraminiferal assemblages. Their composition differs considerably from that of the Bajocian assemblage, being more diverse: these assemblages include up to 65 species of 42 genera and 24 families.

The assemblages became dominated by forms with agglutinated tests, their secretory species are of secondary importance. There are new and scarce planktonic foraminifera of a single species *Globuligerina bathoniana* (Pazdro). According to their composition, the Bathonian assemblages, which inhabited the Syrian territory, can be classified into two main types. The first type found in the Anti-Lebanon includes abundant forms of Lituolidae, Lenticulinidae, Polymorphinidae, Ophtalmidiidae, Trocholinidae, Ceratobuliminidae, and planktonic Globuligerinidae. The assemblage is similar in composition to the Bathonian foraminiferal assemblage from the Sinai Peninsula, the Jebel Maghara Range (Said and Barakat, 1958). The most typical forms are *Reophax horridus* (Schwager), *Recurvoides bartouxi* Said et Barakat, *Ammobaculites fontinensis* Terquem, *A. suprajurassicus* (Schwager), *A. hermonensis* sp. n., *Lenticulina polymorpha* (Terquem), *Citharina proxima* (Terquem), *Lamarckella antiqua* Kapt., and *Globuligerina bathoniana* (Pazdro). The Bathonian strata of the Coastal Mountains, Kurd-Dag and Palmyrides contain another assemblage, which is dominated by the Tethyan endemics of the families Cyclamminidae (*Amijiella*, *Dhrumella*), Spirocyclinidae (*Haurania*), Dorothiidae (*Eomarssonella*), Protolixoplectidae (*Pseudomarssonella*, *Riyadhella*), and Dictioconidae (*Kilianina*, *Meyendorffina*, *Paracoscinolina*). The family Pfenderinidae is represented by numerous species of the genera *Paleopfenderina*, *Pfenderella*, *Praekurnubia*, and *Kurnubia*, which is of the utmost importance in this case.

The succession of foraminiferal assemblages enables us to subdivide the Bathonian strata of the

Coastal Mountains, with the most abundant and diverse fauna into lower and upper substages consisting of several zones or fauna beds. A distinct sequence of the assemblages and steady taxonomic composition is characteristic of the whole distribution area of this fauna type. The typical early Bathonian species include: *Haurania deserta* Henson, *Amijiella amii* (Henson), *Redmondoides lugeoni* (Septfontaine), *Pseudomarssonella primitiva* Redmond, *Riyadhella arabica* Redmond, *Protopeneroplis striata* Weynschenk, *Paleopfenderina trochoidea* (Smout et Sugden), *Dhrumella evoluta* Redmond, and *Globuligerina bathoniana* (Pazdro). Noteworthy is the almost complete absence of boreal-cosmopolitan elements typical of the southern Hermon assemblage.

Thus, the beginning of the Bathonian is marked by significant modifications in the foraminiferal assemblages, the appearance of new generic taxa of the Tethyan endemics (Fig. 1), and the decreasing importance of boreal-cosmopolitan elements.

The late Bathonian shows the same trends, four new genera appear near the early-late Bathonian boundary, in addition to the still existing genera known from the early Bathonian (*Paleopfenderina*, *Pfenderella*, *Satorina*, *Sanderella*, *Dhrumella*, *Haurania*, *Amijiella*, *Protopeneroplis*, *Pseudomarssonella*, *Riyadhella*, and *Redmondoides*). The boundary between the substages is defined by the renewal of species composition, a less important role of the genera *Haurania* and *Amijiella*, and the appearance of species of the above listed new Tethyan genera. The most typical late Bathonian species include: *Kilianina blancheti* Pfen., *Meyendorffina bathonica* Auroze and Bizon (zonal index species), *Paracoscinolina occitanica* Peyb., *Praekurnubia crusei* Redm., *Kurnubia bramkampi* Redm., *Berthelinella paradoxa* (Berth.), *Limognella dufaurei* Pell. and Peyb., *Paleopfenderina salernitana* Sart. and Cresc., *Mesoendothyra croathica* Gusič, *Pseudomarssonella bipatriata* Redm., and *Globuligerina bathoniana* (Pazdro) (Pellisse *et al.*, 1984).

The beginning of the Callovian is characterized by a contracting transgression and impoverished foraminiferal assemblages with still evolving Bathonian species and genera. The Callovian assemblages are clearly inherited from the Bathonian foraminifers. Most of the late Bathonian species continued to exist in the Callovian, when no new genera originated. The Tethyan endemics are still of prime importance in the assemblages, but there are also some forms of wide geographical distribution: Polymorphinidae (*Eoguttulina*, *Globulina*) Ammodiscidae (*Ammodiscoides*), Verneuilinidae (*Paleogaudryina*), and Haplophragmoidiidae (Haplophragmoides). During the evolution of the planktonic foraminifera, *Globuligerina bathoniana* (Pazdro) is replaced by the Gallovian species *Globuligerina meganomica* K. Kuznetsova and *G. calloviensis* K. Kuznetsova. They are still rare, but occur both in purely carbonate and in terrigenous-carbonate deposits. Callovian foraminiferal assemblages dominated by agglutinated forms are less diverse than those of the Bathonian, and contain representatives of 16 families, 29 genera, and nearly 60 species.

Like the Bathonian, the Callovian is also characterized by two types of assemblages: in Anti-Lebanon, the forms of wide geographic distribution are still dominant, whereas the Coastal Mountains were inhabited mainly by the Tethyan endemics. The composition of the Callovian assemblages is insufficient to define two units of this stage in Syria (as in the Crimea). In sections of different structural zones the stage varies, but in complete and continuous sections the main species assemblage can be traced as essentially consistent from the uppermost Bathonian to the base of the Oxfordian. In Anti-Lebanon, the most characteristic species are *Lituotuba nodus* Kos., *Kurnubia palastiniensis* Henson, *Paleogaudryina varsoviensis* Biel. et Poz., *Nautiloculina colithica* Mohler, and *Ammobaculites fontinensis* (Terquem).

The assemblage from the Coastal Mountains includes: *Ammodiscoides magharaensis* Said et Barakat, *Sanderella laynei* Redm., *Steinekella crusei* Redm., *Kurnubia palastiniensis* Henson, *Paleopfenderina salernitana* (Sart. et Cresc.), *Astacolus pellucida* Said et Barakat, *Frondicularia spissa* (Terq.), and *Reincholdella dreheri* Bart.

The Oxfordian was the expansion period of the marine transgression, which resulted in wide distribution of deposits of this age in the East Mediterranean, including Syria. These deposits contain extremely rich faunal communities, the most important components of which are foraminifera. Their assemblages are characterized by high taxonomic diversity, a uniform composition over vast areas (as a result of extensive fauna migrations), high density of most species populations reflecting the environmental stability of the paleobasins, the occurrence of planktonic forms, a higher abundance of secreted benthic forms as compared to agglutinated species and the dominance of widespread boreal-cosmopolitan components over the Tethyan endemics. These peculiarities are typical of foraminiferal assemblages from all areas of the Oxfordian deposits in Syria. Their taxonomic diversity (28 families, 46 genera, and more than 100 species) is high enough to reveal successive assemblages, to subdivide the Oxfordian into lower and upper substages, and to distinguish their foraminiferal zones. The early Oxfordian foraminiferal assemblages from the Anti-Lebanon sections (Hadar, Rowda, and Wadi Al-Karn) contain the following species: *Alveosepta jaccardi* (Schrodt), *Ammobaculites coprolithiformis* (Schwag.), *Pseudocyclammina maynci* Hott., *Mesoendothyra* sp., *Lenticulina brueckmanni* (Mjatl.), *L. quenstedti* (Guemb.), *L. russiensis* Mjatl., *Astacolus vacellantes* Esp. et Sigal, *Planularia beierana* (Guemb.), *Citharina entypomatus* Esp. et Sigal, *C. paralella* Biel. et Poz., *Marginulinopsis suprajurassicus* (Schwager), *Conorboides paravalendisensis* Reiss, *Spirillina kuebleri* Mjatl., *Epistomina nemunensis* Grig., *E. porcellanea* Brueckm., and *Globuligerina oxfordiana* (Grig.).

The assemblage consists mainly of widespread secreted benthic forms known from the Boreal province, Madagascar, the Sinai Peninsula, western Europe, Canada, and the Crimea. This permits us to correlate deposits of the lower Oxfordian *Lenticulina brueckmanni–Globuligerina oxfordiana* zone in european Russia, the Crimea, and Caucasus (*Stratigrafiya i Korrelyatsiya* ..., 1985).

The lower Oxfordian strata grade into the middle-upper Oxfordian beds. Their foraminiferal assemblages were clearly inherited from the earlier fauna. The species composition is renewed by the following late Oxfordian forms: *Reophax metensis* Franke, *Haplophragmium lutzei* Hanzl., *Ammobaculites brunsteini* Cushm., *Trocholina transversarii* Paalz., *Lenticulina quenstedti* (Guemb.), *L. audax* Loebl. et Tapp., and *Steinekella steineki* Redm. The last-mentioned species belongs to the Paleopfenderinidae family, peculiar to the Tethys. The Tethyan and Subtethyan endemics are only represented by the genera *Steinekella*, *Pseudocyclammina*, and *Everticyclammina*. The genera are poorly diversified at the species level, but in some beds their forms are very abundant.

The taxonomic stability of the late Oxfordian foraminiferal assemblages is reflected in the widespread zones distinguished in Syria, which can be considered as units of a common stratigraphic scale. Similar, though less diverse foraminiferal assemblages were recovered from the Oxfordian strata of the Palmyrides, despite the fact that previously they were thought to be missing here (Jarmakani *et al.*, 1989).

In Syria, the Kimmeridgian is marked by the beginning of a structural reorganization, extensive uplifts, and sea basin contraction, which influenced the composition, structure, and spatial distribution of foraminiferal assemblages.

Occurrences of Kimmeridgian strata are restricted mainly to Anti-Lebanon (the Wadi Al-Karn and Wadi Favuar sections). The shallow-water sediments here are predominantly clastic, oolitic, and stromatoporitic limestones, and contain impoverished foraminiferal assemblages: *Reophax hounstoutensis* Lloyd., *Triplasia jurassica* Mjatl., *Marssonella doneziana* Dain., *M. hehti* Dieni et Massari, *Citharina lepida* (Schwag.), and *Alveosepta personata* (Tobler). The last form is an index species from a zone of the same name, which occurs widely in the Mediterranean carbonate facies. This form is the only "Tethyan" species in the assemblage, whereas the rest are represented by widespread euryfacies forms. A similar assemblage with more Tethyan elements occurs in the deposits of the Coastal Mountains (the Nicola quarry), here defined as Kimmeridgian. The assemblage contains *Ammobaculites pellucida* Said et Barakat, *Pseudocyclammina* sp., *Alveosepta personata* (Tobler), *Nautiloculina oolithica* Mohler, and *Lenticulina subtilis* (Wins). It includes in general 14 families, 20 genera, and 25 species, most of which are agglutinated forms; planktonic species are lacking.

In the rest of the Syrian territory, there was either no Kimmeridgian sedimentation (Kurd-Dag), or sediments of this age were eroded as a result of the pre-Cretaceous uplifts, as evidenced by ostracode and foraminiferal faunas redeposited in the Cretaceous strata of some localities (the Wadi Jahannam section, Coastal Mountains).

The Tithonian deposits are preserved in only a few sections of Syria because the pre-Cretaceous uplifts involved a major part of the territory. They were studied in the Anti-Lebanon (the Wadi Al-Karn, Sad Al-Karn, and Wadi Favuar sections) and the Coastal Mountains (the Qadmous section), The deposits yielded abundant assemblages of high species diversity. They contain the widespread zonal species *Anchispirocyclina lusitanica* (Egger) and *Melathrokerion eospiralis* Gorb. The corresponding zone is recognizable in Syria, the Crimea, Caucasus, and probably in Morocco. The incompleteness of the Tithonian strata prevents a detailed subdivision. The Tithonian foraminiferal assemblages from Anti-Lebanon are characterized by a mixed composition including both the Tethyan and Subtethyan endemics and cosmopolitan forms, namely: *Gaudryina vadazi* Cushm. et Glaz., *Stomatostoecha compressa* Gorb., *Melathrokerion eospirialis* Gorb., *Alveosepta powersi* Redm., *Verneuilina angularis* Gorb., *Marssonella hehti* Dieni et Mass., *Anchispirocyclina lusitanica* (Egger), *Pseudocyclammina* sp. 1, and *Kurnubia jurassica* Redmond. The Tithonian strata of the Coastal Mountains (the Qadmous section) produced an assemblage differing in species composition and dominated by the Tethyan endemics *Bramkampella arabica* Redm. and the Subtethyan species: *Choffatella decipiens* Schlum., *Anchispirocyclina lusitanica* (Egger), *Pseudocyclammina parvula* Hott., *Feurthillia frequens* Maync, *Torinosuella* sp., and others. All these species are very abundant. In addition, the assemblage includes the Tithonian forms, which appeared in the Tithonian and then evolved in the Cretaceous. This section is likely to exhibit the latest Jurassic strata (the late Tithonian) and the beds transitional to the Berriasian.

Thus, the analysis of the development of the Jurassic foraminiferal assemblages allows the following conclusions.

(1) Study of the foraminifera evolution in relation to the dynamics of the Mediterranean sea basins revealed a number of stages different in the composition, structure, and distribution of their assemblages. Many of these stages correspond in duration to such stratigraphic units as a stage. Biological peculiarities of the studied foraminifera enable the recognition of two large evolutionary stages (megaphases); early-middle Jurassic and late Jurassic–early Cretaceous. These stages are different in their morphotypes of dominants, degree of endemism, tolerance, rates of evolution, intensity of speciation, and area distribution sizes of the foraminifers. The results show that the biological transformations of the fauna were slower than the changes in the abiotic factors that influenced the basins that were their habitat.

(2) The most distinct steps in the fauna renewal are recorded at the beginning of the Bathonian, in the late Bathonian, at the beginning of the Oxfordian, and at the beginning of the Tithonian. All these boundaries are marked by appearance of new taxa of a generic rank.

(3) All genera appearing in the middle Jurassic (Aalenian–Callovian) are tropical endemics. Beginning from the late Jurassic (Oxfordian–Tithonian) till the early Cretaceous (Berriasian–Barremian), new elements of the assemblages are represented exclusively by Subtethyan genera, which had wider distribution areas outside of the Tethys.

(4) In the Mediterranean, the changes in the foraminiferal assemblages near the Jurassic–Cretaceous boundary were of the same nature as in the Boreal province. The fauna was renewed at the specific level only, the Cretaceous and Jurassic assemblages are very similar, new elements (genera) appeared mainly in the Tithonian, and then evolved in the early Cretaceous.

REFERENCES

Gordon, W.A., Biogeography of Jurassic Foraminifera, *Bull. Geol. Soc. Am.*, 1970, vol. 81, no. 6, pp. 1689 - 1704.

Jarmakani, E., Kuznetsova, K., Grigelis, A., Hallak, L., and Bittar, M., The Appearance of Upper Jurassic Deposits in Palmyrides, *Syrian J. Geologie*, 1989, no. 14, pp. 22 - 24.

Pellissie, T., Peybernes, B., and Rey, J., The Larger Benthic Foraminifera from the Middle/Upper Jurassic of SW France (Aquitaine, Causses, Pyrenees), *Biostratigraphic, Paleoecologic, and Paleobiogeographic Interest, Benthos'83, 2nd Symp. Int. Benthic Foraminifera*, Pau, Bordeaux, 1984, pp. 479 - 489.

Said, R. and Barakat, M.G., Jurassic Microfossils from Gebel Maghara, Sinai, Egypt, *Micropaleontology*, 1958, vol. 4, no. 3, pp. 231 - 272.

Basov, V.A., On Some Characteristics of Foraminifera Geographical Spreading in Jurassic, *Paleogeografiya Severa Evrazii v Mezozoe* (Mesozoic Paleobiogeography of Northern Eurasia), Moscow: Nauka, 1974, pp. 63 - 76.

Basov, V.A., Vakhrameev, V.A., Krymgol'ts, G.Ya., Mesezhnikov, M.S., Saks, V.N., and Shul'gina, N.I., A Problem of Continental Drift in the Jurassic and Cretaceous According to Paleobiogeographic Data, *Paleontologiya, Mezhdunarodnyi Geologicheskii Kongress, XXIV Sessiya, Doklady Sovetskikh Geologov* (Paleontology, XXIV Int. Geol. Congr.: Rep. Sov. Geologists), Moscow: Nauka, 1972, pp. 104 - 113.

Kuznetsova, K.I. and Gorbachik, T.N., *Stratigrafiya i Foraminifery Verkhnei Yury i Nizhnego Mela Kryma* (Upper Jurassic and Lower Cretaceous Stratigraphy and Foraminifers of Crimea), Moscow: Nauka, 1985.

Stratigrafiya i Korrellyatsiya Verkhnei Yury SSSR po Foraminiferam (Stratigraphy and Correlation of the Upper Jurassic in USSR by Foraminifers), Moscow: Geological Inst., 1985.

Stratigraphy and Geological Correlation, Vol. 2, No. 1, 1994, pp. 88 - 94. Translated from Stratigrafiya. Geologicheskaya Korrelyatsiya, Vol. 2, No. 1, 1994, pp. 95 - 102.
Original Russian Text Copyright © 1994 by Maisadze.
English Translation Copyright © 1994 by Interperiodica Publishing (Russia).

Upper Eocene Olistostromes on the Southern Slope of the Greater Caucasus

F. D. Maisadze

Dzhanelidze Geological Institute, Academy of Sciences of Georgia, ul. Zoi Rukhadze 1, Tbilisi, 380093 Georgia

Received May 28, 1992

Abstract – The study on the upper Eocene olistostromes of the southern slope of the Greater Caucasus showed that, contrary to previous findings, a part of these formations situated east of the Bol'shaya Liakhvi River does not belong to the wildflysch. The olistostromes were formed in a basin with subcratonic-type sedimentation, in the cordillera zone south of the flysch basin.

Olistostromes of the southern slope of the Greater Caucasus occur at different stratigraphic levels. The upper Eocene formations are the most widespread among them.

The formations are characterized in many works (Vassoevich, 1931; Kandelaki, 1975; Keller, 1945; Kopp, 1990; Leonov, 1981; Maisadze, 1970, 1984; Mamedov, 1968; Mrevlishvili, 1954, 1957) describing their structure, genesis, structural position, and age. Still, many problems remain unsolved or disputable.

The formations are interesting because they are widespread throughout the Alpine foldbelt (Leonov, 1981). As reference beds, the olistostromes are peculiar as they permit us to determine the time and duration of the Pyrenean orogeny, and thus enable us to correlate tectonic events both inside and outside of the Alpine fold system. On the southern slope of the Greater Caucasus, the formations under question occur irregularly, mainly in two regions (Fig. 1).

Their insignificant portion occurs in the Sochi–Adler depression as a member of the regressive Matsesta Formation, which consists of three parts differing in lithology: sandy claystones, an "inclusion-bearing horizon," and clayey sandstones (Maisadze, 1987). The inclusion-bearing horizon (olistostrome) is a typical submarine rockslide formation. It consists mainly of olistoliths of the underlying rocks dominated by the *Lirolepis* marls (the Kuma Formation).

The age of the Matsesta Formation is disputable. Some researchers (Keller and Ul'yanov, 1937; Keller and Menner, 1945; and others) refer it to the Oligocene, others suggest the upper Eocene age (Kacharava, 1944; Papava and Goderdzishvili, 1968; Salukvadze, 1972; and others).

The Oligocene age was based on the small foraminifers previously dated as the early Oligocene assemblage, yet now referred to the latest Eocene age (Salukvadze, 1972).

The complete sequence of the Matsesta Formation and its distinct boundaries with the underlying and covering formations (the foraminiferal marls and Khosta Formation) allow us to date the beginning and duration of the Pyrenean orogeny, which caused the deposition of these rocks (Maisadze, 1984).

The bulk of the upper Eocene olistostromes occurs in the eastern segment of the southern slope of the Greater Caucasus.

From the Rioni River, they stretch eastward as a narrow belt along the frontal thrust of the flysch deposits of the Mestia–Tianeti zone[1].

As a result of thrusting, the deposits under consideration are partly, or in some places entirely overthrusted by the flysch deposits. In turn, the olistostromes are thrusted from the north over the autochtonous normal sedimentary rocks of the Gagra–Dzhava zone with different ages including the upper Eocene.

The upper Eocene olistostromes occur mainly in Georgia, and are sporadic in the Azerbaidzhan part of the Greater Caucasus (the Dashbulag and Talystan outcrops).

There is no agreement on the age of the olistostromes. Different researchers referred them to various levels of the Eocene. Using nummulite fauna, they were assigned to the upper Eocene (Mamedov, 1968). It was initially believed that olistostromes correspond to the entire upper Eocene, or to its basal part. Later, because of new fauna finds (Leonov, 1975) and correlations with the coeval formations of the adjacent regions (Maisadze, 1984), the age was more accurately defined as the uppermost Eocene.

Still, in Kopp's work (1991) the olistostromes are referred to the lower part of the Il'dokan Formation of the middle Eocene. This age interpretation seems disputable, because it is based upon the nummulite fauna, which will be discussed in greater detail later.

In my opinion, the other point of contention concerns the facies and tectonic environments of olistostrome origin east of the Bol'shaya Liakhvi River in

[1] The tectonic subdivisions used in the paper are from the tectonic schematics of Gamkrelidze and Gamkrelidze (1978).

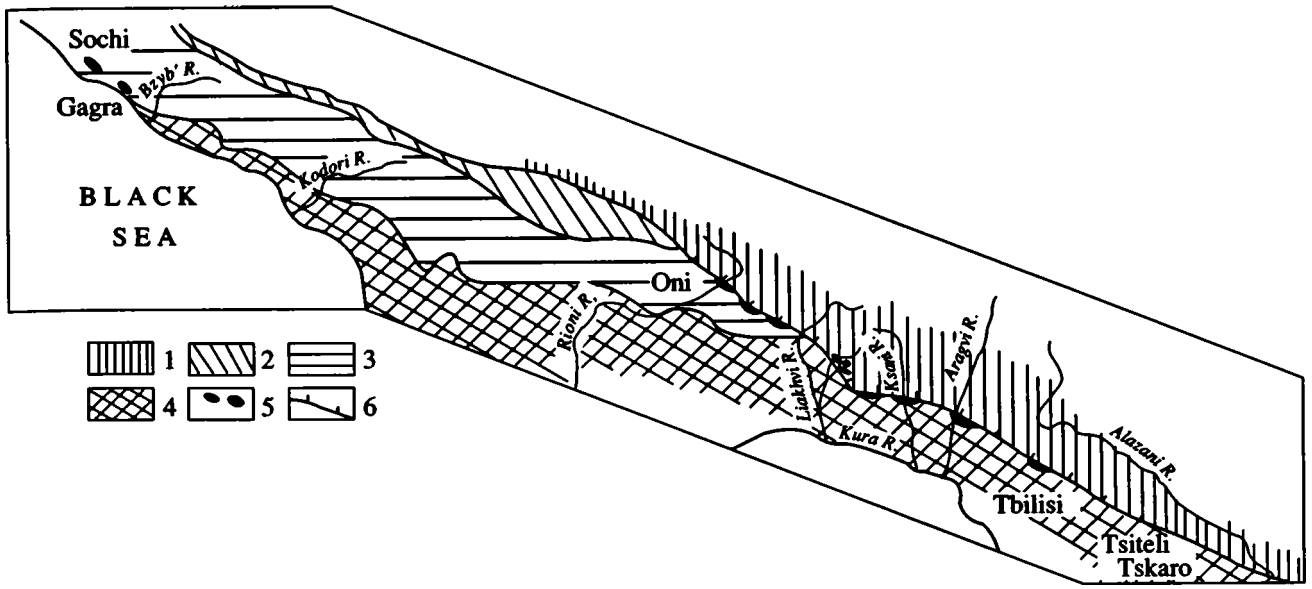

Fig. 1. Scheme of localities of the upper Eocene olistostromes.

1 – Mestia–Tianeti zone; 2 – Chkhalti–Lailash zone; 3 – Gagra–Dzhava zone; 4 – Georgian block; 5 – upper Eocene olistostromes; 6 – thrust boundary of flysch deposits.

the Zhinvali–Gombori subzone of the Mestia–Tianeti zone. These olistostromes have been considered an integral part of flysch deposits and the wildflysch (Gamkrelidze and Gamkrelidze, 1977; Leonov, 1975; Maisadze, 1984; and others). Olistostromes, similar in age and composition, also occur west of the Bol'shaya Liakhvi River outside the Zhinvali–Gombori subzone (Rioni–Liakhvi interfluve) in the northern margin of the Gagra–Dzhava zone. Their affinity with the subcratonic facies is beyond doubt.

So, the upper Eocene olistostromes of the southern slope can be divided laterally into two facies groups: one (the Rioni and Liakhvi interfluve area) belongs to the subcratonic deposits, and second (east of the Bol'shaya Liakhvi River) is of the wildflysch type.

The concept of the wildflysch as a part of the upper Eocene olistostromes of the southern slope was first suggested by Leonov (1975). This concept is based on the great similarity between the rocks of the Zhinvali–Gombori subzone east of the Bol'shaya Liakhvi River and analogous formations of the Alpine fold system of Western Europe.

As the primary features of olistostromes common to both of the regions above, Leonov (1975) noted their present structural position, sediment morphology, peculiarities of sedimentation, and age. It is worth noting that the same similarity in many of these features can be observed for olistostromes situated west of the Bol'shaya Liakhvi River and belonging to the subcratonic deposits of the Gagra–Dzhava zone.

In the Swiss Alps, where the wildflysch was first recognized, olistostromes are constituents of the Ultrahelvetian nappe of central and western Switzerland, tectonically clamped between the marginal subalpine flysch and the schlieren flysch to the south (Trümpi, 1960). As shown below, the study on the Paleogene formations of the southern slope of Greater Caucasus indicates that there are different relations between olistostromes and flysch.

Classifying compatible and coeval deposits of a single region as different facies groups one has to take into consideration both the similar features and differences in composition and structure of these groups, which are observable in the region.

As was noted, the olistostromes have a strict tectonic position. With the exception of three isolated outcrops along the Malaya Liakhvi River, which are in the flysch deposit zone north of the afare said thrust line (Fig. 1) they are confined to the frontal thrust line of flysch formations. Yet, as outlined below, here they are a secondary occurrence as first noted by Kandelaki (1975).

Without going into detailed characteristics of the deposits under consideration, I shall outline only their main features, which persist throughout their distribution areas in the region.

Olistostromes mainly consist of olistoliths of Mesozoic and sometimes Paleogene deposits of the Gagra–Dzhava zone. Dominant among them are the upper Jurassic reef limestone and porphyritic volcanic rocks of the Bajocian. In addition, these olistoliths are the largest in size, especially those of the limestones, which in some outcrops form olistoplaques of several hundreds, and even thousands of cubic meters in volume (Dashbulag, Orbodzala, Alevis-Klde, and others). The huge size of such klippen was formerly the reason why they were accepted as bedrock outcrops of the upper Jurassic rocks.

Small faults and slickensides are abundant inside olistostrome bodies, which thus indicates their tectonic rearrangement. The olistostrome matrix mainly consists of carbonate claystone and siltstone. The thickness varies from dozens to several hundreds of meters.

In various parts of the region under consideration, there are minor differences in the olistostrome composition as described below.

As noted above, the olistostromes of the Rioni–Liakhvi interfluve are confined to the northern part of the Gagra–Dzhava zone.

In the Utsera district (Gomrula River), olistostromes include fragments of the Cretaceous flysch formations. In olistostromes of the Ertso district, besides the Bajocian volcanic rocks I was the first to discover younger volcano-sedimentary rocks bearing inclusions of the upper Jurassic limestones (Maisadze, 1970). These rocks include volcaniclastic and effusive varieties. The former are represented by agglomerate tuff and tuffite, the latter, by basalt and olivine basalt.

Petrography and chemical composition of these rocks indicate their affinity to the normal calc–alkaline series (Maisadze, 1970). The volcanic rocks were considered to be coeval with the olistostrome formation, and thus were accepted as products of the upper Eocene volcanism. Yet, the geologic position of the olistostrome was unclear at that time because of bad exposure conditions and high tectonic rearrangement. As the southern slope of the Caucasus is free of the upper Eocene volcanic rocks, and the olistostrome formation is probably related to the beginning of the nappe formation, the upper Eocene age of the volcanic rocks under discussion seems unreliable.

At the same time, in the Ksani–Arkali para-autochthon, there are outcrops of Albian(?)–Cenomanian volcanic rocks (Gamkrelidze, 1970), the olivine basalt and coarse- to fine-grained tuff and tuffite that, according to chemical composition, belong to the calc–alkaline volcanic series.

The aforesaid suggests that the above-mentioned volcanic rocks with inclusions of the upper Jurassic limestone are products of the Albian(?)–Cenomanian volcanism, enclosed in the olistostrome as olistoliths along with the Bajocian volcanic rocks.

East of the Bol'shaya Liakhvi River, olistostromes occur in the Zhinvali–Gombori zone, which is characterized by an intricate tectonic structure. From the north to the south, there are Alisigori–Chinchveliti, Sadzeguri–Shakhvetility, and Zhinvali–Pkhoveli tectonic nappes, as well as the Ksani–Arkali para-autochthon (Gamkrelidze and Gamkrelidze, 1978).

The Cretaceous–Paleogene flysch deposits are constituents of the first three thrust sheets, whereas the Ksani–Arkali para-autochthon consists of just Mesozoic and Paleogene subcratonic deposits, having been at one time a northern part of the Gagra–Dzhava zone (Gamkrelidze and Gamkrelidze, 1977).

Olistostromes of this subzone occur at the boundary between the Zhinvali–Pkhoveli and Ksani–Arkali nappes, along the line of the flysch thrust (Fig. 2). This can be most clearly observed in the Aleura River section (left tributary of the Ksani River), where the Paleogene flysch and subcratonic deposits of the Zhinvali–Gombori subzone are completely exposed.

The upper Eocene flysch deposits occurring in the Sadgezuri–Shakhvetili and Zhinvali–Pkhoveli nappes are represented by the Il'dokan Formation. In the Alisigori–Chinchveliti nappe these deposits are absent, most probably eroded.

The previously disputed age of the Il'dokan Formation has been established as the late Eocene according to the nummulite fauna (Varentsov, 1950; Kandelaki, 1975; Leonov, 1975) and the stratigraphic position of the section. Small foraminifers collected from these deposits support their upper Eocene level.

The Oligocene age of the upper part of the Il'dokan Formation (Vassoevich, 1931; Leonov, 1975; and others) was justified neither by fauna nor by lithology.

The formation under discussion is divisible lithologically into two parts. The lower part, darker in color, is about 400 m thick, and consists of alternating siltstone and claystone, which are poorly calcareous or carbonate-free. In forms of interbeds, there are marl and arkose quartz sandstone. The claystone is mainly bituminous, and the sandstone contains organic detritus. Lenses of limy dolomite are present in the part of the formation exposed in the Aleura River section.

Enriched in terrigenous material of sand size, the upper part of the Il'dokan Formation is represented by regressive, lightly colored deposits. This part of the formation consists of alternating calcareous arkose–quartz and greywacke–quartz sandstone, foliated claystone, and marl with limestone interbeds. In the upper part of the sequence, there are several horizons of breccia-conglomerate as thick as 6 - 11 m. The clastic material of breccia-conglomerate consists mainly of flysch rocks. Clasts of upper Jurassic reef limestone were not observed among them. The apparent thickness of the regressive part of Il'dokan Formation is 800 - 900 m.

The upper Eocene subcratonic deposits of the Ksani–Arkali para-autochthon occur south of the flysch deposits, and are represented by olistostrome and normal sedimentary rocks. Occurring south of the olistostrome belt, the latter consist of slightly calcareous soft claystone, arkose–quartz sandstone, and claystone with a total thickness of 60 - 70 m.

Of interest, in some sections (Ksani and Aleura rivers) the olistostrome matrix contains members of sedimentary rocks with characteristic flysch elements (hierogliphs and rhythmic alternation). These features of the subcratonic deposits seem to be caused by turbidite penetration into the basin from the north. The process was most likely favored by the straits between cordilleras and the related flysch and subcratonic basins.

Rounded granitoid fragments represent a peculiarity of the olistostromes under discussion.

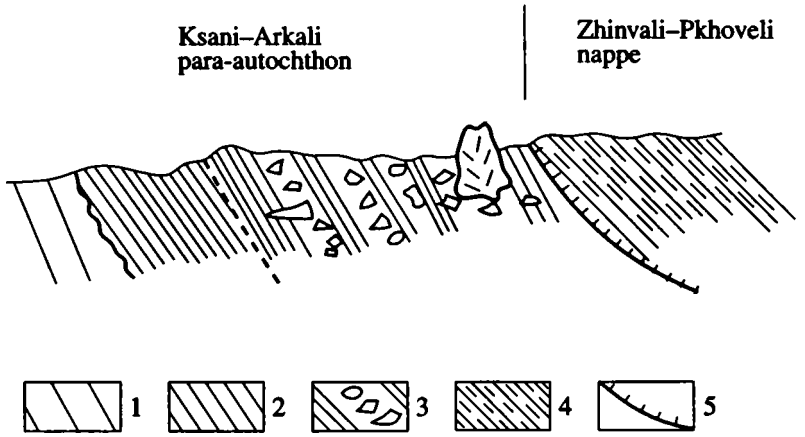

Fig. 2. Schematic cross-section along the Aleura River (left tributary of the Ksani River).

1 – Liassic deposits; 2 – normal sedimentary rocks of the upper Eocene; 3 – upper Eocene olistostromes; 4 – Cretaceous flysch deposits; 5 – nappe lower boundary.

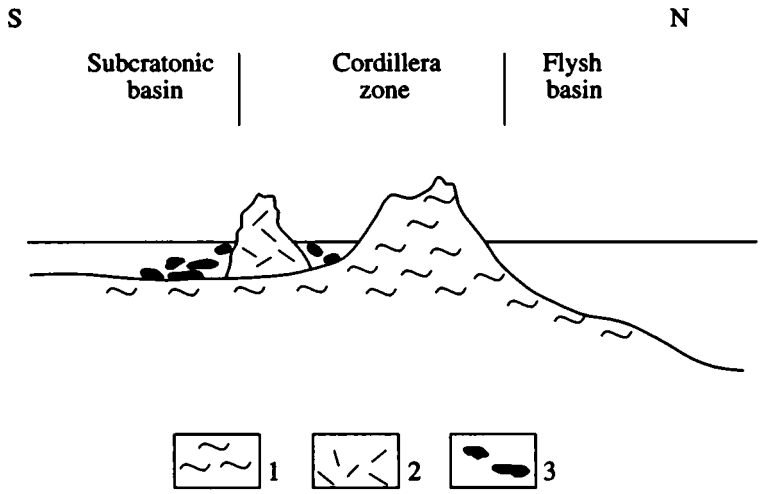

Fig. 3. Paleogeographic schematics of the olistostrome formation.

1 – Mesozoic deposits; 2 – upper Jurassic reef; 3 – olistoliths.

East of the Pshavis-Aragvi River (southern Kakhetiya), the Alisigori–Chinchveliti thrust sheet completely covers the Sadzeguri–Shakhvetili nappe, whereas Zhinvali–Pkhoveli and Ksani–Arkali nappes are incompletely overthrusted. As a result, the upper Eocene formations of the Ksani–Arkali para-autochthon are only exposed in tectonic windows and semi-windows represented by olistostromes, on the one hand (Turdo River), and by conglomerate, granule gravelstone, sandstone, and claystone, on the other hand (Gombori River). Both facies seem to laterally replace each other. Upsection, they give way to loose sandstone and Maikop clay, which are referred to as the Kinta Formation (the Oligocene–lower Miocene).

As was noted, in the Malaya Liakhvi drainage basin there are three isolated olistostrome outcrops, which, contrary to the general distribution mode of olistostromes along the line of a flysch thrust, are inside the Cretaceous–Paleogene flysch zone of the Zhinvali–Pkhoveli nappe, 1.5 - 3 km north of the thrust line (Fig. 1). These are the olistostrome exposures near the Orbodzala and Rekhi mountains, and the Zonkari Village.

Their study revealed that they occur either on various levels of the upper Cretaceous flysch (Zonkari and Rekhi localities), or over the Paleocene deposits (Orbodzala locality). Thus they are not constituents of the Il'dokan Formation, and are located as isolated fragments amid the Cretaceous–Paleogene flysch of the Zhinvali–Pkhoveli nappe.

The aforesaid suggests that these olistostromes are in secondary occurrence as small klippen marking the retrograde thrust faults of tectono-gravitational origin. The sheets were moving northward. In other words, inversely relative to the main mass transportation on the southern slope of the Greater Caucasus. To an extent, the gravitational movement of these sheets was likely caused by the large volume of the upper Jurassic

limestones forming olistoplaques, 250 × 300 m (Rekhi) and 3 × 1 km (Orbodzala) in size.

So, the data presented shows that the upper Eocene olistostromes east of the Bol'shaya Liakhvi River do not superstruct the flysch sequence, and therefore cannot be classified as wildflysch.

It should be suggested that throughout the southern slope of Greater Caucasus, the olistostromes were formed under paleogeographic and tectonic conditions identical to those of a basin with a subcratonic type of sedimentation.

As for the wildflysch, it may include only that part of the Il'dokan Formation containing breccia-conglomerate layers (Aleura and Medzhuda rivers), and crowns the Paleogene flysch sequence.

With respect to the main features of the upper Eocene olistostrome-forming event, I note the following.

During the second half of the upper Eocene, significant paleogeographic and facies changes took place on the southern slope of the Greater Caucasus as a result of the initial stage of Pyrenean orogeny.

At this time, the Sochi–Adler basin with sedimentation of regressive deposits of the Matsesta Formation began its formation in the western part of the southern slope. This is evidenced both by the character of Paleogene deposits in filling the depression and by their thickness pattern. Here, in particular, thin (170 - 200 m) typically subcratonic deposits (marl and limestone) grade into comparatively thick (320 - 350 m) deposits of the clastic rich Matsesta Formation (Maisadze, 1987).

The Pyrenean orogeny is most brightly manifested in the eastern segment of the southern slope (east of the Rioni River). The northern marginal cordillera of the Gagra–Dzhava zone, which served as the main source of clastic material for the upper Eocene basins, is now entirely overlain by flysch deposits.

East of the Bol'shaya Liakhvi River, where a flysch basin continued to exist during the Paleogene, the cordillera separated subcratonic and flysch basins. It was composed mainly of the Mesozoic, and partly Paleogene deposits of the Gagra–Dzhava zone. In the eastern part, rocks of the crystalline basement of the Gagra–Dzhava zone were integral parts of the cordillera structure (Gamkrelidze and Gamkrelidze, 1977). The end of the upper Eocene, when the Pyrenean orogeny was at maximum, was apparently characterized by intense avalanching, the result of strong earthquakes. In consequence, a vast mass of clastic material accumulated around the land areas, and olistostromes were formed in a basin with the subcratonic type of sedimentation (Fig. 3).

A similar process also developed in the Sochi–Adler depression, where the Matsesta Formation includes an "inclusion-bearing horizon," which is a deposit coeval with the olistostromes.

Some researchers (Kopp, 1991; Leonov, 1975; and others) suggest that the clastic material was transported northward, from the cordillera toward the flysch basin. Yet it is more natural to assume that disintegrated cordillera material moved from the north southward, toward the subcratonic basin because it is likely that at this time tectonic nappes began forming in the eastern segment of the southern slope with a mass movement in this direction (Fig. 3).

In the straits between the cordilleras, where the clastic material was smaller in size and limited in supply, conglomerate, granule gravelstone, sandstone, and claystone coeval with the olistostrome formation were deposited, being laterally replaced by the latter.

The cordillera zone also delivered the terrigenous material into the flysch basin. During the second half of the upper Eocene, the regressive rocks of the upper part of the Il'dokan Formation were deposited here. It is likely that inside the basin there were small areas of erosion (probably submarine) providing the flysch basin with clastic material, which caused the deposition of breccia-conglomerate layers in the periods of highest tectonic activity.

To conclude, it should be noted that according to the regressive deposits of Matsesta and Il'dokan formations, and the olistostromes, the period of their deposition ought to be 2 - 3 Ma, which seems to correspond to the duration of the Pyrenean orogeny on the southern slope of the Greater Caucasus (Maisadze, 1984).

REFERENCES

Gamkrelidze, I.P., Tectonic Window in the Ksani River Canyon, *Soobshch. Akad. Nauk Gruz. SSR*, 1970, vol. 59, no. 3, pp. 613 - 616.

Gamkrelidze, P.D. and Gamkrelidze, I.P., *Tektonicheskie Pokrovy Yuzhnogo Sklona Bol'shogo Kavkaza* (Tectonic Nappes of the Southern Slope of the Greater Caucasus), Tbilisi: Metsniereba, 1977.

Gamkrelidze, P.D. and Gamkrelidze, I.P., Main Tectonic Features of the Caucasus and West Carpathians, *Tr. D. Stur's Geol. Inst.*, Bratislava, 1978, no. 69, pp. 21 - 51.

Kacharava, I.V., *Rachinsko-Lechkhumskii Bassein i Smezhnye Raiony v Paleogenovoe Vremya* (Rachi–Lechkhumi Basin and Adjacent Regions in the Paleogene Time), *Tr. Geol. Inst. Akad. Nauk Gruz. SSR, Ser. Geol.*, 1944, vol. 11(VII).

Kandelaki, D.N., History of Geological Development of the Greater Caucasus Piedmont (Likhavi–Iori Interfluve), *Cand. Sci. (Geol.) Dissertation*, Tbilisi: Geol. Inst., Gruz. Akad. Nauk, 1975.

Keller, B.M. and Ul'yanov, A.V., New Data on Stratigraphy and Oil–Gas Fields of the Sochi District, *Neft. Khoz.*, 1937, no. 9, pp. 58 - 61.

Keller, B.M. and Menner, V.V., Paleogene Deposits of Sochi District and Related Submarine Rock Slides, *Byull. MOIP, Otd. Geol.*, 1945, vol. 20, nos. 1, 2, pp. 83 - 100.

Kopp, M.L., Transgressive-Regressive Cycles of the Late Cretaceous–Paleogene and Olistostrome-Forming Stages on the Southern Slope of the Eastern Caucasus, *Byull. MOIP, Otd. Geol.*, 1990, vol. 65, no. 4, pp. 97 - 109.

Kopp, M.L., Transgressive-Regressive Cycles of the Late Cretaseous–Paleogene and Olistostrome-Forming Stages on Southern Slope of the Eastern Caucasus, *Byull. MOIP, Otd. Geol.*, 1991, vol. 66, no. 1, pp. 13 - 23.

Leonov, M.G., *Dikii Flish Al'piiskoi Oblasti* (Wildflysch of the Alpine Province), Moscow: Nauka, 1975.

Leonov, M.G., *Olistostromy v Strukture Skladchatykh Oblastei* (Olistostromes in the Foldbelt Structure), Moscow: Nauka, 1981.

Maisadze, F.D., Paleogeography and Tectonic Environment during the Origin of Eocene Formations in the Rioni–Liakhvi Interfluve, *Cand. Sci. (Geol.) Dissertation*, Tbilisi: Geol. Inst. Akad. Nauk Gruz. SSR, 1970.

Maisadze, F.D., On the Pyrenean Orogeny in the Caucasus, *Izv. Akad. Nauk. SSSR, Ser. Geol.*, 1984, no. 7, pp. 148 - 152.

Maisadze, F.D., *Paleogeografiya Abkhazii v Paleogenovoe Vremya* (Paleogeography of Abkhaziya during the Paleogene), Tbilisi: Metsniereba, 1987.

Mamedov, A.V., Mode of Occurrence and Origin of Jurassic Rock Klippen in the Piedmont Zone of the Southern Slope of the Greater Caucasus, *Geotektonika*, 1968, no. 4, pp. 85 - 98.

Mrevlishvili, N.I., Fauna and Paleogene Stratigraphy of the Dusheti Region, *Cand. Sci. (Geol.) Dissertation*, Tbilisi: Geol. Inst. Akad. Nauk Gruz. SSR, 1954.

Mrevlishvili, N.I., Geological Structure of the Greater Caucasus Piedmont in the Dusheti Region, *Tr. Geol. Inst. Akad. Nauk Gruz. SSR*, 1957, vol. 10(15), pp. 139 - 147.

Papava, D.Yu. and Goderdzishvili, G.S., On the Age of Khosta Sandstone, *Soobshch. Akad. Nauk Gruz. SSR*, 1968, vol. 52, no. 3, pp. 695 - 698.

Salukvadze, N.Sh., The Paleogene System, *Voprosy Geologii Severo-Zapadnoi Chasti Abkhazii* (Problems of Geology of the Northwestern Abkhaziya), Tbilisi: Metsniereba, 1972, pp. 123 - 143.

Trümpy, R., Paleotectonic Evolution of the Central and Western Alps, *Bull. Geol. Soc. Am.*, 1960, vol. 71, pp. 843 - 908

Varentsov, M.I., *Geologicheskoe Stroenie Zapadnoi Chasti Kurinskoi Depressii* (Geological Structure of the Western Part of the Kura Depression), Moscow: Akad. Nauk SSSR, 1950.

Vassoevich, N.B., Brief Geological Essay on Oil Occurrences in the Central Southern Slope of the Greater Caucasus, *Tr. NGRI, Ser. B*, Leningrad, no. 1, 1931, pp. 95 - 106.

A BRIEF COMMENT ON F.D. MAISADZE'S PAPER

F.D. Maisadze's paper concerns formations that mark one of the most important events in the history of the Caucasus and the entire Alpine-Himalayan belt, and has, in addition, global significance. I consider two of the author's points important: first, his conclusion on the uniform stratigraphic position of the Eocene–Oligocene boundary olistostromes in the western and central parts of the Greater Caucasians slope, and therefore their coeval origin; and second, the data on transportation of the coarse material, composing olistoliths, from the north rather than from the south.

I would like to add to the first point that the olistostrome formations are traceable far east of Georgia into Azerbaidzhan. They occur not only in the northern Adzhinour Steppe, as mentioned by the author with the due reference to A.V. Mamedov, but also much farther, up to the western Shemakha region, where the olistostromes compose the Talystan and Shabian "Rocks" in the Agrychai and Akhsu interfluve area. As a student, I studied the Shabian Rocks almost 60 years ago, but then and long after, I did not understand their origin. Unfortunately, later the rocks were not studied in more detail (in respect to the Talystan Rock, it was done by my student I.A. Voskresenskii). Thus, this olistostrome level is in broad perspective significant in the Caucasus (in the context of the Greater Caucasus). Similar formations of the same level are also known in the northeastern and southeastern slopes of the Lesser Caucasus (T.A. Gasanov).

As for the second point, it should be first noted that F.D. Maisadze's idea differs from M.G. Leonov's previous notion. All the researchers of these olistostromes agree that the olistostromes occurred at the expense of the disintegration of rocks that composed the northern margin of the Transcaucasian microcontinent, which is subdivided into the Gagry–Dzhava (in the west) and Kakhetiya–Vandam (in the east) zones. The most peculiar rocks are the Middle Jurassic porphyrite and upper Jurassic reef limestone, both being the products of the destruction of a volcanic island arc and its barrier reef. Just these rocks form the largest olistoliths. Rather logically, M.G. Leonov suggested that it was the northern margin of the Gagry–Dzhava zone that underwent destruction. Yet, according to F.D. Maisadze, the clastic material was transported from the north, rather than from the south. This led him to believe, again logically, that in the late Eocene there was another uplift consisting of the same rocks as those of the Gagry–Dzhava zone, and further that the olistostromes were formed in a trough related to the uplift. F.D. Maisadze's speculation is confirmed by the fact that in the western- and easternmost parts of the olistostrome belt the Akhtsu and Vandam uplifts are present, respectively, which are well expressed at the surface of the modern structure (the Nialdag Range and others). Yet F.D. Maisadze's idea, illustrated by Fig. 3 of his paper, has one weakness. As noted by its author, in the flysch formations occurring immediately to the north of the olistostrome belt there are no products eroded from the Transcaucasian microcontinent, or its marginal volcanic island arc.

I think that there are two ways of explaining this. First, the uplift could be sharply asymmetric with a steep southern edge and gently dipping northern slope. This may suggest that in fact it was a tectonic thrust sheet, a part of the nappe structure of the Greater Caucasus southern slope. Later, I will try to estimate what it means.

Second, the southernmost, now marginal flysch nappes consist of sediments evidently deposited far away from the postulated uplift. Later, during the deformations in the central part of the southern slope, they were thrusted over the marginal uplift, now in direct tectonic contact with the olistostrome-bearing formations. According to M.L. Kopp, in the easternmost region, northwest of Shemakha, the frontal thrust of the flysch zone (the Zanga Trust) retreats to the north, and the olistoliths of the upper Jurassic limestones already appear on the northern slope of the Vandam uplift.

The formation of the Akhtsu–Vandam tectonic nappe has to be the result of tangent deformations during the upper Eocene, which had a southern vergence and affected the northern margin of the Transcaucasian microcontinent, causing the nappe detachment and its transportation to the south. So, this may indicate the beginning of a collision between the Transcaucasian microcontinent and the southern margin of the Eurasian lithospheric plate.

Now we arrive at the more important problem of the overall Caucasus significance, the problem concerning paleotectonic and paleogeographic environments in the Greater Caucasus during the Oligocene and early-middle Miocene. For a long time, the Greater Caucasus was thought to have undergone the early orogenic stage of its development during the period represented by an insular land of moderate relief. Yet earlier, in his classic work on the Greater Caucasus, V.V. Belousov (1940) suggested another scenario. According to his reconstruction, the sea was not only spread all over the Greater Caucasus during that epoch, but also deposited sediments of maximum thickness; the relief and structure inversion took place later.

It should be noted that V.V. Belousov's early idea has recently received support. In consideration of the following, it was without a doubt favored by M.L. Kopp and I.G. Shcherba. First, the erosion products of the Greater Caucasus rocks appear on its slopes, in particular on the northern one, just in the upper Miocene (Sarmatian) deposits. Second, seismic investigations in the eastern Ciscaucasia using the reflection CDP technique showed that during the entire Paleogene and early Miocene, the clastic material was transported to the future Terek–Caspian basin from the north, as indicated by the clinoform inclination. In the Oligocene olistostrome of Dagestan, the olistoliths of the upper Cretaceous and lower Paleogene rocks have a northern (Nogai Steppe), rather than a southern Caucasian origin. In the southern side of the Terek–Caspian basin, the northward-oriented clinoforms only appear at the Sarmatian, indicating that at this time the Greater Caucasus became a source of the clastic material.

Unfortunately, we do not have the similarly thorough information on Western Ciscaucasia. The oil-bearing shoestring deposits and sand-filled "coves" in the lower part of the Maikop Group, which were described by I.M. Gubkin in his classic work on the Shirvan (Maikop) oil province, are the main subjects of study there. How were these submarine canyons oriented, from the south northward, or vice versa? What are these "coves", can they be distal portions of submarine dejection cones also oriented southward?

Whatever it is, the intensive deformations took place on the southern slope at the end of the Eocene thus indicating the beginning of the collision, which prompts a reconsideration of the paleogeography of the Greater Caucasus during the Oligocene and early-middle Miocene. It seems doubtful that this area remained covered with a deep sea, which deposited thick sediments. It was rather a submarine and partly subaerial (flat islands) uplift restricted by the Main Ridge, because in the northern Eastern Caucasus, as well as in Limestone Dagestan and the Shakhdag zone of Azerbaidzhan, there are basins that preserve the upper Miocene (Sarmatian and Pontian) sediments. In this case, the sediments are thin littoral shallow-water limestones without any coarse clastic material from the Main Ridge. And again, the sediments are deformed together with the underlying deposits, i.e., in post-Pontian time. In this context, it should be noted that during the 1930s, one of the well known Caucasian investigators, L.A. Vardanyants, working in the Mountainous Osetiya region came to the conclusion that the main deformation and orogeny in the Caucasus began during the Meotian. By the way, it was exactly at this time that the Caspian depression became elongated north–south, as it is presently elongated.

East of the Shakhdag, near the village of Budug, one can observe the remnants of the Maikop deposits: the dark clays, which are simultaneously similar and dissimilar to the typical Maicop varieties. The same clays compose the Kinta Formation in the Kakhetian Ridge on the southern slope of the Greater Caucasus. These are likely analogs of the lower Miocene deposits of the upper Maikop Group.

It is also remarkable that the remnants of the middle Miocene limestones, like their counterparts in Shakhdag and Dagestan, are preserved in the Shamkhor region of Azerbaidzhan, even if the crucial character of the Eocene–Oligocene boundary is more evident in the Lesser than in the Greater Caucasus.

So, there are reasons to assume that the collision, which formed the folded-nappe structure of the Greater Caucasus, started at the end of the Eocene, though its main orogenic stage occurred only in the upper Miocene. It was then that the Arabian plate, being detached from the African one, started its movement to the north, and under its pressure the Transcaucasian microplatform was separated into the eastern Black Sea and southern Caspian plates. The intense subaerial volcanism started at that time in the Caucasus, and the Cis- and Transcaucasian intermontane depressions were finally formed. The subject matter of this stage is clear, yet the previous stage, be it the early orogenic or early collisional, deserves attention.

These are some speculations concerning F.D. Maisadze's paper. The fact that it provoked such speculations is itself a good reason for the paper to be published.

V. E. Khain

Stratigraphy and Geological Correlation, Vol. 2, No. 1, 1994, pp. 95 - 98. Translated from Stratigrafiya. Geologicheskaya Korrelyatsiya, Vol. 2, No. 1, 1994, pp. 103 - 107.
Original Russian Text Copyright © 1994 by Glezer.
English Translation Copyright © 1994 by Interperiodica Publishing (Russia).

BRIEF

COMMUNICATIONS

Correlation of Development Stages of the Paleogene Diatom Flora from Marine Epicontinental and Oceanic Basins

Z. I. Glezer

All-Russian Research Institute of Geology, Srednii pr. 74, St. Petersburg, 199026 Russia

Received January 26, 1993

Abstract – The Paleogene is one of the most important stages in the development of diatoms, which play an important part in natural substance cycles. During the Paleogene time, diatoms occupied new ecological niches and new water areas. Some taxa died out, others appeared, and new flora assemblages were formed in the course of evolution. Thick diatomite layers in different regions of the world and diatomaceous mud in sedimentary cover of seas and oceans are the evidence and result of the vital functions of the Paleogene diatoms.

One of the peculiarities of the Paleogene is the wide occurrence of diatoms in the epicontinental marine basins (EMB). These basins existed in the Boreal zone, comprising the territories of the Baltic countries, the Dnepr–Don depression, the Voronezh anteclise, the Volga region, the Caspian Sea depression, the western part of the area adjacent to Mugodzhars, the Turgai trough, the West Siberian plain, and Mangyshlak. During different stages of the Paleogene, the diatom flora of the EMB had more or less close biogeographic relations with the flora of the open seas and oceans (OSO). The correlation of the development stages between the diatom flora from the EMB and OSO is of great scientific and practical importance, especially for the elaboration of zonal schemes.

This paper is based on the analysis and summary of original and published data on the taxonomy, evolution, and biostratigraphic significance of the Paleogene diatoms. The publications used are mostly from the bibliography of summary reports (*Diatomovye* ..., 1974, 1988; *Plankton Stratigraphy*, 1985; Strel'nikova, 1992). In addition, I used papers by different authors dealing with diatomology (Baldauf and Barron, 1987; Barron and Park, 1985; Fourtanier, 1991; Glezer, 1986, 1991; Gladenkov, 1987, 1988; Harwood, 1988; Pushkar', 1987; Ross and Sims, 1980, 1985, 1987; Sims, 1986; Sims and Ross, 1988; Yanagisawa and Suzuki, 1987).

Ten stages are distinguished in the development of marine diatom flora of the Paleogene. Each of them was peculiar in its flora taxonomic composition and evolution specifically manifested in different paleobasins. Each had a characteristic biogeography and distribution pattern. There are smaller-scale stages in the flora development recognized in separate paleobasins, or basin groups of a single paleobiogeographic province (area). They are reflected in corresponding zonal schemes.

The results of the comparative analysis of the development stages of Paleogene diatom flora from epicontinental and oceanic basins are presented in the table. The characteristics of the flora assemblages, named after the index species of zonal subdivisions, are given in corresponding publications, and hence will not be discussed in this paper. Below, there are brief descriptions of the ten largest stages in the development of marine Paleogene diatom flora.

During the first, early Paleocene stage, the evolutionary processes were weakly manifested only at the specific level. The flora mainly consisted of transit Cretaceous species with dominant forms representing the families Biddulphiaceae and Hemiaulaceae of the order Biddulphiales.

This prosperous stage of the EMB diatom flora of the early Paleocene resulted in the formation of thick diatomite deposits composed of diatom shells. Rich and diverse diatom flora widespread in the Syzran' [1] (Middle Volga region) and Marsyaty (eastern slope of the Urals) basins bear a close resemblance to the flora of the Tasman Sea and eastern Antarctic. The similarity is evident from both the identity of evolutionary stages and the flora inhabiting the neritic zone. The second stage in the development of diatom flora occurred at the beginning of the late Paleocene. Possibly after the onset of the regression and pertinent hydrodynamic changes, the area of diatom distribution in the EMB sharply decreased. This stage in the development of diatom flora is known only from the Nizhnii Saratov (Kochelai) basin (Middle Volga region). It mainly consists of transit, predominantly benthic species. Its relations with the oceanic flora of that time from the Tasman Sea and Indian Ocean are obscure.

The third stage of the diatom flora began to flourish in the late Paleocene. In particular the evolutionary processes in different phyla were activated by the end of Paleocene. The order Buddulphiales progressively developed; the new genus *Soleum* appeared in the family Hemiaulaceae. Speciation was characteristic of the *Trinacria*, *Sheshukovia*, and *Hemiaulus* genera. The

[1] The basins here and below are named after the formations where the corresponding flora were found.

Correlation of the development stages of Paleogene diatom flora from the OSO and EMB

Principal stages			OSO	EMB (according to author's data)	
Oligocene	Late	10	*Rocella gelida	⟷ Flora with *Actinoptychus thumii, Synedra jouseana linearis-Cavitatus linearis*	
			*Bogorovia veniaminii		
	Early	9	*Rocella vigilans		
			*Coscinodiscus reticulatus		
			*Coscinodiscus excavatus		
Eocene	Late	8	*Baxteriopsis brunii	*Bipalla oamaruensis, Cosmiodiscus* aff. *radiatus*	
			*Asterolampra marylandica a/b		
	Middle	7	*Btightwelia imperfecta	⟷ *Coscinodiscus senarius, C. succinctus, C. praenitidus*	
			*Hemiaulus gondolaformis	⟷	
		6	*Hemiaulus alatus	⟷ *Pyxilla oligocaenica tenuis*	
			*Pyxilla caput-avis	⟷ *Pyxilla gracilis* s. l.	*Brightwellia hyperborea*
			*"Triceratium" kanayae	⟷	
	Early	5	*Craspedodiscus oblongus	⟷	*Coscinodiscus decrescens*
			**Craspedodiscus undulatus	*Coscinodiscus payeri*	
			***Pyxilla gracilis	*Coscinodiscus josephinus*	
			***Hemiaulus incurvus	⟷ *Hemiaulus proteus* a/b	
		4			
Paleocene	Late	3		⟷ *Trinacria ventriculosa*	*Sheshukovia mirabilis*
					Stephanopyxis ferox
		2	***Hemiaulus peripterus		*Coscinodiscus* aff. *mutabilis*
	Early	1		*"Triceratium" gombasii*	
			****T. senta (heibergiana) H. rossicus	⟷ *Trinacria senta*	

Note: Zonal associations defined by: * J. Fenner*, ** M. Gombos*, *** E. Fourtanier (1991), **** A.P. Zhuze*;
⟷ species interchange, * see Plankton Stratigraphy (1985).

Coscinodiscaceae family from the order Coscinodiscales was supplemented with the new *Craspedodiscus* and *Pseudotriceratium* genera. New species appeared in the genus *Coscidodiscus*. The new family Pyxillaceae with the genus *Pyxilla* came into existence.

At the beginning of the epoch, the diatom flora had a limited distribution in the Truevo basin (Middle Volga region), but during the second half of Paleocene, diatoms spread over the Serov basin (eastern slope of the Urals), Moler Sea (Denmark), Southern Atlantic (the Folkland Plateau and Cap Basin). The increasing number of common species during the late Paleocene indicates the expanding biogeographical connections between the flora of the EMB and OSO. An especially close similarity between the flora of the EMB and Moler Sea appeared at the end of Paleocene, when the Truevo basin flora acquired features of deeper-water forms. At that time, diatom shells composed thick diatomite layers in the northern hemisphere, and diatomaceous muds accumulated in the oceans. These events are thought to be related to the transgression that developed during the late Paleocene and to the water enriched with dissolved silica.

The onset of the fourth stage in the development of diatom flora seems to fall at the beginning of the early Eocene. It is characterized by a slowdown of the evolutionary process. The flora consists chiefly of the species inherited from the Paleocene, and new species are scarce. The flora distribution is restricted by separate areas of the EMB of the east European Platform: the Sambiisk (Kaliningrad region), Kanev (Dnepr–Don depression), Veshenskoe (Voronezh anteclise), Kalinin, and Ozinki (Volga region) basins, as well as the southern regions of the Serov or Irbit sea.

The species similar to modern flora of the Indian Ocean were not found.

The fifth stage, the first half of the early Eocene, is marked by the disappearance of diatom flora in the seas of the east European platform and the gradual occupation of the Asian EMB: the Akchatau (western part of the areas adjacent to Mugodzhars), Tasaran (Turgai through), and Irbit–Lyulinvorsk (eastern slope of the Urals and the West Siberian plain) basins. Diatom flora also prograded into the Barents and Karsk seas. The most favorable conditions were in the Irbit and Akchatau basins, where diatomite accumulated.

This flora is typical of the neritic marine zone. Initially it was principally composed of transit species, but became gradually enriched in new species, mainly of the genera *Coscinodiscus* and *Hemiaulus*. This diatom flora developed in a peculiar way. Biogeographical connections with the flora of the Indian and Atlantic oceans, which are characterized by the evolution of the genus *Craspedodiscus*, were absent.

Apparently, a new transgression began at the very end of the early Eocene. It reached its maximum in the middle Eocene. The hydrochemical regime of the basins changed. The evolutionary peak of the Centrophyceae class occurs in the middle Eocene, when the new families Asterolampraceae, Triceratiaceae, Trigoniaceae, and Aspeiziaceae appeared, along with new genera in the families Hemiaulaceae, Coscinodiscaceae, and Radialiplicataceae. Species of the genera *Asterolampra*, *Rylandsia*, and *Azpeitia* supplemented the composition in the diatom oceanic assemblage in the neritic plankton of the EMB. They occur only sporadically, and a significant part of flora composition consists of species of the genera *Pyxilla* (including *Pyxilla gracilis* typical of the flora of the Indian Ocean at the very beginning of the Eocene), *Coscinodiscus*, and *Breightwellia*.

The sixth stage in the development of diatom flora coincides with the very end of the early Eocene (Lutetian). At first, diatom flora was most abundant in the EMB, namely in the Vershaut, Tasaran, Akchatau, Irbit, and Nyurol' basins (West Siberian plain), and prograded into the Karsk Sea. At the end of the Lutetian (or at the beginning of the Bartonian), diatom flora survived in some areas of the Nyurol' (or Tavda) basin, but continued to develop widely in more southern, Asian basins. A reverse situation occurred in the OSO, where the areas of the flora distribution widened gradually.

At the beginning of the stage, an important part of the EMB flora consisted of species inherited from the early Eocene. But by the end of the Lutetian, their significance decreased, and new floral elements became more important, including the constantly increasing number of migrant species from oceanic flora. In spite of common species, the flora of the EMB and OSO developed rather independently. Most probably, this was related to the differences in basin depths, temperature conditions and biogeographic zonations.

During the Bartonian (the seventh stage in the development of diatom flora), the diatom flora continued to flourish in the EMB and OSO. The EMB flora contained many species widespread in the OSO, Atlantic and Pacific Oceans, and the Norwegian Sea.

The next stage in the development of diatom flora, the eight stage, occurred in the late Eocene. The flora taxonomic composition resembled that of the Bartonian. Its evolution was slower compared to that of the middle Eocene time, and rare new genera appeared only in the oceanic flora of the Centrophyceae class. In the EMB of the western area adjacent to Mugodzhars and in the Caspian Sea depression, there was highly depleted diatom flora; rich and diverse diatom assemblages developed in the Kas'yanov (Voronezh anteclise) and Obukhov (Dnepr–Don depression) basins.

The Obukhov flora had a great taxonomic diversity of diatoms from the Pennatophyceae class, although some of their species are represented by rare subordinate specimens. Highly diverse Pennatophyceae are also typical of the late Eocene flora of New Zealand.

Despite the great number of common species, it is quite probable that there were no biogeographical connections between the EMB and OSO fauna due to the transit nature of the common species.

The EMB disappeared in the early Oligocene as a result of a regression. Progressively developing diatom flora continued to exist in oceans. The evolutionary process accelerated in the Centrophyceae class. The new family Hemidiscaceae, with the genera *Hemidiscus* and *Actinocyclus*, appeared. The new genus *Asteromphalus* came into existence in the Asterolampraceae family. New genera (*Bogorovia* and *Rocella*) originated in other phyla. The new genera *Rouxia*, *Cavitatus*, and others appeared in the Pennatophyceae class. The species of new genera were of minor importance, while those inherited from the late Eocene flora remained dominant. Biogeographical zonation became more obvious in the early Oligocene.

In the late Oligocene, during the tenth and final stage of Paleogene flora development, a wide adaptive radiation of the genera that originated in the early Oligocene occurred. As a result, new species originated, and the diversity of the Pennatophyceae increased. The areas of the diatom flora distribution significantly widened: in the Pacific, it dispersed from the equator northward up to the Bering Sea; in the Atlantic, it spread from the Malvine Basin to the Norwegian Sea; and flora also populated the Indian Ocean. Abundant diatom flora developed for a short time in the Karagiinsk EMB (southern Mangyshlak) and in the middle Maikop basin. In spite of the peculiarity of the neritic Mangyshlak flora, there were some species in its composition similar to the OSO flora.

Thus, regressive and transgressive stages of the marine Paleogene flora development are evident. The OSO flora underwent more profound evolutionary transformations whereas the EMB flora evolved more slowly, mainly at the specific level.

Compared to contemporaneous OSO flora, the EMB flora had a more stable taxonomic composition. Stages of diatom flourishing in the EMB were principally manifested not in the appearance of new taxa but in the unusually high energy of reproduction, which resulted in the deposition of thick diatomite layers.

In establishing biogeographical connections between the EMB and OSO flora, beyond the biotic, another important factor was the water current systems induced by transgressions and regressions.

Peculiarities of diatom flora in different paleobasins were caused not only by local environments, but also by the biogeographic zonation, which began to form at the beginning of the late Paleocene.

REFERENCES

Bardauf, J.C. and Barron, J.A., Oligocene Marine Diatoms Recovered in Dredge Samples from the Navarian Basin Province, Bering Sea, *US Geol. Surv. Bull.*, 1987, no. 1765, pp. 1 - 54.

Barron, J.A. and Park, M., Late Eocene to Holocene Diatom Biostratigraphy of the Equatorial Pacific Ocean, Deep Sea Drilling Project, Leg. 85, *Initial Reports of the DSDP*, Washington: US Govt. Print. Office, 1985, vol. 85, pp. 413 - 456.

Diatomovye Vodorosli SSSR. Iskopaemye i Sovremennye (Diatoms of the USSR. Fossils and Modern), Leningrad: Nauka, 1974, vol. 1.

Diatomovye Vodorosly SSSR. Iskopaemye i Sovremennye (Diatoms of the USSR, Fossils and Modern), Leningrad: Nauka, 1988, vol. 2, issue 1.

Fourtanier, E., Paleocene and Eocene Diatoms: Biostratigraphy and Taxonomy of Eastern Indian Ocean, Site 752, *Proc. of the Ocean Drilling Program, Sci. Research*, 1991, vol. 121, pp. 171 - 187.

Gladenkov, A.Yu., Volcanogenic-Sedimentary Formations of the Bering Island (Comandor Islands) and Their Age, *Voprosy Stroeniya Litosfery* (Problems of the Lithosphere Structure), Moscow: Nauka, 1987, pp. 16 - 22.

Gladenkov, A.Yu., Diatom Stratigraphy of Oligocene Deposits of North Pacific Region, *Geologicheskie Issledovaniya Litosfery* (Geological Study of the Lithosphere), Moscow: Nauka, 1988, pp. 17 - 22.

Glezer, Z.I., Phylogeny of Diatoms of the *Coscinodiscus* Order as Related to a New Classification Development, *Ezheg. VPO* (*VPO Annual*), 1986, vol. 29, pp. 180 - 187.

Glezer, Z.I., New Classification Development of Diatoms, *Aktual'nye Voprosy Sovremennoi Paleoal'gologii* (Actual Problems of Modern Paleoalgology), Kiev: Naukova Dumka, 1986, pp. 65 - 69.

Glezer, Z.I., Diatoms and Silicoflagellates, *Zonal'naya Stratigrafiya Fanerozoya SSSR* (Zonal Stratigraphy of the Phanerozoic in the USSR), Moscow: Nedra, 1991, pp. 140 - 142.

Harwood, D.M., Upper Cretaceous and Lower Paleogene Diatom and Silicoflagellate Biostratigraphy of Seymour Island, Eastern Antarctic Peninsula, Geology and Paleontology of Seymour Island, Feldman, K. and Woodburn, M.D., Eds., *Geol. Soc. Mem.*, 1988, no. 169, pp. 55 - 129.

Plankton Stratigraphy, London: Cambridge Univ., 1985.

Pushkar', V.S., Diatoms from Paleogene Deposits of the Northwestern Pacific, *Palinologiya Vostoka SSSR* (Palynology of the Eastern USSR), Vladivostok: DVNTs Akad. Nauk SSSR, 1987, pp. 60 - 70.

Ross, R. and Sims, P.A., *Syringidium* Ehrenb. *Dextradonator* Ross et Sims, *Nov. Gen., Bacillaria*, Brawnschweig, 1980, vol. 3, pp. 115 - 127.

Ross, R. and Sims, P.A., Some Genera of the Biddulphiaceae (Diatoms) with Interlocking Linking Spines, *Bull. British Museum* (*Natur. Hist.*), *Botany Ser.*, 1985, vol. 13, no. 3, pp. 277 - 381.

Ross, R. and Sims, P.A., Further Genera of the Budulphiaceae (Diatoms) with Interlocking Linking Spines, *Bull. Br. Mus.* (*Natur. Hist.*), *Botany Ser.*, 1987, vol. 16, no. 4, pp. 269 - 311.

Sims, P.A., *Sphynctolethus* Hanna, *Ailuretta* Gen. Nov. and Evolutionary Trends within the Hemiauloideae, *Diatom Research*, 1986, vol. 1, no. 2, pp. 241 - 269.

Sims, P.A. and Ross, R., Some Cretaceous and Paleogene *Trinacria* (Diatom) Species, *Bull. Br. Mus.* (*Natur. Hist.*), *Botany Ser.*, 1988, vol. 18, no. 4, pp. 275 - 322.

Strel'nikova, N.I., *Paleogenovye Diatomovye Vodorosli* (Paleogene Diatoms), St. Petersburg: St. Petersburg Univ., 1992.

Yanagisawa, Y. and Suzuki, Y., Diatoms and Silicoflagellates from the Oligocene Shirasaka Formation of the Joban Coalfield, Northeast Japan, *Bull. Geol. Surv. Jpn*, 1987, vol. 38, no. 2, pp. 81 - 98.

Stratigraphy and Geological Correlation, Vol. 2, No. 1, 1994, pp. 99 - 103. Translated from Stratigrafiya. Geologicheskaya Korrelyatsiya, Vol. 2, No. 1, 1994, pp. 108 - 112.
Original Russian Text Copyright © 1994 by Volkova, Kul'kova.
English Translation Copyright © 1994 by Interperiodica Publishing (Russia).

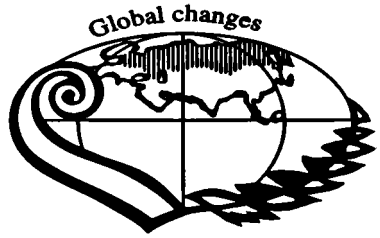

Evolution of the biosphere

BRIEF COMMUNICATIONS

Climatic Optima during the Cenozoic in West Siberia Deduced from Palynological Data

V. S. Volkova and I. A. Kul'kova

Institute of Geology, Siberian Division, Russian Academy of Sciences, Universitetskii pr. 3, Novosibirsk, 630090 Russia

Received October 5, 1992

Abstract – Paleobotanic data bears important information about ancient climates. The analysis of flora allows us to outline the time boundaries and to reveal global climatic changes. The first time boundary during the Cenozoic in West Siberia falls on the end of the early Eocene–beginning of the middle Eocene. The Eocene was a time in which the Paleogene transgression underwent maximum spreading. Seventy percent of the West Siberian platform was submerged at that time. Diatomite and siliceous clays enriched in siliceous shells of radiolarians, silicoflagellates and diatoms accumulated there. These sediments are also rich in dinocysts, pollen and spores.

Eocene palynoflora was examined from the boreholes drilled in the lower reaches of the Pur River, in the basin of the Severnaya Sos'va River, and in the interfluve of the Ob' and Irtysh rivers (in the upper reaches of the Chuzik and Kenga rivers). I.A. Kul'kova (Kul'kova, 1987; Kul'kova and Shatskii, 1990) recently obtained additional data from the boreholes in the Yamal and Taz peninsulas. The marine Eocene of West Siberia was divided by Kul'kova into zones on the basis of dinocyst associations. These zones correspond to three horizons (Irbit, Nyurol'ka, and Tavda). The zonal boundaries were drawn according to the first appearance of zonal forms. Kul'kova, on the basis of the dinocyst data, was able to attribute the Irbit, Nyurol'ka, and Tavda horizons of the marine Eocene to the lower Ypresian, upper Ypresian–Lutetian, and Bartonian–Priabonian, respectively. This presented the opportunity to correlate more reliably on a global scale paleogeographic events and the main evolutionary trends of flora and climate (Volkova *et al.*, 1990). In addition to dinocysts, more complete palynological associations were obtained, which are of great importance in the correlation of marine and continental deposits.

The consistent analysis of pollen assemblages allows us to establish peculiarities of palynoflora. The bulk of the genera of Eocene, flora may confidently be labelled identical to those existing now. Fairly reliable paleogeographic conclusions can be drawn taking into consideration the conditions of the growth of not only present day representatives of individual families and genera but also of plant communities. For example, the development conditions of modern plant formations of the subtropical swamped forests of the *Taxodium-Nyssa* type in the Mexican Gulf coast and south Florida can indicate analogous growth conditions of Eocene plant groups in Siberia.

At the same time, it should be emphasized that Eocene flora was mixed and has no real analogs in the modern flora. The palynological data shows that tropical and subtropical plants (Palmae, Cyrillaeceae, Sapindaceae, Sapotaceae, Santalaceae, *Cardiospermum*, *Loranthus*, Proteaceae, Melaceae, *Aralia*, *Rhus*, and *Casuarina*), moderately warm Turgai (*Carya*, *Pterocarya*, *Juglans*, *Platanus*, and Castanea), and temperate plants (*Betula*, *Alnus*, and *Lonicera*) were present in the Eocene flora. The North and South American-Asian families and genera, presently occupying the subequatorial zone, are of special interest. There are Palmae, Symplocaceae, Cyrillaceae, Bombacaceae, and Podocarpaceae. Palm pollen was noted in Eocene deposits at the high latitudes of North Asia (Shakhmundes, 1966; Kul'kova, 1973; Lyubomirova, 1975). Molds of *Sabal* palm leaves were found in northwestern Kamchatka (Budantsev, 1984). A significant role is played by the North American-South Asian group of plants (Buxaceae, Sapindaceae, and Magnoliaceae, and the *Nyssa*, *Carya*, *Aralia*, and *Comptonia* genera), whose area of distribution is presently limited to 40° - 20°N; by the North American-Mediterranean and South Asian *Liquidambar* and *Carpinus* genera limited to 20° - 50°N; by the East Asian genera (40° - 30°N) and by *Engelhardtia* (30° - 10°N). In addition, there were the species of the *Myrica*, *Alnus*, *Betula*, *Salix*, *Pinus*, *Tilia*, *Juglans*,

Acer, and other genera, whose present areas of distribution vary rather widely. The flora composition suggests an absolutely different arrangement of phytogeographical zones in North Asia. Where boreal–taiga zones presently exist, up to 60°30'N, there were subtropical evergreen forests passing northward into deciduous forests with broad-leaved and Taxodiaceae species, with evergreen plants as an undergrowth. Subtropical, coniferous, and broad-leaved forests with evergreen shrub grew on the coasts and islands of the Paleogene sea in West Siberia. A wide range of broad-leaved plants (*Trochodendron*, maple, plane-tree, hazel, oak, hornbeam, walnut, and *Liquidambar*) and Taxodiaseae (*Sequoia*, *Metasequoia*, *Taxodium*, and *Glyptostrobus*) were found in northeastern Yakutia at 70°N latitude. The remains of fig-tree, magnolia, and the pollen of *Cardiospermum*, Mirtaceae, Protoceae, and Pistaceae were also found there.

The composition of Eocene flora allowed us to define the quantitative parameters of the Eocene climate. It was assumed that the temperature of the hottest month in the central part of West Siberia was +21 to +25°C, of the coldest month, not lower than +12°C. The annual precipitation varied from 800 to 1000 mm in the north, and up to 500 mm in the Pavlodar area near the Irtysh River (Volkova *et al.*, 1990).

The estimation of the quantitative data of some climate elements by plotting the climatograms based on tree genera was as follows. During the Eocene climatic optimum (the end of the early–beginning of the middle Eocene) the coldest month attained a temperatures of +8 to +10°C south of the latitudinal segment of the Ob' River (Fig. 1) and +10 to +12°C in the area of Lake Tastakh (Fig. 2). The temperature of the hottest month was 19.5 - 20°C and 21°C, respectively (Fig. 2). The annual precipitation varied between 1000 - 1200 mm (Volkova *et al.*, 1990).

At the end of the middle–beginning of the late Eocene, the temperature during January varied from 6 to 8°C and that of the hottest month did not exceed 23°C throughout the territory of West Siberia from Kazakhstan to 60°30'N. In the lower reaches of the Kolyma River, the coldest month's temperature was 7 - 9°C and that of the hottest month was 22 - 24°C. The precipitation was not higher than 800 mm.

In West Siberia and northeastern Asia, the cooling took place at the end of the late Eocene (late Tavda time).

The temperature of the coldest month fell to +6 - +2°C. More stable temperatures occurred during warm periods. The January temperatures varied from –22 to –25°C. Mean annual precipitation was 800 - 900 mm (Lyubomirova, 1975).

The analysis of the climatograms showed that the January temperatures during the early and middle Eocene at high latitudes in northeastern Siberia were 1.5 - 2°C above the Eocene January temperatures of West Siberia. The climate was on the whole warm, facilitating the existence of subtropical and some tropical elements of flora in the composition of deciduous and evergreen forests with an admixture of coniferous species. The flora composition united Siberia with Europe and North America. A specific wide zone with a stable climate resembling the subtropical one existed during the Eocene. This conclusion is confirmed not only by the flora composition but also by the data on fauna and lithogenetic features (Sinitsin, 1965). Thus, all the data indicate a significant rise in temperature at the end of the early–beginning of the middle Eocene, which has no equivalent in the entire Cenozoic.

A stage of a stable cooling that seems related to the Antarctic glaciation began at the end of the Eocene. Later, during the most recent geological stage starting from the beginning of the Oligocene, progressive climate deterioration continued, which is reflected in the flora composition (the importance of subtropical species diminished and the importance of coniferous and broad-leaved species increased). There were sharp rises in temperature (optima) and deep falls in temperature related to glacial periods against the background of this gradual climate deterioration.

Among the optima, the following are worth noting: the Miocene optimum (early Kireevskoe time in West Siberia), the Pliocene optimum (Biteke time, 3.5 - 4 Ma), the Kazantsev Pleistocene optimum (120 - 130 ka), and the Holocene optimum.

The Miocene optimum falls at the end of the early–beginning of the middle Miocene (16 - 17 Ma). During the early Miocene, lacustrine–palustrine, in part coal-bearing deposits (Abrosimovka Horizon) accumulated. The flora of the Abrosimovka time still resembled that of the late Oligocene. Its composition indicates the existence of coniferous and broad-leaved forests already containing a great amount of narrow-leaved species and mesophilic deciduous forests with Juglandaceae and Ulmaceae. The significance of the baldcypress diminished, but, on the other hand, the importance of the representatives of the *Picea* genus increased. Subtropical plants, in particular *Nyssa*, became less important. The role of coastal-water herbaceous plants increased. The vegetation was close to the modern south Canadian coniferous-birch-beech forest with the admixture of Juglandaceae and baldcypress. The climate at the latitude of 60°N remained moderately warm but more humid. The average January temperature was close to 0 - +5°C, the July temperature was +20°C. The mean annual precipitation was 700 - 800 mm.

At the end of the early Miocene (Kireevskoe time), during the final stage of lacustrine clay formation, the share of narrow-leaved and broad-leaved species in the flora sharply increased. Among the latter, the dominant position belonged to *Juglans* (up to 19%) and *Quercus* (up to 17%). The importance of forbs increased as well. The vegetation resembled the Canadian birch–hazel forest with oak and beech. The climate was warmer than the that of early Miocene time. The average January temperature was +2°C and the July temperature was

+20°C. The mean annual precipitation remained at the same level of 700 - 800 mm.

The Pliocene optimum (Biteke time). According to the latest paleomagnetic data, it lasted from 3.3 to 3.9 Ma (Gnibidenko, 1989) or from 3.5 to 4 Ma (Zykin *et al.*, 1989). V.S. Zykin, based on data from malacofauna and small mammals, thinks that optimum climatic conditions existed before the Biteke time. It is difficult to say anything about earlier Pliocene optimum conditions from palynological data.

Coarse alluvium was formed during the Biteke time. The predominance of the plants typical of West Siberia was characteristic of the flora of that time. Among trees and shrubs, the representatives of broad-leaved plants (oak, elm, hazel, and linden) were only present for short time spans. Plant communities often changed during the Biteke time. Sagebrush–grass and sagebrush–goosefoot steppes with Ephedra were wide spread during the first half of the Biteke time. The vegetation composition resembled that of the present-day northern Black Sea steppes. The average January and July temperatures were 0 - 8°C and +20 to +22°C, respectively, in southern West Siberia and North Kazakhstan. The average annual precipitation was about 250 mm. The steppe vegetation was replaced by forest-steppe during the humid periods. Linden, elm, oak, ilex, and hazel grew along the river valleys. The amount of precipitation rose to 250 - 500 mm during humid periods. The climate changed from arid to semiarid. The climatogram for the Biteke time (forest-steppe phase based on 8 genera: *Alnus*, *Ulmus*, *Quercus*, *Juglans*, *Ephedra*, *Rubus*, *Osmunda*, and *Chenopodium*) shows that during humid periods the present-day climate was similar to the climate of the Shanghai region. The temperature of the warmest month was 26 - 28°C and that of the coldest one was −5 to +4°C. The annual precipitation was 500 mm. During the cold seasons, the deviation from modern temperatures was 20°C.

During *the late Pleistocene optimum* (Kazantseva time, 120 - 130 ka), marine sediments were formed in the northern plain and lacustrine, lacustrine–palustrine and alluvial deposits accumulated south of the Kazantseva sea. Spores and pollen compositions and their ratio suggest that most of the marine sands with moderately thermophilic mollusks and arctoboreal foraminifers in the lower reaches of the Yenisei River (sections along the Lukovaya Channel and near the village of Agapa) were formed during the development of forest vegetation. The climate at that time was much warmer and more humid than now. Average July (Fig. 3) and January temperatures were as much as +15 - 16°C and −22°C, respectively. The annual precipitation was close to 450 mm. The shift of the vegetation zone boundaries during that period is estimated to be 5 - 6°; i.e., the northern boundary of the forest zone shifted 700 km northward. It coincided with the shoreline of the Kazantseva marine basin, the temperature of which, according to S.L. Troitskii (1979), never fell below 0°C.

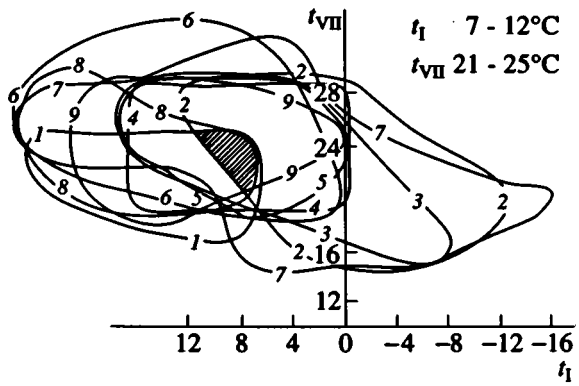

Fig. 1. Climatogram for the middle Eocene (Agana continent).

1 – Protea, 2 – Fagus, 3 – Castanea, 4 – Corylopsis, 5 – Platycarya, 6 – Engelhardfia, 7 – Rhus, 8 – Sterculia, 9 – Taxodium. Hatched field is the center of the maximum concentration of ecologically similar plants.

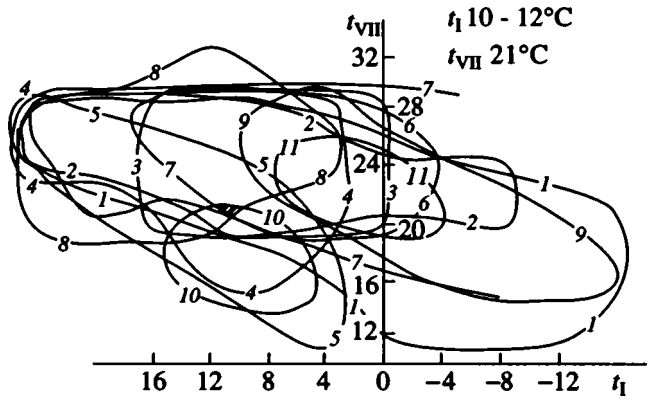

Fig. 2. Climatogram for the Eocene optimum (the end of the early–beginning of the middle Eocene, Tastakh Formation).

1 – Acer, 2 – Carya, 3 – Corylus, 4 – Castanopsis, 5 – Dacrydium, 6 – Liquidambar, 7 – Moraceae, *8 – Sabal, 9 – Hamamelis, 10 – Sequoia, 11 – Sciadopitys.*

The conclusions about the climatic conditions are supported by the study of buried peat along the Irtysh River near the village of Gornaya Subbota. The analysis of palynological data shows that the peat was formed under conditions of the boreal taiga vegetation with an admixture of broad-leaved species (Volkova, 1966, 1977; Gurtovaya and Krivonogov, 1988).

When plotting the climatogram, 6 taxa (*Picea*, *Abies*, *Quercus*, *Pinus sibirica*, *Lycopodium alpinum*, and *Menyanthes trifoliata*) were taken into account. As a result, a general field was obtained, which characterizes the temperature conditions allowing the coexistence of the species under consideration. The average temperatures in July and January were +18 to 20°C and −28°C, respectively. The July temperature was almost the same as the modern one, but the January temperature was 4.5°C higher (+8°C from carpological data). The climate was warmer and even more than during the

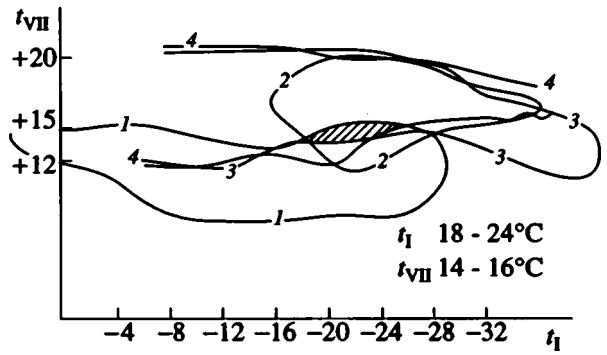

Fig. 3. Climatogram for the Kazantseva optimum (outcrops along the Lukovaya Channel on the Yenisei River). Constructed on the basis of climatic fields of four species (14 taxa were taken into account).

1 – Lycopodium alpinum L., *2 – Pinus sibirica* Du. Tour., *3 – Menyanthes trifoliata* L., *4 – Pinus silvestris* L.

Holocene optimum. The annual precipitation was 100 mm higher than the present value.

Holocene optimum. We consider the Holocene duration to be 10 000 years. This time boundary is well defined by paleobotanical data and is displayed in the replacement of periglacial plant formations by forest-tundra and forest ones. The Holocene flora was represented by modern species now growing in West Siberia. The analysis of a great number of palynological and radiocarbon data demonstrates that the Holocene environment was not stable. The general trend of vegetation evolution remained the same in the Siberian and European part of the country. The climate was colder than now in Preboreal time and at the beginning of Boreal time. The most favorable climatic conditions (optimum) in West Siberia began only in late Atlantic time and lasted till the beginning of the Subboreal interval (5500 - 4500 years). This time span corresponds to a general optimum throughout North Asia. The Boreal and middle Subboreal warmings were not manifested everywhere. The analysis of broad-leaved species, of their appearance, flourishing and degradation, allows us to trace the dynamics of their development during Atlantic, Subboreal and the beginning of Subatlantic times. In West Siberian forests, at first elm, then linden, and finally oak appeared about 7000 years ago. The blossom of the broad-leaved flora occurred at the end of the Atlantic time, and its degradation occurred about 2200 years ago. V.A. Klimanov, on the basis of palynological data and using an informational-statistic method, obtained quantitative parameters of some climate elements. It was found that the largest deviations of temperature and precipitation from modern values took place during the Holocene optimum (Volkova and Klimanov, 1988). The deviations of the average July and January temperatures from the modern values at the latitude of 67° - 70°N, in the Yamal Peninsula, were 4 - 5°C and 1°C, respectively. The amount of precipitation was 100 mm higher than today and attained 400 - 500 mm. The temperature deviation exceeded 1°C for the central regions. The precipitation was 100 mm higher, but it was 50 mm lower than present values, between the middle reaches of the Yenisei and Ob' rivers (Volkova and Klimanov, 1988). The July and January temperatures during the Holocene optimum were similar to contemporary ones south of 55°N. The comparison of the climatic conditions of the late Pleistocene and Holocene optima leads us to the conclusion that the climate was warmer during Kazantseva time. Tundra and forest-tundra landscapes were absent. The areas, occupied now by these plant assemblages, at that time were inundated with water.

The northern areas of West Siberia, the Yamal and Taz peninsulas were characterized by the greatest temperature deviations from the modern values during the Holocene optimum, which was reflected in the position of the upper boundary of the permafrost. Thus, during the late Pleistocene and Holocene optima, the greatest changes in temperatures and landscape patterns took place in the northern regions of West Siberia. This data should be taken into account when predicting future climates.

REFERENCES

Budantsev, L.Yu., On the Problem of the Boundary Between the Early and Late Cenophytic in the North Pacific, *Sreda i Zhizn' na Rubezhakh Epokh Kainozoya v Sibiri i na Dal'nem Vostoke* (Environment and Life at the Boundary of the Cenozoic Epochs in Siberia and the Far East), Novosibirsk: Nauka, 1984, pp. 20 - 24.

Gnibidenko, Z.N., Magnetostratigraphic Sequence and Paleomagnetic Characteristics of Pliocene Deposits in the South of the West Siberian Plain, *Kainozoi Sibiri i Severo-Vostoka SSSR* (Cenozoic of Siberia and the Northeast of the USSR), Novosibirsk: Nauka, 1989, pp. 26 - 31.

Gurtovaya, E.E. and Krivonogov, S.K., Phytologic Characteristic of Continental Sediments of the Kazantseva Horizon, *Mikrofitofossilii i Stratigrafiya Mezozoya i Kainozoya Sibiri* (Microphytofossils and Stratigraphy of the Mesozoic and Cenozoic in Siberia), Novosibirsk: Nauka, 1989, pp. 69 - 91.

Kul'kova, I.A., Palynological Investigations of the Eocene Sediments of the Yana–Indigirka Lowland, *Palinologiya Kainofita* (Palinology of the Cenophytic), Moscow: Nauka, 1973, pp. 105 - 109.

Kul'kova, I.A., Stratigraphy of Paleogene Deposits of West Siberia Based on Palyntological Data, *Geol. Geofiz.*, 1982, no. 6, pp. 11 - 17.

Kul'kova, I.A. and Shatskii, S.B., Zonal Division of the Marine Paleogene of the West Siberian Plain According to Dinocysts, *Geol. Geofiz.*, 1990, no. 1, pp. 25 - 31.

Lyubomirova, K.A., Paleogene, *Paleofitogeografiya Severa SSSR v Melu i Paleogene* (Paleophytogeography of the Northern USSR during the Cretaceous and Paleogene), Leningrad: Nedra, 1975, pp. 69 - 84.

Shakhmundes, V.A., On the Floral Relations Between the Northern West Siberia and Europe in the Early Eocene, *K Metodike Paleopalinologicheskikh Issledovanii* (On the Methods of Paleopalynological Investigations), Leningrad: Nedra, 1966, pp. 172 - 196.

Sinitsin, V.A., *Drevnie Climaty Evrazii, Chast' 1: Paleogen–Neogen* (Ancient Climates of Eurasia, Part 1: Paleogene–Neogene), Leningrad: Leningrad Univ., 1965.

Troitskii, S.L., *Morskoi Pleistotsen Sibirskikh Ravnin. Stratigrafiya* (Marine Pleistocene of Siberian Plains. Stratigraphy), Novosibirsk: Nauka, 1979.

Volkova, V.S., *Chetvertichnye Otlozheniya Nizov'ev Irtysha i Ikh Biostratigraficheskaya Kharakteristika* (Quaternary Sediments of the Lower Reaches of the Irtysh River and Their Stratigraphic Characteristic), Novosibirsk: Nauka, 1966.

Volkova, V.S., *Stratigrafiya i Istoriya Razvitiya Rastitel'nosti Zapadnoi Sibiri v Pozdnem Kainozoe* (Stratigraphy and Evolution of Vegetation of West Siberia in the Late Cenozoic), Moscow: Nauka, 1977.

Volkova, V.S. and Klimov, V.A., Palynology and Climate of West Siberia and Main Thermal Optima of the Holocene, *Mikrofitofossilii i Stratigrafiya Mezozoya i Kainozoya Sibiri* (Microphytofossils and Stratigraphy of the Mesozoic and Cenozoic of Siberia), Novosibirsk: Nauka, 1988, pp. 91 - 95.

Volkova, V.S., Kul'kova, I.A., and Fradkina, A.F., *Klimat Eotsena Sibiri (na Primere Zapadnoi Sibiri)* (Climate of Eocene of Siberia: with Reference to West Siberia), Novosibirsk: IGIG SO Akad. Nauk SSSR, 1990.

Zykin, V.S., Zazhigin, V.S., and Prisyazhnyuk, V.A., Stratigraphy of Pliocene of the South of the West Siberian Plain, *Kainozoi Sibiri i Severo-Vostoka SSSR* (Cenozoic of Siberia and the Northeast of the USSR), Novosibirsk: Nauka, 1989, pp. 9 - 17.

MEETING ANNOUNCEMENT

WEDDELL SEA TECTONICS AND GONDWANA BREAKUP

Convenors: Ed King, Roy Livermore, Bryan Storey

Cambridge, UK

6 - 7 June 1994

The aim of the meeting is to bring together those working on tectonic problems related to the breakup of Gondwana in the Weddell Sea sector. Apparently conflicting evidence concerning plate kinematics and the dispersal of Gondwana fragments will be reviewed and, hopefully, reconciled. Key areas for the acquisition of new data will be identified.

The meeting will provide a publishing opportunity for those working on large regional datasets, such as aeromagnetic and satellite gravity data, as well as more local land and marine data, to summarise progress to date.

The second circular, which contains further details of presentations, the venue and a registration form can be obtained from the address below.

Gill McDonnell
Weddell Sea Meeting
British Antarctic Survey
High Cross, Madingley Rd.
Cambridge, CB3 0ET, UK
tel.: +44 22 361188
fax: +44 22 362616

III Symposium on the CRETACEOUS of Brazil

(meeting and field trip: July 24 - 31, 1994)

The general objective of the Symposium is to open room for the discussions and publications of new data disclosed by recent researches on the Cretaceous of Brazil. The topics to be covered are wide ranging and embrace:

- *Tectonics*
- *Stratigraphy* (including *Sequence Stratigraphy* and *Sismo-Stratigraphy*)
- *Sedimentology*
- *Biostratigraphy*
- *Paleobiology*
- *Paleoecology*
- *Paleoceanography*
- *Geochemistry*
- *Geophysics*
- *Geomorphology*
- *Magmatism*

Deadline for submission of abstracts **April 15, 1994.**

Contact:

Dimas Dias-Brito
Departamento de Geologia Sedimentar
Universidade Estadual Paulista (UNESP)
Rua 10 nº 2527
Rio Claro-SP, CEP. 13506-230
BRASIL

Phone: 011-55-0195-340327

Fax: 011-55-0195-242445-15

PALAEWORLD

An English-language series publication of *the Laboratory of Palaeobiology and Stratigraphy*

Nanjing Institute of Geology & Paleontology, Academia Sinica

The Laboratory of Palaeobiology and Stratigraphy is pleased to announce its English-language publication, *Palaeoworld*, which is a non-periodical series reporting our most recent research activities and achievements in palaeobiology, paleontology, and stratigraphy, including collections of individual papers, collected papers of important research programs organized by the Laboratory and significant monographs. The available and upcoming issues of *Palaeoworld* are as follows:

Number 3: Taxonomic Studies of Upper Jurassic (Tithonian) Radiolarian from the Taman Formation, East-Central Mexico. Monography by Yang Qun. (Extensive systematic paleontology on Tithonian radiolarians, one new fam., 7 new gen., 49 new spp.; the radiolarians associated with ammonites, calpinellids and pectenacids; correlation with radiolarian faunas of Oman, Japan and the east Atlantic Cape Verde basin; outer neritic to bathyal environment; northern Tethyan province; 165 p., 26 pls. 35 text-figs).
Available: November, 1993.

Number 4: Permian Stratigraphy, Environment and Resources of China. Edited by Jin Yugan, J. Utting and B.R. Wardlaw. (Section one – detailed correlation of Permian, south China with a proposal on candidate GSGP sections for P/T boundary. Section two – biostratigraphy of conodonts, fusulinids, radiolarians, etc. Section three – stage level paleogeographic maps based on computerized database, isotopic analysis and integrated studies on Permian coal-bearing series and oil-basins in China).
Available: June, 1994.

Number 5: Base of the AUSTRODENTATUS Zone as a Level for Global Subdivision of the Ordovisian. Edited by Chen Xu and S.M. Bergstrom. (Proposed candidate boundary stratotype section for Ordovisian subdivision in Chejiang, south China; graptolites, conodonts and related fossil groups).
Available: October, 1994.

Palaeoworld numbers 1 & 2 contain individual research papers mostly written in Chinese.

For those interested, each copy of all issues of *Palaeoworld* costs 28 US dollars (postage included). Orders by cashier's or personal checks are acceptable and should be addressed to:

Prof. Jin Yugan
Laboratory of Palaeobiology and Stratigraphy
Nanjing Institute Geol. & Palaeontol.
Chi-Ming-Ssu, Nanjing 210008
CHINA

Continental Processes

VII International Symposium on the Observation of the Continental Crust Through Drilling

• Santa Fe, New Mexico, USA, April 25 - 30, 1994 •

Themes for Scientific Sessions

• **Global change** – evolution of surface environments through time; the sedimentary basin record of global change; seismic stratigraphy; impact features; ice-coring; short-term surface thermal history

• **Active tectonic processes** – active faulting and deformation; lithospheric dynamics and in-situ stress

• **Fluids in crustal processes** – fluid generation, migration and trapping; energy and mineral resources; waste transport; basin evolution

• **Thermal regimes** – volcanic, metamorphic and deep magmatic processes; hydrothermal systems

• **Evolution of continental lithosphere** – Crustal structure; continental margins and continental accretion; testing of geological, geochemical and geophysical models

• **Downhole sampling and measurements** – logging, fluid sampling and testing; geophysical & geochemical experimentation in drillholes

Field Excursions

• Continental Scientific Drilling in California

• Jemez Volcanic Field (included with registration fee)

Registration Information

US$400.00 – if registering before March 1, 1994

US$450.00 – if registering after March 1, 1994

US$ 50.00 – student participants

US$100.00 – accompanying persons

For Further Information Contact:

Dr. Earl Hoskins, DOSECC, College of Geosciences and Maritime Studies,
Texas A&M University, College Station, TX 77843-3148 USA,
Ph: (409) 862-1146, Fax: (409) 845-0056, E-mail: hoskins@pluto.tamu.edu.

Sponsored by the Department of Energy, the National Science Foundation, and the US Geological Survey, convened by Drilling, Observation, and Sampling of the Earth's Continental Crust, Incorporated, and by Los Alamos National Laboratory.

Russia's leading geological research brought to you in English direct from Moscow by INTERPERIODICA

PETROLOGY

Editor-in-Chief
Vilen A. Zharikov
Director of the Institute of Experimental Mineralogy, Russian Academy of Sciences

PETROLOGY is a journal of magmatic, metamorphic, and experimental petrology, mineralogy, and isotopic geochemistry. The journal offers comprehensive information on all multidisciplinary aspects of theoretical and experimental petrology. By giving special consideration to studies on the petrography of different regions of the former Soviet Union, PETROLOGY will provide all readers with a unique opportunity to refine their understanding of the geology of the vast territory of the Eurasian continent.

Coverage includes:

- petrology of magmatic, metamorphic, and metasomatic rocks in continental and oceanic environments
- experimental petrology and mineralogy
- geothermobarometry
- physiochemical analysis of mineral assemblages
- isotopic geochemistry and geochronology.

Bimonthly. 1993 Vol. 1. ISSN 0869-5911.
North America, $540 Rest of World, $576

STRATIGRAPHY AND GEOLOGICAL CORRELATION

Editor-in-Chief
Boris S. Sokolov
Academician and Adviser of the Presidium, Russian Academy of Sciences

Previously combined with PETROLOGY in the original Russian, this new journal fully explores stratigraphy and the chronological features of the world's geological record. STRATIGRAPHY AND GEOLOGICAL CORRELATION is the only journal in the world to provide comprehensive coverage of fundamental and applied aspects of stratigraphy and the correlation of geological events and processes in time and space. Articles are based on the results of multi-disciplinary research and cover a wide area of interests including:

- problems of general and regional stratigraphy of continents and the oceans sedimentary cover
- theory and methods of stratigraphic analysis
- geochronology including isotopic geochronology
- the evolution of the biosphere
- development of sedimentary basins
- aspects of geological correlation and global secular changes in ecosystems.

Bimonthly. 1993 Vol. 1. ISSN 0869-5938.
North America, $540 Rest of World, $576

GEOLOGY OF ORE DEPOSITS

Editor-in-Chief
Nikolai P. Lowerov
Director of the Institute of Geology of Ore Deposits, Petrology, Mineralogy and Geochemistry, Russian Academy of Sciences

Founded in 1959, GEOLOGY OF ORE DEPOSITS is one of only a few devoted to the study of metallic and non-metallic minerals and the conditions of their formation and distribution. Since restrictions on publishing classified geological data have been lifted, more complete and concrete findings on important deposits throughout the former USSR — including such unique ore districts as Noril'sk, Udokan, and Muruntau — are now available. Also included are articles by foreign contributors on strategic deposits through the world. GEOLOGY OF ORE DEPOSITS covers:

- economic geology of metal and non-metal ore deposits
- geological environments of ore formation
- mineral composition of ores
- experimental studies of ore-forming systems
- ore-forming processes and their evolution
- geochronology of ore-forming processes and their evolution
- criteria of forecasting and estimating mineral deposits.

Bimonthly. 1993 Vol. 35. ISSN 0016-7770.
North America, $540 Rest of World, $576

INTERPERIODICA

pledges to give you the best quality and service:

- Immediate access to unique scientific research
- Superior translations — produced by a carefully chosen team working closely, in Moscow, with the Russian authors and editors
- High quality printing in North America...journals attractively designed and printed with high standards to ensure rapid delivery
- Centralized customer service — responsive attention to your needs through our North American subscription office
- Reasonable prices...and now offering special discounts
- Full no-risk, money-back guarantee if you are not completely satisfied

▼

ALL 1993 JOURNALS WILL BE PUBLISHED IN 1993!

▲

For more information call
1 800 633-4931 (US and Canada)
or 205 995- 1567 (Rest of World)
or write
INTERPERIODICA
P.O. Box 1831
Birmingham, AL 35201-1831